STUDIES ON SYNTHESIS OF SILICA COATED SILVER NANOPARTICLES FOR DETECTION AND THERAPEUTICS

A Thesis Submitted to

D. Y. PATIL EDUCATION SOCIETY

(INSTITUTION DEEMED TO BE UNIVERSITY)

For the Degree of

DOCTOR OF PHILOSOPHY

In

NANOBIOTECHNOLOGY

By

MS. PRIYANKA SINGH

M. Sc.

Under the Supervision of

Dr. RAGHVENDRA A. BOHARA

M.Sc., Ph.D., Pharm Dip, MRSC(UK)

2024

DECLEARATION

I hereby declare that the thesis entitled "Studies on synthesis of silica coated silver nanoparticles for detection and therapeutics" submitted for the degree of Doctor of Philosophy (Ph.D.) in the Centre for Interdisciplinary Research faculty of the D. Y. Patil Education Society (Institution Deemed To Be University), Kolhapur is completed and written by me, has not before made the basis for the award of any degree/diploma/other related heading of this or any other university in India/any other country/examining body to the best of my knowledge. Further, I assert that, I have not dishonored any of the requirements under copyright and piracy/cyber/IPR act amended by UGC from time to time.

(Research Student)

Place: Kolhapur

Date: / /202 **Ms. Priyanka Singh**

CERTIFICATE OF GUIDE

This is to certify that the thesis entitled **"Studies on synthesis of silica coated silver nanoparticles for detection and therapy"**, which is being submitted here with for the award of The Degree of Doctor of Philosophy in **Nanobiotechnology** from D. Y. Patil University Kolhapur (Estd. u/3 of the UGC Act 1956), under the faculty of interdisciplinary studies, is the result of original Research work completed by **Priyanka Singh** under our supervision and guidance and to the best of our knowledge and belief the work bound in this thesis has not formed earlier the basis for the award of any Degree or similar title of this or any other University or examining body.

Date:

Place: Kolhapur

Research Guide

Dr. Raghvendra A. Bohara

(M.Sc., Ph.D., Pharm.Dip,MRSC)

Acknowledgment

It started with a dream framed into a plan and the rest is the journey of hard work, resilience, and dedication supported by family, friends, research mates, my professors, College staff, and my mentor. I am filled with joyous emotions so fulfilling that can be felt not described. I feel short of words but filled with heartful emotions to bow down to my father ***Mr. Chandra Bhushan Singh,*** my mother ***Mrs. Rita Singh,*** and my aunt (My godmother) ***Mrs. Veena Karki,*** who provided me the strength to take every small or big step and in the accomplishment of this thesis.

"अज्ञान तिमिरान्धस्य ज्ञानाञ्जन शलाकया। चक्षुरुन्मीलितं येन तस्मै श्री गुरवे नमः॥" (Regards to the Guru who opened the eyes of people blinded by the darkness of ignorance with the light of knowledge).

I am indebted to my Guide and mentor ***Dr. Raghvendra A. Bohara*** who has channelized my hard work, dedication, and knowledge to attain the destination it meant to be. I am grateful to him for being so patient and at the same time equally demanding so that I could be focused and felt hand holed properly to achieve my thesis. His acumen, guidance, and unequivocal support have honed my knowledge and skill to upscale my expertise.

I would like to express my special thanks and gratitude to The Registrar ***Dr. V. V. Bhosale Sir***, and our Research Director ***Prof. C. D. Lokhande Sir*** for giving me the opportunity, resources, and support to complete my research. My research and thesis would have not been so fulfilling without their help. My humble gratitude to ***Dr. Umakant Patil Sir***, for the right guidance and timely help.

Worth mentioning is the role of my soul brother ***Dr. Pranav Katkar***, who has not spared any chance of supporting me. I am grateful to my friends, and my seniors in the Centre for Interdisciplinary Research. Of course, the help and guidance rendered by them in the department will be remembered. And a heart-warming thanks to all the teaching and non-teaching staff members for their support during my doctoral work.

Last but not least I would like to thank the special people who supported me throughout my journey both in academics and life, my family. I must acknowledge my stress buster, (my best friend) my daughter ***Neev***, whose magical words have been the source of eternal energy to me.

To my Alma mater, ***D. Y. Patil Education Society, Kolhapur*** for having me as an alum of the institute.

-Priyanka Singh

Date: / /2024

LIST OF PUBLICATIONS AND CONFERENCES ATTAINED

Articles Published

1. **Priyanka Singh,** Pranav K. Katkar, Umakant M. Patil, Raghvendra A. Bohara, A robust electrochemical immunosensor based on core-shell nanostructured silica-coated silver for cancer (carcinoembryonic-antigen-CEA) diagnosis, RSC Adv., 2021, 11, 10130-10143.
2. **Priyanka Singh**, Pranav K. Katkar, Tomasz Walski, Raghvendra A. Bohara, Three in-one fenestrated approaches of yolk-shell, silver-silica nanoparticles: A comparative study of antibacterial, antifungal, and anti-cancerous applications, Heliyon, 2023, 9, e18034.
3. Raghvendra A. Bohara, **Priyanka Singh**, Multiple Myeloma: Role of Magnetic Nanoparticles, Magnetic Nanoheterostructures, Nanomedicine and Nanotoxicology, Springer, 2020.
4. **Priyanka Singh,** Shivang Singh, Balaji Maddiboyina, SaiKrishna Kandalam, Tomasz Walski, Raghvendra A Bohara, Hybrid silver nanoparticles: Modes of synthesis and various biomedical applications, Electron/ Volume 2, Issue 2/ e22.

Conference Participation

1. Participated in International workshop on "Ph.D. Program for Medical Innovations" (IWPPMI) organized by Centre for Interdisciplinary Research, D. Y. PATIL UNIVERSITY, KOLHAPUR on Feb. 16th & 17th 2014.
2. Attended the 5th international conference on Angiogenesis research: Targeted Anti-Angiogenic Therapy held on 26th -27th October, 2018 at D.Y.Patil Education Society Kolhapur.
3. Participated in paper(poster) presentation in International conference on Nanostructured materials & Devices (ICNSMD-2018) jointly organized by the Society for Technologically Advanced Materials of India (STAMI) and University of Delhi from 17/12/18 to 20/12/18.

INDEX

CHAPTER 1

Nanotechnology at Glance

CHAPTER 2

Coated silver nanoprticles: synthesis methods and applications

CHAPTER 3

Experimental and characterization techniques

CHAPTER 4

Synthesis and characterization of silver and silica coated silver nanoparticles

CHAPTER 5

Fabrication of electrochemical immunosensor for detection of CEA

CHAPTER 6

Evaluation of the anti-cancer potential of Ag nanoparticles and $Ag@SiO_2$ nanoparticles

CHAPTER 7

Comparative antimicrobial studies of Ag nanoparticles and Ag@SiO_2 hybrid nanoparticles against microbes (bacteria and fungus)

CHAPTER 8

Summary and conclusion

LIST OF FIGURES

Chapter 1: Nanotechnology at glance Page No

Chapter 2: Hybrid silver nanoparticles: Synthesis methods and applications

Chapter 3: Experimental and Characterization Techniques

Chapter 4: Synthesis and Characterization of Silver and Silica Coated Silver Nanoparticles

Chapter 5: Fabrication of Electrochemical Immunosensor for Detection of CEA

Chapter 6: Evaluation of the Anti-Cancer Potential of Ag Nanoparticles and Ag@SiO_2 Nanoparticles

Chapter 7: Comparative Antimicrobial Studies of Ag Nanoparticles and Ag@SiO_2 Hybrid Nanoparticles Against Microbes

Chapter 8: RECOMMENDATIONS

LIST OF TABLES

Abbreviations

A:

Ag: Silver

Au: Gold

AgCl: Silver chloride

ASA: Acetylsalicylic acid

As: Arsenic

AOT: Dioctyl sodium sulfosuccinate

ASCO: American society of clinical oncology

$AgNO_3$: Silver nitrate

AAD: Amino-actinomycin dye

Ag@Cu: Silver-copper

Ag@Pt: Silver-platinum

AFP: Alpha-feto protein

AFM: Atomic force microscopy

B:

BLCA: Biotinylated lens culinaris agglutinin

BPP: Banana peel powder

BSA: Bovine serum albumin

C:

CoO: Cobalt(II) oxide

Co_3O: Cobalt(III) oxide

Cr_2O_3: Chromic oxide

$Cu(OAC)_2.2H_2O$: Cupric acetate dihydrate

CFU: Colony-Forming Unit

CEA: Carcinoembryonic-antigen

CTAB: Cetyl-tri-methyl-ammonium-bromide

CEACAM: CEA-associated cell-adhesion molecules

COPD: Chronic obstruction pulmonary disease

CV: Cyclic voltammetry

CTB: Cell titer blue

D:

D: Dimension

DMF: Dimethylformamide

DDA: 1,12-Dodecanedioic acid

E:

EPR: Enhanced permeability and retention

EG: Ethylene glycol

EDX: Energy-dispersive X-ray spectroscopy

EIS: Electrochemical impedance spectroscopy

E.coli: Escherichia coli

EC: Electrical conductivity

F:

FWHM: Full width at half maximum

$Fe(NO_3)_3$: Ferric nitrate

FTIR: Fourier-transform infrared spectroscopy

FITC: Fluorescein-iso-thio-cyanate

FACs: Fluorescence-activated cell sorting

FDA: Food and drug administration

G:

GQD: Graphene quantum dots

H:

H_2O_2: Hydrogen peroxide

$HAuCl_4$: Chloroauric acid

HCC: Hepato cellular carcinoma

HRP: Horse-radish-peroxidase

I:

ITO: Indium tin oxide

IZ: Inhibition zone

K:

Kv: Kilovolt

L:

LSPR: Localized surface plasmon resonance

LSV: Linear sweep voltammetry

M:

MEF: Metal enhanced fluorescence

MRI: Magnetic resonance imaging

MWCNT: Multi wall carbon nanotube

MOFs: Metal organic frameworks

MSSA: Methicillin susceptible Staphylococcus aureus

MRSA: Methicillin resistant Staphylococcus aureus

MIC: Minimum inhibitory concentration

MBC: Minimum bacterial concentration

MTT: 3-(4,5-dimethylthiazolyl-2)-2,5-diphenyltetrazolium bromide

MSN: Mesoporous silica nanoparticles

N:

N_6: Hexazine

nm: Nanometer

NP: Nanoparticle

NM: Nanomaterials

Ni_2O_3: Nickel-oxide

NaCl: Sodium chloride

Na_3CA: Lazurite

NaOH: Sodium hydroxide

Na-LS: Na-lauryl sulfate

Na-NS: Na-naphthalene sulfonate

NH_4OH: Ammonium hydroxide

$NaHB_4$: Sodium borohydride

O:

1-D: One dimensional

P:

PA: p-aminoazobenzene

PEG: Polyethylene glycol

PVP: Polyvinyl pyrrolidone

PSA: Prostrate specific antigen

P.aeruginosa: Pseudomonas aeruginosa

PI: Propidium iodide

PBS: Phosphate buffer solution

Q:

QD: Quantum dots

R:

ROS: Reactive oxygen species

RT: Room-temperature

S:

SiO_2: Silicon dioxide

SFS: Sodium formaldehydesulfoxylate

SDS: Sodium lauryl sulfate

SERS: Surface-enhanced Raman scattering

SDBS: Sodium dodecyl benzene sulfonate

SAED: Selected area electron diffraction

SEM: Scanning electron microscope

S. aureus: Staphylococcus aureus

SIF: Silver island film

SD: Standard deviation

SCE: Saturated-calomel electrode

T:

TiO_2: Titanium dioxide

TSC: Tri sodium citrate

TAA: Tumor-associated-antigen

TMA: Thiomalic acid

2-D: Two dimensional

3-D: Three dimensional

TEM: Transmission electron microscopy

TEOS: Tetraethyl orthosilicate

U:

UV-vis: Ultraviolet visible

X:

XRD: X-ray diffraction

Z:

Zn: Zinc

ZnO: Zinc oxide

Z0-D: Zero dimensional

Chapter 1

Nanotechnology at Glance

Chapter 1: Nanotechnology at Glance

1.1. Introduction

Nanotechnology is managing matter on the atomic as well as the molecular scale. It is a developing field of science that comprehends the engineering and studying of nanosized particles of numerous materials. It is evident that nanoscience and nanotechnology entirely deal with very tiny-sized objects and systems. Conventionally, the United States National Science Foundation[1] classified nanotechnology as research that demonstrate materials and systems possessing below mentioned key properties-

- Building block property- Such materials can be combined to create larger structures.
- Process- Formulated with strategies that reveal fundamental command over the chemical and physical aspects of molecular-scale structures.
- Dimension- Partially one dimension should be from 1 to 100nm (nanometer).

The primary interest of nanostructured materials is their ability to fashion, coat, and the outstanding flexibility that they possess in being synthesized to meet the requirement of a specific application. For many years, few of the pre-existing technologies relied mainly on methods that occur on the nanoscale. Lithography, ion exchange, adsorption, drug design, plastics, catalysis, and composites are a few examples of this technology. Several dynamic research fields of nanotechnology and nanoscience include nanocomputers, nanodevices, nanolithography, nanolayers, nanorobotics, nanopowders, nanoporous materials, and nanostructured catalysts, molecular nanotechnology, organic as well as inorganic nanostructure, medicine, cancer prognosis, avoidance, and treatment by nanotechnology amongst others.

One of the prominent contributions of nanotech is that organic nanostructured materials can be effortlessly integrated with regular inorganic nanostructures (e.g. semiconductor devices), consequently providing extra functionality to contemporary photonic circuits and components. The ultimate goal of nanotechnology is to gain a finer understanding of the basic molecular processes and abilities of organic and inorganic nanostructures that are influenced by grain barriers and interfaces for their technological applications in various fields. Numerous advances have been contrived over time with the development of approaches to nanoscience and nanotechnology. Amidst evolution in nanotechnology, an exceptional climb has taken place in the utilization of nanoparticles in various fields of biomedical sciences, mainly in diagnosis[2]. Amid numerous kinds of nanoparticles accessible at the current time, nanoparticles having core-shell architectonic possess excellent properties, collaborating multiple functionalities into a sole hybrid nanocomposite. Alteration in silver nanoparticle's functionality with silica gives the nanoparticle idiosyncratic effects, because of the biocompatibility, hydrophilicity, and optical transparency along with thermal and chemical stability of

the silica; unexpectedly in aqueous media also[3]. The flexibility of silica in surface moderation as well as in synthesis demeanor, offers an outstanding edge to the employment of this material for therapeutic purposes[4],[5] because, for the applicability in medicine, immune-compatibility is a prerequisite condition, that will clinch the non-toxic nature of the material[6]. Cancer is an ambidextrous malady exceptionally unpredictable in its unveiling, evolution, and aftermath. One of the typical sorts of cancer is prostate cancer, which commences whilst cells of the prostrate evolve anomalously[7]. There are certain limitations associated with conventional chemotherapeutic drugs[8]. Silver nanoparticles have the prospective to circumvent assorted drawbacks of typical therapeutic implementations[9]. Tailor-made silver nanoparticles coated with specific biocompatible nanomaterial can target cancerous cells in a foreseeable demeanor because these can be specifically intended for expanded drug loading, upgraded half-life inside the body, unflappable release as well as selective distribution by altering their size[10], composition, surface chemistry, and morphology[11]. In the same manner, antimicrobial chemotherapy also demands attention because lately, resistance to antibiotics by disease engendering fungus and bacteria has been growing at a breathtaking pace and thus become major trouble. Bacterial and fungal contaminations are a colossal source of mortality and morbidity. To overcome such resistance mechanism of pathogenic microbes[12], consideration has been given to silver nanoparticles as an encouraging tool since they work miraculously on a span of targets in contrast to antibiotics, which have a particular site of execution[13]. Silver nanoparticles showcased magnificent outcomes in detecting and remedying microbial infections by enabling the pick out of target pathogens, reactive and combinatorial freightage of antibiotics, successful antibacterial vaccination as well as swift detection of pathogens[14].

In recent years, several immunoassay techniques for the diagnosis of different tumor markers for more effective governance of cancer have been investigated. Gradually, electrochemical immunoassay has acquired acceptance and is therefore broadly utilized to detect tumor markers because of the intrinsic benefits such as lofty selectivity, sensitivity, suitable label-free manipulation, low cost, minute size, and very fast analysis[15]. A sailing way for the observation of cancer has been the evaluation of serum tumor markers.

The employment of indium tin oxide (ITO) for sensing purposes can be increased by incorporating nanoparticles on its outer layer[16]. Metal nanoparticles give a biocompatible environment for the sake of biomolecules which remarkably enhance the surface-to-volume proportion of a stagnant biomolecule onto the surface of the electrode, both of them finally affect electrical signal improvement[17]. Experts in the area of biosensors are invariably eager to unearth novel materials possessing acceptable abilities to increase the activity of biosensors. Composite nanomaterials are appropriate to generate a constant electric field as well as elevate the transferred ratio of electrons in

comparison to sole nanoparticles. Therefore, they can successfully fasten the regeneration action of sensors[18].

1.2. Overview of nanoparticle

Conventionally, the nanotechnology word rises from the Greek word, meaning "dwarf". Around the world nanotechnology has been employed by craftsmen since 2600 BC though[19], the conceptualization of nanotechnology was first proposed on 29th December 1959 at the meeting of the American Physical Society by the famous Nobel laureate Richard P Feynman[20] in the famed lecture given by him- "there's plenty of room at the bottom". Ever since, numerous revolutionary occurrences in the arena of biology, physics, and chemistry have supported Feynman's idea of exploiting matter across the atomic scale.

Three main physical approaches that are co-related that every nanoparticle exhibits-

- They have a towering surface area per unit volume, providing electronic functions and collaboration with outward impacts greatly.
- Nanoparticles show high mobility both in the free state as well as in absorbent media.
- Every nanoparticle displays quantum impact because of the corresponding dimension and the electrical wave function frequency. Nanoparticles- Materials having a size of at least one dimension with a size span of 1 to 100nm.

The word "nano" normally specifies a size 10^{-9} or "one billionth" of something. In the year of 1974, one of the professors at Tokyo University of Science, named Norio Taniguchi innovated the term "nanotechnology" to explain the ultra-fine dimensions and extra-high precision. Based on developments and miniaturization in optoelectronic devices, integrated circuits, computer memory devices, and mechanical devices: he proposed the "top-down approach". About ten years later following this idea, the “bottom-up approach" was introduced by K Eric Drexler when he explained the formation of larger objects from their molecular and atomic element as the future of nanotechnology[21].

It is worth mentioning nanotechnologies can bring benefits in multi-dimensional areas, like water contamination, drug development, fabrication of lighter and stronger materials, and communication and information technologies.

1.3. Types of nanoparticles

Classification of nanoparticles revolves around factors governing the application or area of research it will use. Innumerable standards have been taken into scrutiny for the classification of nanoparticles by researchers and scientists like morphology, origin, dimensionality, geometry, toxicity, aggregation, chemical constituents, and so on. [19] Now we want to throw light on a few of the criteria for the classification of the nanoparticles, that have been employed more frequently.

1.3.1. Based on "Dimension"

Technically, all nanoparticles have a minimum of one dimension in the nano metric size span of one to hundred nanometres[22]. These are classified into four main types on the basis of the dimension, as displayed in the fig. 1.1.

0-dimensional nanoparticles- Conceding that all peripheral proportions of a nanoparticle are placed within the nanoscale or have no dimension, such nanoparticles are designated as 0-dimensional. The best example of zero dimensional nanoparticles are- quantum-dots(QD)[23]. Individual single molecules isolated from each other studied as nanoparticles, also fall in this category.

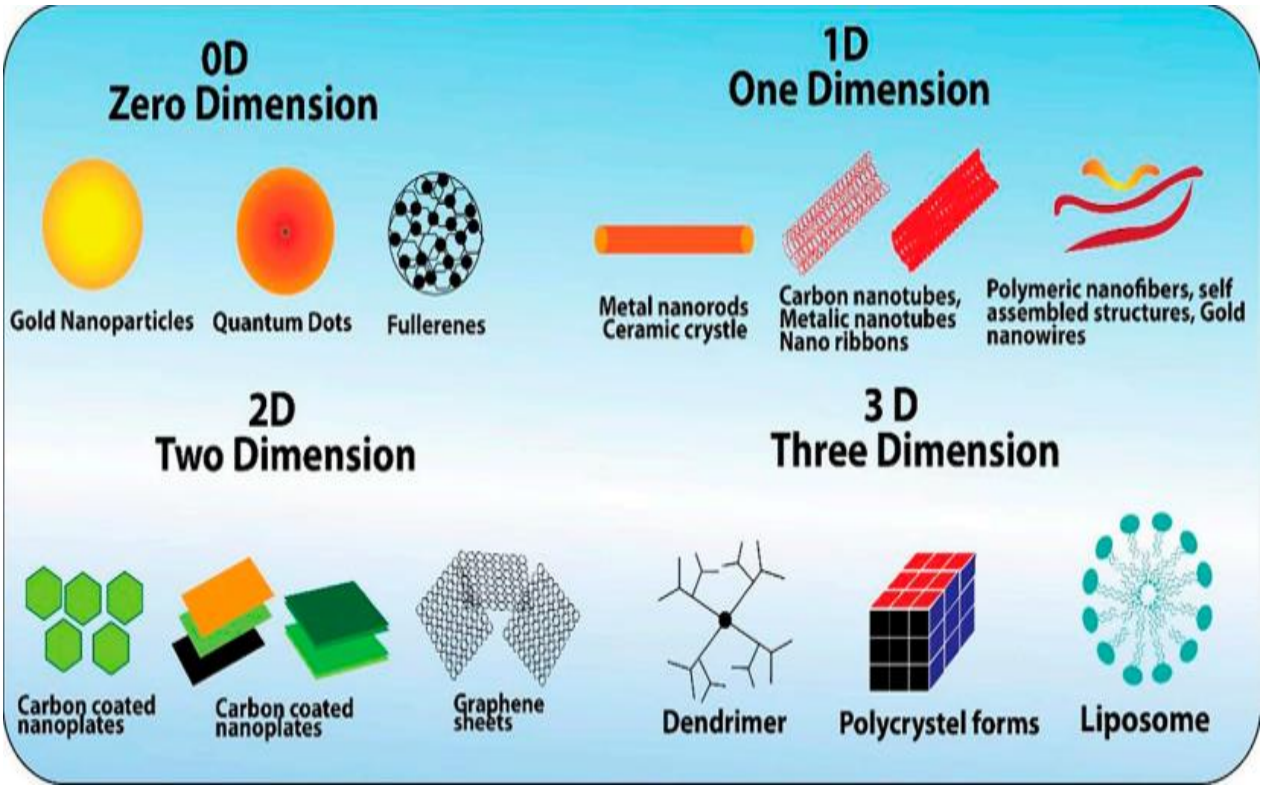

Figure 1.1: Classification of Ag nanoparticles based upon dimension[24].

1-dimensional nanoparticles- Particles having a single dimension out on the nanometric size span along with auxiliary two-fold dimensions at nanoscale size span are designated as 1-dimensional nanoparticles[24]. Such nanoparticles are very crucial in the fabrication of nanotubes, nanowires, nanobelts, nanorods[25] etc. These nanoparticles play a key role in hierarchical nanostructures.

2-dimensional nanoparticles- 2-D- nanoparticles are those particles, comprising two dimensions on the size range of nanometeric-scale. Such class of nanoparticles show qualities of nanosheets[26], nanocoatings or thin films. These nanoparticles possess outstanding applications in the fabrication of sensors and nanoreactors[27].

3-dimensional nanoparticles- These are the class of nanoparticles that exhibit nanoscale character interior even after neither of the three peripheral dimensions are on the nanometric size range. Multilayer particles, polycrystalline materials, fibrous particles together with a few types of powders fall into this category[28]. Building blocks of such types of nanoparticles are geometrically comprised of lower dimensionality of elements. In modern nanotechnology, three-dimensional nanoparticles possess extraordinary importance.

1.3.2. Established on "origin"

Nanoparticles feasibly halved into three main classes based on the "origin"-

Natural nanoparticles- The name itself says such nanoparticles rise naturally, particularly as highly fine particles. Frequent origins of such nanoparticles in around in nature are waves of the sea, crystalline structures, sand storms, oil, volcanoes, space, living organisms,[29] etc.

Manipulated nanoparticles- Imposing advanced equipment, a bundle of chemical catalysts, along with innovative methods of synthesis; nanoparticles nowadays are manufactured synthetically to make improvements in targeted features that meet the requirements of certain specific functionalities[30].

Incidental nanoparticles- Such types of nanoparticles are defined as ultra-fine, emitted particles that are co-incidental by-products of composing activities of the human being such as material welding, building demolition, power generation, engine exhaust, cigarette smoke, food processing, etc.

1.3.3. On the basis of "morphology"

Various applications related to nanoparticles need a particular range of sizes and shapes of nanoparticles. Following this reason, there is a requirement for a separate categorization based on morphology. Various geometry of nanoparticles designated as- spherical, cubic, prism-shaped, triangular, helical, hexagonal, tube-like, oval-shaped, rod-like, etc. They can possess distinct intrinsic crystal structures namely icosahedron, face-centered cubic, decahedron, simple cubic, and so on[19].

1.4. Consolidation of nanotechnology and Life sciences

Nanotechnology is the most celebrated, growing, and expanding division of science and technology. Improvements in nanotechnology are progressively being employed in the field of life sciences. Clinical implementation of nanotechnology is developing day by day and its frequency will extend with current research development into practice. Nanotechnology is called a young field to some extent while having the extraordinary potential to refabricate existing industries and remarkably brush-up standards of living.

Rationale designing and structures of particles at the nanometer range are being utilized in various fields like biotechnology, tissue engineering[31], pharmaceuticals, and diagnostics. In the field of medicine, the application of nanotechnology has exceptional prospects with new technologies upgrading drug-delivery[32] together with innovative methods of diagnosis of various diseases.

1.4.1. Influence of nanotechnology on life sciences

Nanotechnology is a growing field that is expected to provide solutions to various technical problems and economically advantageous products in different fields of application. Already there are numerous products contributed by nanotechnology is available in the market but still, it needs intensive research and works in this field. There are a wide number of industries in existence, that uses a set of techniques in mainly three overlapping areas, named nanomaterials, nanobiotechnology, and nanoelectronics,[23] which has wide application in a number of fields such as - agriculture, pharmaceutics, information technology, transport, materials, metrology, electronics, environment, healthcare, robotics[33], and so on.

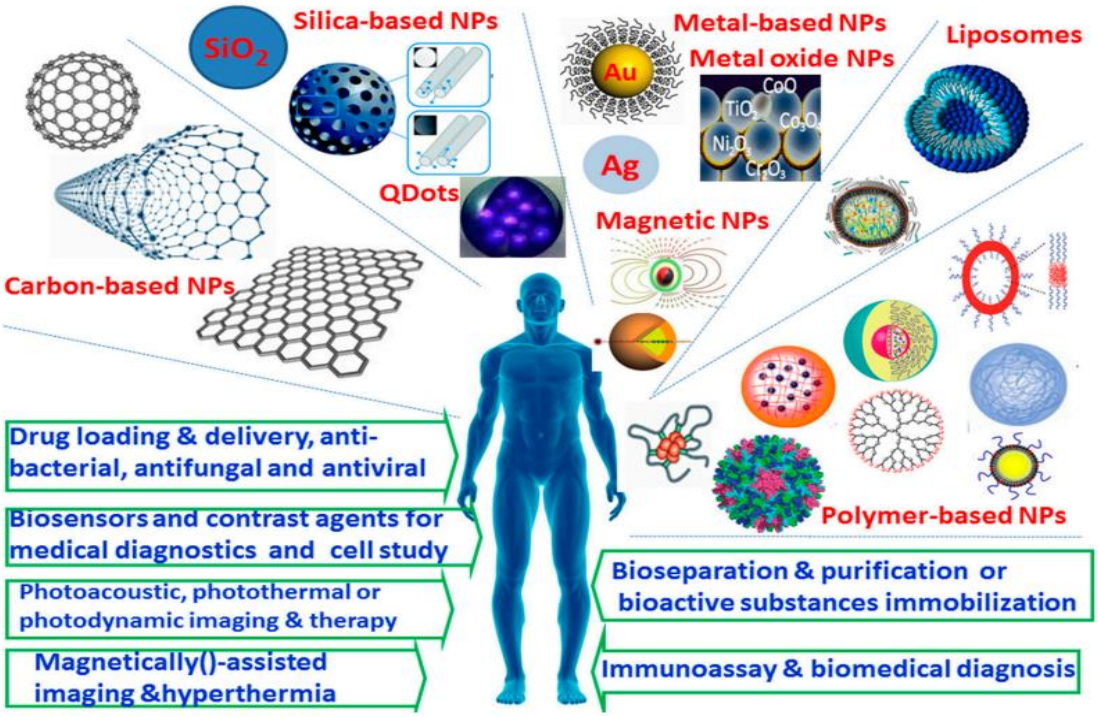

Figure 1.2: Types of nanoparticles and their applications[34].

1.4.2. Impact on the diagnostic field

Molecular diagnostic is the latest revolutionary area of nanotechnology, which needs less time is a quick process, has a small number of samples, and is trustworthy for various kinds of analysis. We can fabricate a tiny chip analyzer by employing lab-on-chip technology which can interpret the desired samples within a few minutes[35]. Such chip analyzers need merely picolitre or nanogram-sized samples which can give more scope for systematic analysis and reliability. The lab-on-a-chip[36] method is the basis for conjoining screening approaches which can dramatically accelerate the novel drug discovery process when combined with dynamic computers.

1.4.3. Influence of nanotechnology in the field of drug-delivery

Nanotechnology has given a broad range of potentially valuable prospects for its utilization in drug delivery systems and it can be employed efficiently to carry a particular drug to the desired target locations, by delivering specific solubility of appallingly water-soluble drugs. This is mainly significant in the treatment of cancer where there is the risk of damage of healthy cells by the chemotherapeutic drugs in the surrounding area of the tumor, that is how it brings forth the benefits of diminished accumulation in healthy tissues. Materials at the nanoscale possess a very specific property named EPR-effect(enhanced permeability and retention effect)[37] which is particularly significant for the treatment of cancer. A few of the other areas which utilize nanotechnological efforts are- vaccine adjuvants and their delivery systems, wound management, and in orthopedics[38].

1.4.4. Influence in tissue-engineering

Tissue engineering is the connection between the biomedical industry and pharmaceutical where nanotechnology shall have an actual impact. This field growing at a very fast pace in developed countries in terms of commercial significance day by day. Internal tissue implant is one of the best examples of this thing. Nanotech can be utilized to develop tissues and organs synthetically on nanopatterned scaffolds[36] to give the platform for internal tissue-implant because of the shortfall in producing replacement organs which leads to xenotransplants[36]. One of the other speculative areas is nanorobot therapeutics, which can take so far as possible twenty years, and hereafter it's been predicted that nanorobots will hover around the body and can perform targeted healing jobs. Miniaturization methods are key to various applications that merge actuators and sensors with nano-scale features to create personal healthcare-related testing devices and sensors that can be employed to detect cancer and other multiple classes of infections and diseases.

1.5. Metallic nanoparticles

Since ancient times, metals had been mined and utilized by humans. Although the date of the initial employment of metals is still not known, the estimated date of the discovery of metals, e.g. Ag, As, Pb, Fe, Zn, Cu, Hg, Au, dates back 4000-300 b.c. Colloidal metals have also been utilized since Ancient Roman times[39]. For example, colloidal gold has been employed in decorative objects like staining glass windows, ornaments, and beads. Michael Faraday prepared colloidal gold nanoparticles having been brightly colored in the mid-1850s. It is still in London in the Royal Institution’s Faraday Museum for display[39]. In the last two decades, noteworthy development has been made in the present area because of the evolution of novel instruments capable of manipulating and characterizing nanostructured materials. For the sake of a proper understanding of materials, one needs to know their basic anatomical structure. The requirement of determining the classes of atoms that form their building blocks and the routes by which such atoms are organized compared to one another is very important. Nanoparticle systems possess amazing photocatalytic, photo-electronic, photochemical,

and photo-physical systems. Nanoparticles possess a high surface-to-volume ratio which leads to electronic and structural alteration that in turn, bring about other qualities that eventually be different from that of the bulk material[40]. Their properties rely on the specific geometry of the particle and their surface characteristics. The extraordinary specifications of inorganic particles are belonging to their particular size being lesser than the scattering length or associated mean free path of their electrons(10-100nm).

Noble metals are highly stable when they are in bulk but once they are in the nanometer regime, they are exceptionally "active". At the nanometer range, particles possess high surface energy which turns them exceedingly localise, in addition, whole system goes through aggregation devoid of passivation or else protection of their specific surfaces. In the case of semiconductors, the optoelectronic properties of the nanoparticles altered with their nano crystallite size. This is because of the charge carriers associated with the quantum mechanical confinement which happens in the 1 to 10 nm arrangement.

Modified phase transformation behaviors, non-linear optical phenomena, and lower melting temperatures have been seen in nanoparticles[41]. An immensely lofty area of surface to the volume ratio has been achieved through the decline of particle size which leads to a surge in surface-specific active areas for chemical reactions as well as photon absorption to increase the reaction along with absorption capabilities. The enhancement in the surface area also enhances surface states, which alters the working of holes and electrons, and influences the dynamics of chemical reactions in semiconductors. For example, the constant associated with the charge carrier transfer ratio is comparatively elevated in nanoparticles as compared to the bulk material.

When the size of the particles declines under the first excitation state of the Bohr radius, a result, quantum size effect could happen because of the confinement of charge carriers[23]. Conduction and valence bands split by quantum size effect; resulting in discrete electronic states, after the size subordination of electronic and optical abilities develop into a much more pronounced state. Eventually, nanoparticles can create the possibility of electron transitions directly at the borderline of the crystals and perceive the required improvement of light absorption[42].

If there is more surface area then there are more active points and speedy chemical reactions, therefore enhancing the efficacy, on the other hand diminishing the cost of platforms and devices. Tuning of optoelectronic functionalities and properties can be done by simply controlling nanocrystal shape, size, and surface chemistry. In preparation of bimetallic colloidal nanoparticles and/or anisotropic catalysts, the size and shape of the nanoparticle can influence the activity along with the selectivity of the catalysts.

Despite the fact, the absorbance of the light rays is conceivably greater as compared to the particles, the nanoparticles react strongly and firmly with light waves. They exhibit different properties from the same materials when they are in bulk, which does not show quantum effects. Metallic nanoparticles exhibit localized external electromagnetic fields due to "plasma oscillations" which conduct strong resonances at particular wavelengths which relied on the particle shape, size as well as the local dielectric environment, which combined action are eventually responsible for the amazing colors of nanoscale materials. It is important to mention here, that the nanospheres exhibit only one plasmon band whereas anisotropic-shaped nanowires or nanorods show two plasmon bands; one related to light absorption along with the long axis of the nanoparticle and the other related to the light absorption along with the shorter axis of the nanoparticle.

The plasmon bands of nanoparticles are adjustable as a feature of nanoparticles aggregation state, shape, aspect ratio, size, and local environment[43]. Additionally, particles having sharp features, such as nanotriangles, nanocubes, nanorods, etc. are anticipated to act like optical antennae by focusing on the local field in a very small volume. Along with this, Resonant Rayleigh scattering [43] through metallic nanoparticles is an extraordinary characteristic of metals at the nanoscale and it is size and shape-dependent. Various colors of the nanoparticle can be achieved depending on the shape of the nanoparticle. Such features are prominent for biological applications when there is a requirement for nanoparticle infiltration, and tracking. Particles at the nanometer scale are mainly important because of their ability to adjust their properties(composition, functionalities, surface area, reactivity, shape, size) and direct them concerning their specific applications: monitoring/imaging site-specific targeted drug-delivery systems[44], targeted diagnostic studies, etc.

1.6. Silver nanoparticles

Metallic nanoparticles which contain beneficial metals like gold and silver show extraordinary physical, chemical, biological, and optical abilities which conceivably exploited in an extensive range of applications[45].

Figure 1.3: Numerous applications of Ag nanoparticles.

The silver nanoparticle is one of the leading nanomaterials widely used in numerous applications. Silver nanoparticles have been the topic of interest for scientists and researchers because of their distinctive qualities, which can be integrated into biosensor materials, composite fibers, anti-microbial applications, cryogenic super-conducting materials[46], electronic components, and cosmetic products as well.

Silver nanoparticles are associated with a wide range of applications including toxicity, electrical resistance, and specific surface plasmon resonance. Based on these qualities, exhaustive studies have been accomplished to observe their function as well as broad implementations in various functions namely bactericidal, fungicidal, anticancerous purposes, water treatment, designing of electronic devices, etc[47].

Silver nanoparticles possess extraordinary properties such as shape and size-dependent antimicrobial, anticancerous, optical, and electrical properties and because of this, it has been a matter of research. Over time, numerous synthesis techniques for the preparation of silver nanoparticles have been investigated, few remarkable examples include, electron irradiation, gamma irradiation, laser

ablation, microwave processing, biological synthetic methods, microwave processing, and chemical reduction methods[48]. Among all of the synthesis routes, the chemical reduction method has many advantages e.g. ease of preparation, ability to command the various conditions of reaction, inexpensive, high yield, etc. The chemical reduction method also enables alteration in the reactant's molar concentration, and proper seeding of reactants to synthesize silver nanoparticles with controlled particle shapes, sizes, and particle size distribution[49].

There are a wide variety of synthesis techniques for silver nanoparticles have been reported to date. A few of the remarkable methods include-

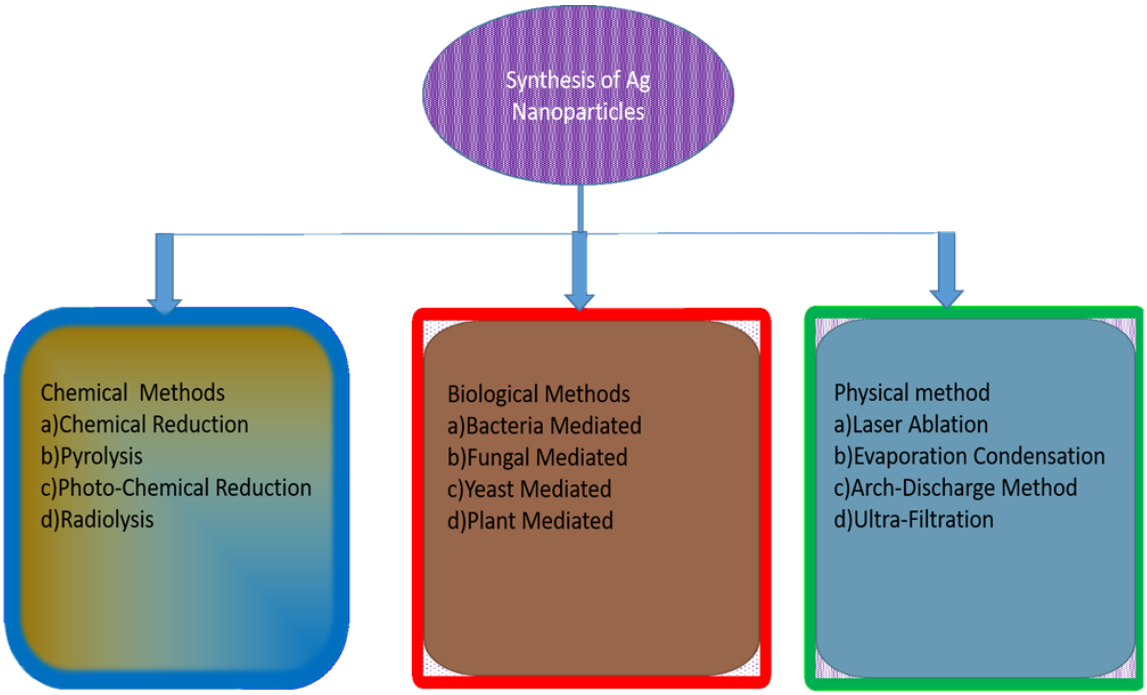

Figure 1.4: Various paths of synthesis of Ag nanoparticles.

1.6.1. Reducing agents associated with silver nanoparticle synthesis:

The picking of a proper reducing agent is a prominent factor, as the geometry and size distribution of the particle are completely dependent on the deportment of the particular agents responsible for synthesis. Consolidation of reductant brings about the reduction of the precursor agent of metal nanoparticles[50]. The salt responsible for metal reduction requires transformation attributed to the acuteness based on the involved reductants responsible for the redox potential of the metal nanoparticles. Few relevant reducing and stabilizing agents used in chemical-reduction of Ag nanoparticles are shown in table format in table no.1.1.

If the rate of the reaction is too fast during the synthesis process, fast preparation of metal nuclei will take place with high yield and it will result in very small particles. In addition, agglomeration of the particles occurs if the rate of the reaction is too slow. Furthermore, the selection of the reducing

agent is very important since it determines the reactivity, dispersibility, solubility, and stability as well as the shape and size of the particles at the time of the synthesis. Silver nanoparticles can be obtained through two prominent methods designated as the "bottom-up" and "top-down" processes[51]. The well-known "bottom-up" method can be achieved by electrochemical methods, sono-composition, and chemical reaction. The "top-down" technique deals with the mechanical grating of bulk metals and following its stabilization by utilization of colloidal protecting agents.

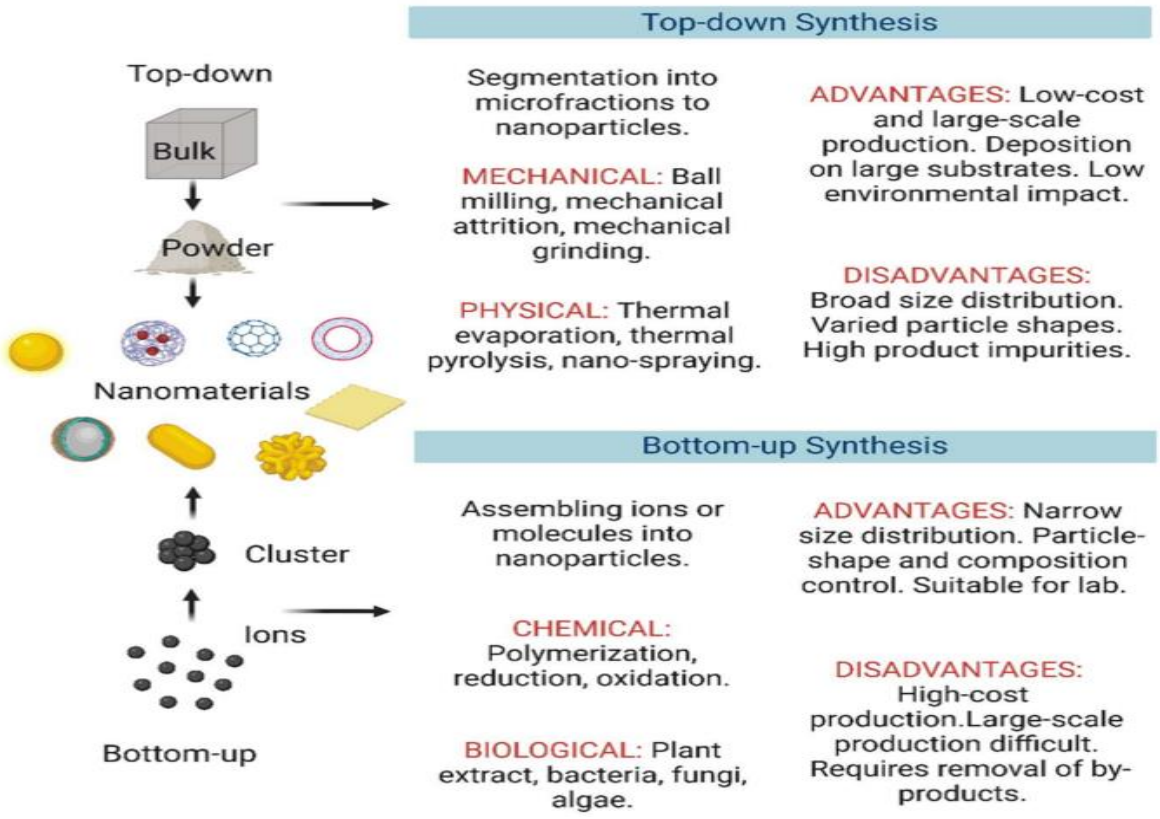

Figure 1.5: Variety of synthesis paths of Ag nanoparticles[52].

Table 1.1- Few relevant reducing and stabilizing agents used in chemical-reduction of Ag nanoparticles[46]

Reducing agents for synthesis	Silver precursor	Size(nm)
Trisodium-citrate	Trisodium -citrate	30-60
Ascorbic-acid	-	200-650
DMF	-	<25
$NaHB_4$	Surfactin	3-28
Trisodium-citrate(initial)+SFS(secondary)	Trisodium-citrate	<50

$NaHB_4$	DDA	~7
Dextrose	PVP	22±4.7
Paraffin	Oleylamine	10-14
Ethylene glycol	PVP	5-25
Hydrazine	-	2-10
Glucose	Gluconic acid	40-80
Ethylene glycol	PVP	50-115
Hydrazine-hydrate	AOT	2-5
m-Hydroxy benzaldehyde	SDS	15-260
Hydrazine-hydrate	AOT	<1.6

1.7. Core-shell nanoparticles

In the past few decades, advanced materials from core-shell nanoparticles are of wide and extensive technological and scientific interest due to their capabilities to finely tune their properties. Such particles can be conveniently modified in a manipulable manner to tailor their mechanical, optical, magnetic, electro-optical, thermal, electrical, and catalytic characteristics[53]. Core-shell nanomaterials comprised of a core configurational domain encapsulated by a shell domain. Both the shell and core can be made of numerous kinds of materials which includes metals, inorganic solids, and polymers. Furthermore, they also possess qualities that may be distinct from the shell or the core material[54]. The fabrication of the yolk-shell nanoparticles is fascinating for the researchers due to their appropriateness for various purposes. They are also interesting from scientific as well as fundamental points of view. They can be employed as model systems for the examination of factors that deals with the interaction between colloidal and their stabilization along with collecting information on the abilities of concentrated dispersions.

Till now, various ways have been evolved for the fabrication of core-shell nanomaterials namely the layer-by-layer method, sol-gel process, template-directed self-assembly, and encapsulation of nanomaterials through in situ polymerization[55]. Normally, the surfaces of nanoparticles have dangling bonds and they are afflicted to coalescence, oxidation, and other instabilities. Additionally, the quantum dots that are prepared in organic mixtures are not soluble in water, whereas biomedical applications require fine-quality water solvent quantum dots. Therefore, the problem is making the fine quality of hydrophobic quantum dots[56] soluble in water and also acute during bioconjugate reactions. So, materials are coated/encapsulated for numerous reasons. Coatings can transform a particle into compatible material, they can enhance mechanical, chemical, and thermal stability,

improve durability or lifetime, inhibit corrosion, and decrease friction, in other words, alter the whole biological and physicochemical qualities of the particles. Coatings can also inhibit the aggregation in a colloidal solution, as compared to bare particles, and gives a biofunctional platform for alteration and subsequent bioconjugation[57]. There are numerous benefits of coating of particles' surface with inert silica shells-can be employed as a stabilizing technique.

1.7.1. Silica-coating of nanoparticles

Most often, nanoparticles can not be employed directly because of a few limitations associated with them, namely hydrophobicity, toxicity, interactions with oxygen, etc. Such complications can most often be resolved by the intermediate shells or layers. Thus, derivatization is necessary most often before the utilization of nanoparticles for its potential application-either to activate(functionalize) surfaces or to stabilize functional cores. Silica is considerably the most adaptable and robust surface. It does not perturb redox reactions of the materials at the core surface because silica is chemically inert. Moreover, in the visible region silica layer is optically transparent, consequently, chemical reactions can be observed spectroscopically and as a result, the emitted light is not impeded[55]. Besides, the competence to command the consistency of the silica layer indicates that the bifurcation of the neighboring particles can be adjusted, and so the collective nature of the particles inside a nanostructure can be customized. The entire chemistry of such types of core/shell nanoparticles is renowned and additional functional groups can also be included to make it adaptable for desired applications.

Considerable work has been accomplished to observe the configuration of the silica shell on the outer surface of the nanoparticles. Silica-encapsulated colloidal nanoparticles are a class of nanomaterials broadly utilized in a variety of materials and colloidal sciences. Numerous coating techniques have been evolved for these samples. Such surface encapsulation permits embellishment of the intercommunication capabilities as well as compels it to disseminate colloidal particles in a wide class of solvent materials beginning from polar to apolar. Aforementioned Stober[58] (sol-gel) process of silica-coating by adding tetra ethoxy silane to the colloidal mixture of the nanoparticles into an ammonia/ethyl-alcohol solution mixture gives even layer after the development takes place close to molecular level. An outer silica encapsulation also provides opportunities for commanding the geometry of a particle. The external encapsulation by silica permits regulation of the optical abilities of the crystal structure and also the interaction potential of the nanoparticles. One of the broadly utilized coating methodologies by silica is the altering of colloid-particles which is stable merely in the liquid solution to ethyl-alcohol where the old traditional Stober method is performed[59].

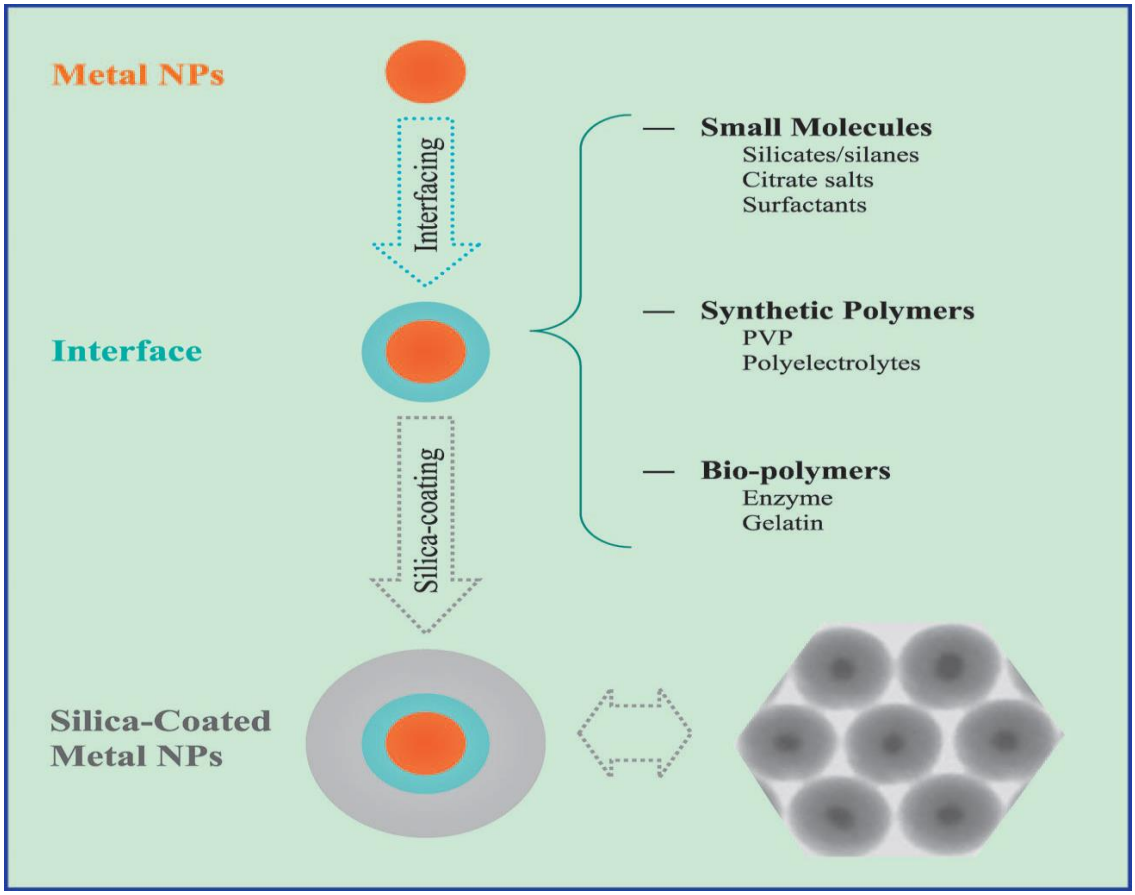

Figure 1.6: Encapsulation of silica on metal nanoparticles: metal nanoparticles obtained from various sources can be coated with biocompatible material silica by the specific sol-gel process[60].

1.8. Statement of the problem

After reaching the nanoscale, particles of silver have a miraculous change in physicochemical properties and they turn out to have exceptional biological activities. The uniqueness of silver nanoparticles broadens their pertinency in anti-bacterial, anti-fungal, and anti-cancer therapy[61].

Amid numerous kinds of nanoparticles accessible at the current time, nanoparticles having core-shell architectonic, possess astounding properties, collaborating multiple functionalities into a sole hybrid nanocomposite. The assorted pattern of efforts was given for the study of the anti-cancerous, anti-bacterial, and anti-fungal effectiveness of silver nanoparticles. Still, scant or no attention is given to the comparative study of silver and yolk-shell silver-silica nanoparticles. Alteration in silver nanoparticle's functionality with silica gives the nanoparticle idiosyncratic effects, because of the biocompatibility, hydrophilicity, and optical transparency along with thermal and chemical stability of the silica; unexpectedly in aqueous-media also. The flexibility of silica in surface moderation as well as in synthesis demeanor offers an outstanding edge to the employment of this material for therapeutic purposes because for the applicability in medicine, immunocompatibility is a prerequisite condition, that will clinch the non-toxic nature of the material.

Cancer is an ambidextrous malady exceptionally unpredictable in its unveiling, evolution, and aftermath. There are numerous drugs available for cancer- therapy but most of them are inefficacious to set foot on-target site in adequate concentrations and systematically deploy the desired pharmacological upshot without triggering irreversible undesired harm to normal cells and tissues.

There are certain limitations associated with conventional chemotherapeutic drugs. Silver nanoparticles have the prospective to circumvent assorted drawbacks of typical therapeutic implementations. Tailor-made silver nanoparticles coated with specific biocompatible nanomaterial can target cancerous cells in a foreseeable demeanor, because these can be specifically intended for expanded drug loading, upgraded half-life inside the body, unflappable release as well as selective distribution by altering their size, composition, surface chemistry, and morphology. In the same manner, antimicrobial chemotherapy also demands attention because lately, resistance to antibiotics by disease engendering fungus and bacteria has been growing at a breathtaking pace and thus became major trouble. Bacterial and fungal infections are colossal causes of morbidity and mortality[62]. To overcome this resistance mechanism of pathogenic microbes, consideration has been given to silver nanoparticles as an encouraging tool since it works miraculously on a span of targets in contrast to antibiotics, which have a particular site of execution. Silver nanoparticles showcased magnificent outcomes in detecting and remedying microbial infections by enabling the pick out of target pathogens, reactive and combinatorial freightage of antibiotics, successful antibacterial vaccination as well as swift detection of pathogens[15].

In recent years, a number of immunoassay-techniques for the diagnosis of different tumor markers for more effective governance of cancer have been investigated. A sailing way for the observation of cancer has been the evaluation of serum tumor markers. Gradually, electrochemical immunoassay has acquired acceptance and therefore broadly utilized to detect tumor markers because of the intrinsic benefits such as lofty selectivity, sensitivity, suitable label-free manipulation, low cost, minute size, and very fast analysis[15]. There exist numerous kinds of electrochemical immunosensor built upon conductometry, amperometry, potentiometry, and electrochemical-impedance-spectroscopy [15]. Evolving a CEA (carcinoembryonic-antigen) immunosensor having good selectivity and sensitivity but lacking a complex fabrication procedure still fascinates researchers.

Based on the above-explained consideration current thesis describes the preparation of silver nanoparticles along with their coating by silica, followed by the characterization of both the nanoparticles, for their applications in therapy and detection purposes.

In view of this issue, output in the current thesis has been given with the below-mentioned aims-

- Preparation of silver nanoparticles by Turkevich procedure by employing chemical reduction method

- Coating of silver nanoparticles with silica through modified Stober method.
- Characterization of both the nanoparticles to observe their spectroscopic, elemental, and morphologic properties.
- Fabrication of electrochemical immunosensor for the detection of carcinoembryogenic antigen (CEA).
- To examine the antibacterial, antifungal as well as anticancerous properties of both the synthesized nanoparticles.

References

1. Mansoori GA. An Introduction to nanoscience and nanotechnology: Springer Soil Biology series. 2017;48:1-16. doi:10.1007/978-3-319-46835-8
2. Burdușel AC, Gherasim O, Grumezescu AM, Mogoantă L, Ficai A, Andronescu E. Biomedical applications of silver nanoparticles: an up-to-date overview. Nanomaterials. 2018;8(9):1-24. doi:10.3390/nano8090681
3. Fan Y, Shi S, Ma J, Guo Y. A paper-based electrochemical immunosensor with reduced graphene oxide/thionine/gold nanoparticles nanocomposites modification for the detection of cancer antigen 125. Biosens Bioelectron. 2019. doi:10.1016/j.bios.2019.03.063
4. Liu H, Wu X, Zhang X, Burda C, Zhu J jie. Gold nanoclusters as signal amplification labels for optical immunosensors. J. Phys. Chem. C: 2012:**2548**-2554. doi.org/10.1021/jp206256j
5. Zhu L, Xu L, Jia N, et al. Electrochemical immunoassay for carcinoembryonic antigen using gold nanoparticle-graphene composite modified glassy carbon electrode. Talanta. 2013;116:809-815. doi:10.1016/j.talanta.2013.07.069
6. Chen W, Peng J, Ye J, Dai W, Li G, He Y. Aberrant AFP expression characterizes a subset of hepatocellular carcinoma with distinct gene expression patterns and inferior prognosis. J Cancer: 2020;11. doi:10.7150/jca.31435
7. Fanelli GN, Naccarato AG, Scatena C. Recent advances in cancer plasticity: cellular mechanisms, surveillance strategies, and therapeutic optimization. Front Oncol. 2020;10(April):1-10. doi:10.3389/fonc.2020.00569
8. Dolscheid-pommerich RC, Manekeller S, Walgenbach-brünagel G. AFP in gastrointestinal cancer using LOCI ^{TM} -based assays. J Cancer: 2017;360. doi:10.21873/anticanres.11329
9. Song Z, Yuan R, Chai Y, Yin B, Fu P, Wang J. Multilayer structured amperometric immunosensor based on gold nanoparticles and prussian blue nanoparticles / nanocomposite functionalized interface. Electrochimica Acta : 2010;55:1778-1784. doi:10.1016/j.electacta.2009.10.067

10. Hong H. Clinical characteristics of novel coronavirus disease 2019 (COVID-19) in newborns, infants and children. Pediatr Neonatol: 2020; (Apr);61(2):131-132. doi:10.1016/j.pedneo.2020.03.001
11. Lippi G, Henry BM. Chronic obstructive pulmonary disease is associated with severe coronavirus disease 2019 (COVID-19). Meta -Analysis> Respir Med:2020; (jun);167:105941: doi:10.1016/j.rmed.2020.105941
12. Devi JS, Bhimba BV. Antibacterial and antifungal activity of silver nanoparticles synthesized using hypnea muciformis. Biosci Biotechnol Res Asia. 2014;11(1):235-238. doi:10.13005/bbra/1260
13. Dey A, Dasgupta A, Kumar V, Tyagi A, Verma AK. Evaluation of the antibacterial efficacy of polyvinylpyrrolidone (PVP) and tri-sodium citrate (TSC) silver nanoparticles. Int Nano Lett. 2015;5(4):223-230. doi:10.1007/s40089-015-0159-2
14. Sintubin L, Verstraete W, Boon N. Biologically produced nanosilver : current state and future perspectives. Biotechnol Bioeng: 2012;(Oct):1-15. doi:10.1002/bit.24570
15. Kasithevar M, Periakaruppan P, Muthupandian S, Mohan M. Antibacterial efficacy of silver nanoparticles against multi-drug resistant clinical isolates from post-surgical wound infections. Microb Pathog. 2017;107:327-334. doi:10.1016/j.micpath.2017.04.013
16. Huang X, Deng X, Wu D. Reagentless amperometric immunosensor for a -1-fetoprotein based on assembly of nano-Au@SiO_2 composite. Analytical Methods : 2012:3575-3579. doi:10.1039/c2ay25778e
17. Cho I hoon, Lee J, Kim J, et al. Current technologies of electrochemical immunosensors : perspective on signal amplification. Sensors. 2018:1-18. doi:10.3390/s18010207
18. Lokina S, Stephen A, Kaviyarasan V, Arulvasu C, Narayanan V. SC.Cytotoxicity and antimicrobial activities of green synthesized silver nanoparticles: Eur J Med Chem. 2014. doi:10.1016/j.ejmech.2014.02.010
19. Khan S, Hossain MK. 2-Classification and properties of nanoparticles: nanoparticle-based polymer composites; 2022.(15-54).doi.org/10.1016/B978-0-12-824272-8.00009-9
20. Pedley JT. Current research in fluid mechanics. Journal of Fluid Mechanics. 2016:17-20; doi:10.1007/978-3-319-31063-33
21. Benelmekki M. An introduction to nanoparticles and nanotechnology. Des Hybrid Nanoparticles. 2014; 1-1 ;1-14: doi:10.1088/978-1-6270-5469-0ch1
22. Ealias AM, Saravanakumar MP. A review on the classification, characterisation, synthesis of nanoparticles and their application. IOP Conf Ser Mater Sci Eng. 2017;263(3). doi:10.1088/1757-899X/263/3/032019

23. Goyal RK. Nanomaterials and nanocomposites: synthesis, properties, characterization techniques, and applications.Crc Press. 2018:1-10; doi:10.1201/9781315153285-1
24. Abbas M, Yan K, Li J, Zafar S, Hasnain Z, Aslam N. Agri-nanotechnology and tree nanobionics : augmentation in crop yield , biosafety , and biomass accumulation. Front Bioeng Biotechnol: 2022;10(April):1-13. doi:10.3389/fbioe.2022.853045
25. Maiyalagan T. Synthesis , characterization and electrocatalytic activity of silver nanorods towards the reduction of benzyl chloride. Applied Catalysis A: General: 2008;340:191-195. doi:10.1016/j.apcata.2008.02.016
26. Wang H, Wang Y, Zhang Y, et al. Photoelectrochemical immunosensor for detection of carcinoembryonic antigen based on 2D TiO 2 nanosheets and carboxylated graphitic carbon nitride. Nat Publ Gr. 2016;(March):1-7. doi:10.1038/srep27385
27. Mansour HH, Eid M, El-Arnaouty MB. Effect of silver nanoparticles synthesized by gamma radiation on the cytotoxicity of doxorubicin in human cancer cell lines and experimental animals. Hum Exp Toxicol. 2018;37(1):38-50. doi:10.1177/0960327116689717
28. Sengupta A, Kumar Sarkar C. Introduction to nano: basics to nanoscience and nanotechnoogy. Springer.;2015.http://choicereviews.org/review/10.5860/CHOICE.195358%0Ahttp://link.springer.com/10.1007/978-3-662-47314-6
29. Dadashpour M, Firouzi-Amandi A, Pourhassan-Moghaddam M, et al. Biomimetic synthesis of silver nanoparticles using Matricaria chamomilla extract and their potential anticancer activity against human lung cancer cells. Mater Sci Eng C. 2018;92(June):902-912. doi:10.1016/j.msec.2018.07.053
30. Navya PN, Kaphle A, Srinivas SP, Bhargava SK, Rotello VM, Daima HK. Current trends and challenges in cancer management and therapy using designer nanomaterials. Nano Converg. 2019;6(1). doi:10.1186/s40580-019-0193-2
31. Makvandi P, Wang C yu, Zare EN, Borzacchiello A, Niu L na, Tay FR. Metal-Based Nanomaterials in Biomedical Applications: Antimicrobial Activity and Cytotoxicity Aspects. Adv Funct Mater. 2020;30(22). doi:10.1002/adfm.201910021
32. Simon M, Stefan N, Plückthun A, Zangemeister-Wittke U. Epithelial cell adhesion molecule-targeted drug delivery for cancer therapy. Expert Opin Drug Deliv. 2013;10(4):451-468. doi:10.1517/17425247.2013.759938
33. Tsekenis G, Chatzipetrou M, Massaouti M, Zergioti I. Comparative assessment of affinity-based techniques for oriented antibody immobilization towards immunosensor performance optimization. Journal of sensors. 2019; doi.org/10.1155/2019/6754398
34. Suriati G, Mariatti M, Azizan A. Synthesis of silver nanoparticles by chemical reduction method:

effect of reducing agent and surfactant concentration. Int J Automot Mech Eng. 2014;10(1):1920-1927. doi:10.15282/ijame.10.2014.9.0160

35. Trindade EKG, Silva BVM, Dutra RF. A probeless and label-free electrochemical immunosensor for cystatin C detection based on ferrocene functionalized-graphene platform. Biosens Bioelectron. 2019. doi:10.1016/j.bios.2019.05.016
36. Wongkaew N, Simsek M, Griesche C, Baeumner AJ. Functional nanomaterials and nanostructures enhancing electrochemical biosensors and lab-on-a-chip performances : recent progress , applications , and future perspective. Chem Rev. 2018;119:120-194. doi:10.1021/acs.chemrev.8b00172
37. He C, Lu J, Lin W. Hybrid nanoparticles for combination therapy of cancer. J Control Release. 2015;219:224-236. doi:10.1016/j.jconrel.2015.09.029
38. Bheemidi VS, Tiruckovela M, Chettipalli ND, Yanamadala SV. Novel applications of nanotechnology in life sciences. J Bioanal Biomed. 2011;3(3):1-4. doi:10.4172/1948-593X.R1-001
39. Hunyadi Murph S. Metallic and hybrid nanostructures: fundamentals and applications, in applications of nanomaterials. Nanomaterials and Nanostructures:2012;(January 2012).doi.osti.gov/biblio/1097597
40. Sannegowda LK. Metal nanoparticles for electrochemical sensing applications. Handb Nanomater Sens Appl. 2021:589-629. doi:10.1016/B978-0-12-820783-3.00001-4
41. Kumar CSSR: Raman spectroscopy for nanomaterials characterization. Springer: 2012: http/link.springer.com/book/10.1007/978-3-642-20620-7
42. Alqudami A, Annapoorni S. Fluorescence from metallic silver and iron nanoparticles prepared by exploding wire technique. Plasmonics: 2007:5-13. doi:10.1007/s11468-006-9019-2
43. Tsuji M, Gomi S, Maeda Y, et al. Rapid transformation from spherical nanoparticles, nanorods, cubes, or bipyramids to triangular prisms of silver with PVP, citrate, and H 2O 2. Langmuir. 2012;28(24):8845-8861. doi:10.1021/la3001027
44. Firer MA, Gellerman G. Targeted drug delivery for cancer therapy: the other side of antibodies. J Hematol Oncol. 2012;5(1):1. doi:10.1186/1756-8722-5-70
45. Hagarová I, Nemček L. Application of metallic nanoparticles and their hybrids as innovative sorbents for separation and pre-concentration of trace elements by dispersive micro-solid phase extraction: a minireview. Front Chem. 2021;9(May):1-9. doi:10.3389/fchem.2021.672755
46. Iravani S, Korbekandi H, Mirmohammadi S V., Zolfaghari B. Synthesis of silver nanoparticles: chemical, physical and biological methods. Res Pharm Sci. 2014;9(6):385-406.pubmed.ncbi.nlm.nih.gov/26339255/

47. Abdel-Fattah WI, Ali GW. On the anti-cancer activities of silver nanoparticles. J Appl Biotechnol Bioeng. 2018;5(1):43-46. doi:10.15406/jabb.2018.05.00116
48. Quintero-Quiroz C, Acevedo N, Zapata-Giraldo J, et al. Optimization of silver nanoparticle synthesis by chemical reduction and evaluation of its antimicrobial and toxic activity. Biomater Res. 2019;23(1):1-15. doi:10.1186/s40824-019-0173-y
49. Iravani S, Korbekandi H, Mirmohammadi S V., Zolfaghari B. Synthesis of silver nanoparticles: chemical, physical and biological methods. Res Pharm Sci. 2014;9(6):385-406. pubmed.ncbi.nlm.nih.gov/26339255/
50. Shenava A. Synthesis of silver nanoparticles By chemical reduction method and their antifungal activity. Int Res J Pharm. 2013;4(10):111-113. doi:10.7897/2230-8407.041024
51. Baig N, Kammakakam I, Falath W, Kammakakam I. Nanomaterials: a review of synthesis methods, properties, recent progress, and challenges. Mater Adv. 2021;2(6):1821-1871. doi:10.1039/d0ma00807a
52. Harish V, Ansari M, Tewari D, Gaur M, Yadav AB. Nanoparticle and nanostructure synthesis and controlled growth methods. Nanomaterials (Basel): 2022:1-30.doi: 10.3390/nano12183226
53. Singh P, Katkar PK, Patil UM, Bohara RA. A robust electrochemical immunosensor based on core-shell nanostructured silica-coated silver for cancer (carcinoembryonic-antigen-CEA) diagnosis. RSC Adv. 2021;11(17):10130-10143. doi:10.1039/d0ra09015h
54. Raveendran J, Docoslis A. Detection and quantification of toxicants in food and water using Ag–Au core-shell fractal SERS nanostructures and multivariate analysis. Talanta. 2021;231(March):122383. doi:10.1016/j.talanta.2021.122383
55. Bastakoti BP, Guragain S, Yusa SI, Nakashima K. Novel synthesis route for Ag@SiO 2 core-shell nanoparticles via micelle template of double hydrophilic block copolymer. RSC Adv. 2012;2(14):5938-5940. doi:10.1039/c2ra20316b
56. Gerion D, Pinaud F, Williams SC, et al. Synthesis and properties of biocompatible water-soluble silica-coated CdSe/ZnS semiconductor quantum dots. J Phys Chem B. 2001;105(37):8861-8871. doi:10.1021/jp0105488
57. Tan W, Wang K, He X, et al. Bionanotechnology based on silica nanoparticles. Med Res Rev. 2004;24(5):621-638. doi:10.1002/med.20003
58. Kobayashi Y, Katakami H, Mine E, Nagao D, Konno M, Liz-Marzán LM. Silica coating of silver nanoparticles using a modified Stöber method. J Colloid Interface Sci. 2005;283(2):392-396. doi:10.1016/j.jcis.2004.08.184
59. Wong YJ, Zhu L, Teo WS, et al. Revisiting the Stöber method: inhomogeneity in silica shells. J Am Chem Soc. 2011;133(30):11422-11425. doi:10.1021/ja203316q

60. Liu S, Han MY. Silica-coated metal nanoparticles. Chem - An Asian J. 2010;5(1):36-45. doi:10.1002/asia.200900228
61. Kovács D, Igaz N, Gopisetty MK, Kiricsi M. Cancer therapy by silver nanoparticles: fiction or reality? Int J Mol Sci. 2022;23(2). doi:10.3390/ijms23020839
62. Prasher P, Sharma M, Mudila H, et al. Emerging trends in clinical implications of bio-conjugated silver nanoparticles in drug delivery. Colloids Interface Sci Commun. 2020;35(December 2019):100244. doi:10.1016/j.colcom.2020.100244

Chapter 2

Coated silver nanoparticles: Synthesis methods and applications

Chapter 2: Coated silver nanoparticles: Synthesis methods and applications

2.1. Introduction

The evolution of humans has been closely intertwined with the history and manipulation of materials. From the ancient times, nature provided humans with an amazing selection of exceptional materials. However, surprisingly, in the modern world, their abundance and assortment are still limited. To address this, researchers are continuously working to discover innovative and improved materials that have the potential to ensure a higher and more sustainable standard of living for future generations. Thenceforth, a wide variety of captivating nanoscale materials have appeared ranging from metallic, insulators, polymers, semiconductors, and composite nanostructures[1].

Coated nanoparticles are combinations of nano-sized elements differing in their composition and category, such as nanoplates, nanotubes, nanoparticles, and nanofibers. These nanoparticles often contain nanostructures and are typically within the nanometer size range as well. Composite nanoparticles are an important part of nanotechnology because they are formulated by combining two or more multifunctional dispersed nano object possessing the same scale at the nano level. This class of nanoparticles can be created by merging two or more than two organic components, two or additional inorganic components, or at the minimum one of both types of components[2]. Conventionally, such nanoparticles are attained by establishing a satellite-like structure which is the coagulation of spherical types of particles having different composition and size, where the larger component behaves like a central platform and firmly grasp the smaller particles to create unitary nano object and they exhibit synergistic properties of both particles. Coated silver nanoparticles are combinations of two or more than two materials created by a synergistic combination of both materials at the nanometer scale. From the morphological perspective, coated nanoparticles can be categorized into Janus-type of nanostructures[3] by merging two (or more than two) components of similar size, core-shell-type structures, and nanostructures with nanocomponents that are either deposited or encapsulated on the surface. The combination of various components in the same nanostructures sums up the properties of separate components and at the same time provides the composite structure having novel properties as a consequence of their synergistic effect. It is noteworthy to mention that coated nanoparticles and nanosystems are not exclusively needed for biology and medicine, green chemistry, sensor technology, and other fields, additionally, these are also favorable for the advent of novel potent analytical procedures[4] worthy of overcoming problems of identification

and detection of impurities, poor water solubility, immunogenicity[5], low bioavailability, high toxicity etc. Analysis of various research articles dedicated to coated nanoparticles revealed that the horizon of their application is often designated by the qualities of one of the components[6]. Other components either increase the functional abilities in the same area or elevate the overall system efficiency. Such as nanostructures having magnetic nanoparticles can be manipulated by an outer magnetic field, which is employed as contrast agents in targeted drug delivery[7] or for magnetic resonance imaging (MRI); whereas coated nanoparticles based on magnetic nanoparticles[8] along with the incorporation of luminescent nanostructures[9] can be used to envision the specific site of delivery. In this experiment, core material determines the properties whereas shell material improves the efficiency[10].

2.2. Coated silver nanoparticles and structures

Hybridization of the noble metal nanomaterial with another stabilizing material is very promising to ameliorate colloidal stability and dispersibility[11]**.** Metal nanoparticles have an inclination towards aggregation in aqueous media. Thus, the advancement of proper synthesis methods to assemble metal nanoparticles along with other stabilizing materials is in need of metal-nanoparticle-based applications,[12] as shown in Fig. 1.

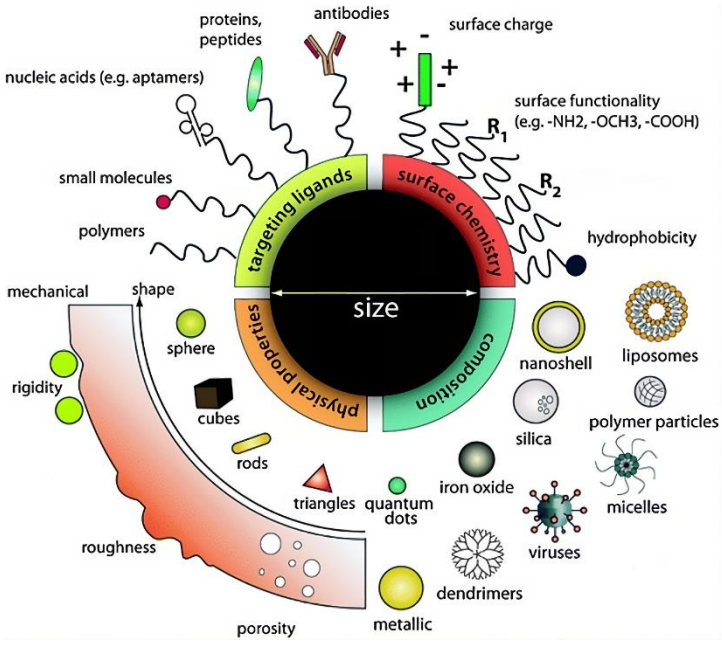

Figure 2.1: Principal elements involved in designing coated nanoparticles[13].

Recently, restrained synthesis of Ag nanoparticles (AgNPs) has gained much attention because of their successful applications in catalysis, surface-enhanced Raman spectroscopy, biological and chemical sensors[14], and a number of other fields as well. Since ages ago, people have used Ag as a disinfectant and antimicrobial agent, as it is documented in a book of Chinese herbal medicine named Compendium of MateriaMedica[15].

In the past, due to the excellent optical properties (plasmonic resonance) of Ag nanostructures, it has been an active area of research[16]. These qualities of AgNPs greatly rely on the composition, size, and shape of the silver. Control over the shape of the nanoparticle is very important to amend the optical significance of the resulting nanostructures. Among all of the available techniques, the most significant method is the chemical method[17].

A group of researchers prepared a well-controlled Ag nanostructure through ethylene glycol (EG) by varying the molar ratio of silver ions and stabilizer, reaction temperature, precursor concentration as well as by adding helper agents[18]. Nevertheless, during these procedures, the reaction conditions are very complicated and often difficult to control.

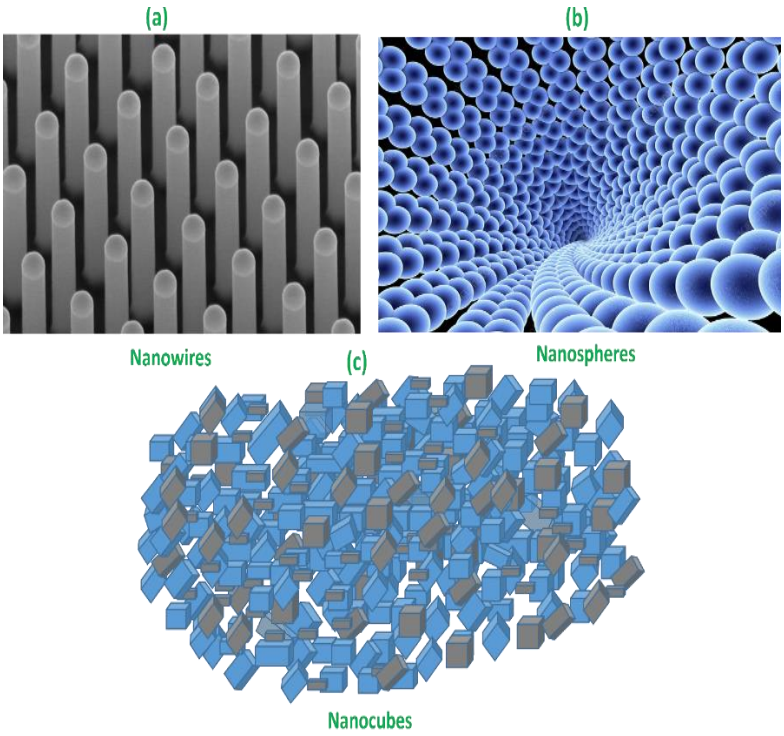

Figure 2.2: Various nanostructures of coated AgNPs. Representative images show (a) nanowires, (b) nanospheres, and (c) nanocubes of coated AgNPs (blue-AgNPs, grey-coated AgNPs).

One of the groups of scientists formed Ag nanowires by catching benefits of the collectively adsorption on the facets i.e. (100) of PVP. The final products are mainly nanospheres, if PVP is added in low amounts or absent. They also discovered that AgNPs having irregular shapes were produced in the presence of diminished molecular weight of the PVP. It is also found that the morphology of AgNPs can also be controlled through varying the molecular weight[19].

The role of different ions also plays a great role in the morphology of the Ag nanostructure. By adding Br^-, Fe^{3+} and Cl^- helps in the synthesis of Ag nanowires, nanocubes (shapes are displayed in Fig. 2) and right bipyramids respectively[20]. If the growth process and reactant conditions are not properly controlled then the attained Ag nanostructures are in very low amount and huge amounts of byproducts are also yielded[21]. Therefore, there is an immense need for a facile and reliable technique for the preparation of Ag nanostructures having the desired shape and size in a large amount.

Lee and co-workers[22] discussed two different types of unconventional processes counting template-based technique and lithography to synthesize metallic nanostructure with high surface area. A wide variety of nanostructures with particular sizes and shapes and various compositions can be made easily by utilizing templates such as polymer membranes etched through ion-tracking or anodized nanoporous alumina membranes[23]. Despite the fact that such unconventional techniques are very efficient; their post-processing is relatively complicated, which can influence the purity of end products.

2.3. Different routes and methods involved in the synthesis of core-shell Ag nanostructures

Basically, there are three main routes of the synthesis of core-shell nanoparticles until now.

2.3.1. Aggregation

This method is actually an expansion of the 'bottom-up' synthetic scheme which implies the fabrication of nanomaterials and then their aggregation to develop a single structure[8]. This synthesis method does not only form nanoparticles but also involves in the subsequent emergence of complex multicomponent nanomaterials above aggregation of the foremost material to form the final core-shell nanoparticles[24].

2.3.2. Parallel

The second approach involves the parallel synthesis of coated nanoparticles[25] and nanostructures to produce the composite beyond the pretreatment of the components.

2.3.3. Sequential

The most famous third method involves a sequence of reactions, that results in multilayer film structures, core-shell nanostructures, or nanoparticles in the matrix notch[26].

2.4. Modes of synthesis of coated Ag nanostructures

The synthesis of complex nanostructure that have upscale functions by a multistep method using chemicals is a hotspot of research[27]. In this part of the review, we will discuss the three illustrative methods to synthesize Ag nanostructures having well-controlled shapes and sizes, combined with double-reductant technique, etching method, and fabrication of core-shell nanostructures[28].

All three techniques can not only synthesize properly shaped Ag nanostructure, but it is also beneficial for numerous applications by showing extraordinary optical properties, useful in localized surface plasmon resonance (LSPR) effect and surface-enhanced Raman scattering (SERS), this nanostructure also possesses excellent anti-bacterial, anti-fungal, and anti-cancerous purposes[29]. They are also extremely useful for the detection of various diseases. Through the mechanism of preparation of hybrid Ag nanostructures by double-reductant technique, we can synthesize affirmative surface of Ag nanocrystals by numerous reductants. These can be utilized to synthesize complex nanostructures like nanoflags having an ultranarrow resonant band and a few other nanostructures whichever are tedious to prepare by using other techniques[30]. By using the etching method; shape-controlled hollow nanostructures and nanoflower preparation are possible[31].

2.4.1. Etching method

Adjusting the size of nanostructures is crucial to tailor their optical and other properties. Furthermore, nanoflowers or nanostars[32] are the kind of nanostructure, that possess sharp horns so they can concentrate electromagnetic-field approaching their tips, which leads to a notable SERS effect. Nowadays, the increasement of SERS enhancement controlled shape and size mediated synthesis of Ag nanostructure has attracted the attention of researchers[33]. Etching techniques are also used to create advanced nanostructures, such as hollow nanostructures or hot spots[34]. Various etchants, including $Fe(NO_3)_3$ or NH_4OH, hydrogen peroxide (H_2O_2), can be employed to alter the shape of Ag nanostructures, and sometimes NH_4OH is combined with H_2O_2. $Fe(NO_3)_3$ or NH_4OH have a significant role in the synthesis of Au nano boxes[35]. This method involves formation of Au/Ag nano boxes by layering Au onto the outer surface of Ag

nanocubes, followed by etching away the Ag layer with $Fe(NO_3)_3$ or NH_4OH[36]. By subsequently adding NH_4OH or $Fe(NO_3)_3$, the nano boxes can be converted into nanoframes and nanocages[102].

One notable benefit of this technique is the ability of NH_4OH or $Fe(NO_3)_3$ to effectively remove Ag from the outer surface of the Au/Ag nanoboxes, which leads to precise control over the broadness of nanocages, which is challenging to achieve using other methods[2].

2.4.2. Hydrogen peroxide

In the 1950s, H_2O_2 was used for etching pits in metals, and it played a crucial role in determining the mechanical properties of crystalline materials[37]. Additionally, H_2O_2 can also be utilized as an effective etchant to diffuse metallic silver. Few nanostructures of Ag cannot be simply synthesized in large amounts in mono-dispersed sizes; to overcome this problem etching techniques can be employed to control the shape/size of AgNPs[38]. Out of numerous shapes of AgNPs, triangular and nanoprisms have gained much interest because of their extraordinary optical qualities and other related properties. M'etraux and Mirkin[23] discovered an innovative reduction route by employing $AgNO_3$/$NaBH_4$/polyvinyl pyrrolidone/tri-sodium citrate(Na_3CA)/H_2O_2 to synthesize Ag nanoprisms; that is an amazing development in the controlled size of Ag nanostructure. They found that in the absence of H_2O_2, the end products were nanospheres, highlighting the significant role of H_2O_2 in the formation of Ag nanoprisms. Subsequently, Zhang et al.[39] have given a detailed explanation of the prominent role played by H_2O_2 in this very reaction mechanism. They showed that H_2O_2 efficiently eliminates unstable nanoparticles in the stage of nucleation and avail the anisotropic structure formation[40], which leads to the transformation of silver nanoplates[41]. However, it was observed that when the concentration of H_2O_2 is extremely high, the produced nanoprisms may disappear due to excessive etching. Tsuji et al. further promoted this study by focusing their work on the role of time-dependent SPR band to increase the rate of etching from prism to sphere[42]. The considerable difference between the Zhang and Tsuji is that the reduction of Ag^+ ion and etching of Ag nanostructure can occur simultaneously, during the reaction process. On the other hand, Tsuji's approach involves the final breaking up of Ag nanowires into Ag^+ ions in the first step followed by the reduction of Ag^+ ions into Ag^o. They also successfully transformed nanocubes and nanobipyramids into Ag nanoprisms, representing a significant improvement in synthesizing large quantities of Ag nanoprisms from various Ag nanostructures. Metallic nanoparticles with hollow nanostructure, e.g., frames and cages having higher surface area gained the researchers'

interest due to their remarkable catalytic, optical[43], and electronic properties and their highly adjustable localized surface plasmon resonance nature[44]. In a related development, Zhang et al. introduced an innovative technique based on the etching of H_2O_2 to synthesize Au nanoboxes.

Silver nanoboxes can be diversified into gold nanoboxes according to a set of chemical reactions. Through titration of Ag nanocubes by aqueous $HAuCl_4$; Au-Ag alloy nanoboxes can be synthesized. The thickness of nanoboxes can be controlled by the aqueous $HAuCl_4$; which causes the redshifting of LSPR peaks. Further with the help of H_2O_2 etching, Ag atoms can be eliminated from the prepared nanoboxes. A similar method was used for the preparation of gold nanoframes via decahedral AgNP[45]. In this method, by tuning the concentration of deposited gold; the broadness of the frames was controlled. Later, they tried to synthesize similar nanoframes by utilizing other Ag nanostructures. All these results showed that merely nanostructure's having (111) facets i.e. icosahedra and nanorods might be employed for the synthesis of nanoframes. They showed that gold tends to stick onto the (111) facets, which are more amenable to the preparation of nanocoatings or nanocages.

The etching method is a proficient technique to synthesize hollow nanostructure with controlled size and shape. It can also be useful for making flower-like Ag nanostructures and can be also beneficial to making the nanocrystal's surface rough; because it has been found that the nanostructure possessing gaps or spiked edges can increase the intensity of SERS[45,46]. The inherent applications of SERS substrates in various fields suggest extensive potential for utilizing the etching method in this area.

2.4.3. Double-reductant method

Every reductant exhibits its unique reducibility, playing a significant role in the shape and size control of nanostructures. Furthermore, desirable facets of nanocrystals can be decided by the reductants employed[15]. Few of the reductants have the tendency to favor the growth of (100) facets, while others promoting (110) or else (111) facets. Accordingly, selecting particular reductants at each step, it becomes possible to craft tailor-made complex nanostructures, a task that is not easily achievable otherwise. Consequently, in this section of the article, we will discuss the reductants used for controlled size and shape-mediated synthesis of a nanostructure. Liz and Marzan et al.[47] used DMF, a well-known organic solvent and very efficient reductant. They utilized DMF for the reduction of silver nitrate, to synthesize Ag nanostructure that creates a novel pathway for size and shape-controlled preparation.

Fabrication of nanowires, nano prisms, and nanospheres can be possible through the reduction of AgNO3 with the help of DMF, while PVP plays the role of second reductant in this process. Lu et al. explored the synthesis of 20 to 50 nm sized nanoplates by using the various concentration of PVP and DMF[48]. Hexagonal, triangular, cubes, bipyramids, pentagonal, icosahedrons as well as decahedrons shape of the nanostructure can be prepared by the use of DMF[49,42,36,50]. Tsuji and co-workers prepared triangular as well as octahedra nanostructures by the reduction of $AgNO_3$ in the presence of EG followed by the shape-transformation of these nanoparticles by DMF[42]. Later these researcher's synthesized nanoflags of Ag by utilizing a 2-step process through making Ag nanorods in EG as seeds and then preparing Ag nanoflags into DMF. The consecutive reductant $AgNO_3$ is employed for whole reduction process in two steps. In the initial step, nanorods of silver were prepared by the reductant $AgNO_3$ in EG via PVP, further it was diluted in DMF for seeding. In the next step, solution containing seed was combined in DMF solution having both - PVP as well as $AgNO_3$. Gradually, with the enhancement of the concentration of $[AgNO_3]_2$/[$AgNO_3]_1$, various structures of silver were detected. They elucidated the advancement of the transformation of silver nanoflags[15] from nanorods. In the next step, several plates were formed shaped in trapezoid form from the facet of nanorods of silver and later develop into twin plates having a triangular shape. In the later step, the triangular flags of Ag were reshaped in tetrahedral Ag flags through two determined tracks[51]. Hence double reductant technique provides a novel route for controlled fabrication of various shapes of Ag nanostructure in large amounts which is generally challenging to achieve the single-step process. Apart from DMF and EG, one of the most intermittently used reductants is $NaBH_4$ for the preparation of colloidal AgNPs[52,41]. Various groups of researchers reported Ag^+ ion reduction in $NaBH_4$; bring in use along with a few of the stabilizers, e.g., PVP[53] and citrate[54]. It was investigated that altering the growth and rate of nucleation during the reduction of Ag^+ ion through the help of PVP, tri-sodium citrate, and $NaBH_4$; controlled the synthesis of Ag nanostructure with desired shape and size[52,41]. It was observed that sodium citrate contributes to the reduction of Ag^+ ion in nanospheres, while PVP prevents AgNPs aggregation and boosts nucleation.

Yang and co-workers invented a new double reductant technique that completes in three steps. According to this method, Ag nanospheres were formed by the silver-nitrate-reduction via $NaBH_4$ and Na_3CA. In the next step, there is the need for a stabilizer that is fulfilled by sodium

dodecyl sulfate (SDS). After incorporation of SDS in the colloidal Ag nanostructure, Ag nanospheres (initially stabilized by citrate) were transformed into SDS-stabilized Ag nanospheres. Finally, in the last step, there is the formation of Ag nanoplates occurs, covered by the reductant - SDS, citrate, and NaCl solution. Few researchers reported on the utilization of Acetylsalicylic acid (AsA) to synthesize string forms and flower-like Ag nanostructure. Luo and co-workers described the reduction of $AgNO_3$ via AsA and in the presence of Na_3CA to gain a hyperbranched Ag nanostructure[55]. They reported the yield of multifaceted AgNPs having bulbous tips through the reduction of silver nitrate via AsA. Zhang and co-researchers also reported on the synthesis of silver dendrites after the reduction of silver-nitrate through AsA; there is a prominent role of SDS and CTAB (cetyl-tri-methyl-ammonium-bromide) in the whole procedure.[56]

Various desirable facets of Ag nanocrystals formed in different reductants are the basis of double reductant method[15]. In the etching method, there is the utilization of an etchant for selective removal of nanoparticle to obtain the controlled shape of the nanostructure[36]. The fabrication of the core-shell nanostructure is derived from epitaxial growth of the core seeds[57]. The various properties of such nanostructure can be regulated by these methods by tuning the size and shape of the nanostructure, which leads to significant and powerful applications in numerous areas.

2.5. Synthesis of Ag core-shell nanostructure

Despite Ag, nanostructures attained huge attention due to their specific optical properties and broad area of applications, researchers are continuously striving to innovate new nanostructures to meet more advanced requirements. By controlling the composition of elements, the optical properties of nanostructures can be altered[58]. The properties of various nanostructures were also highly dependent upon the internal as well as surface structures of the nanoparticles. In the last decade, major consideration has been given to the core-shell type of nanostructure[59] because it presented a novel system with adjustable properties. The nanostructure having core-shell nanoparticles can be accomplished in different ways, such as photochemical method[33], nanosphere-lithography[46], chemical reduction method[60].

The core or the shell material demonstrates the unique core-shell nanostructure abilities. It is noteworthy to mention that we can govern the functionality of core-shell material by altering

the constituting materials or the concentration of either core or the shell[61]. The acting of the coating material involves enhancing stability, functionalization, or restrained release of the core substance[62]. The core-shell nanoparticles, as it is exhibited in Fig. 3, are beneficial in numerous fields namely, drug delivery, bioimaging, and various other biomedical applications. The core-shell hybrid nanoparticles can be categorized in accordance with the coating substances in two broad classes-inorganic and organic. Inorganic nanoparticles are mainly metal-based compounds and can be subdivided into metal salts, metal oxide nanoparticles, and metal nanoparticles. Whereas, organic nanoparticles are referred to the carbon-based compounds, generally polymers. Metal nanoparticles are usually synthesized primarily through the reduction of their corresponding metal salts.

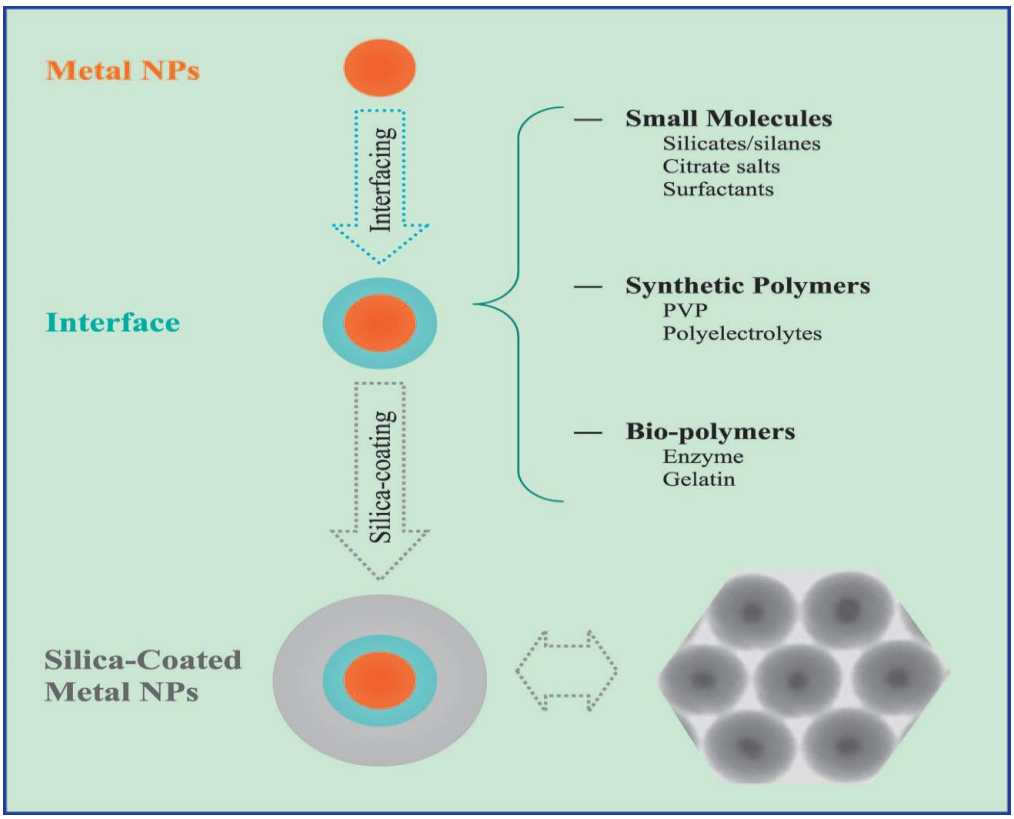

Figure 2.3: Encapsulation of silica on metal nanoparticles: metal nanoparticles obtained from various sources can be coated with biocompatible material silica by the specific sol-gel process[63].

2.5.1. Organic coated AgNPs

Clustering and ionization of the various functionalizing agents, on the surfaces of AgNPs for a longer period of time, lead to the diminished functionalization of the surface. Later, coating

them by utilizing a layer-by-layer method via an organic material (i.e. xanthate, polyethylene glycol, thiol-derivatives, etc.) plays a significant role in protecting them from ionization processes[64]. On the other hand, the dimension of the organic structure is normally incomplete, the size-distribution of the organic nanoparticle is wide and the spatial arrangement of the organic nanoparticle is irregular as well. Thus, the evolution of effective methods for the fabrication of hybrid structures that can overcome these challenges is of great importance[65]. Organic-inorganic nanocomposite material has fascinated researchers to incorporate inorganic components onto polymer matrices[66]. The formation of inorganic nanostructures dissipated in mats of electrospun polymer nanofiber[67] has gained very attention due to the type of nanocomposite material, which merges the amazing qualities of the inorganic nanoscale component in addition to the extraordinary peculiarity of polymer nanofibers[68]. This type of polymer/inorganic nanocomposite can fulfill numerous types of possible applications, such as photonic, electric-sensors, catalysts, filters, antibacterial and antifouling agents along with artificial tissues[69].

Organic materials like polyethylene glycols (PEGs), PVP, Na-lauryl sulfate (Na-LS), SDBS (sodium dodecyl benzene sulfonate), Na-naphthalene sulfonate (Na-Ns) act as a stabilizer to prevent the AgNP from aggregation/sintering. Such a glaring spectrum of applications indicates the need for the utilization of these materials in the fabrication of hybrid nanoparticles[70]. The specific abilities of coated AgNPs give rise to a multitude of applications in various areas, e.g., PVP coated AgNPs can work as an angiogenic factor[71]. Triangular silver nanostructure coated with chitosan demonstrates the ability to act as photothermal agents against non-small human lung cancer cells[72]. This is attributed to its remarkable performance in generating powerful resonances upon exposure to near-infrared light source[73]. PVP-encapsulated AgNPs of different sizes possess an excellent anti-leukemic reaction[74] in the case of acute myeloid leukemia in humans. PVP-coated AgNPs can also be successfully employed for applications in biosensing for food control[75], medical diagnostics as well as environmental protection as a color indicator[76]. It was reported that a cluster of amides present in the protein of a few plant extracts has the capability to stick on the surface of the metallic particles[77]. Such a process leads to the shielding of the outer layer of AgNPs from oxidation and at the same time blocks the agglomeration process[78]. AgNPs toxicity is co-related with the living cells and their various outer surface properties[79].

Numerous metal nanoparticles have been encapsulated in polymer fibers, among which nanoscale AgNPs have gained much interest due to their broad array of significant properties, including high electrical conductivity, remarkable catalytic activity, and amazing antimicrobial activity[80]. So far, countless shapes of silver nanostructure have been synthesized by this method. Polyol-assisted methods[81] are very beneficial due to their controlling abilities in the reduction of precursor ions and in nucleation and growth modes. Kan et al. reported PVP-assisted polyol synthesis of the hybrid Ag nanostructure[82], with proper shapes-nanocubes and nanorods by balancing the synthesizing parameters.

The hierarchical fabrication process of nanoparticles has been broadly used to synthesize nanowires, nanorods, dendrites, nanorings, and so forth. Amid all of these nanoparticles, the dendritic supramolecular nanoparticles are mainly fascinating for researchers because of their applications in sensors, catalysts, electronic and optical systems, along with fluorescence-enhancement materials[48]. Li et al. reported the novel dendritic Ag nanostructure combining $AgNO_3$ and p-aminoazobenzene (PA)[83]. They investigated the SERS technique to find out the use of PA molecules while the seeding-growth of the dendritic Ag nanostructure[34]. These Ag nanostructures may be useful for the SERS substrate for exploring PA molecules adsorbed onto their surfaces, that can be supportive for understanding the part of PA molecules through crystal growth[64].

Wang et al. reported the synthesis of Ag@agarose nanoparticles. In their work, they prepared AgNPs by chemical reduction of sodium-citrate and then incorporated it into agarose by fusing to produce silver-containing agarose film i.e. Ag@agarose[84]. Varying the concentration of AgNPs in the Ag@agarose film together with the broadness of the layering has been controlled by chitosan and sodium alginate. These composite AgNPs were employed to detect metal-enhanced fluorescence (MEF)[85].

Abdal-hay and coworkers reported a specific hybridized AgNPs; in this work, a colloidal mixture of silver nanostructures was fabricated and deposited onto electrospun nylon 6 fibers aside from the use of a surface modifier in the pattern of an ultrathin conformal encapsulated layer through hydrothermal treatment. Nylon 6(N6) is an excellent biocompatible polymer that is broadly utilized in various industrial areas because of its superior fiber forming ability, low cost, strong thermal and chemical stability, and good mechanical strength[66]. Mollaee et al. have reported a novel 2-D polymer named Quinoxaline-benzopyrazine-mediated Ag nanostructure

synthesis. Silver displays a tendency to produce coordinationpolymers with extraordinary metal-metal and metal-carbon interactions[86].

2.5.2. Inorganic coated AgNPs

Several inorganic substances fall into this category for coating of AgNPs namely - silica, metal, metal salt, metal-oxide, and bimetal materials. The resulting coated materials offer versatile applications, being relevant not only in the field of biomedical science but also in various other industries and research areas.

2.5.3. Core-shell nanostructure with the metal core

The ore-shell kind of nanostructure can be synthesized by numerous core and shell combinations relying upon the nature of the material-metal, semiconductor, dielectric. The preferred material noticeably alters the procedure employed for the synthesis of the composite nanostructure[81]. Nanostructures that have metals, generally silver, cobalt and gold, are utilized most often. For this purpose, the shell is normally tailored through a dielectric material balancing by the metal nanoparticles[87].

Gold nanoparticles are incapable of being directly encapsulated with silicon dioxide because the chemical compatibility between them is very weak. Thus, the layer of Au nanoparticles is altered through amphiphilic nonionic PVP. By employing the Stober process, established upon hydrolysis of tetraethoxysilane in ethanol by using ammonia as a catalyst, a group of researchers prepared Au nanoparticles encapsulated with silica shell[88]. Aside from the Stober process, coating with silica shells can also be achieved through the modified citrate method[89] by the use of tri-sodium citrate; in this process citrate ion works as the reducing agent. The heating of the reaction mixture resulted in the oxidation reaction of citrate-ions, which gives itaconic acid and acetone dicarboxylic acid[90]. These acids can be attached to the outer surface of metal nanoparticles, so they work as stabilizing agents and therefore diminish the nanoparticle growth. The synthesis of silver particles encapsulated in silica through citrate reduction method in a mixture of dimethylamine and tetra-ethyl-ortho-silicate in liquid ethanol for more than 5h has been demonstrated[91].

Later, the coated nanoparticles were washed with ethanol with the help of a centrifuge. The coating is an outstanding way to increase the quality of any nanoparticle material. It can improve the stability of AgNPs by the electrostatic stabilization between the particles and can reduce their agglomeration. Another advantage of coating is that it can prevent the cytotoxic

efficiency of AgNPs against living cells[92]. Numerous coating materials have been widely accepted in stabilizing AgNPs, which also maintain their particular shape and degrade ions of Ag, which are specific things that contribute to the toxicity of AgNPs. The process of coating is immensely reliant on the qualities of the material used for the coating, e.g. inorganic coating materials (sulfides, chloride, etc.) and organic coating substances (polymer, polysaccharides, proteins, etc).

2.5.4. Bimetal nanostructure or metal core metal-shell nanostructure

Bimetal nanoparticles possess extraordinary physical, chemical, electrical, and optical qualities over metal nanoparticles that are not coated e.g. Au-Ag (metal-metal) yolk core, yolk-shell nanoparticles displayed unique physical and optical properties as compared to bare metal nanoparticles[81]. Another instance is silver-platinum nanoparticles. Ag/TiO_2 composite nanoparticles have beneficial properties namely visible light photocatalysis, antimicrobial activities, and biological compatibility[93]. Fe_3O_4 integrated into AgNPs can be utilized for the filtration of water and can effortlessly eliminate contamination with the help of magnetic field[67].

Numerous groups of researchers have chosen Au nanoparticles as the core material to synthesize Au@Ag nanostructure; which contains extraordinary properties in catalysis, sensors, and numerous other applications[94]. For the development of the Ag layer on Au nanoparticle, the shape and specific size of the core nanoparticle i.e. Au are very crucial. Liu and coworkers explained two different ways to coat the Au nanoparticle with silver for the very first time[95]. Among these, in one route they had taken sodium citrate as a stabilizer to reduce $AgNO_3$ in the presence of AsA in the outer layer of Au nanorods, however, the results are not that great because of the employment of an elevated concentration of sodium citrate. Therefore, in their next attempt, they selected PVP as a stabilizer. The outcome of the results is in low-pH solution, reduction of Ag ions is not achievable due to the altered redox potential of the reagent (AsA) with pH changes. Because the redox potential of the reagent - AsA altered with pH. Thus, when NaOH was supplemented or else AsA was eliminated through citric acid, which is known to be a weak acid; shells of the Ag nanostructure developed. The results obtained showed that with the enhancement of the concentration of $AgNO_3$ in the reaction mixture; the Ag shells tend to increase in thickness and the blue-shifting of the mode of longitudinal plasmon of the Au nanorods was increased. Another method for the synthesis of Au@Ag was developed by Seo and coworkers[28]. They showed that the nanorods of Ag can be developed directly from the Au

nanorods and decahedrons. Taking the benefit from this method, we can properly understand the procedure of the nanorod formation[96]. For this, first reduction of Ag^+ ions occur, and then deposition onto the decahedral seeds of the Au nanoparticle takes place. After that, Ag nanocrystal particles developed in the longitudinal direction with inconsiderable variation assigned to the particular adsorption of PVP[97].

Another Au@Ag nanostructure coating mechanism was described by Sanchez-Iglesias and co-workers[98]; in their work, they managed to control the broadness of the covering layer of Ag by synthesizing thin to thick shells of Ag by the use of various feature ratios of Au nanorods. They also used methoxy-poly-thiol as a counterbalance[99], that can attach at the tips of Au nanorod to chunk the development of Ag with the longitudinal direction, which leads to the synthesis of Ag octahedrons[100]. They have also described that the thickness of Ag shells is co-related with the optical properties of the core-shell nanostructure. Tsuji et al. explained a merging of polyol reduction and microwave application as a way to synthesize triangles of Au@Ag core-shell nanostructure[101]. Metal oxide nanoparticles are also a very good candidate for coating purposes, because of the fact that they play a significant role in catalysis as well as in drug delivery. Ag coated with iron-oxide core-shell nanostructure permits a magnetic activity to AgNPs[102]. This unique nanostructure can overcome the problem of biocompatibility of AgNPs and diminish the chances of their direct contact with tissues[66]. AgNPs coated with metal salt play a significant role in the fabrication of sensors, battery cathodes, and solar cells. Silver copper sulfide core-shell nanostructure utilized as Ag nanowire enhances the electrochemical properties of copper-sulfide via decreasing its resistance during charge transfer.

Zinc is also very beneficial for the synthesis of composite nanoparticles. Hu and co-workers reported that nanoflowers shapes of ZnO@Ag can be synthesized by settling powder of zinc on the silver shells by employing a vapor-transportation technique under an atmosphere of oxygen[103]. Few researchers have reported on the synthesis of Ag@Pt bimetallic nanoparticles, through the route of chemical reduction[104].

Fu et al. designed a coated Ag nanostructure geometry that contains fluorescent emitters sandwiched between AgNP and silver island film (SIF). A relevant number of polyelectrolyte layers were deposited on the surface of the SIF, formerly the self-assembly of the second layer of AgNP. This layer-by-layer configuration structure provided a well-defined dye position. The

yielded coated Ag nanostructure was used to study the photophysical nature of the fluorophores[105].

2.6. Biomedical applications of coated AgNPs

After reaching the nanoscale, particles of silver have a miraculous change in physicochemical properties, and they turn out to have exceptional biomedical activities. The uniqueness of silver nanoparticles broadens their pertinency in anti-bacterial, anti-fungal, and anti-cancer therapy[106].

Amid numerous kinds of nanoparticles accessible at the current time, nanoparticles having core-shell architectonic, possess astounding properties, collaborating multiple functionalities into a sole coated nanocomposite. The assorted pattern of efforts was given for the study of the anti-cancerous, anti-bacterial, and anti-fungal effectiveness of silver nanoparticles. Still, scant or no attention is given to the comparative study of silver and yolk-shell silver-silica nanoparticles. Alteration in silver nanoparticles' functionality with silica gives the nanoparticle idiosyncratic effects, because of the biocompatibility, hydrophilicity, and optical transparency along with thermal and chemical stability of the silica; unexpectedly in aqueous-media also. The flexibility of silica in surface moderation as well as in synthesis demeanor offers an outstanding edge to the employment of this material for therapeutic purposes because for the applicability in medicine, immunocompatibility is a prerequisite condition, that will clinch the non-toxic nature of the material.

Cancer is an ambidextrous malady exceptionally unpredictable in its unveiling, evolution, and aftermath. There are numerous drugs available for cancer- therapy but most of them are inefficacious to set foot on-target site in adequate concentrations and systematically deploy the desired pharmacological upshot without triggering irreversible undesired harm to normal cells and tissues.

There are certain limitations associated with conventional chemotherapeutic drugs. Silver nanoparticles have the prospective to circumvent assorted drawbacks of typical therapeutic implementations. Tailor-made silver nanoparticles coated with specific biocompatible nanomaterial can target cancerous cells in a foreseeable demeanor, because these can be specifically intended for expanded drug loading, upgraded half-life inside the body, unflappable release as well as selective distribution by altering their size, composition, surface chemistry, and morphology. In the same manner, antimicrobial chemotherapy also demands attention because

lately, resistance to antibiotics by disease engendering fungus and bacteria has been growing at a breathtaking pace and thus became major trouble. Bacterial and fungal infections are colossal causes of morbidity and mortality[107]. To overcome this resistance mechanism of pathogenic microbes, consideration has been given to silver nanoparticles as an encouraging tool since it works miraculously on a span of targets in contrast to antibiotics, which have a particular site of execution. Silver nanoparticles revealed magnificent outcomes in detecting and remedying microbial infections by enabling the pick out of target pathogens, reactive and combinatorial freightage of antibiotics, successful antibacterial vaccination as well as swift detection of pathogens[108].

In recent years, a number of immunoassay-techniques for the diagnosis of different tumor markers for more effective governance of cancer have been investigated. A sailing way for the observation of cancer has been the evaluation of serum tumor markers. Gradually, electrochemical immunoassay has acquired acceptance and therefore broadly utilized to detect tumor markers because of the intrinsic benefits such as lofty selectivity, sensitivity, suitable label-free manipulation, low cost, minute size, and very fast analysis. There exist numerous kinds of electrochemical immunosensor built upon conductometry, amperometry, potentiometry, and electrochemical-impedance-spectroscopy [108]. Evolving a CEA immunosensor having good selectivity and sensitivity but lacking a complex fabrication procedure still fascinates researchers.

Based on the above-explained consideration current thesis describes the preparation of silver nanoparticles along with their coating by silica, followed by the characterization of both the nanoparticles, for their applications in therapy and detection purposes.

In view of this issue, output in the current thesis has been given with the below-mentioned aims-

- Preparation of silver nanoparticles by Turkevich procedure by employing chemical reduction method
- Coating of silver nanoparticles with silica through modified Stober method.
- Characterization of both the nanoparticles to observe their spectroscopic, elemental, and morphologic properties.
- Fabrication of electrochemical immunosensor for the detection of carcinoembryogenic antigen (CEA).

-To examine the antibacterial, antifungal as well as anticancerous properties of both the synthesized nanoparticles.

2.6.1. Antibacterial effectiveness of coated AgNPs

Romans, Egyptians, and Greeks anciently used different metals as well as metal salts for wound care, taking advantage of their antimicrobial effectiveness. However, with the discovery of antibiotics, the use of antimicrobial metals in the biomedical field declined. Nowadays, clinicians face a growing problem as an increasing number of pathogens have devolved resistance to antibiotics[109]. It was demonstrated by various researchers that AgNPs exhibit increased growth inhibition of numerous bacterial colonies. They can bind to the exterior surface of the bacterial membrane significantly disturbing its basic functions (e.g. respiration, permeability). Additionally, AgNPs can penetrates the bacterial cell wall and interact with their DNA leading to their destruction[110]. Coated AgNPs have emerged as a fascinating option for combating antibiotic-resistant bacteria, displaying enhanced activity against various multi-drug resistant strains. Silver ions can bind with the negatively charged molecules like proteins, DNA, and RNA, making them highly toxic against many human pathogens, as depicted in Fig. 4. The disabling of bacteria is related to the nanoparticles' shape, concentration, size, the presence of Ag^{+}, and bacterial type. The antibacterial effectiveness of AgNPs enhances on the basis of their extensive whole surface area per unit volume[109].

In general, silver releases their ions under specific physiological conditions and such ions assemble on the functional (phosphoryl-, sulfhydryl-) enzymatic groups and proteins, which are prominent for the intrinsic metabolism of bacterial cells. As a result of this, vital enzymes became inactivated and DNA loses its ability to replicate, and changes occur in the structure of the cell membrane. As a result, the bacteria are effectively inactivated[111].

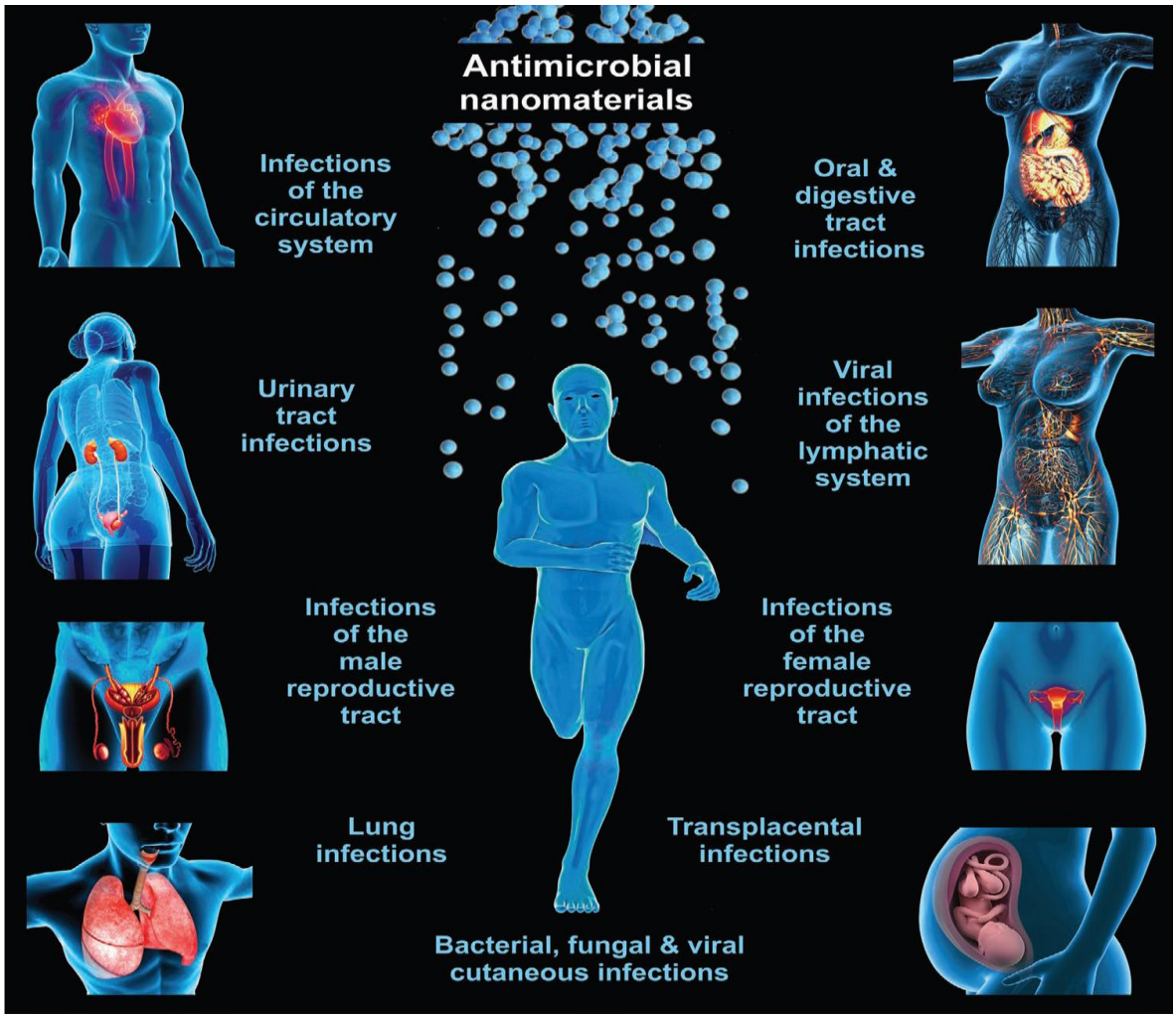

Figure 2.4: Representative image showing the potential of coated AgNPs in combating antimicrobial infections in different parts of the human body[112] harnessing their various disease-repelling properties.

Due to their incredible cytotoxicity, AgNP is competent to work as a medical antiseptic as well as an antimicrobial agent against both Gram -ve as well as Gram +ve bacteria. AgNPs make use of their bacterial effectiveness by disrupting bacterial cell membranes and triggering the release of specific reactive oxygen species (ROS), leading to the generation of free radicals with potent bactericidal capabilities[113].

Table 2.1: showing anti-bacterial efficacy of core-shell AgNPs.

Hybrid AgNP	Bacterial strain	Methods of analysis	Effects	Ref.

Ag@SiO_2-Penicillin NP	methicillin-susceptible *S. aureus* and methicillin-resistant *S. aureus*	MIC, MBC and IZ (diameter of the inhibition zone)	$AgSiO_2$ NPs showed an rate of inhibition of about 40% at the MIC. The bactericidal results displayed the minimal MIC for Ag@SiO_2-Penicillin as compare to that for penicillin and $AgSiO_2$ NPs.	[114]
Zeolite-Ag-zinc	*Escherichia coli (E. coli)*	MBC	The specific nanoparticle exhibit minimum bacterial concentration of 78μg/ mL	[111]
AgNP stabilizes onto hyperbranched polymers	*S. aureus, E. coli, K. mobilis, B. subtilis*	MIC, IZ (diameter of the inhibition zone)	Microbial activity enhances as Ag concentration in polymer diminish when AgNP size reduces.	[115]
AgNP-aerosol	*B. subtilis*	MIC	76% CFU decreases after implementing AgNP aerosol on *B. subtilis*	[116]
Ag-MSNs (mesoporous silica nanoparticles)	*E. coli* *S. aureus*	Bacterial kinetic test	Ag-MSNs exhibit long-lasting anti-bacterial activity on Gram +ve and Gram	[117]

			-ve bacteria at very low concentration	
Ag/SiO_2	*E. coli, S. typhimurium, B. cereus, S. aureus*	Kirby-Bauer disk-diffusion method	Ag/SiO_2NPs exhibits unique antibacterial activity	[91]
Polystyrene-silver-silica	*S. aureus, E. coli*	MIC, MBC	Ag-Si nanocomposite comprising of polystyrene particles displayed excellent antibacterial efficacy against *S.aureus* as well as against *E. coli*.	[111]
SiO_2@Ag	*E. coli, P. aeruginosa, S. aureus, Enterobacter cloacae*	MIC	The hybrid nanoparticle showed more potent toxicity towards Gram -ve bacteria than Gram +ve bacteria	[118]
$Ag@TiO_2$ and $Ag@SiO_2$	*E. coli, S. aureus*	MIC and IZ (inhibition zone)	The MIC observed in the case of $Ag@TiO_2$ nanoparticle are 100 µg/mL for *S. aureus* and 200 µg/mL for E.coli while it is 100 µg/mL for both *S. aureus* and *E. coli* in case of $Ag@SiO_2$	[119]

Bryaskova et al. reported the excellent antibacterial efficacy of AgNPs/PVP against a few groups of bacteria namely *Staphylococcus aureus* (Gram +ve), *Escherichia coli* (Gram -ve),

Pseudomonas aeruginosa (Gram -ve), *Bacillus subtilis* (Gram +ve). Metal-organic coated nanoparticles showed excellent antimicrobial effectiveness and particularly minimal toxicity towards eukaryotic calls[68], as shown in Table 1. Thiagamani and co-workers reported about the cellulose / banana peel powder / AgNP coated nanoparticles against gram +ve (*S. aureus* and *B. licheniformis*), gram -ve (*P. aeruginosa* and *E. coli)*. Aymonier et.al. described the various amphiphilic hyperbranched molecules integrated with AgNPs, displaying antimicrobial properties[120]. Apalangya et al. fabricated calcium-carbonate along with AgNP by mechanochemical milling method and exploit it to study its antimicrobial behavior and got extremely good results[69]. Chen et al. described the function of Graphene Quantum Dot / Ag core-shell nanoparticle for antimicrobial purposes against Staphylococcus aureus and *E. coli*[113].

2.6.2. Anti-cancerous approaches of coated AgNPs

According to the World Health Organization, 19.3 million new patients with cancer were noted in 2020[121]. Despite immense efforts and advancements in cancer research, treatment failure rates are very high, principally because of dose-limiting toxicity, drug resistance, and serious side effects[27]. Therefore, there is a critical need for potent strategies for the treatment of cancer without compromising the patient's quality of life. Among metallic nanoparticles, AgNPs and their related core-shell nanomaterials have gained prominence due to their wide range of applications. Recently, AgNPs have acquired a special interest in the field of nanomedicine because numerous groups of researchers' reported the effective anti-tumoral activities in both *in vitro* and *in vivo* tumor models. These findings suggest that AgNPs hold promise for a variety of oncotherapy modalities and can also be beneficial in the development of diagnostic tools.

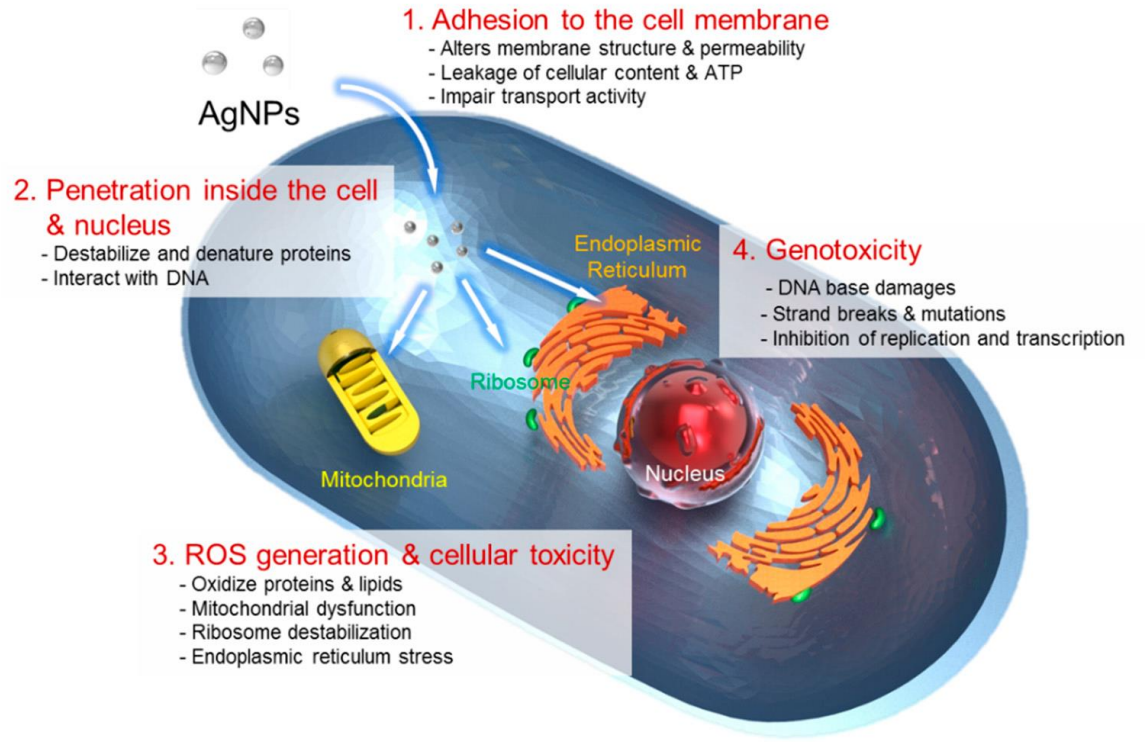

Figure 2.5: The four primary mechanisms of cytotoxicity execution of AgNPs[122].

AgNPs exhibit promising qualities for cancer therapies. Although the actual mechanism of action of AgNPs against cancerous cells is not yet fully explained, it is well known that their cytotoxicity depends on the propagation of ROS[123], as shown in Fig.2.5. Among various classes of nanoparticles available at the present time, core-shell nanoparticles with multiple functionalities possess astounding properties. Cytotoxicity reactions originated by enhancing the extent of ROS, decreasing the levels of intracellular glutathione as well as degrading the potential of the mitochondrial membrane. AgNPs can create inflammation of lung cells (epithelial) and can also cause macrophage inflammation[124]. According to numerous reports, coated AgNPs cytotoxicity, shown in Table 2.2, is dependent on the size as well as on the coating material.

Table 2.2: showing applications of cell-cytotoxicity of bare and coated AgNPs.

Hybrid AgNPs	Cell-cytotoxicity assay	Tested cell	Finding	Ref.
PEG (poly-ethylene-glycol) coated AgNPs	MTT	Hep G2	The two types of coated AgNS diminished cell-viability and proliferation with a same toxicity contour.	[125]
Peptide (L-cysteine L-lysine L-lysine) coated AgNPs	Cell titer blue cell viability assay(CTB)	V79, Hep G2 and Caco-2	The smaller uncoated nanoparticles exhibit much toxic outcome as compared to larger ones.	[126]
PVP (poly-vinyl-pyrrolidone) capped AgNPs	MTT	HT29 and J77A.1	Bare AgNPs are much toxic as compared to coated ones and diminish the cell-viability at about concentration of 1 µg mL^{-1}, whereas the viability of cells of coated AgNS diminish near the concentration of 25 µg mL^{-1}	[127]
ZnO integrated AgNPs	MTT	A431	Slighter cytotoxicity has been noticed because of the core-shell hybrid nanostructure as compared to bare AgNPs	[103]
Polysaccharide coated AgNPs	MTT	Mammalian cells	Cell-viability of bared AgNPs was kept at 50% whereas for the coated AgNPs; the viability of cells	[128]

			was diminished to merely 20%.	
PEG capped AgNPs-B (Betulin)	MTT and Annexin v-FITC	B16 melanoma 4A5 and B160va;human keratinocytes and melanocytes	PEG-capped AgNPs-B shows selective high toxicity at minimal doses and absence of toxicity for healthy cells in comparison to AgNPs-B.	[129]
PVP coated AgNPs	MTT and FACs	T24 bladder carcinoma cells	Both PVP coated and bare AgNPs displayed toxicity towards T24 bladder carcinoma cells.	[130]
PEG coated AgNPs	Alamar blue assay and MTT	Human keratinocytes-HaCat cells	PEG-coated AgNPs showed cytotoxicity even at minimal concentration as a main aspect of reduced toxicity.	[131]
PVP coated AgNPs	MTT and comet-assay	Hep G2 cells	The amount of damage of DNA was higher in case of bare AgNP was higher as in the PVP-AgNP. On the other hand, PVP-AgNP create extra serious chromosomal aberration compared to bare AgNP.	[132]
Ag-Au bimetallic NPs	MTT and comet-assay	HTC116 and 4T cell lines	Ag-Au bimetallic nanoparticles showed maximal antitumor effect as compare to bare AgNPs.	[133]

Researchers have suggested that the capping or hybridization of the nanoparticle surface enhances the dissolution and stability of the nanoparticles. Several factors influence the cytotoxic activity of the coated AgNP:

1. Coating: Proper coating of AgNPs generally decreases their cytotoxic activity[187].
2. Aggregation: Aggregated AgNPs tend to degrade the cytotoxic activity[162].
3. Size: Smaller particle size is associated with a higher degree of toxicity[134].

The cytotoxicity mechanism of AgNPs relies on their chemical attraction with the cell's surface and the removal of the silver ions from the nanoparticles; the surface coating of the AgNPs influences their cytotoxic mechanisms[125]. Specific size and surface area are also main factors, used to demonstrate the levels of cytotoxicity. Thus, the coating material used to fabricate coated nanoparticles can impact the cytotoxicity process, as it can magnificently influence shape, surface area, and physical properties[62]. In one of the studies, the AgNPs coated with zinc oxide diminished the cell cytotoxicity of AgNPs as against to the cancer cell line A431[103].

The surface coating of AgNP can alter their interactions with cells and the bacterial cell, consequently affecting their antimicrobial activity and toxicity. However, the impact of the same coating on antimicrobial activity can vary depending on the starting nanometals.

2.6.3. Coated AgNPs application in detection

Nowadays, nanomaterials have developed at a fast pace as an encouraging candidate for the detection of various diseases as they may solve long-term problems such as systemic distribution and solubility of various drugs, tumor acquired resistance, and can enhance the working performance of diagnostic methods[135]. Experts in the area of biosensors are invariably eager about unearthing novel materials possessing acceptable abilities to increase the activity of biosensors[136]. The investigative tools for the detection of biomarkers must be efficient in working at the level of distinctive diagnosis and be special to not generate various false positive results. Metal nanoparticles give a desired favourable environment which remarkably enhance the surface-to-volume proportion of a stagnant biomolecule onto the surface of the electrode, which can affect electrical signal improvement. It is noteworthy to mention that, AgNPs are very fascinating materials for application in detection because of their catalytic activity, plasmonic properties, and high conductivity[137]. All of these properties can be used to upgrade the performance of biosensors. For the diagnosis of minimal concentration of an analyte, the

sensitivity of the sensor is a prominent factor[138]. AgNPs have been utilized to enhance the electroactive field of the electrodes and accordingly the electron-transfer rate, thereby increasing the biosensor's sensitivity, as shown in Table 2.3.

Table 2.3: showing applications of coated AgNPs for various detection purposes.

Hybrid AgNPs	Detecting Biomarker/ cells/bacteria	Purpose	Type of biosensor	Linear range of detection	Limit of detection	Ref.
Au-Ag-graphene hybrid nanosheets	AFP (alpha fetoprotein)	Detection of liver cancer	Amperometric immunosensor	0.1-200 ng/mL	0.04 ng/mL	139
Si-AgNPs	PSA	Detection of prostate cancer	Label free voltametric immunosensor	0.2-200 ng/mL	0.01 ng/mL	140
B-LCA-AgNPs (Biotinylated Lens culinaris agglutinin-AgNP)	AFP-L3	Detection of HCC (hepato-cellular-carcinoma)	Electrochemical biosensor	25-15000 pg/mL	12 pg/mL	141
Ag/Fe-MOFs (metal organic frameworks)	α2,6-sialylated-glycans	Detection of carcinoma cells (colon, breast, cervix, liver)	Electrochemical affinity biosensor	1 fg/mL to 1 ng/mL	0.09 fg/mL	142

AgNPs-MWCNT (multi wall carbon nanotube)	H_2O_2 detection	For the diagnosis of oxidative stress	Non-enzymatic electrochemical sensor	1-1000 µM	0.38 µM	[143]
AgNPs-TMA (Thiomalic acid)	sensing of cysteamine	Neuroprotection in neuro-degenerative diseases	Colorimetric biosensor	0.2-10.0 µM	46 nM	[144]
Sulfo-NHS-terminated AgNPs	sensing of cholesterol	Prevention from cardiovascular diseases	Colorimetric sensor	10-250 nM	0.014 nM	[145]
M-AgNPs (Melamine functionalized AgNPs)	detection of clenbuterol	Protection against pulmonary disease	Electrochemical biosensor	10 pM to 100 nM	10 pM	[146]

Core-shell nanomaterials are appropriate to generate a constant electric field as well as elevate the transferred ratio of electrons in comparison to sole nanoparticles. Therefore, they can successfully fasten the regeneration action of sensors[147]. Li et al. reported a sensor for alpha-fetoprotein (AFP) detection by utilizing coated AgNPs to tag the target analyte seized through the electrode, by amplifying the electrode to enhance the sensitivity of the entire sensing system[148]. Chen et al. described the synthesis of coated AgNPs for the diagnosis of human telomerase efficacy[149]. In this procedure, AgNPs were integrated into telomerase binding sites moderately conjugated with the complementary strands of DNA. While the functional telomerase hybridized with its domain, the conjugated cohesion has enhanced, diminishing salt-induced aggregation; consequently, the color of the mixture remains yellow. However, if telomerase is inactive, the hybridized solution aggregate results in a change in color from yellow to gray[150].

Dewangan and colleagues[145] explained the use of coated AgNPs as colorimetric probes for the detection of cholesterol. The entire system has relied on the oxidation of cholesterol through ChOx which culminate in the generation of H_2O_2. The produced H_2O_2 finally oxidizes the AgNPs (Ag^0) into Ag^+, creating a change in color of the solution mixture from yellowish to colorless. Cheng et al. employed coated AgNPs to increase the signal amplification twice. At first, a hairpin fixated on the electrode which is opened via the target miRNA is misplaced after a biotinylated hairpin gets added[151]. Subsequently, in the second step, binding of AgNPs takes place altered with streptavidin onto the electrode surface. This mentioned biosensor showed a minimum limit of diagnosis of 0.4 fM. All of these studies revealed how the physicochemical qualities of AgNPs have been researched in the fabrication of various classes of sensors, mainly for biomedical purposes, contributing to the field of point-of-care detection of various diseases.

2.7. Conclusions

Novel strategies for fabricating core-shell nanoparticles by merging different functionality into one nanomaterial are in high demand. The current review shed light on various types of coated nanoparticles with a brief elucidation of the core-shell silver nanoparticles with a different way of synthesis and types of coated silver nanoparticles. We also explained core-shell AgNPs and numerous types of core and shell association. The flexibility of synthetic methods of hybrid AgNPs and facile consolidation of AgNPs into various media have gained the keen interest of researchers to explore the mechanistic aspects of various properties of such nanoparticles. A large number of such synthetic routes are still in the advanced stages and the challenges involve in the aggregation and stability of nanoparticles, morphology, control of crystal growth, difficulties in the proper management of the synthesis, and size distribution of the nanoparticles. Although, the separation of synthesized nanoparticles for additional applications is still a significant issue, by employing different stabilizers and reducing agents, the morphology and particle size of coated AgNPs have been restrained. Synthesis of these coated nanoparticles promises a chance for its applications in various areas from therapy to detection. Core-shell AgNPs have drawn the notice of researchers due to their extraordinary properties and manifest applicability in various areas, namely water treatment, optics, electronics, medicine, textile engineering, catalysis, bioengineering sciences, nanobiotechnology, and biotechnology. Additionally, diverse applications of coated AgNPs in various fields were also highlighted. Prominent inhibitory effects of coated AgNPs, against microbial pathogens and cytotoxic effects

on cancerous cells, are also discussed. Their applicability in diagnosis has also been explained. Nevertheless, even greater experimental methods are required for tailor-made well- characterized core-shell AgNPs.

References

1. Carpen LG, Acsente T, Sătulu V, et al. Hybrid nanostructures obtained by transport and condensation of tungsten oxide vapours onto cnw templates. *Nanomaterials*. 2021;11(4). doi:10.3390/nano11040835
2. Lee SJ, Begildayeva T, Yeon S, et al. Eco-friendly synthesis of lignin mediated silver nanoparticles as a selective sensor and their catalytic removal of aromatic toxic nitro compounds. *Environ Pollut*. 2021;269:116174. doi:10.1016/j.envpol.2020.116174
3. Botha TL, Elemike EE, Horn S, Onwudiwe DC, Giesy JP, Wepener V. Cytotoxicity of Ag, Au and Ag-Au bimetallic nanoparticles prepared using golden rod (Solidago canadensis) plant extract. *Sci Rep*. 2019;9(1):1-8. doi:10.1038/s41598-019-40816-y
4. Mohsen E, El-borady OM, Mohamed MB, et al. Synthesis and characterization of ciprofloxacin loaded silver nanoparticles and investigation of their antibacterial effect. *J Radiat Res Appl Sci*. 2020;13(1):416-425. doi:10.1080/16878507.2020.1748941
5. Hasanzadeh M, Shadjou N. Electrochemical and photoelectrochemical nano-immunesensing using origami paper based method. *Mater Sci Eng C*. 2016;61:979-1001. doi:10.1016/j.msec.2015.12.031
6. Sun C, Ma L, Qian Q, et al. A chitosan-Au-hyperbranched polyester nanoparticles-based antifouling immunosensor for sensitive detection of carcinoembryonic antigen. *Analyst*. 2014;139(17):4216-4222. doi:10.1039/c4an00479e
7. Hindler JA, Humphries RM. Colistin MIC variability by method for contemporary clinical isolates of multidrug-resistant gram-negative bacilli. *J Clin Microbiol*. 2013;51(6):1678-1684. doi:10.1128/JCM.03385-12
8. Glackin CA. *Nanoparticle Delivery of TWIST Small Interfering RNA and Anticancer Drugs : A Therapeutic Approach for Combating Cancer*. Vol 44. 1st ed. Elsevier Inc.; 2018. doi:10.1016/bs.enz.2018.08.004
9. Saptarshi SR, Duschl A, Lopata AL. Interaction of nanoparticles with proteins : relation to bio-reactivity of the nanoparticle. Published online 2013:1-12.

10. Shamsi M, Sedaghatkish A, Dejam M, Saghafian M, Mohammadi M, Sanati-Nezhad A. Magnetically assisted intraperitoneal drug delivery for cancer chemotherapy. *Drug Deliv*. 2018;25(1):846-861. doi:10.1080/10717544.2018.1455764
11. Benelmekki M. Designing hybrid nanoparticles. *Des Hybrid Nanoparticles*. 2015;(April):1-68. doi:10.1088/978-1-6270-5469-0
12. Sharifi M, Avadi MR, Dashtestani F, Ghorchian H, Rezayat SM, Saboury AA. Author ' s Accepted Manuscript. Published online 2018. doi:10.1016/j.bios.2018.11.026
13. Rachel Ouvinha de Oliveira. Development and evaluation of nanoparticles for cancer treatment.2014.http://www.bdtd.uerj.br:8443/handle/1/15635
14. Gupta K, Patra AK. Luminescent Europium(III) "Turn-On" Sensor for G-Series Chemical Warfare Simulants: A Mechanistic Investigation. *ACS Sensors*. 2020;(Iii). doi:10.1021/acssensors.9b02552
15. Zhang T, Song YJ, Zhang XY, Wu JY. *Synthesis of Silver Nanostructures by Multistep Methods*. *Sensors*. 2014. Vol 14(4), 5860-5889; doi:10.3390/s140405860
16. Fernandes T, Fateixa S, Ferro M, Nogueira HIS, Daniel-da-Silva AL, Trindade T. Colloidal dendritic nanostructures of gold and silver for SERS analysis of water pollutants. *J Mol Liq*. 2021;337:116608. doi:10.1016/j.molliq.2021.116608
17. Marinescu L, Ficai D, Oprea O, et al. Optimized Synthesis Approaches of Metal Nanoparticles with Antimicrobial Applications. *Journal of Nanomaterials*. 2020; doi:10.1155/2020/6651207
18. Wiley B, Sun Y, Xia Y. Synthesis of silver nanostructures with controlled shapes and properties. *Acc Chem Res*. 2007;40(10):1067-1076. doi:10.1021/ar7000974
19. Selim H, Mohamed D, Eskander H. Silver nanoparticles : synthesis , medical application , and toxicity effects. International Journal of Nanotechnology and Allied Sciences. 2017;Vol 1, doi:10.13140/RG.2.1.2581.4241
20. Holtz RD, Souza Filho AG, Brocchi M, Martins D, Durán N, Alves OL. Development of nanostructured silver vanadates decorated with silver nanoparticles as a novel antibacterial agent. *Nanotechnology*. 2010;21(18). doi:10.1088/0957-4484/21/18/185102
21. Botsa SM, Kumar YP, Basavaiah K. Facile simultaneous synthesis of tetraaniline nanostructures/silver nanoparticles as heterogeneous catalyst for the efficient catalytic reduction of 4-nitrophenol to 4-aminophenol. *RSC Adv*. 2020;10(37):22043-22053.

doi:10.1039/d0ra03327h

22. Lee SY, Jeon HC, Yang SM. Unconventional methods for fabricating nanostructures toward high-fidelity sensors. *J Mater Chem*. 2012;22(13):5900-5913. doi:10.1039/c2jm16568f
23. Métraux GS, Mirkin CA. Rapid thermal synthesis of silver nanoprisms with chemically tailorable thickness. *Adv Mater*. 2005;17(4):412-415. doi:10.1002/adma.200401086
24. Malola S, Nieminen P, Pihlajamäki A, Hämäläinen J, Kärkkäinen T, Häkkinen H. A method for structure prediction of metal-ligand interfaces of hybrid nanoparticles. *Nat Commun*. 2019;10(1). doi:10.1038/s41467-019-12031-w
25. Saraidarov T, Levchenko V, Popov I, Reisfeld R. Superlattices and Microstructures Shape control synthesis of spheroid and rod-like silver nanostructures in organic – inorganic sol – gel composite. *Superlattices Microstruct*. 2009;46(1-2):171-175. doi:10.1016/j.spmi.2008.10.015
26. Lara S, Perez-potti A. Applications of Nanomaterials for Immunosensing. *Biosensors* 2018; 8(4), 104; doi:10.3390/bios8040104
27. Silvestri B, Armanetti P, Sanità G, et al. Silver-nanoparticles as plasmon-resonant enhancers for eumelanin's photoacoustic signal in a self-structured hybrid nanoprobe. *Mater Sci Eng C*. 2019;102(April):788-797. doi:10.1016/j.msec.2019.04.066
28. Zhang XF, Liu ZG, Shen W, Gurunathan S. Silver nanoparticles: Synthesis, characterization, properties, applications, and therapeutic approaches. *Int J Mol Sci*. 2016;17(9). doi:10.3390/ijms17091534
29. Kovács D, Igaz N, Gopisetty MK, Kiricsi M. Cancer Therapy by Silver Nanoparticles: Fiction or Reality? *Int J Mol Sci*. 2022;23(2). doi:10.3390/ijms23020839
30. Li Z, Jiang S, Huo Y, et al. 3D silver nanoparticles with multilayer graphene oxide as a spacer for surface enhanced Raman spectroscopy analysis. *Nanoscale*. 2018;10(13):5897-5905. doi:10.1039/c7nr09276h
31. Benelmekki M. An introduction to nanoparticles and nanotechnology. *Des Hybrid Nanoparticles*. 2014. doi:10.1088/978-1-6270-5469-0ch1
32. Chandra P, Singh J, Singh A, Srivastava A, Goyal RN, Shim YB. Gold Nanoparticles and Nanocomposites in Clinical Diagnostics Using Electrochemical Methods. *Journal of Nanoparticles*. 2013; doi:10.1155/2013/535901

33. Wang TJ, Huang Y Te, Liu ZY, Barveen NR. Photochemical synthesis of ZnO/Ag heterogeneous nanostructure on chemically patterned ferroelectric crystals for high performance SERS detection. *J Alloys Compd*. 2021;864:158120. doi:10.1016/j.jallcom.2020.158120
34. Shiao MH, Wu T, Huang HJ, et al. Dendritic forest-like ag nanostructures prepared using fluoride-assisted galvanic replacement reaction for sers applications. *Nanomaterials*. 2021;11(6). doi:10.3390/nano11061359
35. Huynh KH, Pham XH, Kim J, et al. Synthesis, properties, and biological applications of metallic alloy nanoparticles. *Int J Mol Sci*. 2020;21(14):1-29. doi:10.3390/ijms21145174
36. Zumpano R, Polli F, D'Agostino C, Antiochia R, Favero G, Mazzei F. Nanostructure-Based Electrochemical Immunosensors as Diagnostic Tools. *Electrochem*. 2021;2(1):10-28. doi:10.3390/electrochem2010002
37. Chen CC, Hendrickson AA. New dislocation etchant for silver. *J Appl Phys*. 1971;42(13):5375-5378. doi:10.1063/1.1659952
38. Li Z, Jia L, Li Y, He T, Li XM. Ammonia-free preparation of Ag@SiO 2 core/shell nanoparticles. *Appl Surf Sci*. 2015;345:122-126. doi:10.1016/j.apsusc.2015.03.159
39. Zhang Q, Li N, Goebl J, Lu Z, Yin Y. A Systematic Study of the Synthesis of Silver Nanoplates. *Biomaterials*. 2011;133(46):18931-18939.
40. Chen B, Jiao X, Chen D. Size-controlled and size-designed synthesis of nano/submicrometer Ag particles. *Cryst Growth Des*. 2010;10(8):3378-3386. doi:10.1021/cg901497p
41. Yi Z, Xu X, Wu X, et al. Silver nanoplates: Controlled preparation, self-assembly, and applications in surface-enhanced Raman scattering. *Appl Phys A Mater Sci Process*. 2013;110(2):335-342. doi:10.1007/s00339-012-7256-0
42. Tsuji M, Gomi S, Maeda Y, et al. Rapid transformation from spherical nanoparticles, nanorods, cubes, or bipyramids to triangular prisms of silver with PVP, citrate, and H 2O 2. *Langmuir*. 2012;28(24):8845-8861. doi:10.1021/la3001027
43. Popov A, Brasiunas B, Kausaite-Minkstimiene A, Ramanaviciene A. Metal nanoparticle and quantum dot tags for signal amplification in electrochemical immunosensors for biomarker detection. *Chemosensors*. 2021;9(4). doi:10.3390/chemosensors9040085
44. Abdal-Hay A, Khalil KA, Lim J, Lim JK. Fabrication and characterization of silver

nanostructures conformal coating layer onto electrospun N6 nanofibers with improved physical properties. *J Sol-Gel Sci Technol*. 2014;71(1):184-191. doi:10.1007/s10971-014-3337-1

45. Rycenga M, Cobley CM, Zeng J, et al. Controlling the synthesis and assembly of silver nanostructures for plasmonic applications. *Chem Rev*. 2011;111(6):3669-3712. doi:10.1021/cr100275d
46. McEachran M, Keogh D, Pietrobon B, et al. Ultrathin gold nanoframes through surfactant-free templating of faceted pentagonal silver nanoparticles. *J Am Chem Soc*. 2011;133(21):8066-8069. doi:10.1021/ja111642d
47. Pastoriza-Santos I, Liz-Marzán LM. Formation of PVP-protected metal nanoparticles in DMF. *Langmuir*. 2002;18(7):2888-2894. doi:10.1021/la015578g
48. Lu L, Kobayashi A, Kikkawa Y, Tawa K, Ozaki Y. Oriented attachment-based assembly of dendritic silver nanostructures at room temperature. *J Phys Chem B*. 2006;110(46):23234-23241. doi:10.1021/jp063978c
49. Kumar A, Choudhary A, Kaur H, Mehta S, Husen A. Metal-based nanoparticles, sensors, and their multifaceted application in food packaging. *J Nanobiotechnology*. 2021;19(1). doi:10.1186/s12951-021-00996-0
50. Meng XK, Tang SC, Vongehr S. A Review on Diverse Silver Nanostructures. *J Mater Sci Technol*. 2010;26(6):487-522. doi:10.1016/S1005-0302(10)60078-3
51. Sannegowda LK. Metal nanoparticles for electrochemical sensing applications. *Handb Nanomater Sens Appl*. Published online 2021:589-629. doi:10.1016/B978-0-12-820783-3.00001-4
52. Zhang Y, Yang P, Zhang L. Size- and shape-tunable silver nanoparticles created through facile aqueous synthesis. *J Nanoparticle Res*. 2013;15(1). doi:10.1007/s11051-012-1329-z
53. Guo D, Zhu L, Huang Z, et al. Anti-leukemia activity of PVP-coated silver nanoparticles via generation of reactive oxygen species and release of silver ions. *Biomaterials*. 2013;34(32):7884-7894. doi:10.1016/j.biomaterials.2013.07.015
54. Kim YJ, Rahman MM, Lee SM, et al. Assessment of in vivo genotoxicity of citrated-coated silver nanoparticles via transcriptomic analysis of rabbit liver tissue. *Int J Nanomedicine*. 2019;14:393-405. doi:10.2147/IJN.S174515
55. Li M, Luo Z, Zhao Y. Self-Assembled Hybrid Nanostructures : Versatile Multifunctional

Nanoplatforms for Cancer Diagnosis and Therapy Self-Assembled Hybrid Nanostructures : Versatile Multifunctional Nanoplatforms for Cancer Diagnosis and Therapy. Published online 2017. doi:10.1021/acs.chemmater.7b03924

56. Zhang T, Song Y jun, Zhang X yang, Wu J yuan. *Synthesis of Silver Nanostructures by Multistep Methods*.; 2014. doi:10.3390/s140405860
57. Raveendran J, Docoslis A. Detection and quantification of toxicants in food and water using Ag–Au core-shell fractal SERS nanostructures and multivariate analysis. *Talanta*. 2021;231(March):122383. doi:10.1016/j.talanta.2021.122383
58. Lee SH, Jun BH. Silver nanoparticles: Synthesis and application for nanomedicine. *Int J Mol Sci*. 2019;20(4):1-23. doi:10.3390/ijms20040865
59. Singh P, Katkar PK, Patil UM, Bohara RA. A robust electrochemical immunosensor based on core-shell nanostructured silica-coated silver for cancer (carcinoembryonic-antigen-CEA) diagnosis. *RSC Adv*. 2021;11(17):10130-10143. doi:10.1039/d0ra09015h
60. Zhu S, Du CL, Fu Y. Localized surface plasmon resonance-based hybrid Au-Ag nanoparticles for detection of Staphylococcus aureus enterotoxin B. *Opt Mater (Amst)*. 2009;31(11):1608-1613. doi:10.1016/j.optmat.2009.03.009
61. Fahmy HM, Mosleh AM, Elghany AA, et al. Coated silver nanoparticles: Synthesis, cytotoxicity, and optical properties. *RSC Adv*. 2019;9(35):20118-20136. doi:10.1039/c9ra02907a
62. Azizi M, Ghourchian H, Yazdian F, Bagherifam S, Bekhradnia S, Nyström B. Anti-cancerous effect of albumin coated silver nanoparticles on MDA-MB 231 human breast cancer cell line. *Sci Rep*. 2017;7(1):1-18. doi:10.1038/s41598-017-05461-3
63. Liu S, Han MY. Silica-coated metal nanoparticles. *Chem - An Asian J*. 2010;5(1):36-45. doi:10.1002/asia.200900228
64. Fateixa S, Nogueira HIS, Trindade T. Hybrid nanostructures for SERS : materials development and chemical detection. Published online 2015. doi:10.1039/C5CP01032B
65. Pazos E, Sleep E, Rubert CM, Lee SS, Tantakitti F. Nucleation and Growth of Ordered Arrays of Silver Nanoparticles on Peptide Nano fi bers: Hybrid Nanostructures with Antimicrobial Properties. Published online 2016:4-7. doi:10.1021/jacs.6b01570
66. Khalil AA hay, Khalil A, Lim J, Kyoo J. Fabrication and characterization of silver nanostructures conformal coating layer onto electrospun N6 nanofibers with improved

physical properties. Published online 2014:184-191. doi:10.1007/s10971-014-3337-1

67. Pencheva D, Bryaskova R, Kantardjiev T. Polyvinyl alcohol/silver nanoparticles (PVA/AgNps) as a model for testing the biological activity of hybrid materials with included silver nanoparticles. *Mater Sci Eng C*. 2012;32(7):2048-2051. doi:10.1016/j.msec.2012.05.016
68. Bryaskova R, Pencheva D, Nikolov S, Kantardjiev T. Synthesis and comparative study on the antimicrobial activity of hybrid materials based on silver nanoparticles (AgNps) stabilized by polyvinylpyrrolidone (PVP). *J Chem Biol*. 2011;4(4):185-191. doi:10.1007/s12154-011-0063-9
69. Apalangya V, Rangari V, Tiimob B, Jeelani S, Samuel T. Development of antimicrobial water filtration hybrid material from bio source calcium carbonate and silver nanoparticles. *Appl Surf Sci*. 2014;295:108-114. doi:10.1016/j.apsusc.2014.01.012
70. Podagatlapalli GK, Hamad S, Rao SV. Trace-level Detection of Secondary Explosives using Hybrid Silver-Gold Nanostructures and Nanoparticles Achieved with Femtosecond Laser Ablation.
71. Gurunathan S, Lee KJ, Kalishwaralal K, Sheikpranbabu S, Vaidyanathan R, Eom SH. Antiangiogenic properties of silver nanoparticles. *Biomaterials*. 2009;30(31):6341-6350. doi:10.1016/j.biomaterials.2009.08.008
72. Loiseau A, Asila V, Boitel-Aullen G, Lam M, Salmain M, Boujday S. Silver-based plasmonic nanoparticles for and their use in biosensing. *Biosensors*. 2019;9(2). doi:10.3390/bios9020078
73. Gurunathan S, Kang MH, Kim JH. Combination effect of silver nanoparticles and histone deacetylases inhibitor in human alveolar basal epithelial cells. *Molecules*. 2018;23(8). doi:10.3390/molecules23082046
74. Mele G, Pinna S, Loseto G, Melpignano A, Quarta G. A482 What is the Best Maintenance Therapy for Multiple Myeloma. *Clin Lymphoma Myeloma*. 2012;9(February):S77. doi:10.1016/s1557-9190(11)70600-x
75. Dawadi S, Katuwal S, Gupta A, et al. Current Research on Silver Nanoparticles: Synthesis, Characterization, and Applications. *J Nanomater*. 2021;2021. doi:10.1155/2021/6687290
76. Garcia T, Lafuente D, Blanco J, et al. Oral subchronic exposure to silver nanoparticles in

rats. *Food Chem Toxicol*. 2016;92:177-187. doi:10.1016/j.fct.2016.04.010

77. Tolaymat TM, El Badawy AM, Genaidy A, Scheckel KG, Luxton TP, Suidan M. An evidence-based environmental perspective of manufactured silver nanoparticle in syntheses and applications: A systematic review and critical appraisal of peer-reviewed scientific papers. *Sci Total Environ*. 2010;408(5):999-1006. doi:10.1016/j.scitotenv.2009.11.003
78. Javed B, Ikram M, Farooq F, Sultana T, Mashwani Z ur R, Raja NI. Biogenesis of silver nanoparticles to treat cancer, diabetes, and microbial infections: a mechanistic overview. *Appl Microbiol Biotechnol*. 2021;105(6):2261-2275. doi:10.1007/s00253-021-11171-8
79. Fatima A, Younas I, Ali MW. An Overview on Recent Advances in Biosensor Technology and its Future Application. *Arch Pharm Pract*. 2022;13(1):5-10. doi:10.51847/ltogi43jil
80. Moodley N. Antimicrobial activity of ciprofloxacin-coated gold nanoparticles on selected pathogens. *Thesis*. 2014;61(21):196.
81. Shnoudeh AJ, Hamad I, Abdo RW, et al. *Synthesis, Characterization, and Applications of Metal Nanoparticles*. Elsevier Inc.; 2019. doi:10.1016/B978-0-12-814427-5.00015-9
82. Kan CX, Zhu JJ, Zhu XG. Silver nanostructures with well-controlled shapes: Synthesis, characterization and growth mechanisms. *J Phys D Appl Phys*. 2008;41(15). doi:10.1088/0022-3727/41/15/155304
83. Li M, Luo Z, Zhao Y. Self-Assembled Hybrid Nanostructures: Versatile Multifunctional Nanoplatforms for Cancer Diagnosis and Therapy. *Chem Mater*. 2018;30(1):25-53. doi:10.1021/acs.chemmater.7b03924
84. Wang X, He F, Zhu X, Tang F, Li L. Hybrid silver nanoparticle/conjugated polyelectrolyte nanocomposites exhibiting controllable metal-enhanced fluorescence. *Sci Rep*. 2014;4:1-6. doi:10.1038/srep04406
85. Wang X, He F, Zhu X, Tang F, Li L. Hybrid silver nanoparticle/conjugated polyelectrolyte nanocomposites exhibiting controllable metal-enhanced fluorescence. Published online 2014:1-6. doi:10.1038/srep04406
86. Mollaee J, Molaei F, Morsali A, Joo SW, Bruno G, Rudbari HA. Preparation of silver nanostructures from a new benzopyrazine silver(I) nitrate coordination polymer. *Inorg Chem Commun*. 2014;43:67-69. doi:10.1016/j.inoche.2014.01.018

87. Kim T, Braun GB, She ZG, Hussain S, Ruoslahti E, Sailor MJ. Composite Porous Silicon-Silver Nanoparticles as Theranostic Antibacterial Agents. *ACS Appl Mater Interfaces*. 2016;8(44):30449-30457. doi:10.1021/acsami.6b09518

88. Tan W, Wang K, He X, et al. Bionanotechnology based on silica nanoparticles. *Med Res Rev*. 2004;24(5):621-638. doi:10.1002/med.20003

89. Dong P Van, Ha CH, Binh LT, Kasbohm J. Chemical synthesis and antibacterial activity of novel-shaped silver nanoparticles. ??? Published online 2012:1. doi:10.1186/2228-5326-2-9

90. Zhang H, Zhang C. Transport of silver nanoparticles capped with different stabilizers in water saturated porous media. 2014;5(1):231-236.

91. Allafchian AR, Banifatemi SS, Jalali SAH. Synthesis and Characterization of Ag/SiO2 Nanoparticles Embedded in TPS and TEOS Sol-gel Matrix with Excellent Antibacterial Activity. *Nanosci &Nanotechnology-Asia*. 2017;8(1):33-40. doi:10.2174/2210681207011704191502O9

92. Gurunathan S, Han JW, Eppakayala V, Jeyaraj M, Kim J hoi. Cytotoxicity of Biologically Synthesized Silver Nanoparticles in MDA-MB-231 Human Breast Cancer Cells. 2013;2013.

93. Oda M. Metal Nano-Particles. *J Japan Inst Electron Packag*. 2002;5(6):523-528. doi:10.5104/jiep.5.523

94. Austin LA, MacKey MA, Dreaden EC, El-Sayed MA. The optical, photothermal, and facile surface chemical properties of gold and silver nanoparticles in biodiagnostics, therapy, and drug delivery. *Arch Toxicol*. 2014;88(7):1391-1417. doi:10.1007/s00204-014-1245-3

95. Liu M, Guyot-sionnest P. Synthesis and Optical Characterization of Au / Ag Core / Shell Nanorods. Published online 2004:5882-5888.

96. Product GN, Two R. Chapter 1 : Introduction Chapter 1 : Introduction. *Fluid Mech*. Published online 1966:1-16.

97. Machulek A, Moisés De Oliveira HP, Gehlen MH. Preparation of silver nanoprisms using poly(N-vinyl-2-pyrrolidone) as a colloid-stabilizing agent and the effect of silver nanoparticles on the photophysical properties of cationic dyes. *Photochem Photobiol Sci*. 2003;2(9):921-925. doi:10.1039/b302943c

98. Ye W, Krüger K, Sánchez-iglesias A, et al. CTAB Stabilizes Silver on Gold Nanorods. Published online 2020. doi:10.1021/acs.chemmater.9b05139

99. Oziri OJ, Wang Y, Watanabe T, et al. PEGylation of silver nanoparticles by physisorption of cyclic poly(ethylene glycol) for enhanced dispersion stability, antimicrobial activity, and cytotoxicity. *Nanoscale Adv*. 2022;4(2):532-545. doi:10.1039/d1na00720c

100. Fratoddi I. Hydrophobic and hydrophilic au and ag nanoparticles. Breakthroughs and perspectives. *Nanomaterials*. 2018;8(1). doi:10.3390/nano8010011

101. Song YJ, Wang M, Zhang XY, Wu JY, Zhang T. Investigation on the role of the molecular weight of polyvinyl pyrrolidone in the shape control of highyield silver nanospheres and nanowires. *Nanoscale Res Lett*. 2014;9(1):1-8. doi:10.1186/1556-276X-9-17

102. Chandra S, Barick KC, Bahadur D. Oxide and hybrid nanostructures for therapeutic applications ☆. *Adv Drug Deliv Rev*. 2011;63(14-15):1267-1281. doi:10.1016/j.addr.2011.06.003

103. Fahmy HM, Mosleh AM, Elghany AA, et al. Coated silver nanoparticles: Synthesis, cytotoxicity, and optical properties. *RSC Adv*. 2019;9(35):20118-20136. doi:10.1039/c9ra02907a

104. Kota S, Dumpala P, Anantha RK, Verma MK, Kandepu S. Evaluation of therapeutic potential of the silver/silver chloride nanoparticles synthesized with the aqueous leaf extract of Rumex acetosa. *Sci Rep*. 2017;7(1):1-11. doi:10.1038/s41598-017-11853-2

105. Aslan K, Wu M, Lakowicz JR, Geddes CD. Fluorescent core-shell Ag@SiO2 nanocomposites for metal-enhanced fluorescence and single nanoparticle sensing platforms. *J Am Chem Soc*. 2007;129(6):1524-1525. doi:10.1021/ja0680820

106. Kovács D, Igaz N, Gopisetty MK, Kiricsi M. Cancer Therapy by Silver Nanoparticles: Fiction or Reality? *Int J Mol Sci*. 2022;23(2). doi:10.3390/ijms23020839

107. Prasher P, Sharma M, Mudila H, et al. Emerging trends in clinical implications of bio-conjugated silver nanoparticles in drug delivery. *Colloids Interface Sci Commun*. 2020;35(December 2019):100244. doi:10.1016/j.colcom.2020.100244

108. Kasithevar M, Periakaruppan P, Muthupandian S, Mohan M. Antibacterial efficacy of silver nanoparticles against multi-drug resistant clinical isolates from post-surgical wound infections. *Microb Pathog*. 2017;107:327-334. doi:10.1016/j.micpath.2017.04.013

109. Arranja AG, Pathak V, Lammers T, Shi Y. Tumor-targeted nanomedicines for cancer theranostics. *Pharmacol Res*. 2017;115:87-95. doi:10.1016/j.phrs.2016.11.014

110. Elechiguerra JL, Burt JL, Morones JR, et al. Interaction of silver nanoparticles with HIV-1. *J Nanobiotechnology*. 2005;3:1-10. doi:10.1186/1477-3155-3-6

111. Egger S, Lehmann RP, Height MJ, Loessner MJ, Schuppler M. Antimicrobial properties of a novel silver-silica nanocomposite material. *Appl Environ Microbiol*. 2009;75(9):2973-2976. doi:10.1128/AEM.01658-08

112. Makvandi P, Wang C yu, Zare EN, Borzacchiello A, Niu L na, Tay FR. Metal-Based Nanomaterials in Biomedical Applications: Antimicrobial Activity and Cytotoxicity Aspects. *Adv Funct Mater*. 2020;30(22). doi:10.1002/adfm.201910021

113. Chen S, Quan Y, Yu YL, Wang JH. Graphene Quantum Dot/Silver Nanoparticle Hybrids with Oxidase Activities for Antibacterial Application. *ACS Biomater Sci Eng*. 2017;3(3):313-321. doi:10.1021/acsbiomaterials.6b00644

114. Malekzadeh M, Yeung KL, Halali M, Chang Q. Preparation and antibacterial behaviour of nanostructured Ag@SiO2-penicillin with silver nanoplates. *New J Chem*. 2019;43(42):16612-16620. doi:10.1039/c9nj03727f

115. Zhang Y, Peng H, Huang W, Zhou Y, Yan D. Facile preparation and characterization of highly antimicrobial colloid Ag or Au nanoparticles. *J Colloid Interface Sci*. 2008;325(2):371-376. doi:10.1016/j.jcis.2008.05.063

116. Yoon KY, Byeon JH, Park JH, Ji JH, Bae GN, Hwang J. Antimicrobial characteristics of silver aerosol nanoparticles against Bacillus subtilis bioaerosols. *Environ Eng Sci*. 2008;25(2):289-293. doi:10.1089/ees.2007.0003

117. Tian Y, Qi J, Zhang W, Cai Q, Jiang X. Facile, one-pot synthesis, and antibacterial activity of mesoporous silica nanoparticles decorated with well-dispersed silver nanoparticles. *ACS Appl Mater Interfaces*. 2014;6(15):12038-12045. doi:10.1021/am5026424

118. Kim YH, Lee DK, Cha HG, Kim CW, Kang YS. Synthesis and characterization of antibacterial Ag - SiO2 nanocomposite. *J Phys Chem C*. 2007;111(9):3629-3635. doi:10.1021/jp068302w

119. Dhanalekshmi KI, Meena KS. Comparison of antibacterial activities of Ag@TiO2 and Ag@SiO2 core-shell nanoparticles. *Spectrochim Acta - Part A Mol Biomol Spectrosc*.

2014;128:887-890. doi:10.1016/j.saa.2014.02.063

120. Thiagamani SMK, Rajini N, Siengchin S, Varada Rajulu A, Hariram N, Ayrilmis N. Influence of silver nanoparticles on the mechanical, thermal and antimicrobial properties of cellulose-based hybrid nanocomposites. *Compos Part B Eng*. 2019;165(February):516-525. doi:10.1016/j.compositesb.2019.02.006
121. Jeevanandam J, Krishnan S, Hii YS, et al. Synthesis approach-dependent antiviral properties of silver nanoparticles and nanocomposites. *J Nanostructure Chem*. 2022;(0123456789). doi:10.1007/s40097-021-00465-y
122. Lee SH, Jun BH. Silver nanoparticles: Synthesis and application for nanomedicine. *Int J Mol Sci*. 2019;20(4). doi:10.3390/ijms20040865
123. Miranda RR, Sampaio I, Zucolotto V. Exploring silver nanoparticles for cancer therapy and diagnosis. *Colloids Surfaces B Biointerfaces*. 2022;210(November 2021):112254. doi:10.1016/j.colsurfb.2021.112254
124. Mauricio MD, Guerra-Ojeda S, Marchio P, et al. Nanoparticles in medicine: A focus on vascular oxidative stress. *Oxid Med Cell Longev*. 2018;2018. doi:10.1155/2018/6231482
125. Bastos V, Ferreira-de-Oliveira JMP, Carrola J, et al. Coating independent cytotoxicity of citrate- and PEG-coated silver nanoparticles on a human hepatoma cell line. *J Environ Sci (China)*. 2017;51:191-201. doi:10.1016/j.jes.2016.05.028
126. Cai L, Qin X, Xu Z, et al. Comparison of Cytotoxicity Evaluation of Anticancer Drugs between Real-Time Cell Analysis and CCK-8 Method. *ACS Omega*. 2019;4(7):12036-12042. doi:10.1021/acsomega.9b01142
127. Nguyen KC, Seligy VL, Massarsky A, et al. Comparison of toxicity of uncoated and coated silver nanoparticles. *J Phys Conf Ser*. 2013;429(1). doi:10.1088/1742-6596/429/1/012025
128. Ahamed M, Karns M, Goodson M, et al. DNA damage response to different surface chemistry of silver nanoparticles in mammalian cells. *Toxicol Appl Pharmacol*. 2008;233(3):404-410. doi:10.1016/j.taap.2008.09.015
129. Danciu C, Pinzaru I, Coricovac D, et al. Betulin silver nanoparticles qualify as efficient antimelanoma agents in in vitro and in vivo studies. *Eur J Pharm Biopharm*. 2019;134:1-19. doi:10.1016/j.ejpb.2018.11.006
130. Castiglioni S, Cazzaniga A, Perrotta C, Maier JAM. Silver nanoparticles-induced

cytotoxicity requires ERK activation in human bladder carcinoma cells. *Toxicol Lett*. 2015;237(3):237-243. doi:10.1016/j.toxlet.2015.06.1707

131. Pinzaru I, Coricovac D, Dehelean C, et al. Stable PEG-coated silver nanoparticles – A comprehensive toxicological profile. *Food Chem Toxicol*. 2018;111(November 2017):546-556. doi:10.1016/j.fct.2017.11.051
132. Wang X, Li T, Su X, et al. Genotoxic effects of silver nanoparticles with/without coating in human liver HepG2 cells and in mice. *J Appl Toxicol*. 2019;39(6):908-918. doi:10.1002/jat.3779
133. Mukha I, Vityuk N, Grodzyuk G, et al. Anticancer effect of Ag, Au, and Ag/Au bimetallic nanoparticles prepared in the presence of tryptophan. *J Nanosci Nanotechnol*. 2017;17(12):8987-8994. doi:10.1166/jnn.2017.14106
134. Mansour HH, Eid M, El-Arnaouty MB. Effect of silver nanoparticles synthesized by gamma radiation on the cytotoxicity of doxorubicin in human cancer cell lines and experimental animals. *Hum Exp Toxicol*. 2018;37(1):38-50. doi:10.1177/0960327116689717
135. Gabizon AA, de Rosales RTM, La-Beck NM. Translational considerations in nanomedicine: The oncology perspective. *Adv Drug Deliv Rev*. 2020;158:140-157. doi:10.1016/j.addr.2020.05.012
136. Najahi-Missaoui W, Arnold RD, Cummings BS. Safe nanoparticles: Are we there yet? *Int J Mol Sci*. 2021;22(1):1-22. doi:10.3390/ijms22010385
137. Zhong Z, Wu W, Wang D, et al. Biosensors and Bioelectronics Nanogold-enwrapped graphene nanocomposites as trace labels for sensitivity enhancement of electrochemical immunosensors in clinical immunoassays : Carcinoembryonic antigen as a model. *Biosens Bioelectron*. 2010;25(10):2379-2383. doi:10.1016/j.bios.2010.03.009
138. Aydın EB, Aydın M, Sezgintürk MK. Author ' s Accepted Manuscript. Published online 2017. doi:10.1016/j.bios.2017.05.056
139. Zhou C, Liu D, Xu L, et al. A sensitive label-free amperometric immunosensor for alpha-fetoprotein based on gold nanorods with different aspect ratio. *Sci Rep*. 2015;5:1-7. doi:10.1038/srep09939
140. Oliveira N, Costa-Rama E, Viswanathan S, Delerue-Matos C, Pereira L, Morais S. Label-free Voltammetric Immunosensor for Prostate Specific Antigen Detection.

Electroanalysis. 2018;30(11):2604-2611. doi:10.1002/elan.201800417

141. Li J, Gao T, Gu S, Zhi J, Yang J, Li G. An electrochemical biosensor for the assay of alpha-fetoprotein-L3 with practical applications. *Biosens Bioelectron*. 2017;87:352-357. doi:10.1016/j.bios.2016.08.071
142. Zhao Y, Chen J, Zhong H, et al. Functionalized Ag/Fe-MOFs nanocomposite as a novel endogenous redox mediator for determination of α2,6-sialylated glycans in serum. *Microchim Acta*. 2020;187(12). doi:10.1007/s00604-020-04608-w
143. Xu D, Hou B, Qian L, Zhang X, Liu G. Non-enzymatic electrochemical sensor based on sliver nanoparticle-decorated carbon nanotubes. *Molecules*. 2019;24(18):1-11. doi:10.3390/molecules24183411
144. Mohammadi S, Khayatian G. Silver nanoparticles modified with thiomalic acid as a colorimetric probe for determination of cystamine. *Microchim Acta*. 2017;184(1):253-259. doi:10.1007/s00604-016-1991-4
145. Dewangan L, Korram J, Karbhal I, Nagwanshi R, Jena VK, Satnami ML. A colorimetric nanoprobe based on enzyme-immobilized silver nanoparticles for the efficient detection of cholesterol. *RSC Adv*. 2019;9(72):42085-42095. doi:10.1039/c9ra08328f
146. Miao P, Han K, Sun H, et al. Melamine functionalized silver nanoparticles as the probe for electrochemical sensing of clenbuterol. *ACS Appl Mater Interfaces*. 2014;6(11):8667-8672. doi:10.1021/am501473m
147. Lokina S, Stephen A, Kaviyarasan V, Arulvasu C, Narayanan V. SC. *Eur J Med Chem*. Published online 2014. doi:10.1016/j.ejmech.2014.02.010
148. Li J, Gao T, Gu S, Zhi J, Yang J, Li G. An electrochemical biosensor for the assay of alpha-fetoprotein-L3 with practical applications. *Biosens Bioelectron*. 2017;87:352-357. doi:10.1016/j.bios.2016.08.071
149. Chen W, Wang L, He R, Xu X, Jiang W. Convertible DNA ends-based silver nanoprobes for colorimetric detection human telomerase activity. *Talanta*. 2018;178(July 2017):458-463. doi:10.1016/j.talanta.2017.09.057
150. Liu Y, Chen Y, Xiang R. DETECTION OF CANCER BIOMARKERS WITH NANOTECHNOLOGY. 2013;9(1):71-89. doi:10.3844/ajbbsp.2013.71.89
151. Cheng Z, Li M, Dey R, Chen Y. Nanomaterials for cancer therapy: current progress and perspectives. *J Hematol Oncol*. 2021;14(1):1-27. doi:10.1186/s13045-021-01096-0

Chapter 3

Experimental and Characterization Techniques

3.1. Introduction

In this thesis, the chemical route of synthesis of silver nanoparticles, followed by its coating through the modified Stober method[1], has been demonstrated. The surface characterization, phase analysis, structural analysis, compositional analysis, and the antimicrobial and anticancerous properties of synthesized nanoparticles against disease-causing micro-organisms and mammalian cells were analyzed by different techniques (shown in figure no. 3.1) through X-ray diffraction (XRD), UV-Visible (UV-Vis) spectroscopy, Energy dispersive X-ray spectroscopy (EDX), Scanning Electron Microscopy (SEM), Transmission Electron Microscopy (TEM), Dynamic Light Scattering (DLS), Fourier Transform Infra-red (FTIR) spectroscopy, Zeta-potential, Electrochemical Impedance Spectroscopy (EIS), Cyclic Voltammetry, Atomic Force Microscopy (AFM), Raman Spectroscopy and cytotoxicity studies by Flow cytometry. The current chapter is consigned to describe the fundamental principle of the techniques employed for characterization.

3.2. Synthesis of silica-coated silver nanoparticles

Over the years, researchers have shown considerable effort in advancing different techniques for synthesizing and tailoring nanostructured materials and nanoparticles. Additionally, the core-shell hybrid material has gained enough attraction because of the proficiency in the management of particles' shape and size, surface properties as well as compositions of the materials.

Figure 3.1: Various characterization techniques utilized for Ag nanoparticles and Ag@SiO_2 nanoparticles.

To study their broad potential applications colloidal silver nanoparticles were prepared by chemical reduction of tri-sodium citrate through the modified Turkevich method[2]. Synthesis of silica-coated silver nanoparticles was accomplished by the altered Stober method. The thickness of the silica shell can be conveniently controlled by the concentration of utilized tetraethyl orthosilicate (TEOS). The shell can modify the surface's functionality, charge, and reactivity, enhancing the stability and dispersive qualities of the core[3]. Later, catalytic, magnetic, and optical functions can be transmitted to the colloidal nanomaterials through the shell material. To exhibit the versatility of the hybrid silica-coated silver nanoparticles; we have illustrated their relevance on two platforms- therapy and detection.

3.3. Structural characterization techniques

3.3.1. Light scattering techniques (Dynamic light scattering)

Dynamic light scattering is a prominent tool; utilized to determine the specific size of the nanoparticles. DLS evaluates light dissipated through a laser provenance that travels through a liquid solution, pictorial representation shown in figure no. 3.2. By evaluating the distortion of the dispersed light intensity along with time, information can be gained about the size of the nanoparticles in the liquid solution. This investigation is established upon the diffusive motion of the nanoparticles in a liquid solution(by Brownian motion); which signifies smaller particles will pass with an increased pace and scatter more light than larger particles. The basic hydrodynamic diameter (width of a contingent nonporous sphere that diffuses at the identical pace as the nanoparticles being characterized) can be estimated from the time subservience of the scattering intensity quantifications. The hydrodynamic diameter is a requisite factor in another sizing calculation namely TEM since it brings forth knowledge about the aggregation condition of particles in colloidal suspension.

Firmly disassembled liquid solutions possess particles with hydrodynamic diameters homogenous to or rather big compared to TEM size, whereas tremendously aggregated suspension will possess a larger hydrodynamic diameter than the TEM size. The DLS measurements of the colloidal samples were performed utilizing a NICOMPIM 380ZIS (Santa Barbara, CA, USA) having a red He-Ne laser diode at 632.8 Å in a fixed angle 90° plastic cell. All of the measurements were accomplished by utilizing a circulating water bath at 25.0+ 0.1°C. Fig 3.2 shows a typical diagram of the DLS instrument. Cylindrical cells of 10mm diameter were employed comprehensively in light scattering technique measurements.

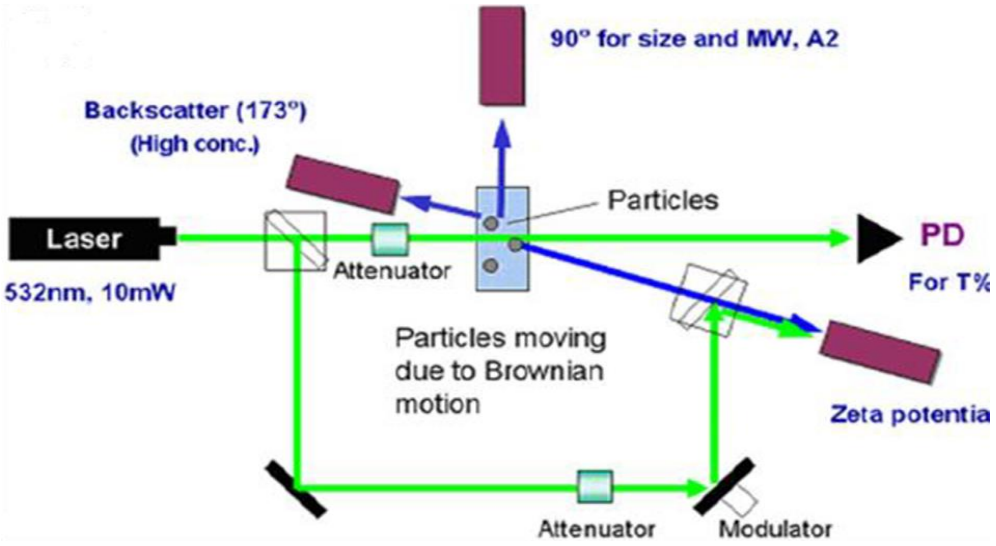

Figure 3.2: Schematic representation of Dynamic Light scattering instrument[4].

3.3.2. X-ray diffraction analysis

X-ray diffraction is a very potent and at the same time very basic methodology for the sake of characterization of thin films and nano-materials. It is a non-destructive, non-contact technique that gives beneficial information for example-specific orientation and size of the grain, composition, presence of phases, thickness of the film, and state of the strain. The XRD technique mainly revolves around the diffraction of x-ray radiation, which takes place, particularly whilst the wavelength of the wave motion is in a similar arrangement of magnitude as the repeat space between scattering centres.

Such diffraction-pattern is acknowledged as Bragg's law (as shown in equation no.3.1) because Bragg theoretically examined the diffraction pattern of crystalline material and framed it in mathematical expression as in the following equation-

$$2d\sin\theta=n\lambda \text{-------(3.1)}$$

Here, d= Interplanar spacing, θ= diffraction angle, λ= wavelength of X-ray, n= order of diffraction

Regular diffractometer comprised of an x-ray source and a detector for the specific detection of diffracted x-rays. The basic depiction of the usual diffractometer is prepared contingent on the geometry proposed by Bragg-Brentano. Fig 3.3 (a) exhibits the graphical illustration of the x-ray diffractometer. Here, a crystalline solid is a unit cell on which atoms are sequenced in a specific periodic pattern referred to along with its inter-atomic spacing corresponding to the wavelength of x-rays (0.5 to 2.5 Aº). Therefore, crystals are the finest gratings for x-ray diffraction studies. The specific directions of diffracted x-rays give details about the ordering of atoms. Thus the structure of the crystal and phase formation can be established by x-ray diffraction studies. The method of fulfilling Bragg's law is devised and can be completed by constantly altering either θ or λ throughout the experiment.

Normally, four distinct diffraction methods are distinguished in which these quantities (θ or λ) are changed: the Bragg x-ray spectrometer, powder, rotating crystal, and Laue photographic methods.

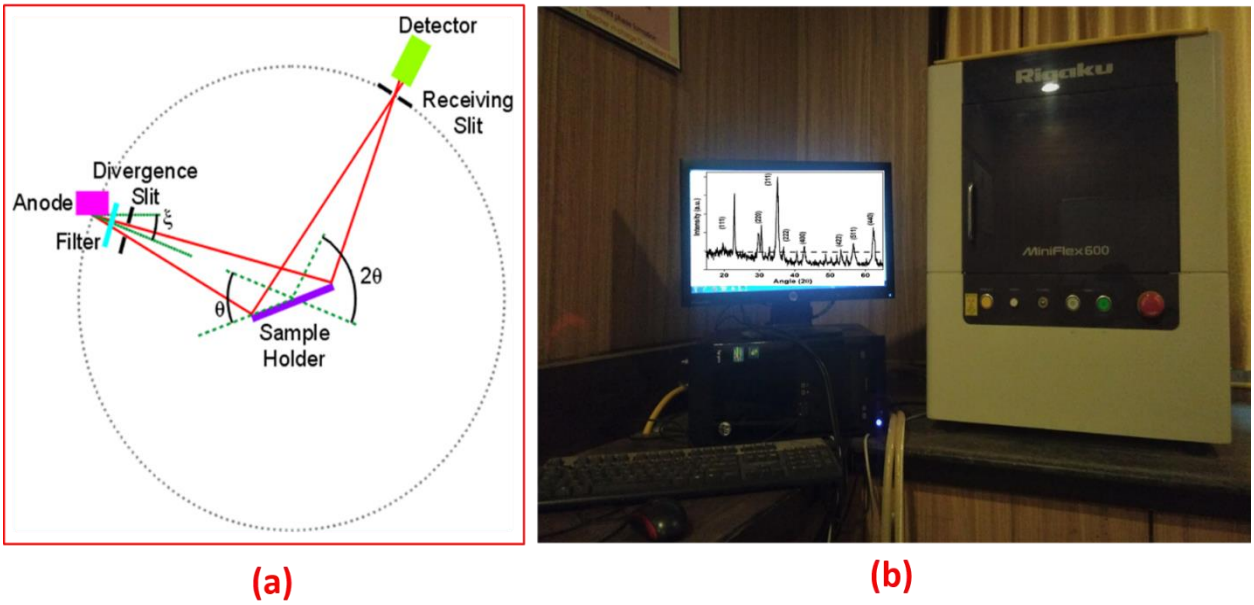

Figure 3.3: (a) Schematic diagram of XRD diffractometer and (b) Photograph of Rigaku Miniflex-600 X-Ray diffractometer[5].

Phase identification

Particular phases can be acknowledged from the d-spacing in a sample employing the standard JCPDS powder diffraction file data offered by the International Centre for Diffraction Data (ICDD) and the reflections can be matched with Miller indices, as displayed in the equation no.3.2. Assuming that, the average crystallite size is very low (less than 2000A° diameter), then there is an added broadening of the beam of the diffracted x-ray.

Crystallite size can be calculated followed by this broadening of the peak; through the Scherrer equation as follows-

$$t = 0.9\,\lambda / \beta \cos\theta_B \text{ ----------(3.2)}$$

Here, t = particle size, θ = diffraction angle, λ = wavelength of x-rays, β = Line broadening at full width at half maxima (FWHM).

In this thesis, the crystalline size and structure of the chemically synthesized and coated hybrid nanoparticles were recorded by Rigaku Miniflex 600 diffractometer Cu Kα (λ =1.54A0) having an accelerating voltage of 40KV and the 2θ range were between 200 to 800.

3.4. Morphological and topographical techniques

3.4.1. Scanning electron microscopy (SEM)

Scanning Electron Microscopy is employed to investigate the topography, morphology, and composition (utilizing EDS) of the samples. The SEM technique relies on the principle that the investigation carried on is centered on a beam of the electron.

Once, a beam of electrons coordinates with the atom of the investigated sample; it resulted in elastic and inelastic scattering. The higher energy electron, that is emitted through elastic scattering is termed a backscattered electron, whereas that is ejected through inelastic scattering is termed a secondary electron. All of these signals are forwarded to the detector and after that, they go through a cathode ray tube via an amplifier, at which point the images are constructed, which provides the specifications about the surface of the sample and other information. A simplified scanning electron microscope is illustrated in fig.3.4.

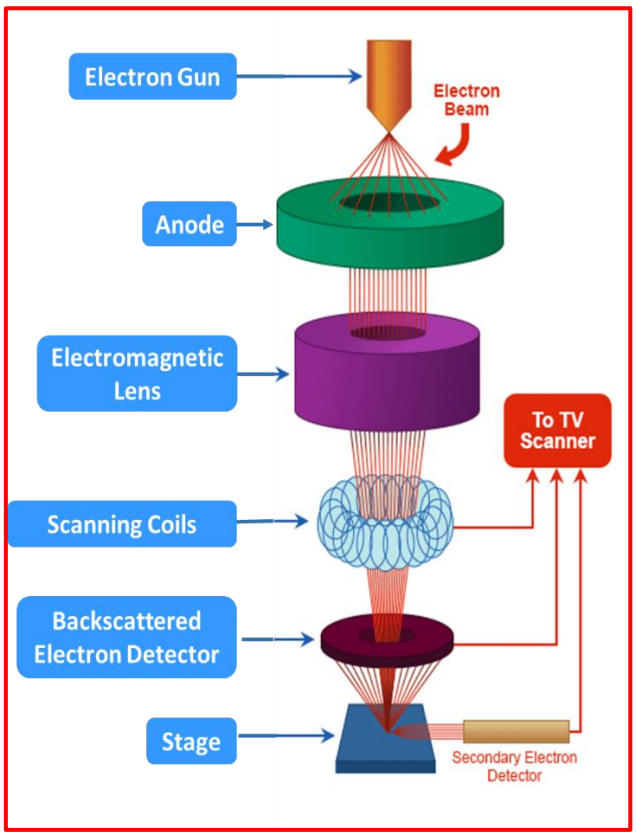

Figure 3.4: Ray diagram of field emission scanning electron microscope[6].

The SEM instrument utilized in the current work is - Sem, Model: JEOL JSM-6360A instrument with an operating voltage of 20 kV.

3.4.2. Transmission electron microscopy (TEM)

Transmission electron microscopy (TEM) is the prominent characterization technique utilized to study the shape, size, morphology, and size distribution of the particles as well as the crystallinity of the nanoparticles. The principle of TEM is that it utilizes a high-power beam of electrons originating through the electron source. To focus the beam of electrons; coherent lenses are used. Once the thin

beam of the electron is focused and falls on the specimen, a number of events take place. The indicated transmitted electron is focussed via the objective lens to create an image. The typical ray diagram of TEM is exhibited in fig.3.5. The desired sample, which is intended for analysis, should be exceptionally thin and the range should be between 0.1 to 1.0µm. The preparation of the sample is a very essential step in the analysis. The standard method for the preparation of the sample involves diffusion of the material in the solvent like- water to make a colloidal solution and out of which a single drop is deposited on a conducting grid of copper (size approx 1µm) and then properly dried.

Such a grid is utilized for the investigation of the sample. It has been noticed that standard TEM instrument utilizes transmitted or dissipated beam for the creation of the image. The description of the instrument employed in the current thesis is- Philips CM 200 model TEM. The operating voltage is in the range of 20-200kV with a 2.4 A° resolution.

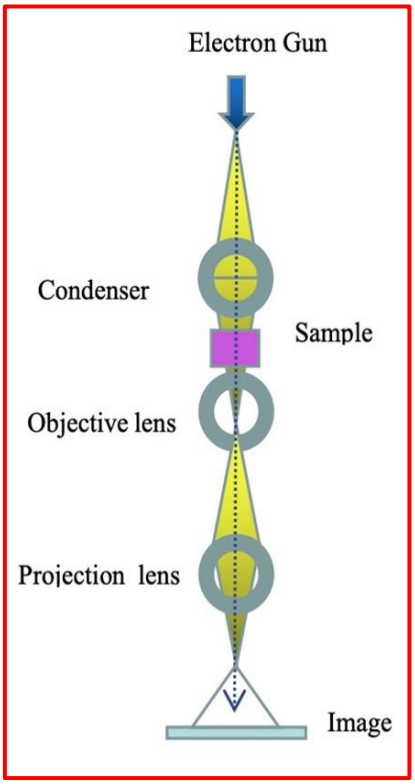

Figure 3.5: Basic ray diagram of TEM[7].

3.4.3. Atomic force microscopy

Atomic force microscopy (AFM) is a non-optical, high-resolution imaging methodology, at first validated by Binnig, Gerber, and Quate in 1985. Afterward, it evolved into an impressive measurement technique for surface analysis. AFM permits precise and non-destructive analysis of the topographical, optical, electrical, mechanical, chemical, magnetic, etc qualities of a sample surface along with high resolution in liquids, air, or ultrahigh vacuum. Such an amazing merger of potentiality executes AFM indispensable in nearly state-of-the-art labs based on science and technology around the world. AFM

intensifies the image of the desired specimen and utilizes a cantilever constructed from silicon nitride or silicon along with a minimum spring constant to make the image of the sample. From the upper side of the cantilever, a laser beam is constantly reflected which detects the bend that takes place in the cantilevers as well as measures the real position of the cantilever. Fig 3.6 shows a typical image of the AFM instrument. AFM records 3 D-image of the outer topography of the specimen with the influence of persistent applied force that resulted concisely into a whole maximum resolution of the image.

The specification of the instrument used for the AFM analysis is INNOVA 1B3BE on the X-Y scan rate of 1-90μm and Z scan rate between 50-7.5 μm. It provides an excellent state-of-the-art system that gives accurate measurements as well as noise levels impending particular open-loop operations.

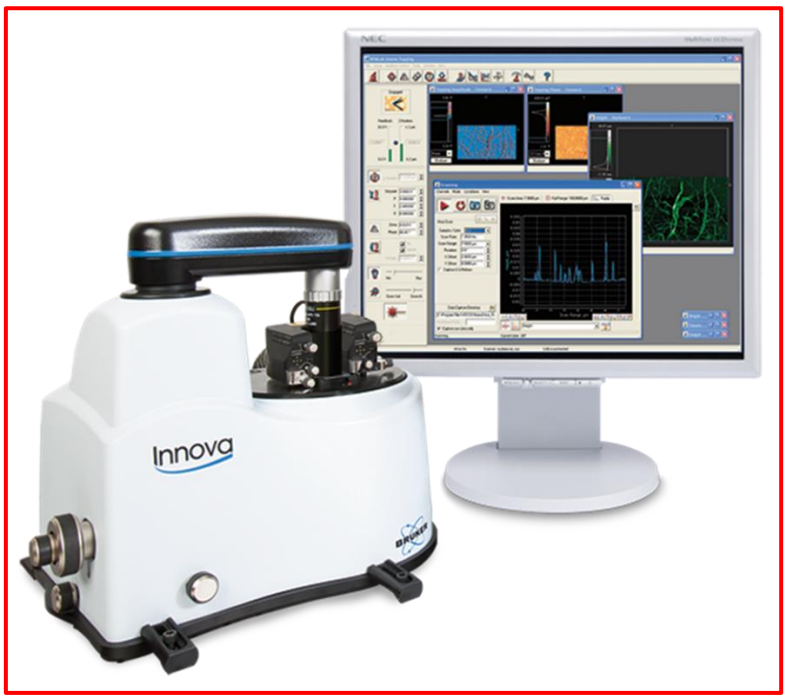

Figure 3.6: Photograph of Atomic force microscopy[8].

3.5. Spectroscopic analysis techniques

3.5.1. UV-Visible spectroscopy

UV-Vis spectroscopy belongs to reflectance spectroscopy or absorption spectroscopy in the ultraviolet-visible spectral region. This spectroscopy has been frequently utilized in analytical chemistry for the quantitative determination of numerous analytes, namely highly conjugated organic compounds, biological macromolecules, and transition metal ions. In recent years, UV-Vis spectroscopy has also been employed with high precision, high energy spectrophotometers are in the field because of the quick enhancement in absorption and reflection assessments on solid samples, which includes films, semiconductors, glass, and absorbing materials, it is exhibited in equation no.3.3.

Such absorption spectroscopy utilizes electromagnetic radiations ranging between 190nm to 800nm and is distributed into the ultraviolet (190-400nm) and visible (400-800nm) regions. It is well known that light is a prominent source of energy and thus absorption of light by matter creates the elevated energy content of the atoms and molecules. The whole potential energy of a molecule (or atom) is given by below-mentioned equation--

$$E = hv,\ v = c/\lambda \text{----------(3.3)}$$

UV-Visible absorptions in organic molecules are the result of the shifting of valence electrons between molecular orbitals.

Whole amount of the change in the energy of the molecule, ΔE_{total} is shown by following mentioned equation no. 3.4--

$$\Delta E_{total} = \Delta E_{elec} + \Delta E_{vib} + \Delta E_{rot} \text{----------(3.4)}$$

Here, ΔEelec, ΔEvib and ΔErot are the variations in electronic, vibrational, and rotational energy respectively.

The whole gain of energy of a molecule is in a series of discrete states or levels. Among the various states, the variation that takes place in energy is in the order. Photons of UV and visible light have sufficient energy to generate transitions among the various levels of electronic energy in some atoms and molecules. The energy needed to transfer an electron from a lower energy level to a higher energy level is the particular wavelength of light absorbed. The fundamental principle of UV-Vis spectroscopy is founded on the Beer-Lambert law, exhibited in equation no.3.5. The phenomenal Beer-Lambert law gives information about the relation of light intensity and concentration as indicated in the equation-

$$I = I0 \times 10^{-Ɛc1} \text{----------(3.5)}$$

Here, Ɛ is the molar extinction coefficient or molar absorptivity and 1 is the path length.

By combining this equation with light intensity and connecting absorbance it provides the expression as mentioned in equation no.3.6--

$$A = C \times Ɛ \times 1 \text{----------(3.6)}$$

Here, A is the calculated absorbance, C is the concentration of the analyte.

It is well known that noble metal nanoparticles exhibit characteristic surface plasmon resonance and at that point, they absorb light dynamically in the visible region.

Therefore, UV-Vis spectroscopy is the main characterization methodology for the analysis of the nanoparticle-synthesis process. The UV-Vis absorption spectra data reported in this thesis was taken by Shimadzu UV-1800 dual beam Spectrophotometer.

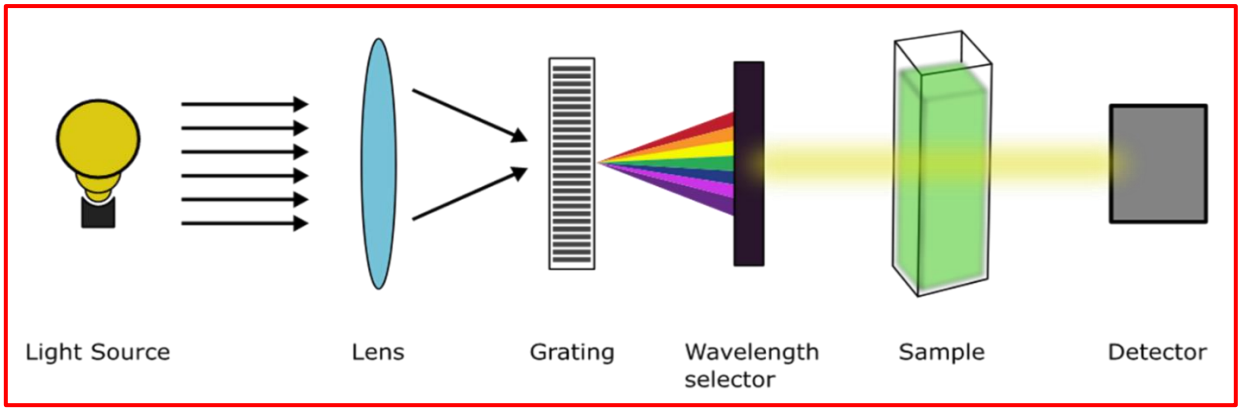

Figure 3.7: Ray diagram of UV-Vis Spectrometry[9].

3.5.2. Fourier Transform Infrared Spectroscopy (FT-IR)

FTIR is one of the dynamic techniques that evolved in 1970 to quantify and qualify materials by using infrared absorption of molecules. This technique is used to analyze both- inorganic as well as organic compounds. It is based on the precept of molecular spectroscopy which signifies that a particular molecule absorbs light energy of a particular wavelength, designated as their resonance frequencies. Thus, verify the presence of a chemical bond or functional group, as one will exhibit a different absorption pattern[10],[11].

So, for the authentication of the functional group present on the facet of silver nanoparticles and silica-coated silver nanoparticles, we have employed FTIR in the current work. It has been observed that infrared (IR) is comprised of a spectral region from the red end side of the visible spectrum (12, 500cm^{-1}, 0.8mm) to the microwave end side (10cm^{-1} to 1000mm) in the electromagnetic spectrum. Such armamentarium is distributed into near (12,500 to 4000cm^{-1}), mid-IR (4000 to 400cm^{-1}), and far-IR (400 to 10 cm^{-1}). Among these, mid-IR (4000 to 400cm^{-1}) is the significant field as almost all of the fundamental vibrations occur in that field only.

The working of FTIR, which is significantly a Michelson interferometer and merely a single mirror, is sliding in current work. The sliding is compelled to create an interferogram, that is transformed through a Fourier transformer. The wavelength of absorption depends on the once constants of the involved bonds, the specific geometry of the atoms, and the relative masses of the atoms. This causes vibrations of the chemical group; present on the surface of the material and produces closed absorption bands which are demonstrated either as absorbance (A) or transmittance (T).

In the present work, the Fourier transform infrared spectra were noted and recorded in transmittance mode with the instrument named Alpha ATR Bruker (Eco ATR 500-400cm^{-1}) spectrum of Ag and Ag@SiO_2 nanoparticles for the study of attachment of functional groups.

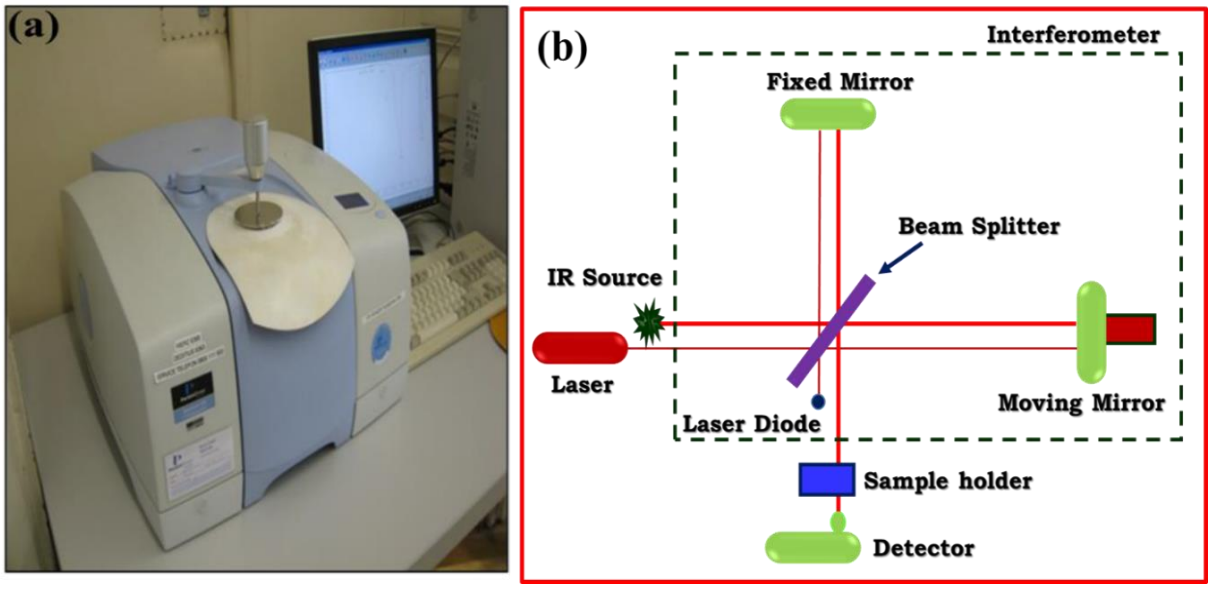

Figure 3.8: (a)illustrates representative FTIR instrument and Fig (b) exhibits the block diagram[12].

Raman Spectroscopy

Raman Spectroscopy is one of the most important, non-destructive chemical investigation methodology which gives exhaustive information about chemical structure, crystallinity, phase, polymorphy and molecular interactions. This technique is founded on the interaction of light coupled with the chemical bonds involved within a material. Raman spectroscopy is based upon the light scattering phenomenon with the help of which a molecular scatters the incident light through a high intensity of laser light source. Maximum of the dispersed light is at the similar wavelength as the source of the laser and it does not deliver beneficial information-which is termed as Rayleigh scatter. Nevertheless, a tiny amount of light (normally 0.0000001%) is dispersed at various wavelength, that hinged on the specific chemical structure of the analyte- this is designated as Raman scatter.

A typical Raman spectrum attributes a number of peaks, displaying the wavelength position and intensity of the Raman scattered light. Every peak correlate to a particular molecular bond vibration, in addition to discrete bonds involved namely- C-H, N-O, C=C, C-C etc, and several group of bonds including polymer chain vibrations benzene ring breathing type, lattice modes etc. The arrangement was accordingly calibrated opposed to silicon wafer peak at 560cm^{-1}. Raman scattering process was excited by a continuous wave argon laser with a power of 100mW(milliwatt). The spectra were resoluted at temperatures of 300 and 78K.

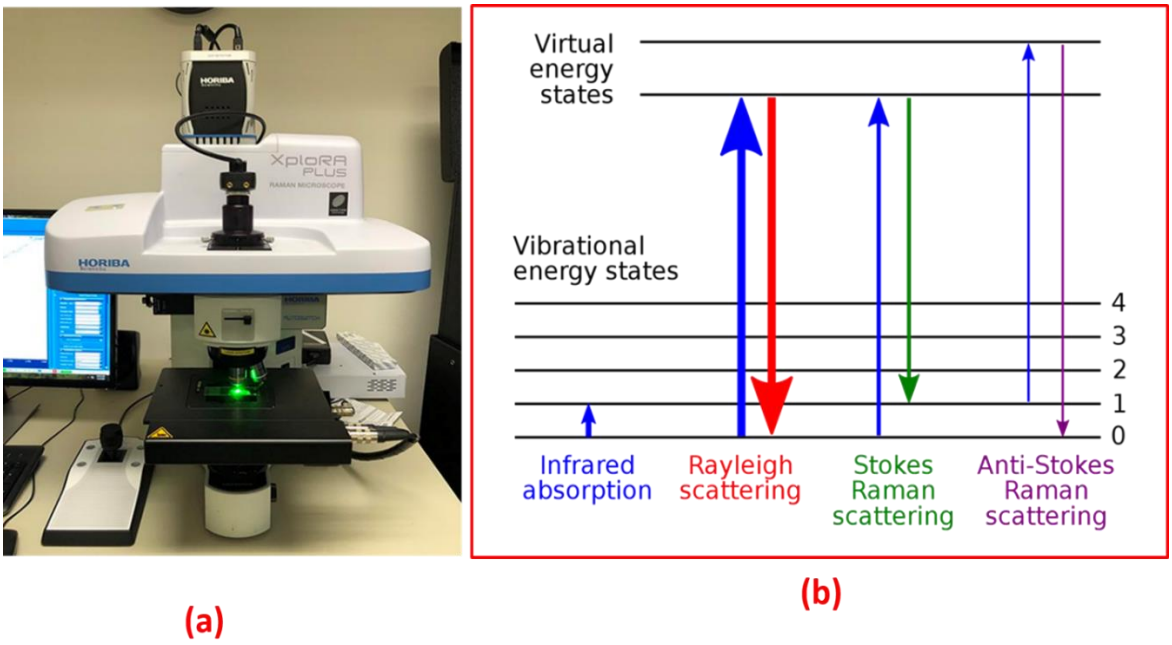

Figure 3.9: (a) Photograph of Raman Spectroscopy,[13] and (b) Energy-level diagram showing the states involved in Raman spectrum[14].

3.6. Electrochemical Analysis

Generally, the three-electrode (half-cell) system is used in electrochemical investigations to determine specific electrochemical properties of a material[15]. The half-cell consists of three electrodes submerged in an electrolyte, namely working electrode, reference electrode, and counter electrode. The schematic of three-electrode cell system described in Figure 3.10.

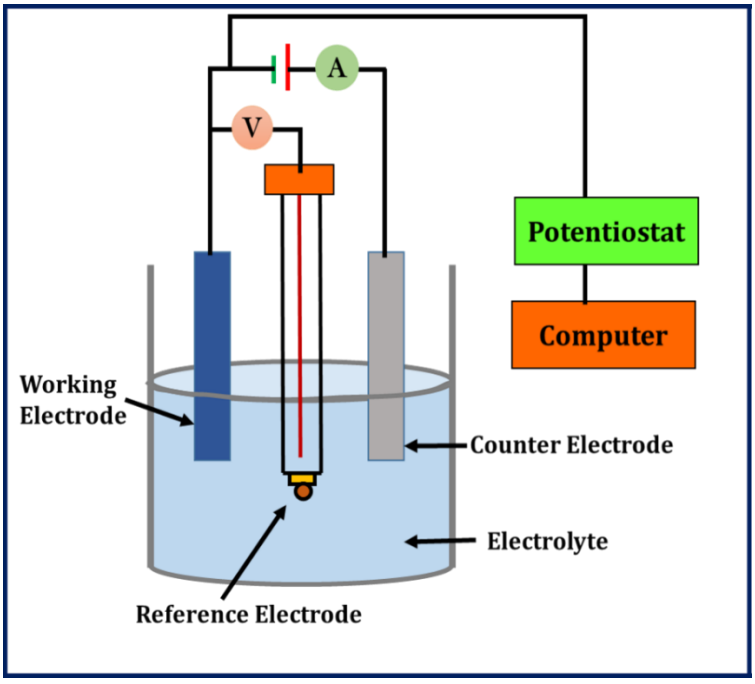

Figure 3.10: Schematic diagram of three-electrode electrochemical (half-cell) system[15]

The electrochemical workstation controllers potential difference betwixt reference and working electrodes and measures the current flowing from counter to working electrode. The obtained current is proportional to voltage developed among working electrode and a reference electrode, then converted to a voltage by a current-to-voltage (I/E) converter and recorded with respect to time by the data-acquisition system. It is noted that, the electrical resistance of an ideal electrometer should be large enough so that it has zero input current. Since, when current passes through a reference electrode, it can change actual potential which in turn affects the precision of data[16].

3.6.1. Electrochemical Impedance Spectroscopy

Electrochemical impedance spectroscopy (EIS) determines the impedance of material in a set of frequencies and is beneficial to bring forth information about the resistance of the electrode-electrolyte interface and charge shifting process[17]. The small AC signal (5 to 50 mV) is applied to the cell over a set of frequencies from 10 μHz to 1 MHz. The output signals are a current response of applied AC signals. The EIS spectra can be analyzed and interpreted by Nyquist[18].

Figure 3.11 illustrates a Nyquist plot with equivalent circuits and involves the following circuit elements: *R*s: ohmic resistance, *R*s+Rct: charge transfer resistance, CPE: constant phase element, and W: Warburg impedance element. The EIS technique is essential because it determines the frequency-dependent and independent electrical components from the Nyquist plot. The imaginary and real parts of impedance are described in the Nyquist plot exhibited in fig. 3.11. In this figure, the semi-circular loop is associated with resistance of charge transfer. In addition, solution resistance is an important term in the impedance of electrochemical cell. The resistance of electrolytic solution depends on the concentration of ions, type of ion, temperature, and geometry of the region in which the electric current flows. Also, the transfer of these charges has fixed kinetics and the kinetics depend on reaction type, temperature, concentration, and potential of reaction products. Furthermore, ionic diffusion can create an impedance called Warburg impedance. Also, impedance is based on the frequency of potential irritability.

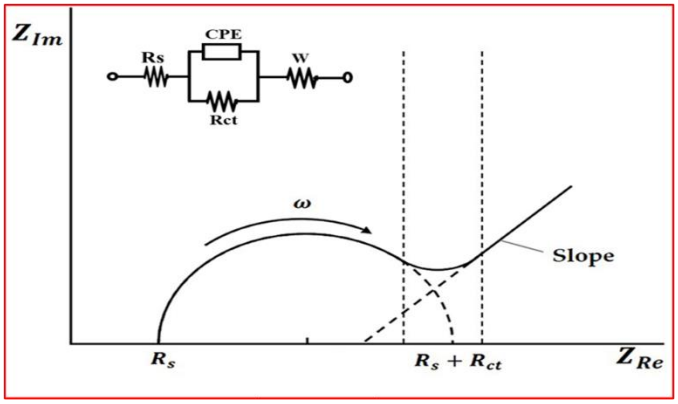

Figure 3.11: Nyquist plot with electrical equivalent circuit[20].

The Warburg impedance is smaller at higher frequencies because the diffusing reactant does not need to go very far. Also, the real-axis intercept (at high frequencies) corresponds to the ohmic resistance. At lower frequencies, the reactors have to diffuse more distance, increasing the Warburg impedance. In the Nyquist plot, Warburg impedance described by a diagonal line with an inclination of 45° arises due to the mass transport of ions. The impedance response mainly depends on the operating voltage[19]. The obtained data were fitted with different interface parameters by algorithms with minimum chi-square values. The EIS was measured under the following circumstances: (i) Open circuit potential condition in the frequency range: 100 kHz-100 MHz; (ii) 10 mV AC-perturbation amplitude of a sinusoidal signal.

3.6.2. Cyclic Voltammetry

Cyclic voltammetry (CV) is electroanalytical technique, it is also called as twoway linear sweep voltammetry (LSV). CV is normally utilized to probe the electrochemical evaluation of active material in an electrolyte solution[20]. It is a potentio dynamic technique whereby the potential of working electrode sweeping between two voltage limits at an anchored voltage scan rate, just as display in fig. 3.12 and, generates basic information about redox behavior, charge transfer kinetics, reversibility and material stability, etc[21].

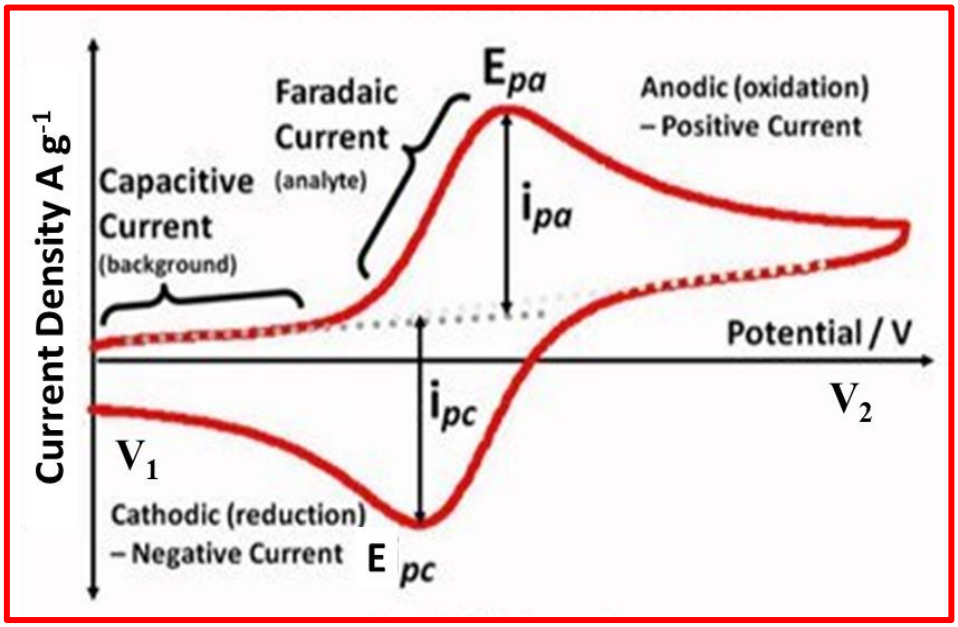

Figure 3.12: Typical CV curve of single electrode with reversible redox reaction[22].

Firstly, selecting initial and final potential is a significant factor for CV measurement. The three-electrode system is used to minimize the ohmic resistance. The potential is applied between a reference electrode and working electrode and current is measured among the working electrode and a counter electrode. The span of operating potentials for a CV in the different electrolytes can varies and not only depends on electrode material but also the composition of electrolytes. Moreover, an

operational potential window of the working electrode depends on redox potential of material and decomposition capacity of electrolytes. Mainly, a positive potential limit is caused by lofty current arising from oxidation of electrolytes as well as reduction of electrolyte brings negative potential limitation.

In CV, the potential is swept within two fixed values (i.e. in a given potential window). When the voltage achieves point V_2, the scan swept back and voltage reversed to point V_1. Where, V_1 and V_2 are the potential limits, i_{pc} and i_{pa} represent the cathodic and anodic peak currents and E_{pc} and E_{pa} are the cathodic and anodic peak voltages of resulted voltammogram. In the course of forward scan, a current surges as potential reaches oxidation potential of the electroactive material, but it declines as potential later increases due to high concentration of electrolytic ions at the electroactive sites. During reversible redox couple, the product formed in initial oxidation reaction reduces during applied reverse potential and generates reverse polarity current.

3.7. Size distribution and colloidal stability characterization techniques

3.7.1. Zeta potential

Zeta potential (also designated as electro-kinetic potential) is a measurement of the functional electric-charge on the facet of the nanoparticle and calculates the charge cohesion of the colloidal nanoparticles. Once a nanoparticle has a net surface charge, the specific charge is screened through an enhanced concentration of ions of opposite charge adjoining the surface. Particles possessing negative zeta-potential will bind to the positively charged surfaces of the nanoparticle and vice versa. Magnitude of the zeta-potential gives details about stability of the particle, with higher magnitude potentials showing enhanced electrostatic repulsion and consequently enhanced stability.

* 40 + mV − Particles are extremely sturdy and stable.
* 20-40mV − Particles are relatively stable.
* 5-20 mV − Particles remain poorly stable.
* 0-5 mV − Particles tend to aggregate or agglomerate.

It is noteworthy to mention that the magnitude of the charge upon the surface of the nanoparticle relies on the pH of the solution. The charge adjacent to the surface can be minimized to zero at a particular pH designated as the isoelectric point. Zeta potential is calculated through incorporating a colloidal solution into a cell, which consists of twin gold electrodes. Once a voltage is exercised to the specific electrode, the particles will flow in the direction of the positively charged electrode.

A Doppler way is employed for the measurement of a particle's velocity as a power of the voltage. A laser ray passes between the cell and as the particles goes constantly through the laser beam the intensity of scattered light varies at a frequency proportional to the speed of the particle. The speed of the particle at different voltages is computed and the following data is utilized to measure the zeta-

potential. Here, the zeta-potential of the chemically synthesized nanoparticles is performed by utilizing a PSS/NICOMP 380 ZLS particles sizing system (Santa Barbara, CA, USA) along with a red He-Ne laser diode at 632.8A° in a stable angle of 90° plastic cell, as displayed in figure no.3.13. The zeta-potential measurements were evaluated at 25°C following a temperature homogenization time interval of 5 min.

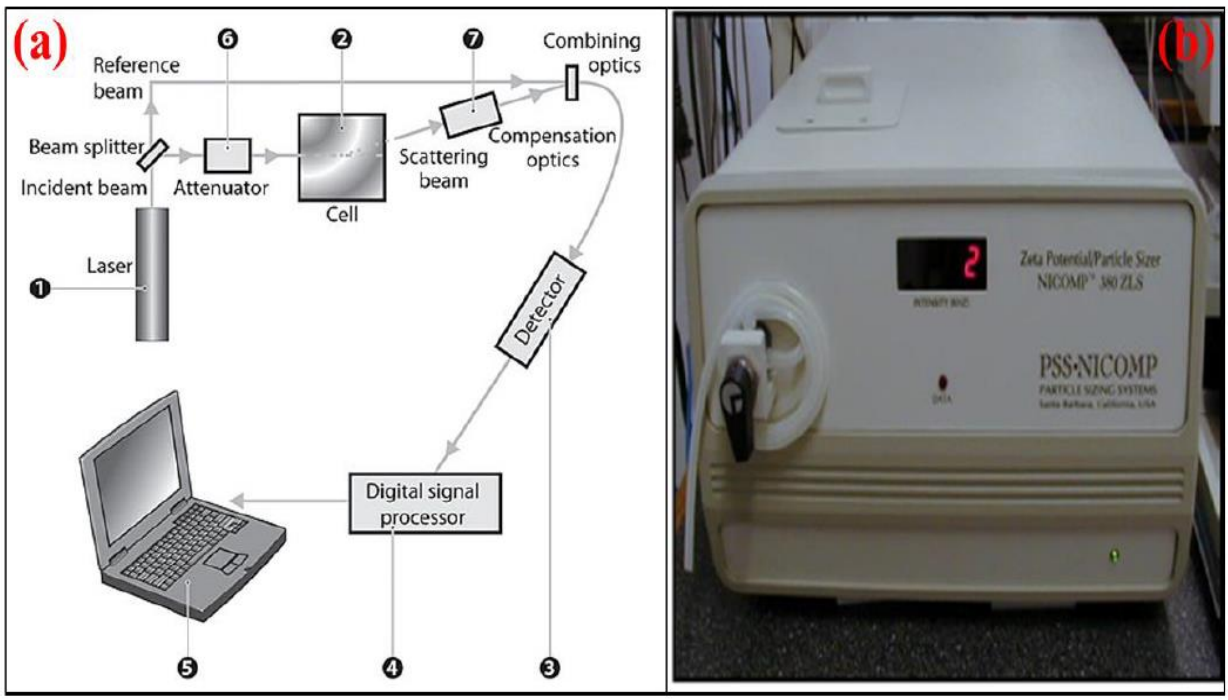

Figure 3.13: (a) Optical configuration of zeta potential instrument, and (b) The zeta potential and particle size analyzer instrument image[23].

3.8. Elemental analysis

3.8.1. Energy dispersive x-ray spectroscopy

In Energy dispersive x-ray spectroscopy (EDS) x-ray is conceivably employed for elemental detection and quantification of the composition of a selected specimen. Such a technique is utilized in combination with a scanning electron microscope (SEM). This method is established on the fact that every element has a distinctive set of atomic structures, which brings about individual sets of peaks, displayed approaching x-ray emission spectrum. In this technique, an x-ray beam or high-energy beam of electrons is focused onto the sample, which is actually studied. The sample consists of electrons, which are in unexcited condition and constrained to the nucleus. The incident x-ray beam can excite an electron in an innermost shell and eliminating it from the shell and generating an electron-hole. Later, the electron from a high energy shell closely packed this space, and among the energy levels of lower energy shell as well as higher energy shell is emancipated in the form of an x-ray. The aforementioned procedure is exhibited in fig 3.14.

Such x-ray energy is the prominent feature of the element from which it was emitted. X-ray detector quantifies the relative profusion of emitted x-rays contrary to their energy. Incident x-ray collides with the detector, which generates a pulse charge, that is then transformed into voltage and finally, it is computed. The spectra of x-ray energy contrary to calculates is estimated to determine the elemental conformation of the relevant sample. Fig.3.14 depicts the prototypical EDX analysis of Ag and Ag@SiO_2 nanoparticles. The specifications of instruments utilized in the present work are JOEL JSM 6360 having an escalating voltage of 20kV and an energy scan in the span of 0-20keV.

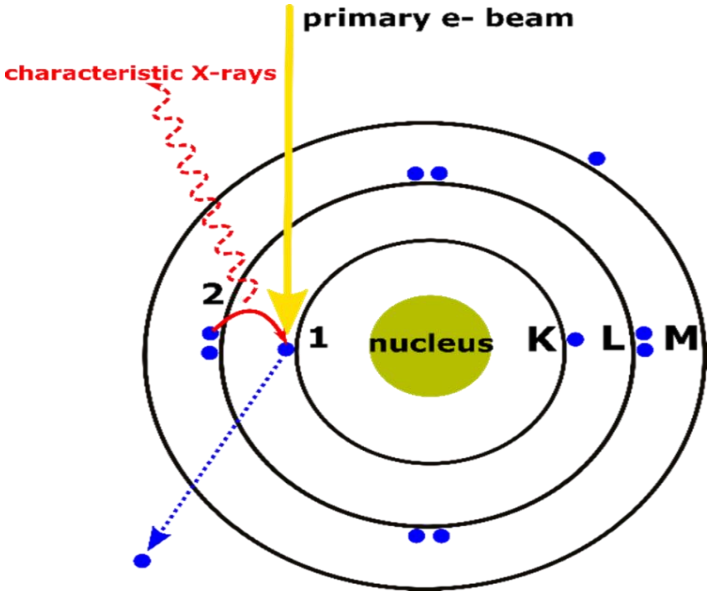

Figure 3.14: Pictorial representation of K, L and M electron shells around nucleus of an atom[24].

3.9. Biological characterization

3.9.1. Anticancerous activity: In-vitro cytotoxicity assays

3.9.1.1. MTT-assay

MTT-assay is a potent methodology to analyze the safe and systematic amount of the drug as well as to observe the cell viability of the cell line. Under particular lab conditions, NADPH adherent cellular oxidoreductase enzymes show the whole number of viable cells. The MTT (3-[4,5-dimethylthiazol-2-yl]-2,5 diphenyl tetrazolium bromide) penetrates the cell membrane and enters the mitochondria. This methodology is developed on the phenomenon of MTT changing into formazan crystals through living cells, which denotes mitochondrial activities. It is a colorimetric assay used for assessing cytotoxicity and can be quantified spectrophotometrically. This assay quantifies the rate of cell proliferation after a metabolic set of events leads to apoptosis or necrosis, resulting in a reduction in cell viability. It is noteworthy to mention that in the absence of cells, the MTT reagent can not gain lofty framework absorbance values.

3.9.1.2. Flowcytometry- assay

Flow cytometry is a quantitative single-cell analysis technique. This technique evolved in the 1970s and soon became an important technology in biological sciences. Flow cytometry is a basic technology that is based on a laser beam. It is utilized in the measurement and detection of chemical as well as physical characteristics of particles or cells in a heterogenous colloidal mixture. Over the years, the employment of flow cytometry has increased because of the fast analysis of numerous characteristics (both quantitative and qualitative) of the cells. The specific properties which can be analyzed by this technique include a particle's granularity or internal complexity, size, and fluorescence intensity. Such unique characteristics are measured utilizing a coupling system named optical-to-electronic systems, which detects the cells dependent on laser dispersed by the cells. Notwithstanding its name, a flow cytometer does not essentially deal with cells; this technique approaches cells most often, however it can deal with molecules or chromosomes or numerous other particles too which can be dispersed in a fluid.

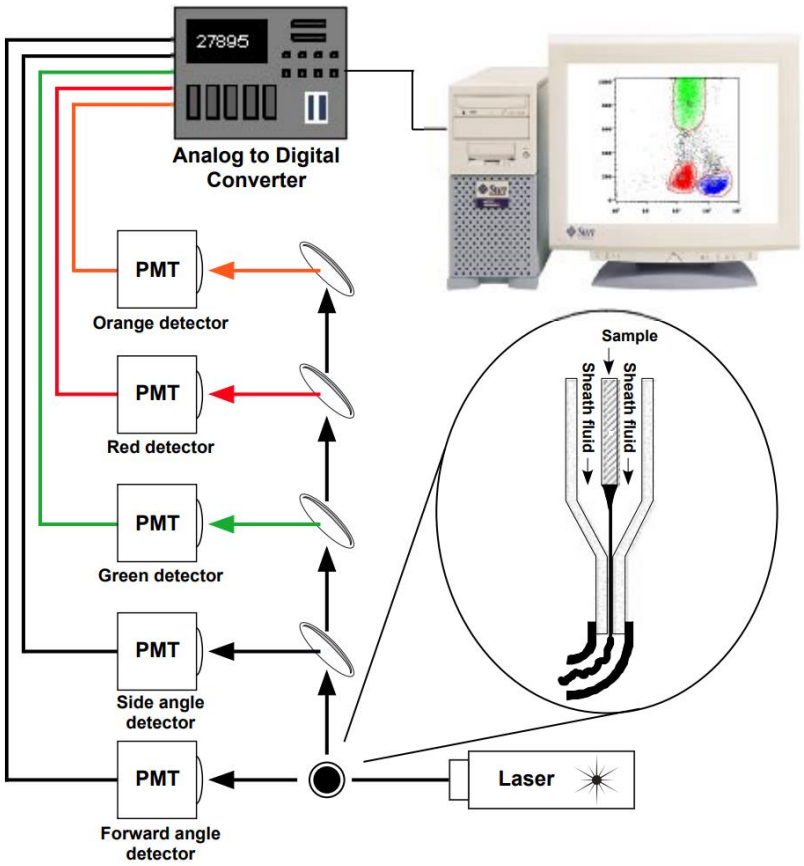

Figure 3.15: Schematic representation of working of Flowcytometry[25].

The fundamental principle of flow cytometry is based on the quantification of light disseminated by the particles, while the fluorescence is perceived when all of these particles have proceeded in a stream via a laser beam (as shown in fig.3.15) A flow cytometer consists of three prominent systems namely optics systems, fluidics, and electronics system. There are four classes of

flow cytometers-Acoustic focusing cytometers, traditional flow cytometers, cell sorters, and imaging flow cytometers. Flow cytometry is utilized in various fields including pathology, immunology, molecular biology, plant biology, virology, and marine biology. Here in the present thesis, we have used flow cytometry for the study of various stages of cell death, necrosis, and apoptosis centered on the biochemical and morphological alteration that takes place in cancerous cells. It provides a fast multi-parametric examination of separate cells in the solution.

3.9.2. Antimicrobial activity

Instead of the fascinating antimicrobial qualities of silver and hybrid silver nanoparticles, it is worthwhile to discuss various methodologies utilized to observe antibacterial as well as antifungal activities. Numerous types of techniques nowadays are available for the evaluation of in vitro antimicrobial performance of antimicrobial agents. Such techniques are listed below-

Agar disc diffusion method

Agar well diffusion method

Shake flask method

3.9.2.1. Agar disc diffusion method

The agar disc diffusion technique is basic and commonly employed for the study of antimicrobial activities, exhibited in figure no.3.16. In such a procedure, desired test organisms are dispersed onto the facet of the nutrient agar medium and after that, the discs of particular antimicrobial agents are allocated on the surface of the plate having sterile nutrient agar medium. Desired tested samples are preserved for 10 minutes in the refrigerator.

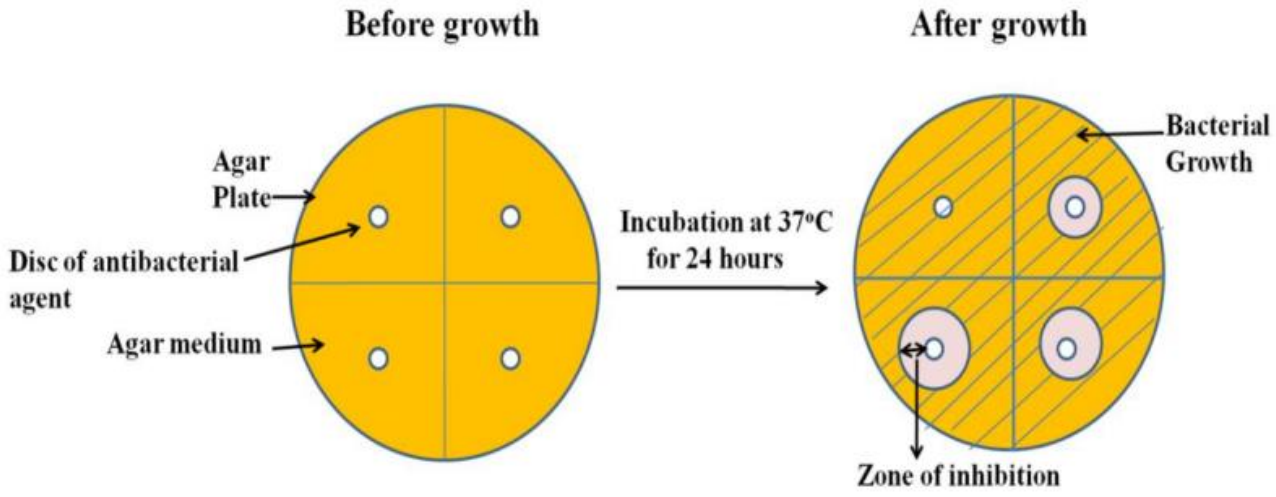

Figure 3.16: Pictorial representation of Agar disc diffusion technique[26]

3.9.2.2. Agar well diffusion method

In this procedure, the plates containing agar are inoculated through a bacterial inoculum onto the whole plate (shown in figure no.3.17). After that, a well is made having a diameter of about 6-8

mm by the use of a tip or sterile cork borer and the desired volume of silver and hybrid silver nanoparticles are poured into the well by the use of sterile micropipette. Further plates of agar are incubated inside the incubator under appropriate conditions according to the test organisms. In the agar plate, both of the nanoparticles are dispersed and hinders the growth of microbial strain. Finally, the zone of inhibition is calculated.

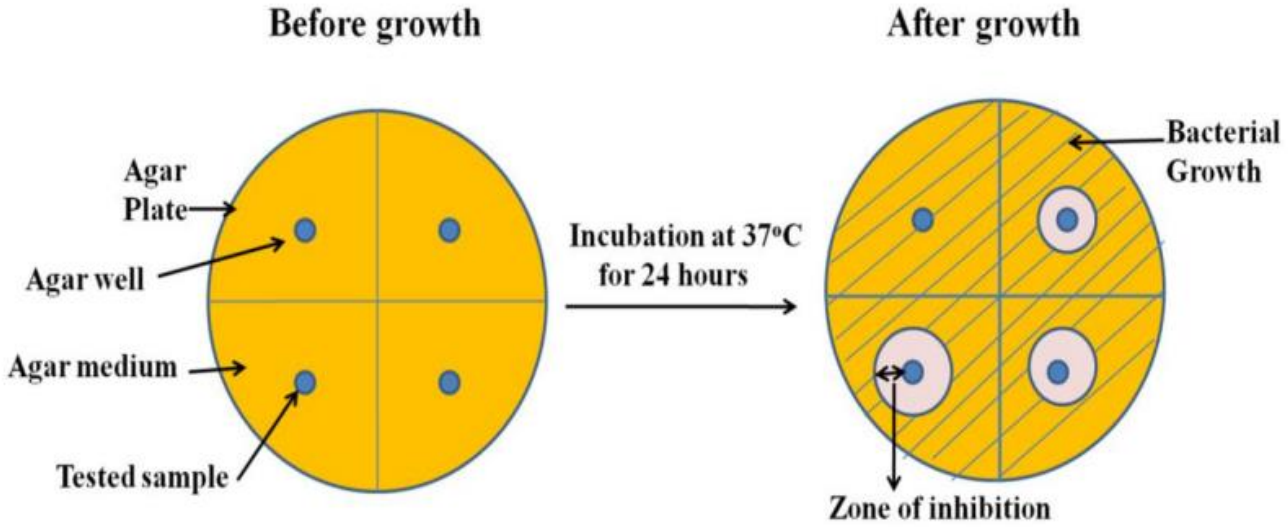

Figure 3.17: Pictorial representation of Agar well diffusion technique [26].

In the present thesis, we have employed the agar-well diffusion technique as well as discussed accordingly in brief in respective chapters.

3.9.3. Minimum Inhibitory Concentration (MIC)

MIC can be determined as the minimal concentration of antimicrobial agents which obstruct the visible growth of the bacteria. There are two main techniques through which MIC of the antibacterial agents can be carried-out i.e. Broth dilution method and the Agar dilution method.

Broth dilution method, utilized for the calculation of MIC in a liquid medium. In this procedure, the growth medium(liquid) possesses enhancing the concentration of antimicrobial agents. Specific micro-dilution is accomplished by utilizing <500µl per well in the microtiter plates. The visualization of the samples exhibits the particular growth of the organisms, subsequently after the incubation period. For the agar dilution process, a certain number of cell-suspension of bacteria are inoculated shortly into the plates containing nutrient agar medium with various concentrations of antimicrobial agents. Most often, this technique is utilized for the antibiotics present in ample quantity. The agar-dilution method is very beneficial for the determination of a huge quantity of bacterial species at a single time.

Each of these techniques mentioned here estimates the minimal concentration of antimicrobial agents, which prohibits the growth of bacteria. The current work evaluates the antimicrobial

performance of the silver and hybrid silver nanoparticles by the agar disc diffusion technique. The MIC was carried out through the broth dilution procedure.

References

1. Kobayashi Y, Katakami H, Mine E, Nagao D, Konno M, Liz-Marzán LM. Silica coating of silver nanoparticles using a modified Stöber method. *J Colloid Interface Sci*. 2005;283(2):392-396.
2. Pinzaru I, Coricovac D, Dehelean C, et al. Stable PEG-coated silver nanoparticles – A comprehensive toxicological profile. *Food Chem Toxicol*. 2018;111(November 2017):546-556.
3. Gong J lai, Liang Y, Huang Y, et al. Ag / SiO 2 core-shell nanoparticle-based surface-enhanced Raman probes for immunoassay of cancer marker using silica-coated magnetic nanoparticles as separation tools. *Biosens Bioelectron*. 2007;22:1501-1507. doi:10.1016/j.bios.2006.07.004
4. Dynamic Light Scattering Particle Size Distribution Analysis [horiba.com] Retrieved (11July 2023)
5. XRD instrument image | Download Scientific Diagram [researchgate.net] Retrieved (20March 2023)
6. https://www.nanoimages.com/sem-technology-overview/sem_img2/ Retrieved (16 June 2023)
7. https://www.acsmaterial.com/transmission-electron-microscope-tem.html Retrieved (8 Jan 2023)
8 https://www.bruker.com/en/products-and-solutions/microscopes/materials-afm/innova-afm.html Retrieved (13 June 2023)
9. https://psiberg.com/uv-vis-spectroscopy/ Retrieved (3 March 2023)
10. "Introduction to Fourier Transform Infrared Spectrometry", by thermo Nicolet Corporation (2001).
11. "Infra-red Characteristics Group Frequencies", John Wiley, Chichester, G. Socrates. (1980)
12. http://hdl.handle.net/10603/327171 Retrieved (10 Feb 2023)
13. http://www.snlabs.com/raman-spectroscopy.html Retrieved (25 May 2023)
14. https://en.wikipedia.org/wiki/Raman_spectroscopy Retrieved (17 March 2023)
15. M. D. Stollera, R. S. Ruoff, Energy Environ. Sci., 3, (2010), 1294-1301.
16. D. A. Skoog, Voltammetry, in Principles of Instrumental Analysis, ed. Fort Worth, Texas Saunders College Pub., (1992).
17. A. Chu, P. Braatz, J. Power Sources, 112, (2002), 236-246.
18. M. E. Orazem, B. Tribollet, Preliminary Graphical Methods in: Electrochemical Impedance Spectroscopy, A John Wiley & Sons, Inc., New Jersey, (2008), pp. 333.

19. D. J. Lee, W. W. Lin, AIChE Journal, 41, (1995), 2314–2317.
20. N A Handayani, E A Krisanti, S Kartohardjono, K Mulia. Cyclic Voltammetry and Oxidation rate studies of ferrous gluconate complex solutions for preparation of Chitosan tripolyphosphate microparticles. *Journal of Chemistry*. 2020; doi:10.1155/2020/3417204.
21. N. Aristov, A. Habekost. Cyclic Voltammetry-A versatile electrochemical method investigating electron transfer processes. *World Journal of. Chemical Education*, 3(5), 2015, 115-119; doi:10.12691/wjce-3-5-2.
22. M. S. Khan, A. Asif, S. Khawaldeh, A. Tekin, J. Electr. Bioimpedance, 9, (2018), 3-9.
23. http://www.pcimag.com/articles, Optical configurations of zeta potential Retrieved (23 June 2023)
24. https://www.thermofisher.com/blog/microscopy/edx-analysis-with-sem-how-does-it-work/ (8 Aug 2023)
25. Roger S. Riley, M.D., Ph.D. ;Michael Idowu MDD. 2 Principles and Applications of Flow Cytometry. Published online 2009:14. http://www.abcam.com/protocols/introduction-to-flow-cytometry
26. http://hdl.handle.net/10603/314179 Retrieved (27 July 2023)

Chapter 4

Synthesis and Characterization of Silver and Silica Coated Silver Nanoparticles

Chapter 4: Synthesis and Characterization of Silver and Silica Coated Silver Nanoparticles

4.1. Introduction

Considering the paradigm of scientific inventions and discoveries from the beginning of human beings on the earth, the advent of nanotechnology is a comparatively recent development. Nanotechnology is a swiftly evolving area due to its amazing usefulness and very wide area of applications[1]. Since time immemorial, certain materials have been part of the medicinal field, due to their outstanding medicinal properties. Silver nanoparticles having dimensions of 1 to 100 nm are remarkably possess significance because of their extraordinary abilities to create various nanostructures, extensively utilized for several applications namely anticancer, antimicrobial qualities, wound healing as well as other therapeutic potential[2]. Among various kinds of nanoparticles accessible at the current time, nanoparticles having core-shell design, possess astonishing abilities, combining multiple functionalities into a single hybrid nanocomposite. The core-shell nanoparticles fascinated attention because of the simplicity of management of particle compositions, ultrastructures, and surface characteristics[3]. It involves modifying the surface features of nanoparticles having a envelop of properly regulated arrangement.[4] The outer envelope can tailor the performance, receptiveness of the surface, and charge and can enhance the stability as well as the dispersive potentiality of the core material[5]. Additionally, optical, catalytic, and magnetic outcomes are conceivably conveyed to the colloidal particles through the encapsulating material.[6]

Many synthesis methods have been reported for the preparation of silver nanoparticles, remarkable examples include gamma irradiation, laser ablation, chemical reduction, electron irradiation, microwave processing, photochemical methods and biological synthetic methods[7]. Among all of these methods, chemical reduction method is normally most preferred, because it is easy to perform, efficient, cost-effective and it permits command in the various structural limitation across optimization of the synthesis circumstances[8]. The most relevant procedure for preparation of silver nanoparticles is its reduction by chemical-reagents. Normally reducing agents namely elemental hydrogen, sodium-borohydride, sodium citrate, ascorbate, tollens reagent, polyol process, N-dimethyl formamide (DMF) are utilized for the reduction of silver nanoparticles. Such reducing agents reduces Ag^{+} ion and makes the way for the preparation of metallic silver (Ag°), afterward agglomeration into oligomeric clusters[7]. Such clusters finally give rise to the synthesis of colloidal silver nanoparticles.
It is crucial to employ protective agents to preserve colloidal nanoparticles during the whole process of metal nanoparticles synthesis and shield the nanoparticles which can stick onto the surface of the nanoparticles and provide the required protection and ultimately avoids their agglomeration.

The current chapter focuses on the preparation of Ag nanoparticles by modified chemical reduction method employing citrate and later the encapsulation of Ag nanoparticles supported by silica

with the use of the modified Stober method (sol-gel)[9]. The layering with silica provides the chemical inertness, robustness, and the adaptability required for the conjugation with the biomolecules. It also shelters silver core from the ions available in biological media. The flexibility of silica in surface moderation as well as in synthesis behaviour, offers an outstanding edge to the employment of this material for multiple purposes. Current chapter also explains approaches of characterization of both of the synthesized nanoparticles. We have prepared silver nanoparticles by one-step chemical reduction and encapsulation of these nanoparticles with silica by employing an altered Stober method[10] to synthesize a composite nanomaterial as it is displayed in Fig.4.1. The morphologies, structure, and size of the nanoparticles were specified by Transmission Electron Microscopy (TEM), Atomic force microscopy (AFM), Scanning electron microscopy (SEM), UV-Visible spectroscopy, X-ray diffraction (XRD), Raman, Fourier Transform Infra Red Spectroscopy (FTIR) and Dynamic Light Scattering (DLS) respectively. The results demonstrates that the average size of Ag nanoparticles & Silica coated Ag nanoparticles is 50 nm and 80 nm respectively. Our TEM results designates that the silica shell consistently envelops the silver core particles.

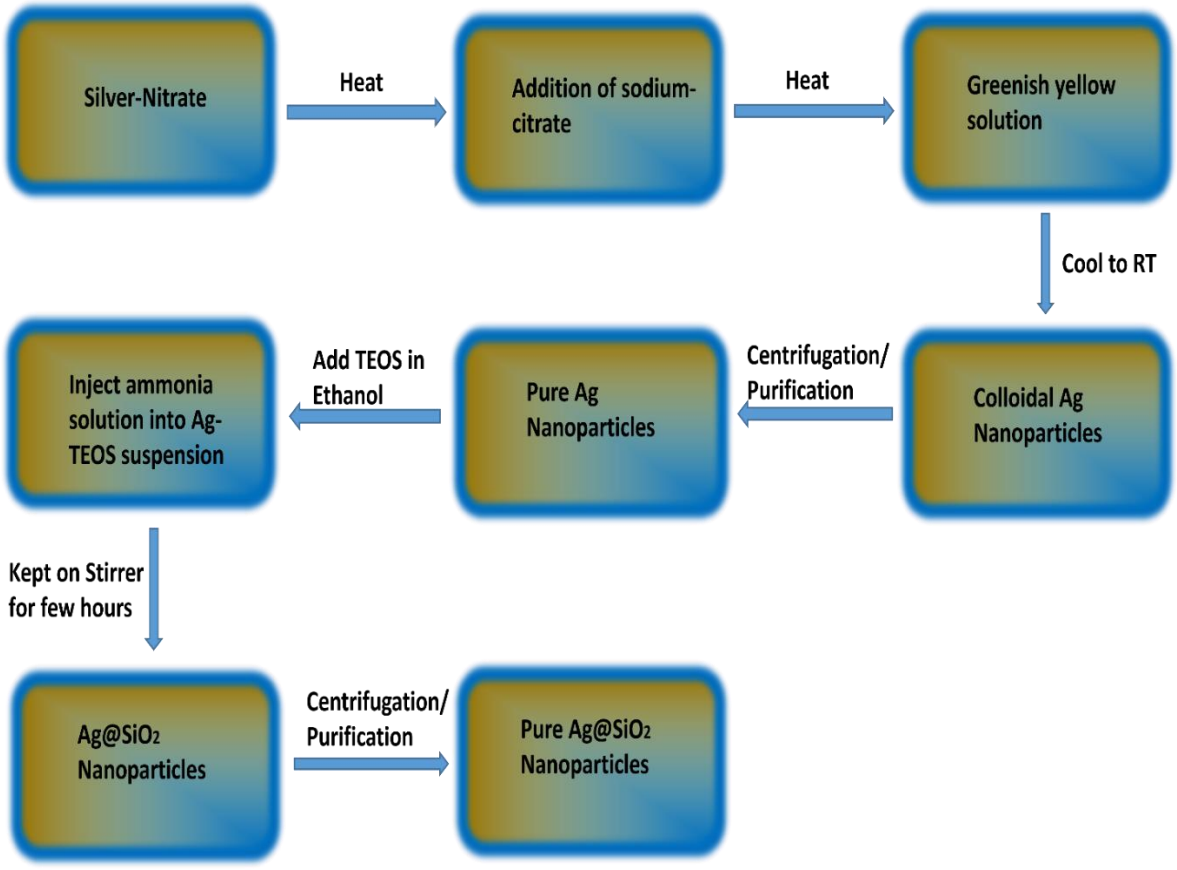

Figure 4.1: Schematic of stepwise synthesis and coating process of Ag nanoparticles.

4.2. Experimental details

Silver nitrate ($AgNO_3$), trisodium citrate dehydrate ($Na_3C_6H_5O_7.2H_2O$) tetra-ethyl-ortho-silicate (TEOS), absolute ethanol, ammonia solution (28-30 wt %). Entire aqueous solutions were processed with deionized double distilled water(18.2 MΩ). All the chemicals were acquired from Sigma-Aldrich and employed without additional purification.

4.2.1. Synthesis of silver nanoparticles

Silver colloidal solutions were synthesized following the chemical reduction method via the altered version of the already known Turkevich method[11]. Concisely, 1.5mM of $AgNO_3$ was dissolved in 98 ml of double distilled water and boiled accurately, under vigorous stirring then 5ml of freshly prepared 1% TSC (Tri - Sodium- Citrate) was combined within 2 minutes into the solution of $AgNO_3$ after that the whole mixture was blended up at 100°C continuously. Further being agitated for one hour, the colloidal mixture was held to chill at room temperature (RT) for extra 10-15 hours for appropriate seeding. The refining of the liquid solution is accomplished by centrifuging the colloids at 10000 RPM for 20 min. Afterward, the silver pellet was collected and washed twice, then fixed quantity of distilled water was added and finally stored at RT for further experimentation.

4.2.2. Coating of silver nanoparticles with silica

Encapsulation of silver nanoparticles with silica can enhance the surface area of the nanoparticle, increasing its porosity, and so the coated nanoparticle becomes more favorable for biomedical applications. The flexibility of silica in surface moderation as well as in synthesis behaviour, offers an outstanding edge to the employment of this material for multiple purposes. The silica encapsulation on silver nanoparticles was done by altered “Stober” method[12]. The as-prepared concentrated silver nanoparticles were brought into a suspension of liquid ammonia (28 to 30 %), pure ethanol (100 ml, 99.9%), and deionized water. Following 35 mins of sonication, known quantity of amounts of TEOS (Tetraethyl orthosilicate) were supplemented drop by drop (gradually starting from 2 to 15 µl) further the mixture was properly blended for 15 h at an ambient temperature. We observed that by modifying the quantity of the TEOS, the diameter of the silica encapsulation can be tuned. Further to separate the suspension mixture, centrifuged it for 40 mins, at 13500 RPM (Rotation per minute) accompanied by washing three times at 8000 RPM in ethanol (100%) for 15 mins all experimentation, the synthesized $Ag@SiO_2$ nanoparticles were re-dispersed in double distilled water.

4.2.3. Characterization of silver nanoparticles and silica-coated silver hybrid nanoparticles

The fundamental composition sizes along with the patterning of the resulting synthesized nanoparticles were examined by utilizing scanning electron microscopy (SEM) and energy-dispersive x-ray spectroscopy (EDX) on Jeol- 6360A instrument with an operating voltage of 20 kV. DLS measurements of both the synthesized samples were performed by utilizing a NICOMPTM 380 ZIS

(Santa Barbara, CA, USA) for the confirmation of hydrodynamic diameter (HDD). Electrochemical Impedance measurements and cyclic voltammetry were performed by utilization of a ZIVE MP1 Electrochemical workstation. XRD measurements were accomplished employing Rigaku mini flex 600 X-ray diffractometer with the help of CuKα radiation at RT at a filament current of 40 mA and voltage of 30 kV in the range of 200 to 800. The UV-Vis absorbance along with fluorescence quantification was noted on a Schimadzu (Model N0. UV 1800) double-beam spectrophotometer amid wavelength 200-1100 nm. Entire Fourier-transform infrared (FTIR) spectroscopic computation was carried out on an Alpha ATR Bruker Spectrometer by utilizing (KBr Pressed disks). Transmission-Electron-Microscopy (TEM) analysis was accomplished to learn the size and morphology, of the AgNPs and Ag@SiO_2 colloidal nanoparticles. Accordingly, we employed Philips CM 200 model TEM, with a working voltage of 20-200 kV along with a resolution of 2.4A°. To quantify the size of the nanoparticles precisely, every peak was Gaussian fitted, besides the instrumental widening was diminished utilizing Si standard sample advancement. The crystallite size of the synthesized nanoparticles is measured from the FWHM of the elevated intense diffraction peak employing Debye Scherrer's formula[13], as shown in equation no.4.1.

$$D = 0.9\lambda/\beta\cos\theta \quad \text{----------(4. 1)}$$

Here, D is the mean crystallite domain size orthogonal to the reflecting planes, λ is the x-ray wavelength, β is the FWHM of the diffraction peak and θ is the diffraction angle. RAMAN spectra[14] was achieved by utilizing an inVia Renishaw micro Raman spectrophotometer. The whole system is automatically calibrated as opposed to a silicon wafer peak at 560cm^{-1}. The Raman scattering was agitated by a continuous wave argon laser along with a power of 100 MW. The spectra were calculated at temperatures of 300 and 78K.

4.3. Results and discussion

4.3.1. Spectroscopic analysis

4.3.1.1. UV-vis spectroscopy

The synthesized silver nanoparticles were acquired by using trisodium citrate dihydrate ($Na_3C_6H_5O_7.2H_2O$) as a coating as well as reducing factor[15]. The mounding of silica on the external surface of silver was executed by an altered "Stober"(sol-gel) method[16]. Our first observation was that the firmness of the shells around silica depended on the circumstances under which they were synthesized.

Ag nanoparticles manifests an intense characteristic peak emerged at 420 nm in UV-visible absorption spectrum and following deposition of the silica coating on Ag nanoparticles, the peak deviate towards longer wavelength, it is shown in Fig.4.2.

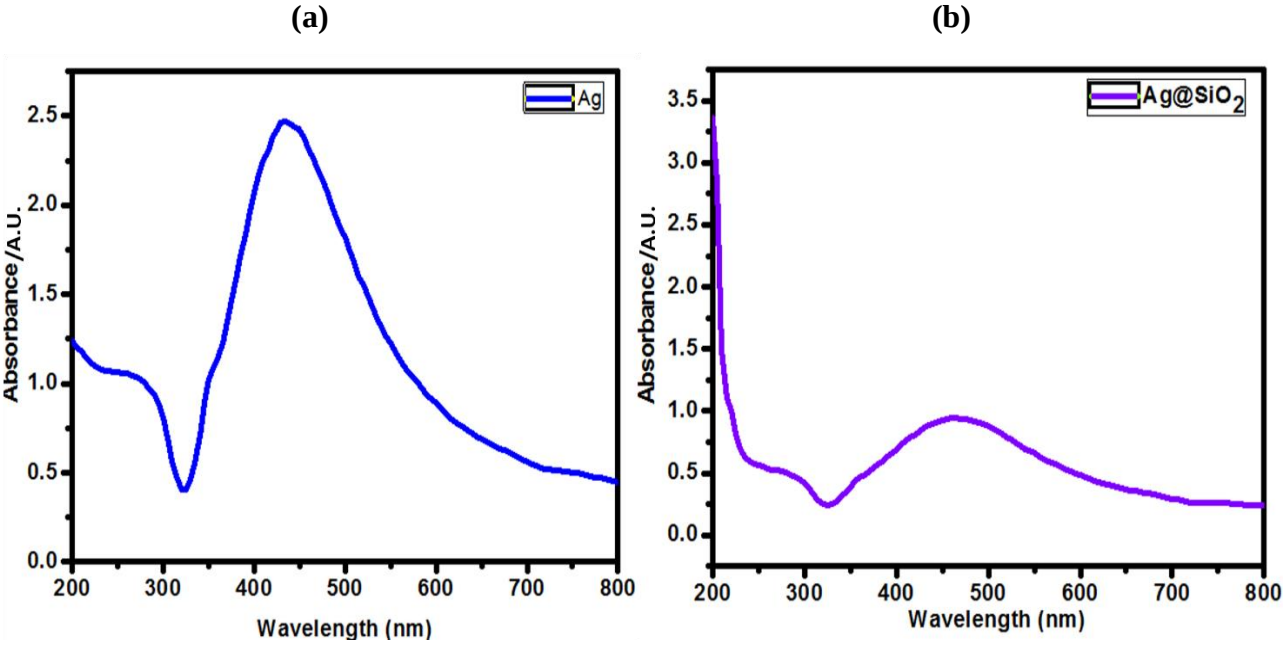

Figure 4.2: The UV-visible spectra of (a) Ag nanoparticles and (b) Ag@SiO_2 nanoparticles.

The change in color from yellow to black the evolution of stable Ag nanoparticles. Ammonia (28-30 wt%) was employed as a stimulant of the reaction. Since, it was needed to acquire an appropriate coating, low ammonia concentration conceivably turns down the decorous rate of reaction to some scale. Additionally, it was unearthed that ammonia and water concentration control the stability between the hydrolysis of TEOS as well as the condensation of its hydrolyzed monomers. Ag nanoparticles revealed a sharp characteristic peak that emerged at 420 nm in UV-visible absorption spectra and subsequently deposition of the silica layer on Ag nanoparticles, resulted in shifting of the peak to a longer wavelength. The thickness of the shell after coating with silica concerning SPR (surface plasmon resonance) signal was assigned through the growing local refractive index of the colloidal nanoparticles and because of this, red shifting of the peaks appeared. The diameter of the peaks of prepared Ag@SiO_2 nanoparticles, denotes the capping of silica layer on the facet of Ag nanoparticles, as it is showed in fig.4.2.

4.3.1.2. Fourier transform infrared spectroscopy (FTIR)

To estimate the functional group, we performed FTIR quantification[17] of the colloidal nanoparticles, which is displayed in Fig.4.3 (a-b). The sole motive of the FTIR was to observe the development of silica shell on the synthesized Ag nanoparticles[18]. The data exhibited that the peaks ascribed to 796 cm^{-1} and 465 cm^{-1} can be due to the existence of silica on the facet of nanoparticles (Si-O-Si and Si-O). Additionally, the specific band at 947 cm^{-1} was attributed to C-N stretching that represents the aliphatic amine. The FTIR spectra of Ag nanoparticles & Ag@SiO_2 nanoparticles reveals that peaks become broad after encapsulation of silica. It is interesting to note that, two peaks

at 1091 and 1048 cm^{-1} are recommended to the asymmetric stretching vibrations of the Si-O-Si and Si-O (H) bonds, and those at 796 cm^{-1} and 465 cm^{-1} can be considered to the symmetric stretching and bending vibrations of the Si-O-Si bond, which confirms the presence of silica shell on the external surface of the Ag nanoparticles.

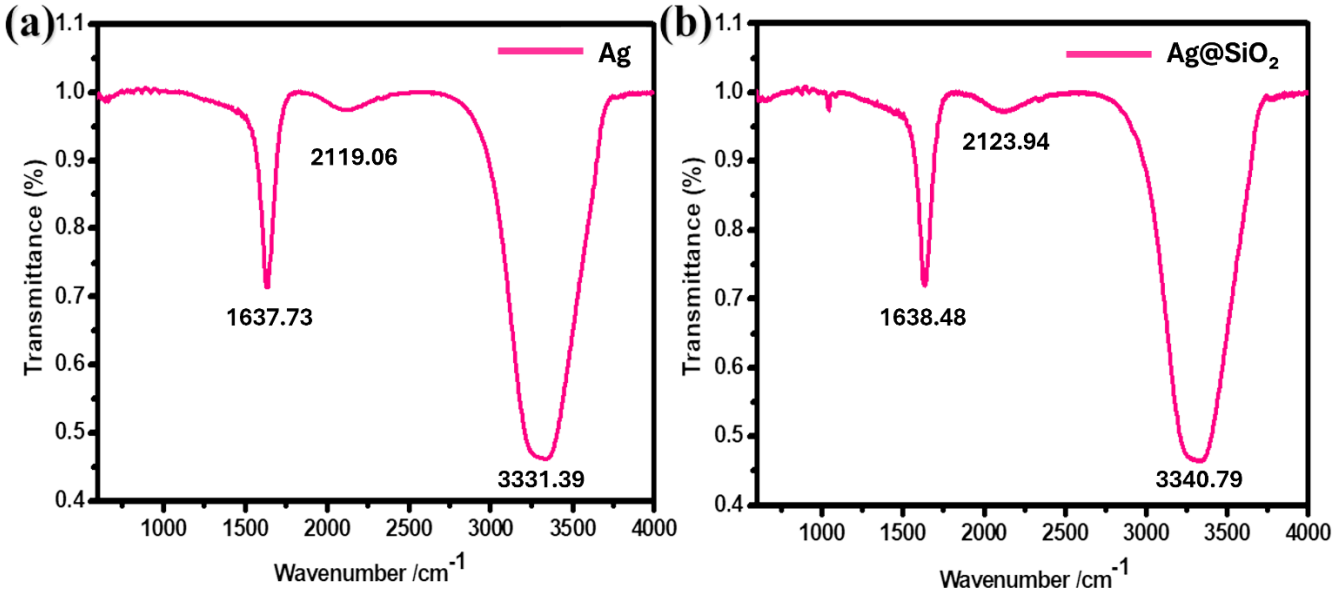

Figure 4.3: FTIR spectra of (a) Ag nanoparticles and (b) $Ag@SiO_2$ nanoparticles.

4.3.1.3. Raman spectroscopy

The RAMAN-spectroscopy assessment was administered to learn the vibrational features of the nanoparticles[19]. These days, this spectroscopic analysis is extensively utilized in cancer-related diagnosis.[3] To the best of our knowledge that colloidal nanomaterials are prone to chemical instability, additionally, the RAMAN method is remarkably less affected by water interferences[14].

It was learned that the fabricated nanoparticles displayed excellent stability. Ag nanoparticles exhibit two substantial peaks at relatively 1569 cm^{-1} and 1396 cm^{-1}, although $Ag@SiO_2$ nanoparticles manifest much lesser scattering at 1630 cm^{-1} and 1328 cm^{-1}, exhibited in Fig.4.4.

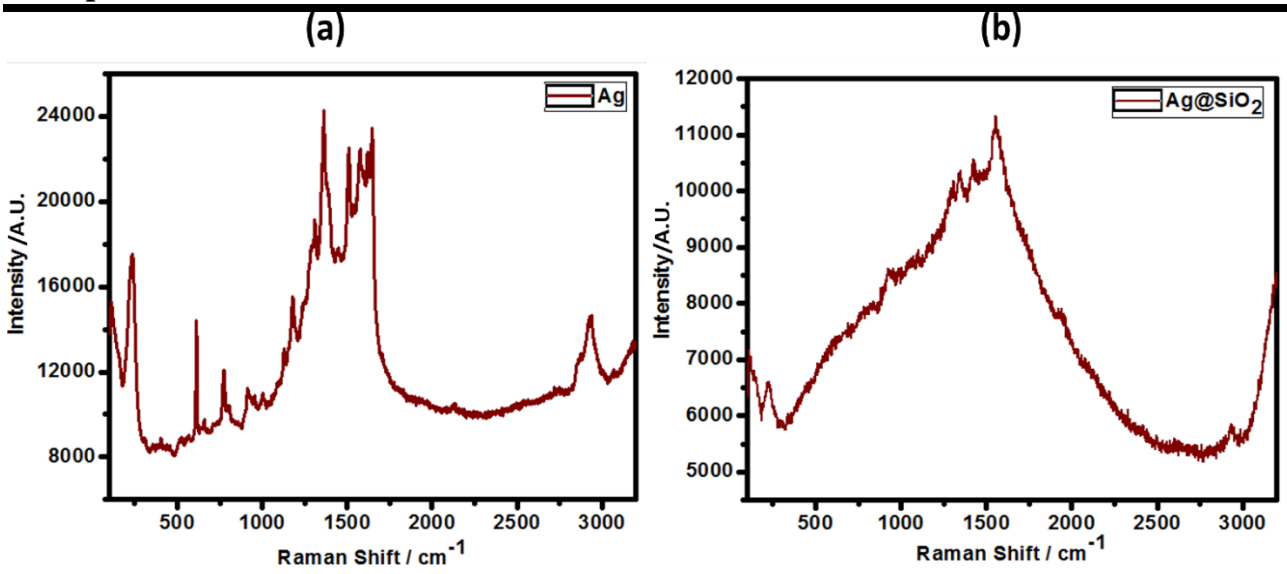

Figure 4.4: RAMAN spectra of (a) Ag nanoparticles and (b) Ag@SiO_2 nanoparticles.

4.3.2. Elemental analysis

4.3.2.1. Energy dispersive x-ray spectroscopy (EDX)

EDX investigation of the silver nanoparticles steadfast the substantial silver peaks in its chemical composition[20]. Additional elemental tip-offs were also noticed in the spectra which were allocated to the presence of some other compounds. EDS analysis reveals that prepared Ag nanoparticles contain sodium, chlorine as well as some amount of nitrogen, and oxygen whereas Ag@SiO_2 nanoparticles display expansion of the peak of silica, shown in fig. 4.5. There are some minor peaks of silver, aluminum, sodium, and oxygen that can be also seen.

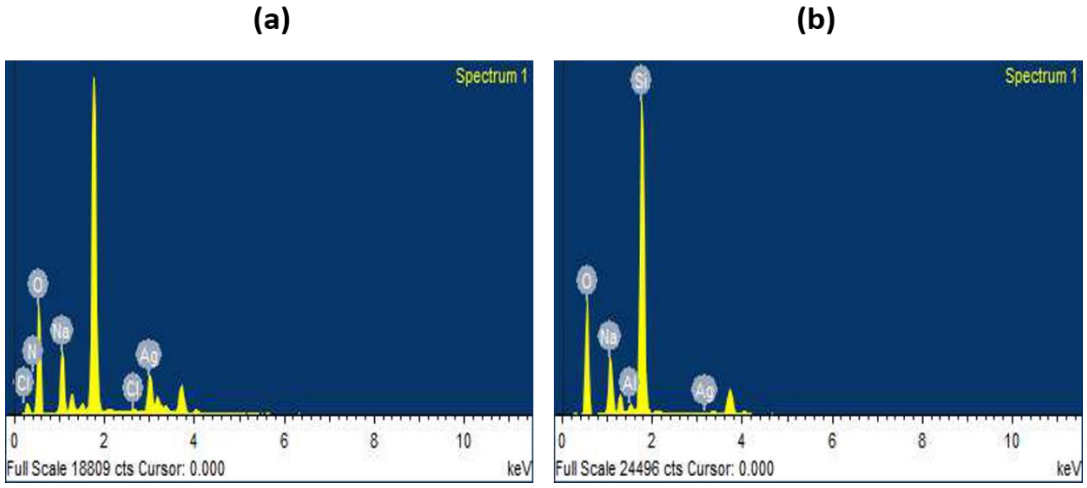

Figure 4.5: Energy dispersive spectra of (a)prepared Ag nanoparticles, and (b) Ag@SiO_2 nanoparticles.

4.3.3. Structural analysis

4.3.3.1. X-ray diffraction

XRD diffraction was employed to explore the variation in the crystal structure among the two nanoparticles[21]. Considering the XRD pattern study of Ag nanoparticles as well as $Ag@SiO_2$ nanoparticles, both of the samples were casted into the surface of the glass and dried in the air, after that the evaluation were accomplished, results are shown in Fig.4.6. The phase identification of the colloidal samples reported is carried out through corresponding peak locations along with comparing the intensities in XRD pattern to those patterns stated in the JCPDS (Joint Committee on Powder Diffraction Standards) data collection. XRD patterns of the Ag nanoparticle are illustrated in fig.4.5. The diffracted intensities were documented from 10° to 80°. By examining the XRD format of Ag nanoparticles and $Ag@SiO_2$ hybrid nanoparticles, three well defined diffraction peaks at 38.2°, 44.03° and 64.2° corresponding to the (111), (200), and (220) Bragg reflections of face-centered-cubic (fcc) crystal structure of Ag nanoparticles were noticed.

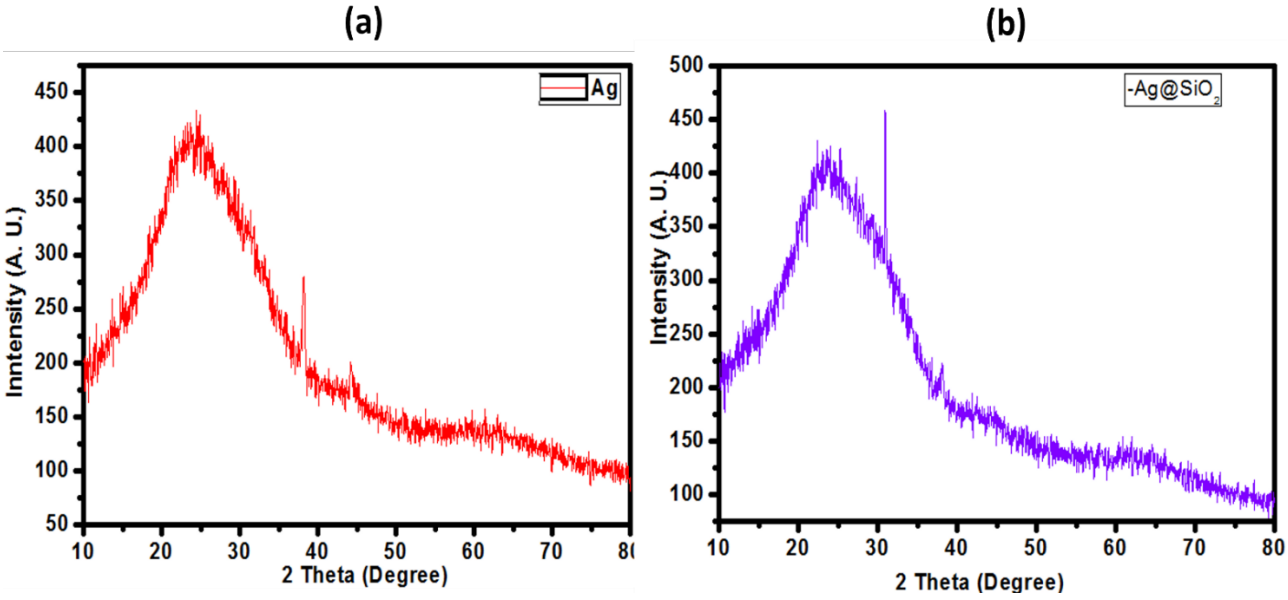

Figure 4.6: XRD patterns of (a) Ag nanoparticles & (b) $Ag@SiO_2$ hybrid nanoparticles recorded in the range from 10° to 80°.

There are several individual peaks are also detectable as a consequence of existence of carbon, and it was connected to the biomaterials. The distinguished peaks at (200), and (220) planes are minor intense whereas, the peak located at (111) planes is more sharp. Fig. also reveals the pattern of the XRD of the silica encapsulated silver nanoparticles. The capping of silica on the facet of Ag does not influence the crystal behaviour of the Ag nanoparticles. The short and substantial peak at 2θ values of around 22° conceivably assigned as a specific layer of silica.

4.3.3.2. Light scattering techniques (Dynamic light scattering)

The hydrodynamic circumference of Ag nanoparticles was decided by utilizing a dynamic-light-scattering (DLS) demonstration[22]. DLS discloses about the proper size distribution of the

nanoparticles. Fig.4.7. (a) displays the DLS of colloidal solution of Ag nanoparticles which exhibits the development of competently distributed nanoparticles starting from 10 to 200 nm, with a mean diameter of 50nm. Although, fig.4.7. (b) is exhibiting DLS of the colloidal solution of $Ag@SiO_2$ nanoparticles showing the increase in the diameter of the nanoparticles starting from size range of 50 to 200 nm, with a mean size of 80nm. It is important to mention that the DLS results are almost alike to the TEM results.

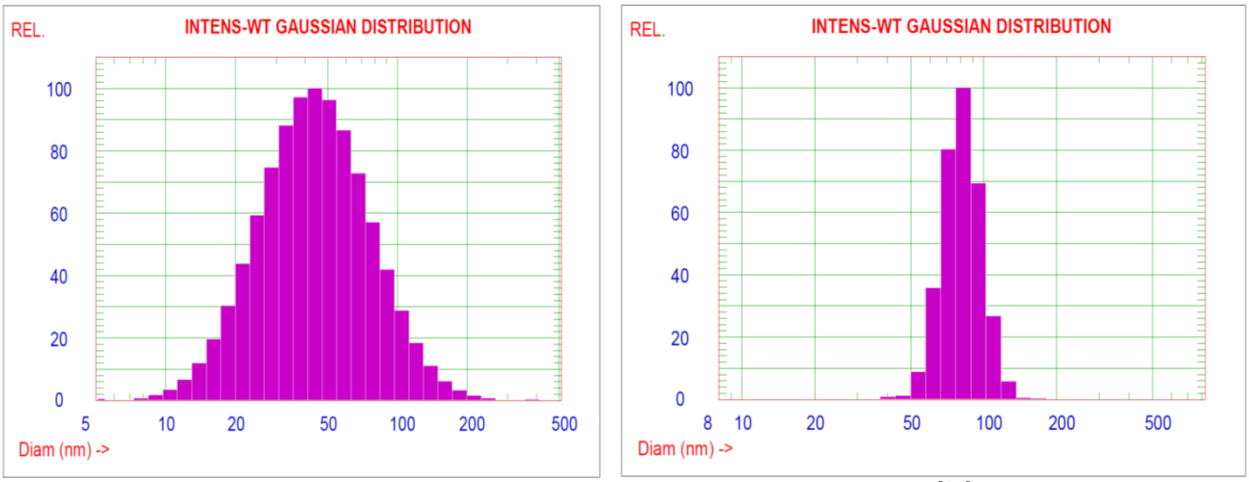

Figure 4.7: The hydrodynamic diameter of the synthesized nanoparticles was determined by the employment of DLS-histograms. (a)Ag nanoparticles, and (b)$Ag@SiO_2$ nanoparticles.

4.3.4. Size distribution and colloidal stability characterization techniques

4.3.4.1. Zeta potential

The stability of both the prepared nanoparticles was calculated in terms of zeta potential by utilizing a zeta sizer, exhibited in Fig. 4.8. The synthesized colloidal nanoparticles maintained a net negative charge[23] on the surface and remained in suspension activated by collective electrostatic-repulsive effectiveness. It is implied that due to the adherent citrate ions, Ag nanoparticles gained a negative charge, and simultaneously because of this, a repulsive force directs the nanoparticles to prevent aggregation. Therefore, there is no requirement for a further stabilizing agent, and nanoparticles in the solution remain in a steady state. Both of the synthesized nanoparticles possess a net negative charge on their surface.

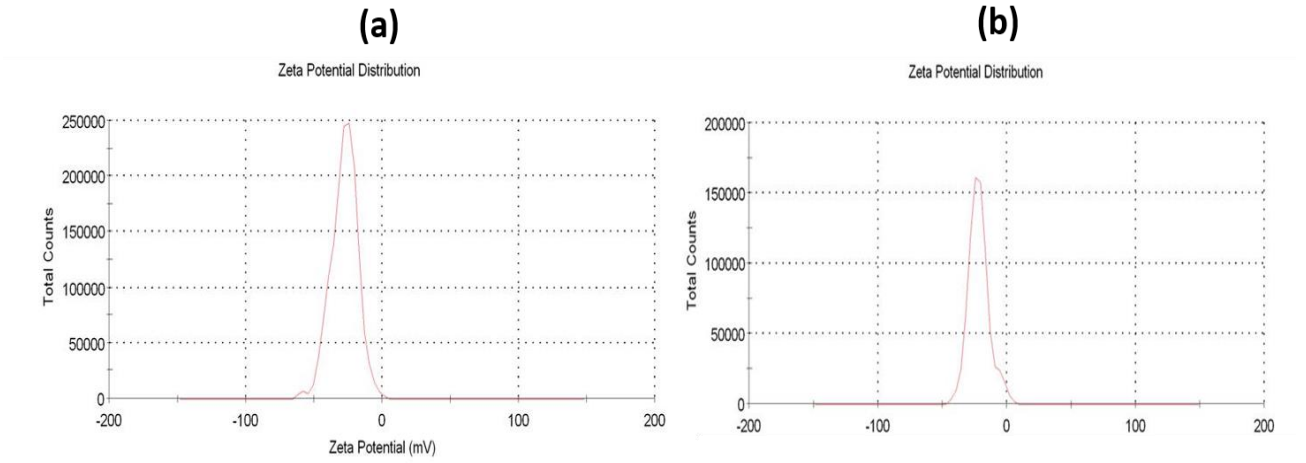

Figure 4.8: The stability of the prepared nanoparticles were measured by utilizing a Zetasizer. Zeta potential of (a) Ag nanoparticles and (b) Ag@SiO_2 nanoparticles.

It was observed that the addition of even a small quantity of silica quickly lowers the zeta potential. The specific colloidal stability of the Ag nanoparticles is -27.7mV while Ag@SiO_2 nanoparticles is -21.7mV. It denotes the diminished stability of the colloidal Ag nanoparticles after coating. Normally higher Zeta potential resulted in stability of the colloid to a greater extent[24].

4.3.5. Morphological and topographical techniques

4.3.5.1. Scanning electron microscopy (SEM)

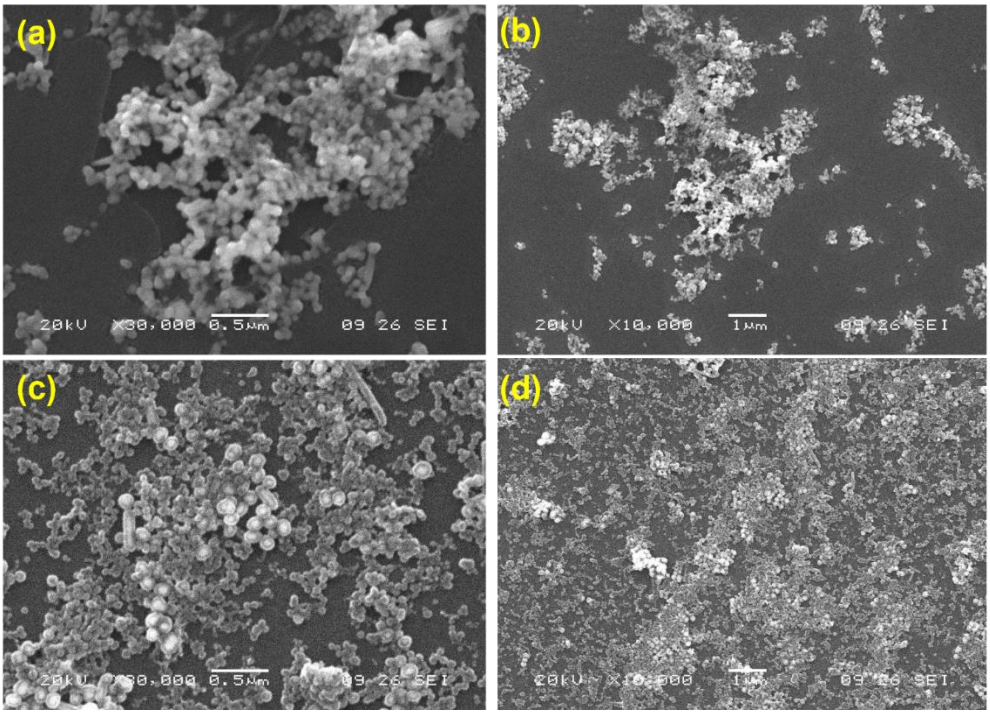

Figure 4.9: SEM images of (a), (b) Ag nanoparticles and (c), (d) Ag@SiO_2 nanoparticles at two magnifications (0.5µm and 1µm).

SEM analysis was accomplished to examine the morphology characteristics of Ag nanoparticles and silica-coated silver nanoparticles at different magnifications. It was evident from the SEM analysis, shown in Fig.4.9, that both the nanoparticles were spherical, and images of $Ag@SiO_2$ nanoparticles exhibit a definite capping of layers of silica on the facet of the silver. It is visible that the Ag nanoparticles have a spherical shape and images of $Ag@SiO_2$ nanoparticles exhibit a definite encapsulation of silica layering on the external surface of the silver.

4.3.5.2. Transmission electron microscopy (TEM)

The TEM interpretation was implemented to study the configuration and dimension of the Ag nanoparticles as well as $Ag@SiO_2$ nanoparticles. Fig. 4.10. manifest TEM images at different magnifications, of prepared Ag nanoparticles and silica encapsulated Ag nanoparticles. To execute this, both of the nanoparticles separately casted on a carbon-concealed copper grid and dried in air. Subsequently, scanning of the grid by using the Philips CM 200 model transmission electron microscopy working voltage is 20 to 200 kV and the resolution was 2.4 A°.

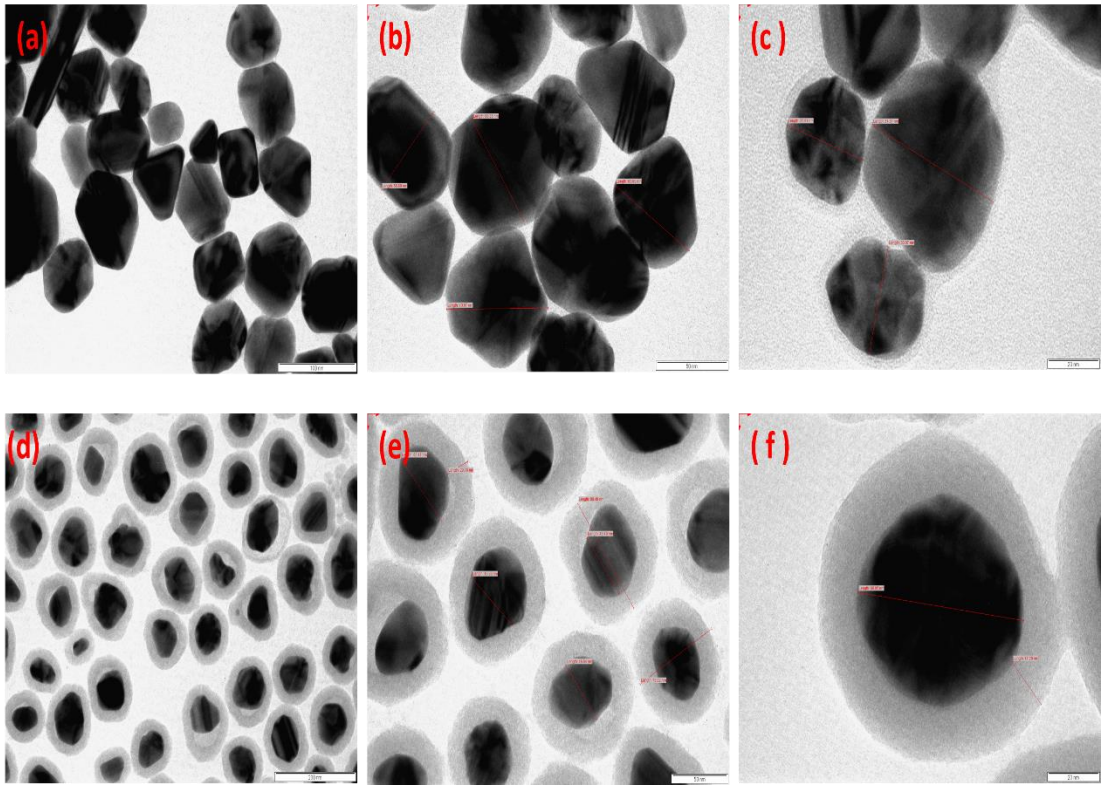

Figure 4.10: TEM micrographs of the prepared (a), (b), (c) Ag nanoparticles, and (d), (e), (f) $Ag@SiO_2$ nanoparticles at different magnifications.

Through the analysis of TEM-micrographs of Ag nanoparticles at different magnifications, it was visible that there is a spherical shape of Ag nanoparticles with extensive size distribution and the average size of particles was 50nm & TEM- micrographs of $Ag@SiO_2$ nanoparticles reveal a uniform, definite and clean coating of silica on the facet of Ag nanoparticles and the $Ag@SiO_2$ nanoparticles

has a mean size of 80 nm. SAED (selected area electron diffraction) pattern of tailored silver nanoparticles depicts a bright randomly dotted ring pattern that describes the crystalline nature of the material, because as we know, the more glaring the spots are, the more crystalline particles will be. Silica-coated silver nanoparticles manifest brighter, thicker, and continuous rings describing the amorphous encapsulation of silica on the facet of silver nanoparticles, as it is shown in Fig.4.11.

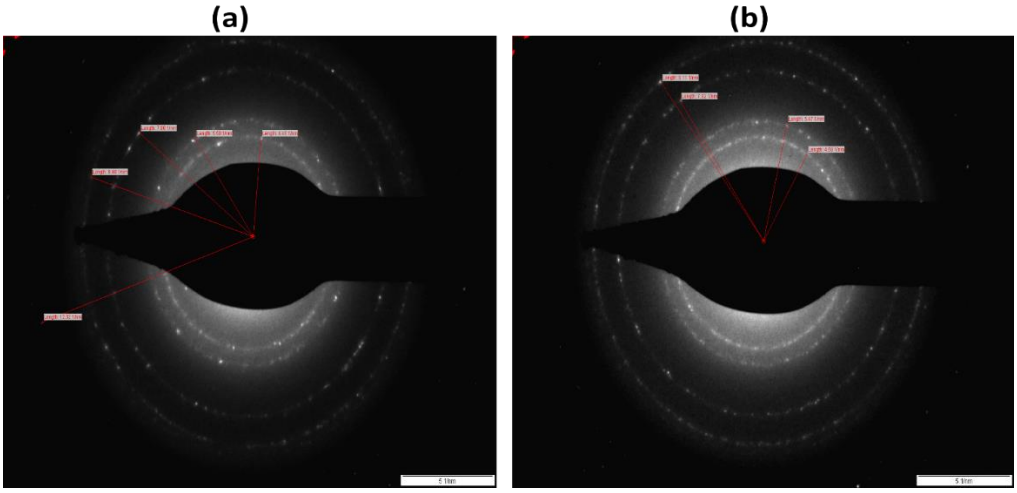

Figure 4.11: Selected Area Electron Diffraction (SAED) patterns of (a)Ag nanoparticles and (b) $Ag@SiO_2$ nanoparticles.

4.3.5.3. Atomic force microscopy (AFM)

Topological observation of both the synthesized nanoparticles was accomplished by AFM onto glass slides. All of these pictures are displayed in fig.4.12. The images assemble in torsional resonance mode, and the interconnection can be noticed. AFM micrographs demonstrate the identical height representation of the synthesized silver and $Ag@SiO_2$ nanoparticles[25]. The maximum number of Ag NPs is detected in the size range of 30 to 80 nm. There exist several larger particles by the observation of AFM data, however according to histogram scanning their number is restricted. The height description of the nanoparticles as proposed by line investigation, is in the same range, just as approved by TEM investigation. From the AFM images it is obvious that once encapsulated with silica, the dimension of the nanoparticles increased, i.e. approx. 80 nm.

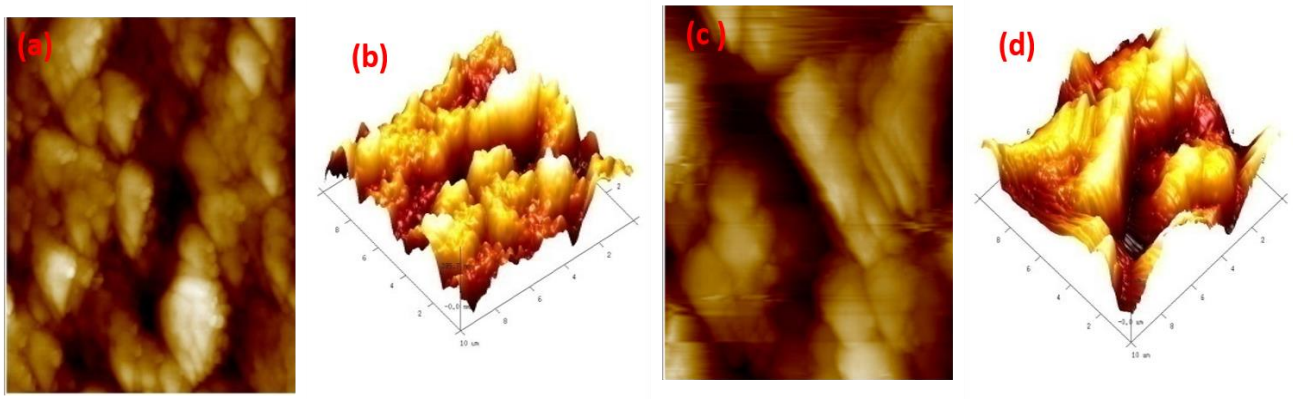

Figure 4.12: Exhibits the topological properties of (a), (b) Ag nanoparticles & (c), (d) Ag@SiO_2 nanoparticles.

Conclusions

In the present study, we have synthesized silver nanoparticles by improvised chemical reduction method by utilizing trisodium citrate dihydrate ($Na_3C_6H_5O_7.2H_2O$) as a reducing as well coating material. By altering the reaction-conditions and amount of the reagent, we obtained firmly silica-encapsulated silver nanoparticles, which was stable even at room-temperature for longer period. The encapsulation of silica on the surface of silver was accomplished by the Stober method. The UV-visible spectroscopy revealed a sharp characteristic peak and after accumulation of the silica layer on Ag nanoparticles, the peak moved towards a longer wavelength. XRD diffraction was employed to regulate the difference of the crystal structure betwixt the two nanoparticles. It also exhibited the phase purity of both synthesized nanoparticles. The synthesized nanoparticles are crystalline having a spherical structure. FTIR, EDX, and RAMAN-spectroscopic evaluation were implemented to learn the functional groups, chemical composition, and vibrational characteristics of the nanoparticles respectively. It was discovered that the prepared nanoparticles displayed good stability. The TEM and SEM interpretations were executed to investigate the configuration and dimensions of the nanoparticles. As confirmed by both results, the silica shell consistently encapsulates silver core particles. The hydrodynamic diameter of both nanoparticles was determined by employing a dynamic-light-scattering (DLS) assessment and they are nearly identical to the TEM results. Topological characterization of both the prepared nanoparticles demonstrates the matching height elucidation. As suggested by line analysis, the height profile of the nanoparticles is in the same range, as confirmed by TEM investigation. It is noteworthy to mention that all of the characterization techniques divulged the average size of the Ag nanoparticles and Ag@SiO_2 nanoparticles were 50 nm and 80 nm. The steadiness of both the prepared colloidal nanoparticles was computed in terms of zeta potential. The synthesized nanoparticles sustained a net negative charge on their surface and remained in a solution prompted by joint electrostatic-repulsive force. Both the synthesized nanoparticles manifest good stability and later employed for medical and health care applications due to their exceptional chemical and physical properties.

References:

1. Almatroudi A. Silver nanoparticles : synthesis , characterisation and biomedical applications. *Open Life Sci*. 2020:819-839.doi:10.1515/biol-2020-0094
2. Sunderam V, Thiyagarajan D, Lawrence AV, Mohammed SSS, Selvaraj A. In-vitro

antimicrobial and anticancer properties of green synthesized gold nanoparticles using anacardium occidentale leaves extract. *Saudi J Biol Sci*. 2019;26(3):455-459. doi:10.1016/j.sjbs.2018.12.001

3. Gong J lai, Liang Y, Huang Y, et al. Ag / SiO 2 core-shell nanoparticle-based surface-enhanced Raman probes for immunoassay of cancer marker using silica-coated magnetic nanoparticles as separation tools. *Biosens Bioelectron*. 2007;22:1501-1507. doi:10.1016/j.bios.2006.07.004
4. Wang T, Wang S, Cheng Z, et al. Emerging core–shell nanostructures for surface-enhanced raman scattering (SERS) detection of pesticide residues. *Chem Eng J*. 2021;424(May):130323. doi:10.1016/j.cej.2021.130323
5. Ghosh Chaudhuri R, Paria S. Core/shell nanoparticles: Classes, properties, synthesis mechanisms, characterization, and applications. *Chem Rev*. 2012;112(4):2373-2433. doi:10.1021/cr100449n
6. Chou K Sen, Chen CC. Fabrication and characterization of silver core and porous silica shell nanocomposite particles. *Microporous Mesoporous Mater*. 2007;98(1-3):208-213. doi:10.1016/j.micromeso.2006.09.006
7. Iravani S, Korbekandi H, Mirmohammadi S V, Zolfaghari B. Synthesis of silver nanoparticles : chemical , physical and biological methods. *Res Pharm Sci*. 2014;9(December):385-406. doi:ncbi.nlm.nih.gov/pmc/articles/PMC4326978
8. Quintero-Quiroz C, Acevedo N, Zapata-Giraldo J, et al. Optimization of silver nanoparticle synthesis by chemical reduction and evaluation of its antimicrobial and toxic activity. *Biomater Res*. 2019;23(1):1-15. doi:10.1186/s40824-019-0173-y
9. Kobayashi Y, Katakami H, Mine E, Nagao D, Konno M. Silica coating of silver nanoparticles using a modified stöber method. *Journal of Colloid and Interface Science*. 2005;283:392-396. doi:10.1016/j.jcis.2004.08.184
10. Wong YJ, Zhu L, Teo WS, et al. Revisiting the stöber method: inhomogeneity in silica shells. *J Am Chem Soc*. 2011;133(30):11422-11425. doi:10.1021/ja203316q
11. Pinzaru I, Coricovac D, Dehelean C, et al. Stable PEG-coated silver nanoparticles – a comprehensive toxicological profile. *Food Chem Toxicol*. 2018;111(November 2017):546-556. doi:10.1016/j.fct.2017.11.051
12. Chen G zhu, Yin Z zhi, Lou J feng. Electrochemical immunoassay of escherichia coli O157 : H7 using Ag @ SiO 2 nanoparticles as labels. *J Anal Methods Chem*. 2014;2014:247034. doi:10.1155/2014/247034.
13. Ghosal G, Singh M. Characterization of silver nanoparticles synthesized using fenugreek leave

extract and its antibacterial activity. *Materials Science for Energy Technologies*. 2022:22-29. doi:org/10.1016/j.mset.2021.10.001.

14. Wang W, Zhao J, Short M, Zeng H. Real-time in vivo cancer diagnosis using raman spectroscopy. *J Biophotonics*. 2015;8(7):527-545. doi:10.1002/jbio.201400026
15. Dey A, Dasgupta A, Kumar V, Tyagi A, Verma AK. Evaluation of the of antibacterial efficacy of polyvinylpyrrolidone (PVP) and tri-sodium citrate (TSC) silver nanoparticles. *Int Nano Lett*. 2015;5(4):223-230. doi:10.1007/s40089-015-0159-2
16. Bokov D, Turki J A, Chupradit S, Suksatan W, Ansari JM, Shewael HI, Valiev HG,Kianfar E, Nanomaterials by sol-gel method: synthesis and application. *Advances in Materials Science and Engineering.* 2021:5102014. doi:org/10.1155/2021/5102014
17. Singh P, Katkar PK, Patil UM, Bohara RA. A robust electrochemical immunosensor based on core-shell nanostructured silica-coated silver for cancer (carcinoembryonic-antigen-CEA) diagnosis. *RSC Adv*. 2021;11(17):10130-10143. doi:10.1039/d0ra09015h
18. Bryaskova R, Pencheva D, Nikolov S, Kantardjiev T. Synthesis and comparative study on the antimicrobial activity of hybrid materials based on silver nanoparticles (AgNps) stabilized by polyvinylpyrrolidone (PVP). *J Chem Biol*. 2011;4(4):185-191. doi:10.1007/s12154-011-0063-9
19. Yilmaz H, Cobandede Z, Yilmaz D, Cinkilic A, Culha M, Demiralay EC. Monitoring forced degradation of drugs using silica coated AgNPs with surface-enhanced raman scattering. *Talanta*. 2020;214(October 2019):120828. doi:10.1016/j.talanta.2020.120828
20. Singh H, Du J, Yi TH. Kinneretia THG-SQI4 mediated biosynthesis of silver nanoparticles and its antimicrobial efficacy. *Artif Cells, Nanomedicine Biotechnol*. 2017;45(3):602-608. doi:10.3109/21691401.2016.1163718
21. Tuteja SK, Kukkar M, Kumar P, Paul AK, Deep A. Synthesis and characterization of silica-coated silver nanoprobe for paraoxon pesticide detection. *Bionanoscience*. 2014;4(2):149-156. doi:10.1007/s12668-014-0129-6
22. Martínez-Castañón GA, Niño-Martínez N, Martínez-Gutierrez F, Martínez-Mendoza JR, Ruiz F. Synthesis and antibacterial activity of silver nanoparticles with different sizes. *J Nanoparticle Res*. 2008;10(8):1343-1348. doi:10.1007/s11051-008-9428-6
23. Salvioni L, Galbiati E, Collico V, et al. Negatively charged silver nanoparticles with potent antibacterial activity and reduced toxicity for pharmaceutical preparations. *Int J Nanomedicine*. 2017;12:2517-2530. doi:10.2147/IJN.S127799
24. Dawadi S, Katuwal S, Gupta A, et al. Current research on silver nanoparticles: synthesis,

characterization, and applications. *J Nanomater*. 2021;2021. doi:10.1155/2021/6687290

25. Gerion D, Pinaud F, Williams SC, et al. Synthesis and properties of biocompatible water-soluble silica-coated CdSe/ZnS semiconductor quantum dots. *J Phys Chem B*. 2001;105(37):8861-8871. doi:10.1021/jp0105488

Chapter 5

Fabrication of Electrochemical Immunosensor for Detection of CEA

Chapter 5: Fabrication of Electrochemical Immunosensor for Detection of CEA

5.1. Introduction

According to the research accomplished by WHO, the fatality rate of cancer in 2018 was 9.6 million, which is expected to be enhanced by 29.5 million by the end of 2040. It was estimated that, out of all the patients who died from cancer, In 2018, 2.09 million casualties were from lung cancer, 2.09 million were from breast cancer, as well as 1.80 million casualties were from colorectal cancer[1]. Tumor markers might have played a crucial role, in all the above-mentioned cancer cases, for early diagnosis of such solid tumor cases[2]. Majority of human cancers are solid tumors (about 85%) till date, including cancers of the breast, prostate, colon, brain, bladder, ovary, rectum, as well as few other tissues. Although there is an exceptional growth in the area of anti-cancer therapeutics, yet proper therapy for cancers associated to solid tumors is unlikely available[3]. Therefore, there is the need of diagnosis of tumor in the initial state, thereby it can be treated properly in advance. This can enhance the life expectancy period of the patient.

Nowadays, nanomaterials have developed at a fast pace as an encouraging candidate for the detection of various diseases as they may decipher long-term problems such as-systemic distribution and solubility of various drugs[4], tumor attained resistance, additionally can enhance the working execution of diagnostic methods[5]. The investigative tools for the detection of biomarkers must be efficient in working at the level of distinctive diagnosis and be special to not generate various false positive results. In recent years, a number of immunoassay techniques for the diagnosis of different tumor markers for more effective governance of cancer have been investigated. An absolutely remarkable method for the observation of cancer is the evaluation of serum tumor markers[6]. Gradually, electrochemical immunoassay has acquired acceptance and therefore broadly utilized to detect tumor markers because of the intrinsic benefits such as elevated selectivity, sensitivity, suitable label-free manipulation, low cost, minute size, and very fast analysis[7]. There exist numerous kinds of electrochemical immunosensor built upon conductometry, amperometry, potentiometry, and electrochemical-impedance-spectroscopy[7]. Evolving a CEA (carcinoembryonic antigen) immunosensor having good selectivity and sensitivity but lacking a complex fabrication procedure still fascinates researchers.

It is noteworthy to mention that, AgNPs are fascinating nanomaterial for requisition in detection because of its catalytic activity[8], plasmonic properties[9], and high conductivity[10]. All of these properties can be used to upgrade the performance of biosensors[11]. For the diagnosis of minimal concentration of an analyte, the sensitivity of the sensor is a prominent factor[12]. AgNPs are utilized to elevate the electroactive field of the electrodes and accordingly the rate of the electron-transfer, thereby enhancing the biosensor's sensitivity[13].

The motive of our study is to combine the benefits of metal nanoparticles, i.e. silver nanoparticles along with silicon dioxide (SiO_2) onto an ITO (indium tin oxide) film to fabricate a new electrochemical immunosensor for the detection of CEA with high sensitivity and selectivity. In the current work, silver nanoparticles were synthesized by an altered chemical reduction procedure by utilizing citrate and further the encapsulation of silver nanoparticles with silica through the revised Stober method (sol-gel). All of the electrochemical experimentation was carried out through cyclic-voltammetric (CV) studies. In addition, the observation of electron transfer resistance by electrochemical–impedance spectroscopic (EIS) studies was also a component of the study. EIS is a specific faradic impedance technique, that happens in the existence of a redox couple. This is a label-free method to discover antigen-antibody reactions on the electrode surfaces by calculating their capacitance as well as interfacial charge transfer resistance. Instantly, a target protein binds with the probe surface which is already functionalized, the electrochemical-impedance of the electrode interface changes, and such types of alteration are detected electrically across an extent of measurement frequencies.

5.2. Background of electrochemical immunosensor based on CEA

In recent years, a number of immunoassay-techniques for the diagnosis of different tumor markers for more effective governance of cancer have been investigated. A sailing way for the observation of cancer has been the evaluation of serum tumor markers. These days, numerous tumor markers (e.g. CA-15-3, CA19-9, AFP, CA-125, HCG, PSA, etc) available in regular clinical work for diagnosis[14]. Amid all of the tumor markers accessible today, CEA gained approval from US food and drug Administration (FDA) and it is an well-known tumor-associated-antigen(TAA)[15]. As stated by Zhu and Basu co-workers, CEA[16] belongs to a class of glycoprotein with molecular weight of approx 180- 200 kDa, it is connected to the superfamily of CEA-associated cell-adhesion (CEACAM). CEA is normally formed during fetal growth, but its production ceases before birth.

In various normal tissues, CEA is expressed inadequately in a variety of normal tissues, which includes the esophagus, tongue, prostrate, colon, stomach, tongue, and cervix. A high level of serum CEA is associated with numerous carcinomas[17]. In view of physiological state, normally CEA is manifested on the luminal segment and apical surface of the normal epithelial cells. CEA fails to gain the polarized distribution in cancer tissues and overexpresses itself, and cleave from the surface of cancerous cells through phospholipase, and it evolved in the uplifted level of serum CEA. Numerous other medical ailments also exist that can elevate CEA levels, which includes cirrhosis of the liver, smoking, pancreatitis, infections, and inflammatory bowel disease[15]. As described by Pommerich and his colleagues, CEA plays a key role in the invasion, adhesion, and migration of

cancer, and on account of its numerous extraordinary qualities, it has become a remarkable target for immunotherapy and medicaments dependent upon antibodies in CEA-positive tumors[18].

In patients with cancer, observation of the level of CEA before surgery is also approved by the ASCO (American Society of Clinical Oncology)[8]. The amount of CEA may also be uplifted in case of emphysema, which is a lung condition, designated as a COPD (chronic obstructive pulmonary disease)[19]. Here it is important to remark that, people suffering from COPD, experience more severe illness due to COVID-19 because of their prevailing lung problems[20],[21]. Therefore, a good strategy is required to accommodate appropriate diagnosis of patients having solid tumors.
Immobilization of antibodies on solid support allows successful capture of analyte in diagnostic assays as in immunosensor. Despite that, several drawbacks exist to employing such approaches as the results of the test are not always faultless, need exorbitant reagents, an exceptional possibility of false or adverse results, and labor-intensive[22]. As stated by Wafik El-Deiry and the co-workers in 2019, exceptional cancer care requires futuristic molecular diagnostics[23].

The employment of ITO for sensing purposes can be apparently increased by incorporating nanoparticles on its outer layer[24]. Metal nanoparticles gives a biocompatible environment for the sake of biomolecules which remarkably enhance the surface-to-volume proportion of an stagnant biomolecule onto the surface of the electrode, both of them finally effect electrical signal improvement[25]. Experts in the area of biosensors are invariably eager about unearthing novel materials possessing acceptable abilities to increase the activity of biosensors. Composite nanomaterials are appropriate to generate a constant electric field as well as elevate the transferred ratio of electrons in comparison to sole nanoparticles. Therefore, they can successfully fasten the regeneration action of sensors[26].

Gradually, electrochemical immunoassay has acquired acceptance and is therefore broadly utilized to detect tumor markers because of the intrinsic benefits such as lofty selectivity, sensitivity, suitable label-free manipulation, low cost, minute size, and very fast analysis[7]. There exist numerous kinds of electrochemical immunosensor built upon conductometry, amperometry, potentiometry, and electrochemical-impedance-spectroscopy[7]. Evolving a CEA immunosensor having good selectivity and sensitivity but lacking a complex fabrication procedure still fascinates researchers.

5.3. Experimental

5.3.1. Materials

All of the chemicals were bought from Sigma-Aldrich® and employed without any purification; trisodium citrate dehydrates ($Na_3C_6H_5O_7.2H_2O$), silver nitrate ($AgNO_3$), tetra-ethyl-ortho-silicate (TEOS), ammonia solution (28-30wt%), absolute ethanol, HCl, NaOH, HRP (horse-radish-peroxidase), bovine-serum-albumin (BSA, 99%), CEA antigen and its corresponding

antibody, acetone, ITO-glass-slides 2x2 cm^2(resistance 30 Ω). The phosphate-buffered saline (PBS) buffer (0.1M) for the assay was made by blending a stock standard mixture of sodium-phosphate-monobasic (NaH_2PO_4) and sodium-phosphate-dibasic (Na_2HPO_4). All of the colloidal solutions were formulated with double distilled water (18.2 MΩ) which is deionized. The entire glass apparatus were precisely cleaned using detergent and finally washed with deionized water prior to use for the experimentation.

5.3.2. Characterization

5.3.2.1. Equipment

The images of the scanning electron microscope (SEM) were obtained from the special edition of EVO-18 CARL ZEISS. Entire electrochemical quantification was practiced by employing an Electrochemical Workstation named ZIVE MP1 which is a basic three-electrode setup comprising of modified ITO as the working electrode, saturated-calomel electrode (SCE) worked as reference electrode and platinum cable was utilized as a counter electrode.

5.3.2.2. Electrochemical Detection

An ambient laboratory temperature of 25ºC was selected for entire electrochemical tests. Phosphate buffer solution (PBS) with pH 6.0 was used as an electrolyte. All electrochemical experimentation of the bare ITO & the modified ITOs was administered by utilizing 0.1M PBS buffer of pH 6.0 comprising of NaH_2PO_4 (pH was maintained by HCl & NaOH) and Na_2HPO_4; for electrochemical impedance spectroscopy (EIS) and cyclic voltammetry (CV) studies.

5.3.3. Synthesis of Ag@SiO_2 nanoparticles

The coating of silica on silver nanoparticles was accomplished by an altered “Stober” process[3]. The fabricated concentrated silver nanoparticles were kept in a solution of deionized water, liquid ammonia (28 to 30 %), and pure ethanol (100 ml, 99.9%). Following 35 mins of sonication, numerous quantities of TEOS (Tetraethyl orthosilicate) were casted dropwise (starting from 2 to 15 µl) further the solution was accurately agitated at ambient room temperature for 15 h. By changing the quantity of the TEOS, the thickness of the silica encapsulation can be controlled. For the segregation of solution, centrifuged at 13500 RPM for the duration of 40 mins accompanied by washing the solution-mixture three times in ethanol (100%) at 8000 RPM for 15 mins. For utilization afterward, the prepared Ag@SiO_2 - nanoparticles were dissolved in purified water.

5.3.4. Fabrication and designing of electrochemical immunosesor for the detection of CEA.

The diagrammatic presentation of the assembling process of immunosensor is depicted in fig.no.5.1. ITO glass -slides (2X2 cm^2) were sonicated by using acetone, ethanol, and water subsequently for about 30 mins, later dried under a flow of nitrogen. After that, 10 µl of prepared Ag@SiO_2 nanoparticles was dropped onto the cleaned ITO-surface and then left to dry at room

temperature overnight. Additionally, 10µl of 10µg/ml anti-CEA liquid solution was casted at Ag@SiO_2 NPs/ITO facet for the period of 8 h at 25C°. Further**,** a 15 µl of 6 µg/ml HRP-enzyme was used to block the non-specific sites on the antibody modified electrode facet. There are few other advantages also associated with HRP-enzyme, as HRP can magnify a frail sign and increase the whole detection procedure of a selected biomolecule. Finally, BSA (1%) was supplemented to the surface of the electrode to hinder the excess active group.

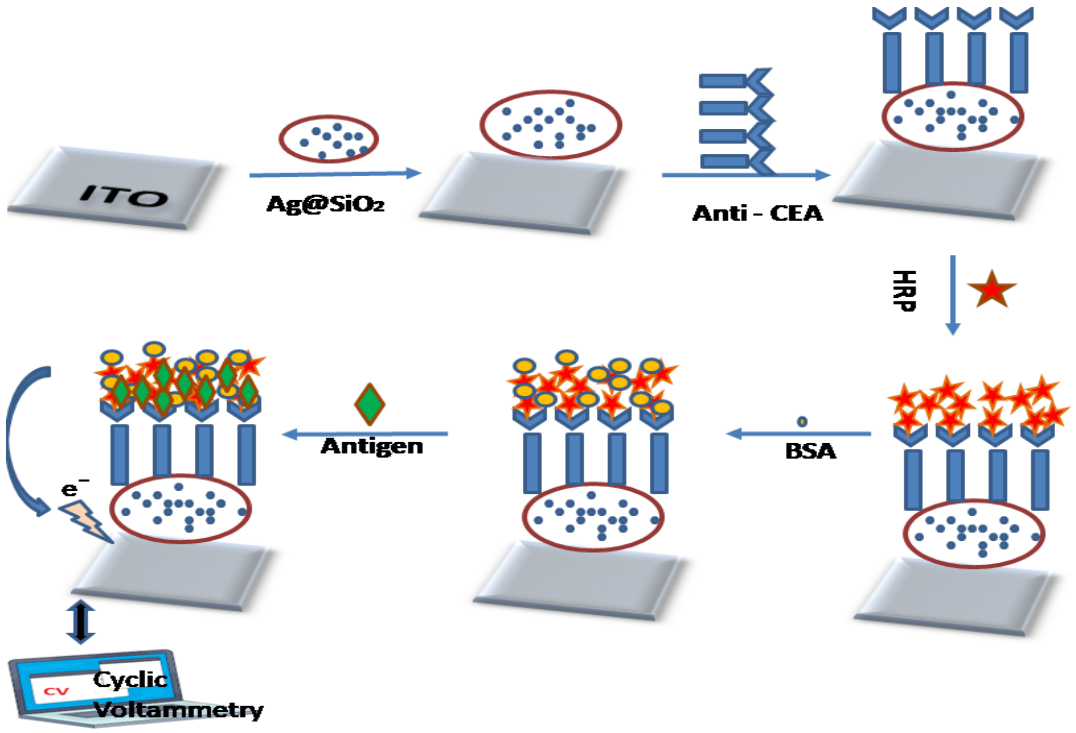

Figure 5.1: Schematic of the step-by-step fabrication process of disposable electrochemical immunosensor.

After desiccating the electrode surface, different concentrations of CEA were added to the electrode surface. Later, the modified ITO (electrode) was put in an incubator for 1 h at 40°C and further washed by the employment of a buffer solution mixture to separate the excess CEA. Here, it is important to mention that, the electrode was dry off by the use of nitrogen after each fabrication step.

5.4. Results and discussion

5.4.1. Optimization of experimental condition

Numerous experimental specifications need to be optimized to fabricate an immunosensor. First, the concentration of the associated antigen (CEA) was optimized to enrich the sensitivity. Even while using low concentrations of CEA, it was unearthed that clearly defined voltammetric peaks were conceivably found, all of these results are displayed in Fig.5.2. Additionally, the peak-current intensities expand, with the increase in the concentration of the CEA. On the other hand, with the

increase in the concentration of CEA, notable gain of high signal, it also included the elevated background at the same time due to the non-specific adsorption method. It was observed that the measuring scale of the current Vs CEA (Fig.5.2.B.) is straight from the range of 0.5ng/ml to 10 ng/ml, therefore, it is suitable for the computable function. The towering signal-to-noise ratio was potentially acquired while keeping the CEA concentration at 10 µl. Thus, 10 µl of antigen was selected as the optimized condition. For this procedure, the limit of the detection was held to be 0.01ng/ml. There are 6 repeated measurements while taking CEA-concentrations of 0.5ng/ml to 10ng/ml was taken.

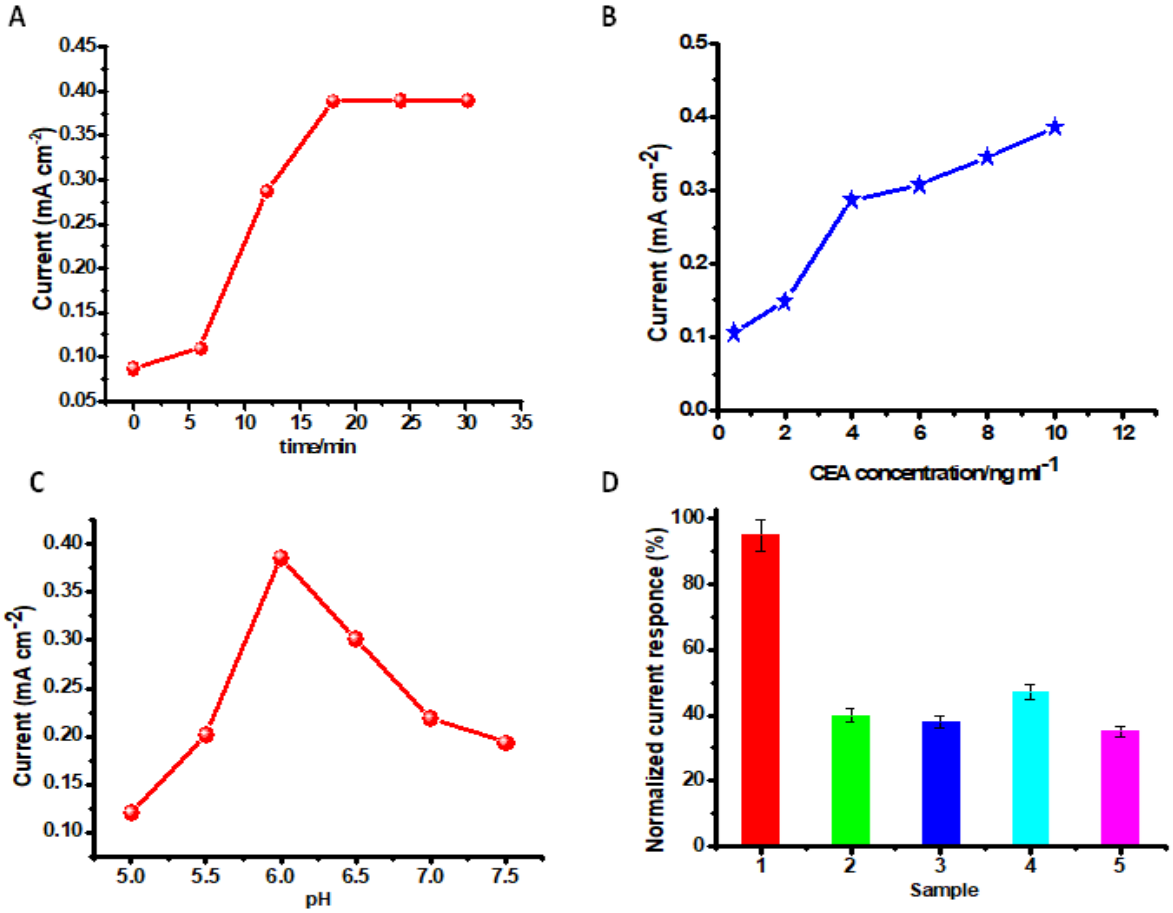

Figure 5.2: Plots of optimizing the experimental specification (A) The variation of peak current, when the fabricated immunosensor was kept for incubation at numerous time intervals. (B) Standardization plot of alteration in peak current rate of the prepared immunosensor Vs concentration of CEA under optimum conditions (C) The observation of the highest electric-current wave of the prepared immunosensor after altering the pH of the PBS buffer mixture. (D) Selectivity of the prepared disposable immunosensor in the presence of (1) CEA (5ng mL^{-1}) (2) 5ng /mL CEA+20ng/mL PSA (3) 5ng/mL CEA+ 20ng/mL AFP (4) 5 ng/mL CEA+ 20 ng/mL Glucose (5) 5 ng/mL CEA+ 20 ng/mL CA-125.

In addition to this**,** the electrochemical reactions which take place in an immunosensor have a high impact on the pH of the detection solution. If pH is unsuitable then protein denaturation can occur. So, the pH of the buffered solvent was investigated thoroughly to acquire an outstanding electric-current signal. Facilitating the concentration of the CEA- persistent (10 µl), the consequence of the value of the pH of the buffer solution on the current intensity was measured by keeping the pH range, starting from 5.0 to 6.0 and after achieving maximum current at pH 6.0, the current-intensity diminished correspondingly when the pH-value increased from 6.0 to 7.5. All of these results define that pH 6.0 is more beneficial for the current response of the immunosensor assembly system. Therefore, pH 6.0 was chosen as the most suitable value. By the employment of PBS buffer at pH 6.0, carefully divulged cyclic voltammograms in addition to properly responding to CEA were recognized. By preserving the concentration of the CEA-20ng/ml, the influence of the incubation period was investigated in the time of 0-30 mins. It was noted that, in the initial 17 mins., ΔI swiftly increased and when the incubation time was more than 17 mins, it approached a constant value. Thus, 17 mins was distinguished as an outstanding condition for incubation. For the sake of practicability in real life, the room temperature was chosen as an ideal temperature to accomplish all the experiments.

5.4.2. Scanning electron microscopy

The productiveness of an ideal electrochemical immunosensor is intertweaved to its physical framework[27]. Accordingly, the positioning of the $Ag@SiO_2$ nanoparticles layer is an important factor. Arrangement of the surface of the film was observed with the help of SEM and in fig.5.3, presumptively it is seen that $Ag@SiO_2$ nanoparticles film displayed a spotless web arrangement. While SEM-images of anti-CEA/HRP/ $CEA/Ag@SiO_2$ NPs/ITO film show the captured biological molecule's abundance through a systematic allotment.

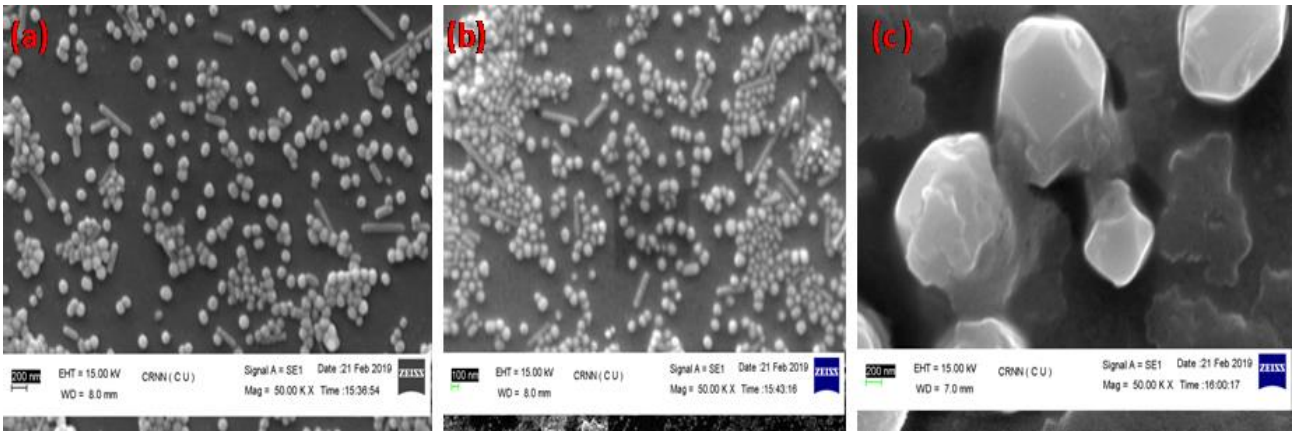

Figure 5.3: SEM images of (a) $Ag@SiO_2$ nanoparticles on ITO surface (b) CEA/HRP/anti-$CEA/Ag@SiO_2$ nanoparticles at Mag 1.00KX (c) CEA/HRP/anti-$CEA/Ag@SiO_2$ nanoparticles at Mag 5.00kx.

Particularly, it is noticeable from the surface analysis that the film of Ag@SiO2 nanoparticles shows a consistent distribution of the nanoparticles. However, from the SEM images of specific anti-CEA/HRP/ CEA/Ag@SiO2 NPS/ITO film, it is evident that there is an aggregate of the constricted biomolecules along with a static dispersal. It was observed that, in the process of immobilization of the anti-CEA, the presence of $Ag@SiO_2$ nanoparticle film plays a leading part in combination with the HRP enzyme which helps in the accurate detection of the CEA antigen.

5.4.3. Cyclic-voltammetry

The current response was markedly increased compared to the bare ITO (shown in Fig.5.4), exactly after $Ag@SiO_2$ nanoparticles were immobilized on the top of it subsequently, recommending that $Ag@SiO_2$ nanoparticles possess outstanding electrochemical features, because of the superconductivity of the Ag nanoparticles. The current response diminished when the payload of CEA antibody, HRP, and CEA was done sequentially on the modified electrode surface successfully, which could be assigned to the hindering of bio-macromolecules.

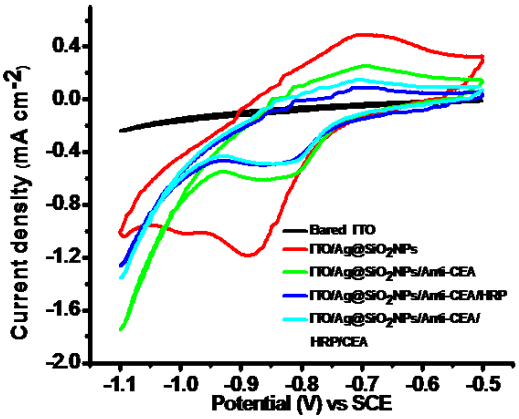

Figure 5.4: (A) CV of the successive immunosensor fabrication procedure, at scan rate 60 mVs-1 by utilizing 0.1M pH 6.0 PBS buffer mixture solution, which possesses Na_2HPO_4 and NaH_2PO_4

.

It has been seen that there is an oxidation peak at 7.5 V and a reduction peak at -1.7 V when the scan rate was 60 mV/s. There exists specific binding of CEA to its equivalent antibody, which creates a hindrance of the electron transfer, just after there is an elevation in CEA concentrations, the peak-current intensities multiply. As noticeable from Fig.5.5., the CV of the electrochemical immunosensor was after using PBS buffer by maintaining the pH 6.0. Peaks were visible after the binding of $Ag@SiO_2$ nanoparticles onto the ITO electrode flat surface attributed to the redox reaction. When there is a reduction in peak-current responses occurs of both the cathodic and anodic, it follows the immobilization methodology of the CEA antibody, which specifies that the steric obstruction effect takes place and it reduced the electron transfer between the solution and the electrode. Although, it is visible that, when HRP binds, the anodic peak-current declines, while the

cathodic peak current rises. Because HRP can amplify even a frail signal and enhance the overall detection process of a selected biomolecule. It is a prototypical electro-catalytic method. When CEA antigens were cast on the electrode surface, they cohered with CEA antibodies and the prepared antibody-antigen combination could further cause hindrance of the rate of the electron transfer because of the strong steric obstruction effect, which resulted in the drop off of retaliation of peak current. The later step-by-step manufacturing process of the immunosensor was also recognized by electrochemical-impedance-spectroscopy to confirm if the response of the surface of the electrode is favorable.

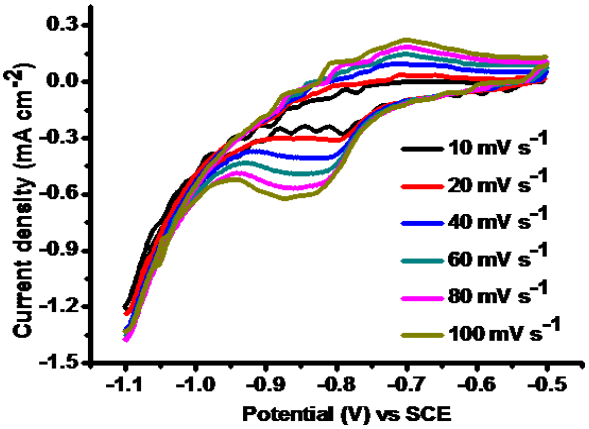

Figure 5.5: CV of prepared immunosensor at various scan rates in 0.1M pH 6.0 PBS buffer solution.

5.4.4. Electrochemical Impedance Spectroscopy (EIS)

The impedance spectrum comprised a linear line at diminutive frequencies and a semi-circle bend at towering frequencies. The electron transfer resistance (Ret) of the modified film was exhibited according to the broadness of the semi-circle diameter. The larger the semi-circle diameter is, the higher the Ret rate is. Thus, the alteration in each step was noticed by the variation in semi-circle broadness. Seemingly, the non-altered ITO electrode demonstrates a minute semi-circle curve in Fig.5.6 while, Ag@SiO_2 nanoparticles modified electrode-facet exhibited significantly higher peak-currents and nanoscopic electron transfer when differentiated with uncoated ITO electrode and over there much smaller semi-circle broadness of the Nyquist-plot and few reversible redox peaks conceivably noticed. The analysis of the redox probe to gain the surface of the electrode was exceedingly influenced by the existence of Ag@SiO_2 nanoparticles as well as it reduced the redox probe. The successive stop-up of the anti-CEA, HRP, BSA, and CEA sequentially give rise to the cumulative advancement of the Ret because of the insulation properties that the protein maintained. It explains that the electric conductivity (EC) of the modified surface of the electrode was enhanced

because of the presence of $Ag@SiO_2$ nanoparticles which possessed a huge surface area as an exceptional conducting element. Furthermore, the incorporation of anti-CEA resulted in an enhancement of the Ret and decreased peak currents, which designates the successful immobilization of the anti-CEA on the film of $AgSiO_2$ nanoparticles has been gained due to the EDC/NHS bonding along with the pi-pi stacking association between proteins and nanoparticles.

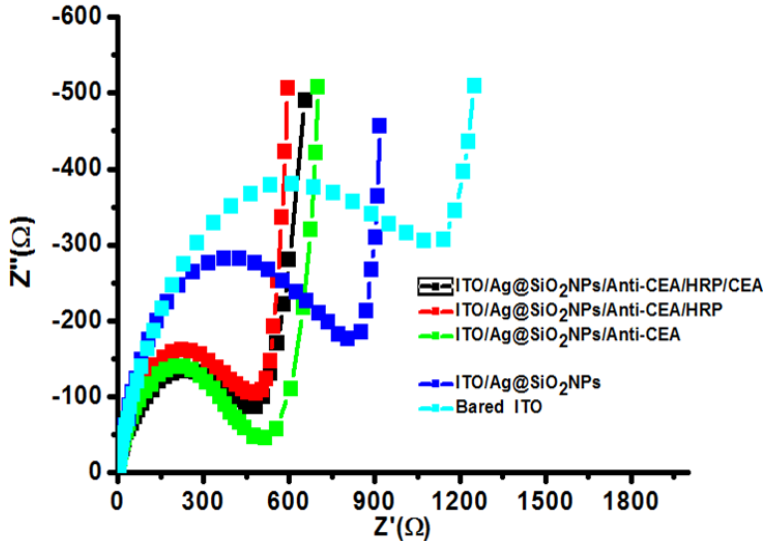

Figure 5.6: The EIS related to the different steps elaborated in the fabrication procedure in the existence of 1% PBS buffer solution, pH was maintained by NaOH and HCl.

The electron transfer resistance (Ret) of the modified electrode surface was denoted by the broadness of the semi-circle of the Nyquist plot. The larger the semi-circle wideness is, the higher the Ret value is. Accordingly, the modified methodology was recorded during the alteration of the semi-circle diameter. ITO electrode that is unchanged, displayed a smaller semi-circle diameter, and the step-by-step immobilization of the anti-CEA, HRP, BSA, and CEA subsequently, led to a progressive elevation in the electron transfer resistance.

All of the results showed that CEA, HRP, anti-CEA, and Ag@SiO2 nanoparticles film were appropriately modified onto the surface of ITO chips in sequence. The previously mentioned proteins can hinder the electron transfer of the electrochemical probe effectively. The parameters discussed here can make a divergence to an extensive range after the incorporation of HRP, which denotes that HRP could block the non-specific sites on the modified electrode. Further, it was noticed that there are decreased peak currents and an augmented Nyquist diagram after the trapping of CEA-antigens. This recommends that the ratio of the electron transfer between electrode and solution was greatly obstructed due to the immuno-reaction of antigen along with its corresponding antibody. The two of the mentioned outcomes were consistent with the reliability that the electrode was modified as

anticipated. Comparison with other previously reported immunosensors for the detection of CEA are shown in table format in table no.5.1.

5.4.5. Selectivity

The findings specified that CEA, HRP, anti-CEA, and Ag@SiO_2 nanoparticles film were readily modified on the surface of the ITO chips in sequence. The mentioned proteins can hinder the electron transfer rate of the electrochemical probe effectively. These parameters can make a divergence at an extensive range after the incorporation of the HRP, which describes that HRP could block the non-specific sites of the modified electrode. Further, it was noticed that there are decreased peak currents and a sharpened Nyquist diagram after the imprisonment of CEA-antigens. This signifies that the specific rate of the electron transfer linking electrode and solution was markedly impeded because of the involved immuno-reaction of antigen following its corresponding antibody. The two mentioned outcomes were consistent with the originality that the electrode was modified as anticipated.

5.4.6. Stability and Reproducibility of the Immunosensor

There are two main components involved in the implementation and evolution of the immunosensors, designated as reproducibility and stability. Five immunosensors were fabricated identically by taking 5 ng/ml CEA to appraise the reproducibility of the suggested immunosensor for the specific detection of the antigen. It was interesting to note that, we obtained a relative standard deviation (RSD) of 3.2%, which illustrated that immunosensor had very good reproducibility. Along with reproducibility, the stability of the immunosensor is a basic need for steady and coveted analysis. The prepared immunosensor remained at 4°C for six weeks and it was explored that only a minute decline in the current response took place. Finally, current-response was investigated, after 2 weeks, 4 weeks, and eventually after 6 weeks. Additionally, it was noticed that the immunosensor maintained 97.1, 96.4, and 94.8% of the previous response independently. It exhibits that the fabricated immunosensor possessed excellent stability.

Table 5.1- Comparison with other previously reported immunosensors for the detection of CEA.

Materials	**Detection Range (ng/ml)**	**Detection Limit (ng/ml)**	**References**
Ba-NH-AuNPs(Organoclay-nanogold composite) film	0.05-5.0; 5.0 - 120	0.01	[30]
CS-MWNT-AuNP Composite	0.3 - 120	0.1	[31]
Carboxylated g- C_3N_4/TiO_2nanosheets	0.01 - 10.0	0.0021	[32]

HRP-anti - CEA - NGGN	0.05 - 350	0.01	[10]
Ng/ chit / nano / Au Composite	0.2 - 120.0	0.06	[33]
Thi @ NPG / AuNPs	0.01 - 100	0.003	[34]
AuNP @ nafion / FC @ CHIT	0.01 - 150	0.0031	[35]
NG / P - PB / nano - Au Composite film	0.5 - 10 & 10 - 120	0.2	[36]
[Ag- Ag_2 O]/ SiO_2 nanocomposite material	0.5 - 160	0.14	[37]
CS - CNTs - GNPs - nanocomposite film	0.1 - 2.0	0.04	[38]
Ag@SiO_2NPs	0.5-10	0.01	This Work

5.5. Conclusions

The current electrochemical disposal immunosensor was prepared by immobilizing anti-CEA onto Ag@SiO_2 nanoparticles encapsulated ITO solid surface for the specific detection of CEA. Our observation was that the presence of silica-coated silver nanoparticles on the flat surface of the electrode, gives an excellent voltammetric advantage, fine stability, and noteworthy biocompatibility towards the detection and additionally gives extensive binding sites for the involved immune reactions. A potent interconnection between the response of the stripping current of the altered ITO flat surface and the particular logarithmic rate of the concentration of CEA was established extended from 0.5ng mL^{-1} to 10ng mL^{-1} with the minimum detection limit of 0.01ng/ml. Such fabrication methodology is more favorable as compared to the metal electrode as it is fabricated from a cost-effective ITO flat surface and may be recreated in bunches. This empirical, low-cost, and flexible electrochemical immunosensor allows a more uncomplicated and more low-budget immunoassay for the detection of CEA, which can provide the goal of CEA detection in clinical analysis in the future and such strategy could be utilized to manufacture immunosensors for other aimed targets also.

References

1. World Health Organization. *Guide to Cancer - Guide to Cancer Early Diagnosis*.; 2017. https://apps.who.int/iris/bitstream/handle/10665/254500/9789241511940-eng.pdf;jsessionid=2646A3E30075DB0FCA4A703A481A5494?sequence=1
2. Paner GP. ♂♀Cystic and Solid Tumors of the Urachus vs. Gynecologic Tract Tumors:

Similarities and Differences. *Gynecol Urol Pathol*. Published online 2019:316-330. doi:10.1017/9781316756423.030

3. Jain A, Jain A, Gulbake A, Hurkat P, Jain SK. Solid tumors : A review. 2011;(September).
4. Ronkainen NJ, Okon SL. Nanomaterial-based electrochemical immunosensors for clinically significant biomarkers. *Materials (Basel)*. 2014;7(6):4669-4709. doi:10.3390/ma7064669
5. Gabizon AA, de Rosales RTM, La-Beck NM. Translational considerations in nanomedicine: The oncology perspective. *Adv Drug Deliv Rev*. 2020;158:140-157. doi:10.1016/j.addr.2020.05.012
6. Kim MH, Choi MK. Relationship Between Serum Tumor-related Markers and Dietary Intakes in Korean Healthy Adults. *Clin Nutr Res*. 2018;7(3):161. doi:10.7762/cnr.2018.7.3.161
7. Kasithevar M, Periakaruppan P, Muthupandian S, Mohan M. Antibacterial efficacy of silver nanoparticles against multi-drug resistant clinical isolates from post-surgical wound infections. *Microb Pathog*. 2017;107:327-334. doi:10.1016/j.micpath.2017.04.013
8. Hao Y, Feng S, Liu Y, Xu J, Wang J. Electrochemical Sensor based on Indium Tin Oxide Glass Modified with Poly (Ethyleneimine)/ Phosphomolybdic Acid Composite Multilayers. Published online 2017:1-10. doi:10.1002/elan.201600672
9. Yamazaki Y, Kuwahara Y, Mori K, Kamegawa T, Yamashita H. Enhanced Catalysis of Plasmonic Silver Nanoparticles by a Combination of Macro-/Mesoporous Nanostructured Silica Support. *J Phys Chem C*. 2021;125(17):9150-9157. doi:10.1021/acs.jpcc.1c01669
10. Zhong Z, Wu W, Wang D, et al. Biosensors and Bioelectronics Nanogold-enwrapped graphene nanocomposites as trace labels for sensitivity enhancement of electrochemical immunosensors in clinical immunoassays : Carcinoembryonic antigen as a model. *Biosens Bioelectron*. 2010;25(10):2379-2383. doi:10.1016/j.bios.2010.03.009
11. Wang B, Akiba U, Anzai J ichi. Recent Progress in Nanomaterial-Based Electrochemical Biosensors for Cancer Biomarkers : A Review. Published online 2017. doi:10.3390/molecules22071048
12. Aydın EB, Aydın M, Sezgintürk MK. Author ' s Accepted Manuscript. Published online 2017. doi:10.1016/j.bios.2017.05.056
13. Society M. Nanoparticles Modified ITO Based Biosensor. 2017;46(4):32-35. doi:10.1007/s11664-016-5172-3
14. Chen W, Peng J, Ye J, Dai W, Li G, He Y. Aberrant AFP expression characterizes a subset of hepatocellular carcinoma with distinct gene expression patterns and inferior prognosis. 2020;11. doi:10.7150/jca.31435
15. Yu S, Li A, Liu Q, et al. Recent advances of bispecific antibodies in solid tumors. Published

online 2017:1-16. doi:10.1186/s13045-017-0522-z

16. Chen GZ, Yin ZZ, Lou JF. Electrochemical immunoassay of escherichia coli O157:H7 using Ag@SiO 2 nanoparticles as labels. *J Anal Methods Chem*. 2014;2014. doi:10.1155/2014/247034
17. Zhu L, Xu L, Jia N, et al. Electrochemical immunoassay for carcinoembryonic antigen using gold nanoparticle-graphene composite modified glassy carbon electrode. *Talanta*. 2013;116:809-815. doi:10.1016/j.talanta.2013.07.069
18. Dolscheid-pommerich RC, Manekeller S, Walgenbach-brünagel G. AFP in Gastrointestinal Cancer Using LOCI ™ -based Assays. 2017;360. doi:10.21873/anticanres.11329
19. Paper O. Comparison of Serum CA 19 . 9 , CA 125 and CEA Levels with Severity of Chronic. Published online 2009:289-293. doi:10.1159/000215726
20. Hong H. Clinical characteristics of novel coronavirus disease 2019 (COVID-19) in newborns, infants and children. 2020;2019.
21. Russell R. Covid-19 and COPD : A Personal Re fl ection. Published online 2020:883-884.
22. Sakamoto S, Putalun W, Vimolmangkang S, Phoolcharoen W. Enzyme - linked immunosorbent assay for the quantitative / qualitative analysis of plant secondary metabolites. *J Nat Med*. 2017;(0123456789). doi:10.1007/s11418-017-1144-z
23. El-Deiry WS, Goldberg RM, Lenz H, et al. The current state of molecular testing in the treatment of patients with solid tumors, 2019. *CA Cancer J Clin*. 2019;69(4):305-343. doi:10.3322/caac.21560
24. Links DA. Analytical Methods Reagentless amperometric immunosensor for a -1-fetoprotein based on. Published online 2012:3575-3579. doi:10.1039/c2ay25778e
25. Cho I hoon, Lee J, Kim J, et al. Current Technologies of Electrochemical Immunosensors : Perspective on Signal Amplification. Published online 2018:1-18. doi:10.3390/s18010207
26. Lokina S, Stephen A, Kaviyarasan V, Arulvasu C, Narayanan V. SC. *Eur J Med Chem*. Published online 2014. doi:10.1016/j.ejmech.2014.02.010
27. Balahura L roxana, Staden R ioana S van, Frederick J, Staden V, Aboul-enein HY. Advances in immunosensors for clinical applications. *J Immunoass Immunochem*. 2018;00(00):1-12. doi:10.1080/15321819.2018.1543704
28. Huang KJ, Niu DJ, Xie WZ, Wang W. A disposable electrochemical immunosensor for carcinoembryonic antigen based on nano-Au/multi-walled carbon nanotubes-chitosans nanocomposite film modified glassy carbon electrode. *Anal Chim Acta*. 2010;659(1-2):102-108. doi:10.1016/j.aca.2009.11.023
29. Wang SX. As featured in : 2013;(207890). doi:10.1039/c3tb00003f

30. Kemmegne-mbouguen JC, Ngameni E, Baker PG, Tesfaye T, Kgarebe B, Iwuoha EI. Carcinoembryonic Antigen Immunosensor Developed with Organoclay Nanogold Composite Film. 2014;9:478-492.
31. Song Z, Yuan R, Chai Y, Yin B, Fu P, Wang J. Electrochimica Acta Multilayer structured amperometric immunosensor based on gold nanoparticles and Prussian blue nanoparticles / nanocomposite functionalized interface. 2010;55:1778-1784. doi:10.1016/j.electacta.2009.10.067
32. Wang H, Wang Y, Zhang Y, et al. Photoelectrochemical Immunosensor for Detection of Carcinoembryonic Antigen Based on 2D TiO 2 Nanosheets and Carboxylated Graphitic Carbon Nitride. *Nat Publ Gr*. 2016;(March):1-7. doi:10.1038/srep27385
33. He X, Yuan R, Chai Y, Shi Y. A sensitive amperometric immunosensor for carcinoembryonic antigen detection with porous nanogold film and nano-Au / chitosan composite as immobilization matrix. 2008;70:823-829. doi:10.1016/j.jbbm.2007.06.002
34. Sun X, Ma Z. Electrochemical immunosensor based on nanoporpus gold loading thionine for carcinoembryonic antigen. *Anal Chim Acta*. 2013;780:95-100. doi:10.1016/j.aca.2013.04.023
35. Shi W, Ma Z. A novel label-free amperometric immunosensor for carcinoembryonic antigen based on redox membrane. *Biosens Bioelectron*. 2011;26(6):3068-3071. doi:10.1016/j.bios.2010.11.048
36. Lv P, Min L, Yuan R, Chai Y, Chen S. A novel immunosensor for carcinoembryonic antigen based on poly (diallyldimethylammonium chloride) protected prussian blue nanoparticles and double-layer nanometer-sized gold particles. Published online 2010:297-304. doi:10.1007/s00604-010-0435-9
37. Yuan Y, Yuan R, Chai Y, Zhuo Y, Mao L, Yuan S. A novel label-free electrochemical immunosensor for carcinoembryonic antigen detection based on the [Ag-Ag2O]/SiO2 nanocomposite material as a redox probe. *J Electroanal Chem*. 2010;643(1-2):15-19. doi:10.1016/j.jelechem.2010.03.014
38. Gao X, Zhang Y, Wu Q, Chen H, Chen Z, Lin X. One step electrochemically deposited nanocomposite film of chitosan-carbon nanotubes-gold nanoparticles for carcinoembryonic antigen immunosensor application. *Talanta*. 2011;85(4):1980-1985. doi:10.1016/j.talanta.2011.07.012

Chapter 6

Evaluation of the Anti-Cancer Potential of Ag Nanoparticles and Ag@SiO_2 Nanoparticles

Chapter 6: Evaluation of the Anti-Cancer Potential of Ag Nanoparticles and Ag@SiO_2 Nanoparticles

6.1. Introduction

These days it is possible to merge chemistry, physics, genetics, and microbiology to tailor structures of nanomaterials for the diagnosis and therapy of various diseases which is core advantage of bionanotechnology[2],[3]. Even though numerous techniques are already available for diagnosing and treating disease, this area fascinates researchers. By utilizing nanotechnology, nanomaterials can appropriately be made lighter, stronger, more reactive, more durable, better electrical conductors, amid other techniques. So, this field encourages researchers to work on it and find some innovative therapies on the nanoscale[4].

Cancer is an ailment exceptionally unpredictable in its unveiling, evolution, and consequences. There are numerous drugs available for cancer- therapy[5]. Most cannot set foot on the target site in adequate concentrations and systematically deploy the desired pharmacological upshot without triggering irreversible undesired harm to normal cells and tissues[6]. One of the typical sorts of cancer is prostate cancer, which commences whilst cells of the prostrate evolve anomalously. Though there is historical evidence advising the existence of this cancer since antiquity, the first scientific description of this cancer was brought to notice in 1851[7]. According to GLOBOCAN 2020, approximately 19.3 million new patients of cancer were notified worldwide, and an estimated 10 million casualties related to cancer happened in 2020. Out of which, 7.3% were because of prostate cancer. There are certain limitations associated with conventional chemotherapeutic drugs[8]. Silver nanoparticles can potentially prevent drawbacks of typical cancer assorted therapeutic implementations[9].

Silver nanoparticles exhibit promising qualities for cancer therapies[10]. Although the actual method of the efficacy of silver nanoparticles against cancerous cells is not completely explained, it is appropriately known that their cytotoxicity depends on the propagation of reactive oxygen species (ROS)[11],[12]. The cytotoxicity methodology of silver nanoparticles relies on their chemical attraction with the cell's surface (showed in Fig.6.1) and the abolishment of the ions attributed to the silver from the nanoparticles; the surface-coating of the silver nanoparticles influences their cytotoxic mechanisms[13]. The specific size and surface area are also the main factors, used to demonstrate the extent of cytotoxicity. Thus, the coating material used to fabricate hybrid nanoparticles can impact cytotoxicity, as it can magnificently influence the shape, surface area, and physical properties[14]. Therefore, hybrid nanoparticles with multiple functionalities fascinate researchers among various classes of nanoparticles available at present due to their astounding properties. Cytotoxicity reactions originated by enhancing the extent of reactive oxygen species, diminishing intracellular glutathione levels, and degrading the potential of the membrane of the mitochondria. Silver nanoparticles can

create inflammation of the lung cells (epithelial) and cause macrophage inflammation[15],[16]. According to various reports, the cytotoxicity of hybrid silver nanoparticles relies on their size and coating material[17].

The synthesized silver nanoparticles coated with specific biocompatible nanomaterial can target cancerous cells in an inevitable wany because these can be specifically intended for expanded drug loading[18], upgraded half-life inside the body, calm release as well as selective distribution by altering their size, composition, surface chemistry, and morphology[19]. MTT assay reveals the appreciable anticancerous advancement of silver and silica-coated silver nanoparticles. Comprehensive results recommended a high perspective of both the nanoparticles for application in the biomedical field.

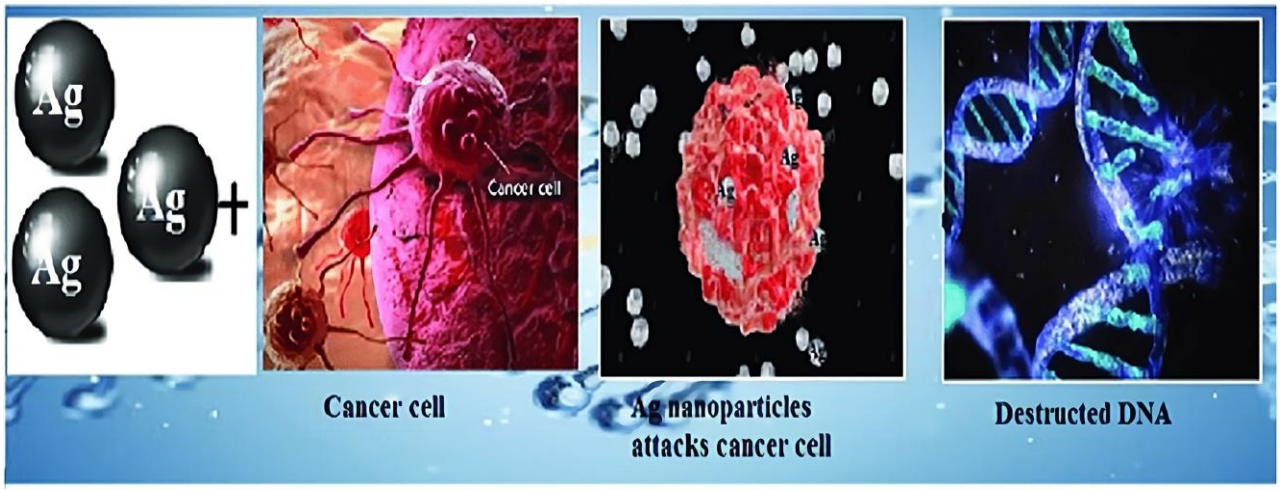

Figure 6.1: Mechanism of working of Ag nanoparticles against cancer cells.[20]

6.2. Experimental details

6.2.1. Materials and Methods

All the reagents required for synthesizing and coating silver nanoparticles were procured from Sigma. Materials used for experimentation of anticancerous activity were bought from HIMEDIA^R. Aqueous solutions were processed by using sterilized double-distilled water. The reagents/chemicals employed were of analytical grade, so utilized precisely without additional purification.

6.2.2. Statistical analysis

All experiments were reiterated thrice, before analyzing the data and then the demonstrated quantitative data were calculated as means ± standard deviation (SD).

6.3. Cytotoxic effects of Ag and Ag@SiO_2 nanoparticles

Despite immense endeavour and advancements in cancer research, treatment failure rates are still very high, mainly because of dose-limiting toxicity[21], drug resistance, and severe side effects[22],[23]

Amid metallic nanoparticles, AgNPs and their related hybrid nanomaterials stand out because of their wide range of applications[24]. Because of the advancement in nanotechnology, novel therapeutic methods have flourished for the utilization of Ag NPs in the field of medicine. Various studies have shown that AgNPs can enter the cells through the process of endocytosis and later their localization into the cell can be settled equally perinuclear space of the cytoplasm as well as the endolysosomal compartment. Cytotoxicity reactions originated by increasing the range of reactive oxygen species, diminishing the levels of intracellular glutathione, and degrading the potential of the membrane of the mitochondria. AgNPs can create inflammation of the lung cells (epithelial) and cause macrophage inflammation[15],[16]. According to numerous reports, hybrid AgNPs cytotoxicity relies on the size and coating material[17], [25], [26].

Researchers have suggested that the capping or hybridization of the nanoparticle surface enhances the dissolution and stability of the nanoparticles[27].

The cytotoxicity method of AgNPs depends upon their chemical gravitation with the particular cell's exterior facet and the nullification of the ions of the silver from the nanoparticles; the surface-encapsulation of the AgNPs impacts their cytotoxic procedure[13]. The specific size and surface area are also the main factors that illustrate the extent of cytotoxicity abilities. Therefore, the encapsulating substance employed to design the hybrid nanoparticles can influence the mechanism of cytotoxicity, while it may excellently impact the physical properties, shape, and surface area[14]. The coating of the surface of the AgNP with silica can alter their interconnection with the cell and in the aftermath, impact their anticancerous activity and toxicity[28],[29].

Currently, the reduction of tetrazolium salts is significantly recognized as a promising course for the investigation of cell multiplication. The yellow-colored tetrazolium salt 3-(4, 5-dimethyl thiazolyl-2)-2, 5-diphenyltetrazolium bromide (MTT) is lessened through metabolically dynamic cells, in part by the action of enzyme -dehydrogenase, which produces NADH and NADPH i.e., reducing equivalents. The consecutive intracellular purple formazan can be evaluated by spectrophotometric means. The assay computed the pace by which the cell proliferated and contrastingly the metabolic set of events that resulted in necrosis or apoptosis.

To analyze the cytotoxic activity of colloidal silver and silica-coated silver nanoparticles, PC-3 cells were trypsinized and added into a centrifuge tube of 5 ml. The cells-pellet was procured by vortexing at 300 × g RPM. The cell count was balanced by using DMEM (Dulbecco's Modified Eagle Medium) media. For every individual well of the 96-well microtiter plate, 200µl of the cell suspension was supplemented and then the plates were incubated at 37°C in the atmosphere of 5% CO_2 for 24

hours. All of these results are exhibited in Fig.6.2 to 6.6. Following this, different concentrations (10, 20, 40, 60, and 80 μg/ml) of the sample were augmented to the respective wells and then kept for incubation. After 24 hours, 10% MTT reagent was added, eventually resulting in crystal formation. The solubilization solution (DMSO) was also used to dissolve the developed formazan. Finally, the absorbance was calculated by utilizing a microtiter plate reader at two different wavelengths, i.e., 570nm and 630nm. The growth inhibition percentage was evaluated by analyzing the nanoparticles' potency to inhibit the cell growth by 50% (IC50 value.)

6.4. Results and Discussion

6.4.1. MTT-assay

Our results exhibit that the measurements of the assay are the outcome of a complex procedure dependent on various factors. The MTT analysis is utilized to detect the metabolic-activity. Here, we employed an MTT assay to determine the PC-3 cell cytotoxicity generated by the anticancerous activity of Ag nanoparticles and silica-coated Ag nanoparticles. The viability of PC- 3 cells, shown in Fig.6.2, was calculated by the yellow-shaded tetrazolium MTT (3-(4, 5-dimethyl thiazolyl-2)-2, 5-diphenyltetrazolium bromide) colourimetric approach, focussed on the capability of live cells to reduce MTT into formazan crystals. The following intracellular purple formazan can be measured by spectrophotometry. The assay ciphered the rate by which the cell multiplies and numerous metabolic sets of events, resulting in necrosis or apoptosis.

Apoptosis is the phenomenon of organized cell death where the cell kills itself without any external factor. Whereas, necrosis is a type of cell death caused by uncontrolled external factors. Process of apoptosis is bit advantageous over necrosis where organelles are still in functioning condition even after the death of the cell.

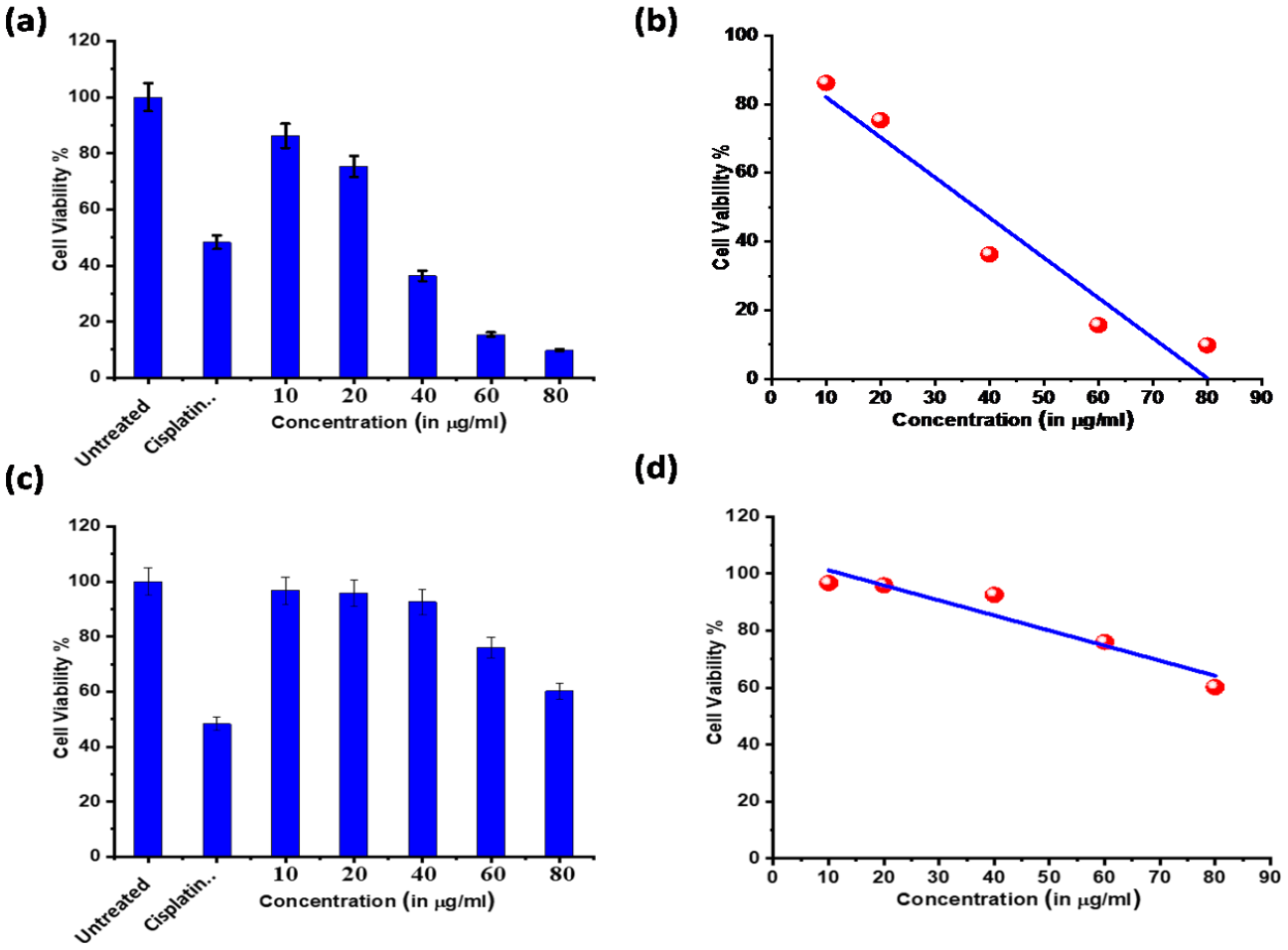

Figure 6.2: Viability of PC-3 cells after treating (for 24 hours, at 37°C, 5% CO_2) with (a) various concentrations of Ag nanoparticles and (c) silica-encapsulated Ag nanoparticles in comparison with untreated cells (negative control) and cells treated with Cisplatin evaluated in MTT reduction assay. The IC50 value was figured based on the MTT assay of (b) Ag nanoparticles and (d) silica-coated Ag nanoparticles.

Table 6.1- The IC_{50} value of the tested nanoparticles for PC-3 cell line for 24 hours of the regimen was discovered to be as mentioned here in table no.6.1:

Sample name	**PC-3 cell line** **IC_{50} (in µg/ml) 24hr**
Cisplatin	15 µg/ml
Sample Ag	37.44µg/ml
Ag@SiO_2	>80µg/ml Calculated value: 106.74µg/ml

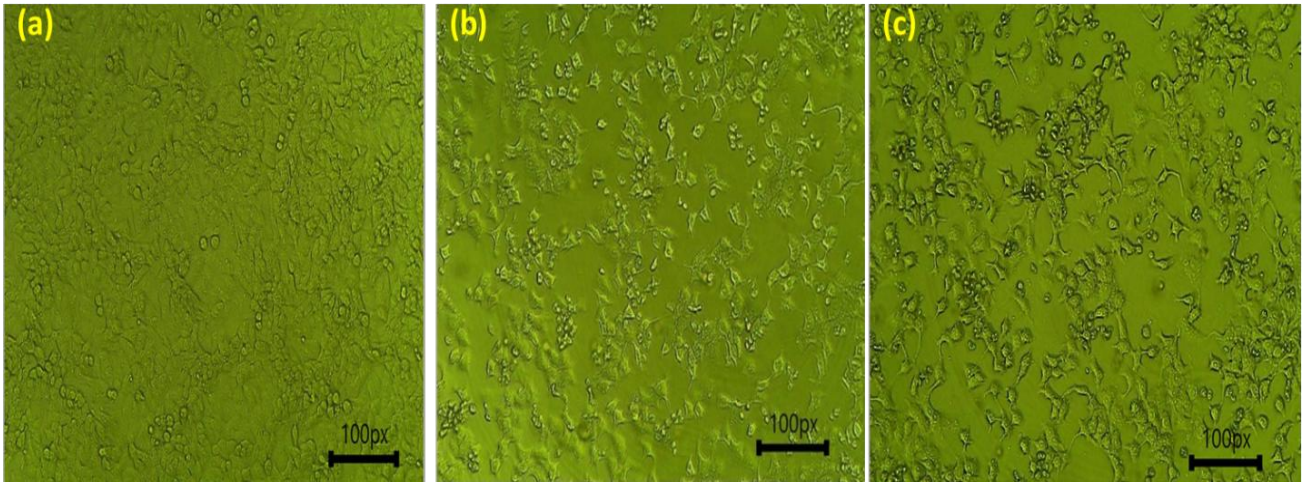

Figure 6.3: Images of (a) PC-3 cell control (b) PC-3 cells treated with Ag nanoparticles (c) PC-3 cells treated with Ag@SiO_2 nanoparticles. Variations in the morphology of the PC-3 cells after exposure to the tailored nanoparticles are evident. All of the images were depicted at a resolution of 100px.

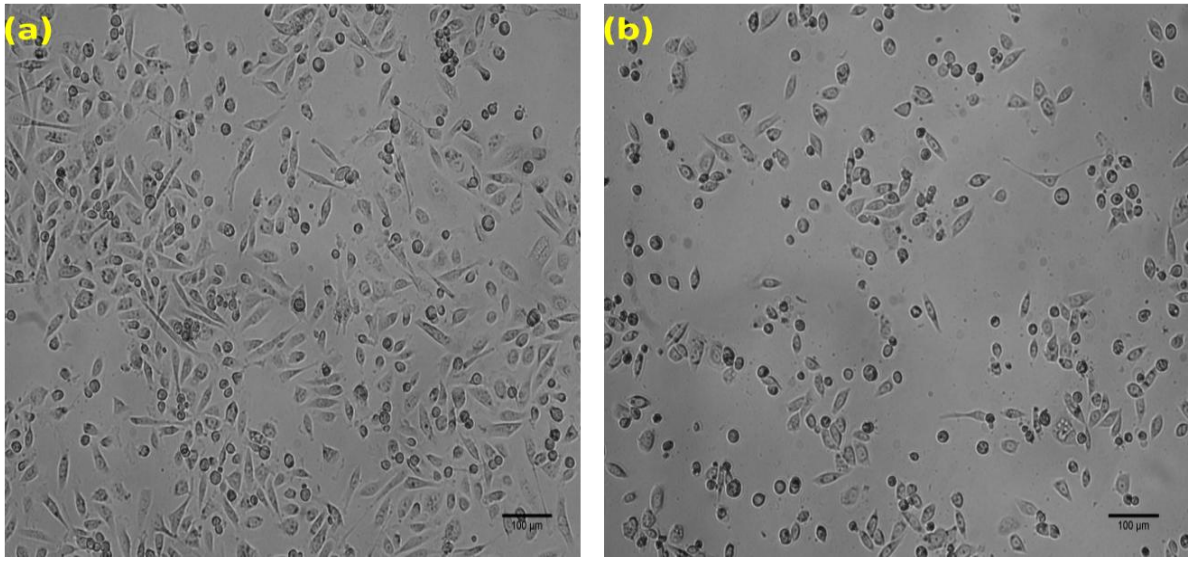

Figure 6.4: Microscopic images depicted at the resolution of 100µm of the (a) Untreated PC-3 cells and (b) cisplatin-treated PC-3 cells. Evident morphological variation is there after treatment with Cisplatin.

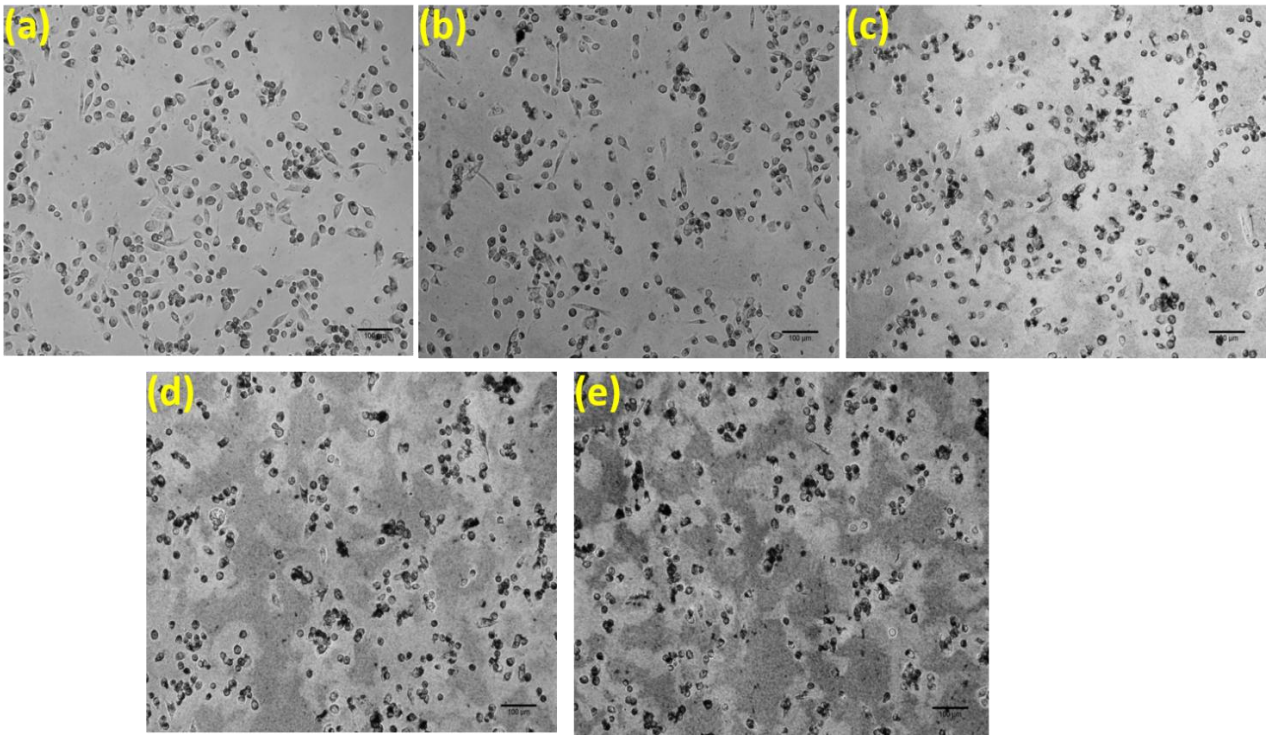

Figure 6.5: Microscopic images depicted at the resolution of 100µm of the Fig. (a) - Morphological variation on the confluency of PC- 3 cell monolayer, when exposed to the Ag nanoparticles 10 µg/ml (b) 20 µg/ml (c) 40µg/ml (d) 60 µg/ml (e) 80 µg/ml; for 24 h.

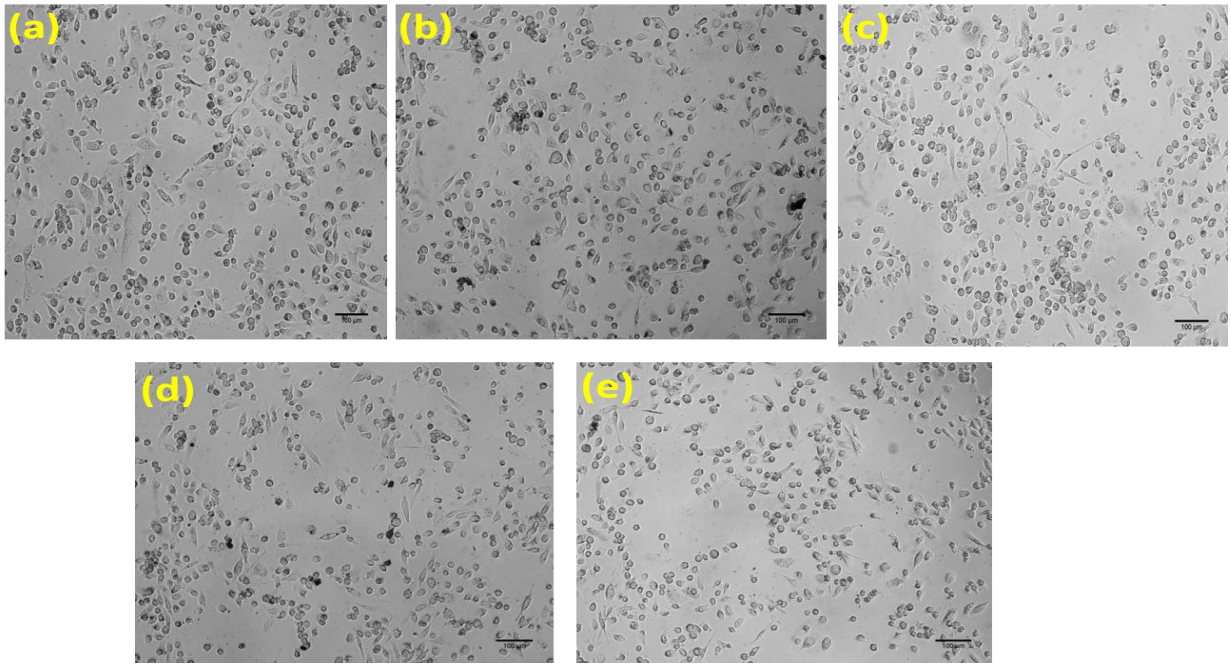

Figure 6.6: Microscopic images to observe the cytotoxic effects depicted at the resolution of 100µm of the Fig. (a) - Morphological dissimilitude on the confluency of PC- 3 cell monolayer, when exposed to the silica coated Ag nanoparticles 10 µg/ml (b) 20µg/ml (c) 40µg/ml (d) 60 µg/ml (e) 80 µg/ml.

6.4.2. Apoptosis

Apoptosis is an organized physiologic mode of cell death, a characteristic feature for anti-cancerous remedial treatment[35]. There are two pathways associated with apoptosis, i.e., extrinsic and intrinsic pathways, that employ caspases to execute this physiologic process with the help of splitting a cluster of proteins. The apoptotic- pathway in cancer is generally inhibited by diversification of overexpression of the protein designated as anti-apoptotic and underexpression of a hallmark of pro-apoptotic proteins[36]. Most of such swapping is the root of intrinsic resistance to the stereotypical anticancer therapy, chemotherapy[37]. Still, there is a dire need for propitious anticancer therapies that will show anticancerous activity by triggering the premeditated cell-death mechanism, i.e. apoptosis[37]. We examined the apoptotic activities of both the synthesized nanoparticles by flow cytometric studies, shown in fig. 6.7. Normally, the apoptotic program is assumed by some specific morphological features, including mislaying of plasma-membrane asymmetry, bonding and condensation of the nucleus and cytoplasm, and fractionalization of DNA of inter-nucleosome[38]. One of the unique earliest features is the forfeiture of the plasma membrane. During cells belonging to apoptosis, the phospholipid phosphatidylserine (PS), which is anchored to the membrane deviated from the internal side to the outer space of the plasma- membrane, therefore demonstrating PS to the outside cellular environment.

The phospholipid-binding protein, Annexin V, is a special Ca2+ fosterling protein with a molecular weight of 35-36 kDa. It possesses very high proximity to PS and interacts with cells to expose PS. Annexin V possibly coalesced with fluorochromes combining fluorescein isothiocyanate (FITC). Since the manifestation of PS occurs in the early phase of apoptosis, staining with FITC Annexin V can recognize apoptosis at the early phase compared to assays based upon DNA-fragmentation. Staining by using FITC Annexin V paves the way for losing membrane integrity and it initiates the latest stages of cell death, which occurs either from necrotic or apoptotic processes, as shown in fig.6.8. In this fig., scatter plot shows cytotoxicity studies of tailored Ag nanoparticles impelled apoptosis on PC-3 Cell monolayer by cell cycle investigation at IC50 concentration for 24 hrs analyzed employing flow cytometry following staining with Annexin v and PI. The findings of this analysis exhibited, a prominent accumulation of cells when they are in the s phase. The proportion of apoptosis was evaluated by the grade of cells that are Annexin v^+/PI^+ and Annexin v^+/PI-, which ultimately activates the apoptotic process. So, FITC Annexin V staining is generally employed in combination with a crucial dye, for instance, 7- Amino- Actinomycin Dye (7- AAD) or propidium-iodide (PI) to make it possible for the researchers to recognize early apoptotic cells (PI negative,

Annexin V positive). Effective cells containing unscathed membranes prohibit PI. Alternatively, membranes of dead and injured cells are penetrable to PI. In particular, viable cells are those cells, that are both-PI negative as well as FITC Annexin V negative, showed in fig. 6.9. In this fig., scatter plot exhibits cytotoxicity studies of tailored silica-coated Ag nanoparticles stimulated apoptosis on PC-3 Cell monolayer by cell cycle investigation at IC50 concentration for 24hrs analyzed employing flow cytometry. Number of apoptosis-associated cells was estimated employing the percentage of Annexin v+/PI+ and Annexin v+/PI- cells; which triggers the apoptosis.

FITC Annexin V positive and PI negative cells are in the stage of early apoptosis. In contrast, late apoptotic or hitherto dead cells are positive with PI as well as FITC Annexin V. It is important to mention that footnoted assay does not discriminate between cells gone through apoptotic death or contrarily died owing to necrotic- route because, in any case the dead cells are bound to stain with both PI and FITC Annexin V. But, if apoptosis is calculated over time then, cells can be mostly traced from PI and FITC Annexin V negative (that means alive or not quantifiable apoptosis), to positive with FITC Annexin V but negative with PI (early apoptotic, presence of membrane integrity), and finally positive with both- FITC Annexin V as well as PI (that means termination of apoptosis which causes death), as shown in 6.10.

As mentioned earlier, the maneuver of cells through all these three phases suggests apoptosis. Even so, this sole monitoring showing cells are twain- PI and FITC Annexin V positive by itself, does not show all the information about the phenomenon through which the cells encounter their death. There is a need for a three-dimensional study of cellular models because almost all of the pronouncements related to apoptosis to date have been churned out in cell culture system that is two-dimensional.

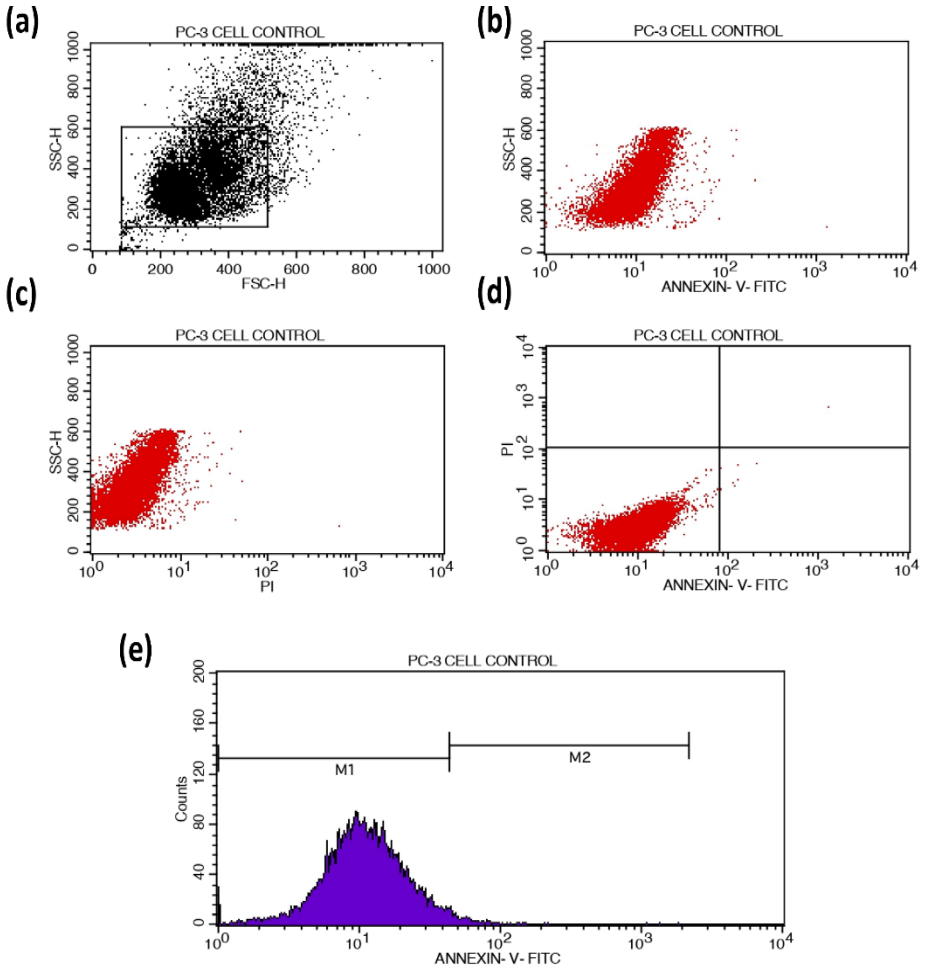

Figure 6.7: Scattergram of cell-cycle analysis by flow cytometry of PC-3 cell control. Here, each dot specifies a single cell. Side vs forward scatter reveals unstained PC-3 Cell Control. Graphs showing percentages of (a) live cells (b) in early apoptosis, (c) cells in late apoptosis, and (d) cells in necrosis were (e) acquired through the autogating operation of flowcyto-software.

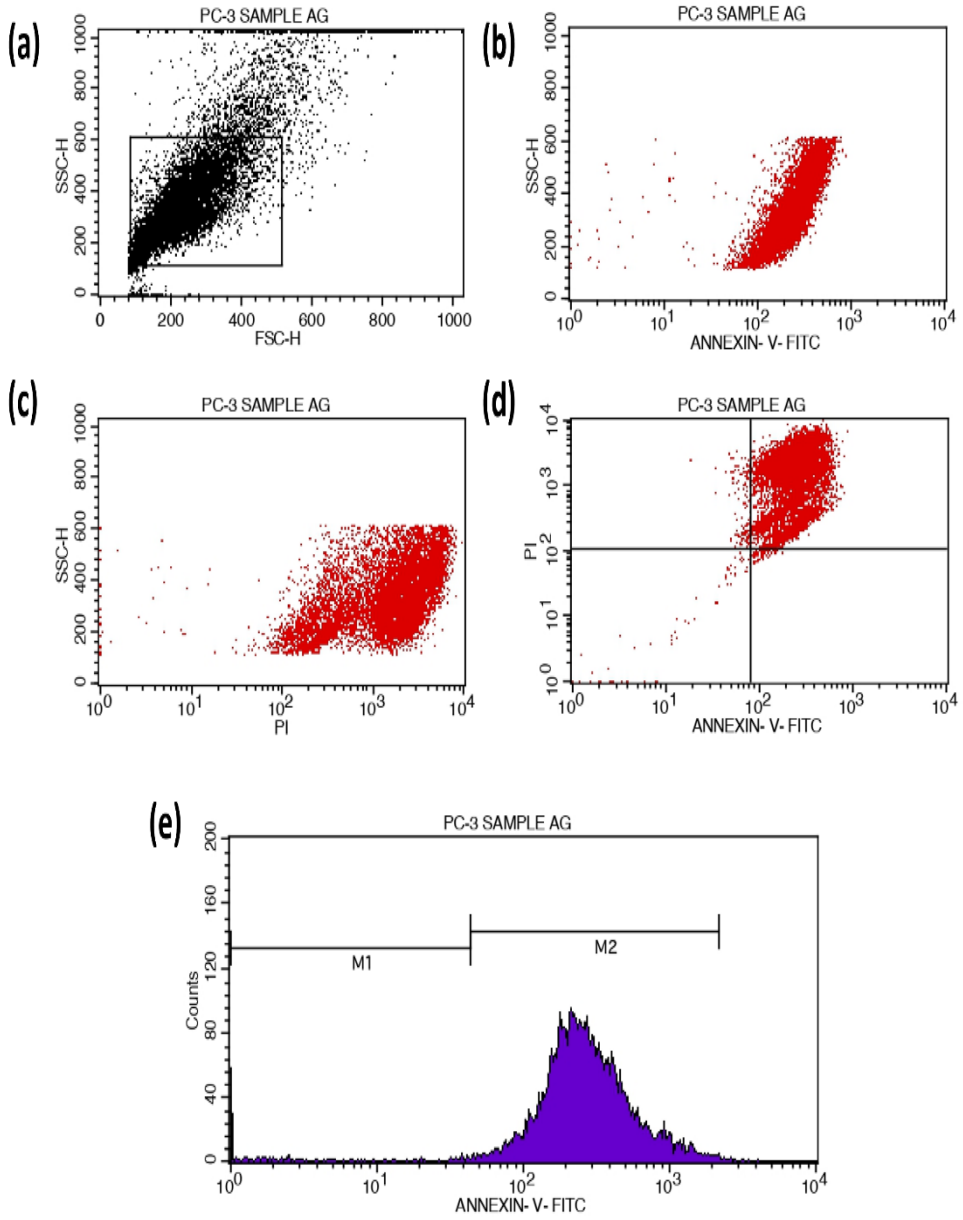

Figure 6.8: Scatter plot showing cytotoxicity studies of tailored Ag nanoparticles impelled apoptosis on PC-3 Cell monolayer by cell cycle analysis. Graphs showing percentages of (a) live cells (b) in early apoptosis, (c) cells in late apoptosis, and (d) cells in necrosis were (e) acquired through the autogating operation of flowcyto-software.

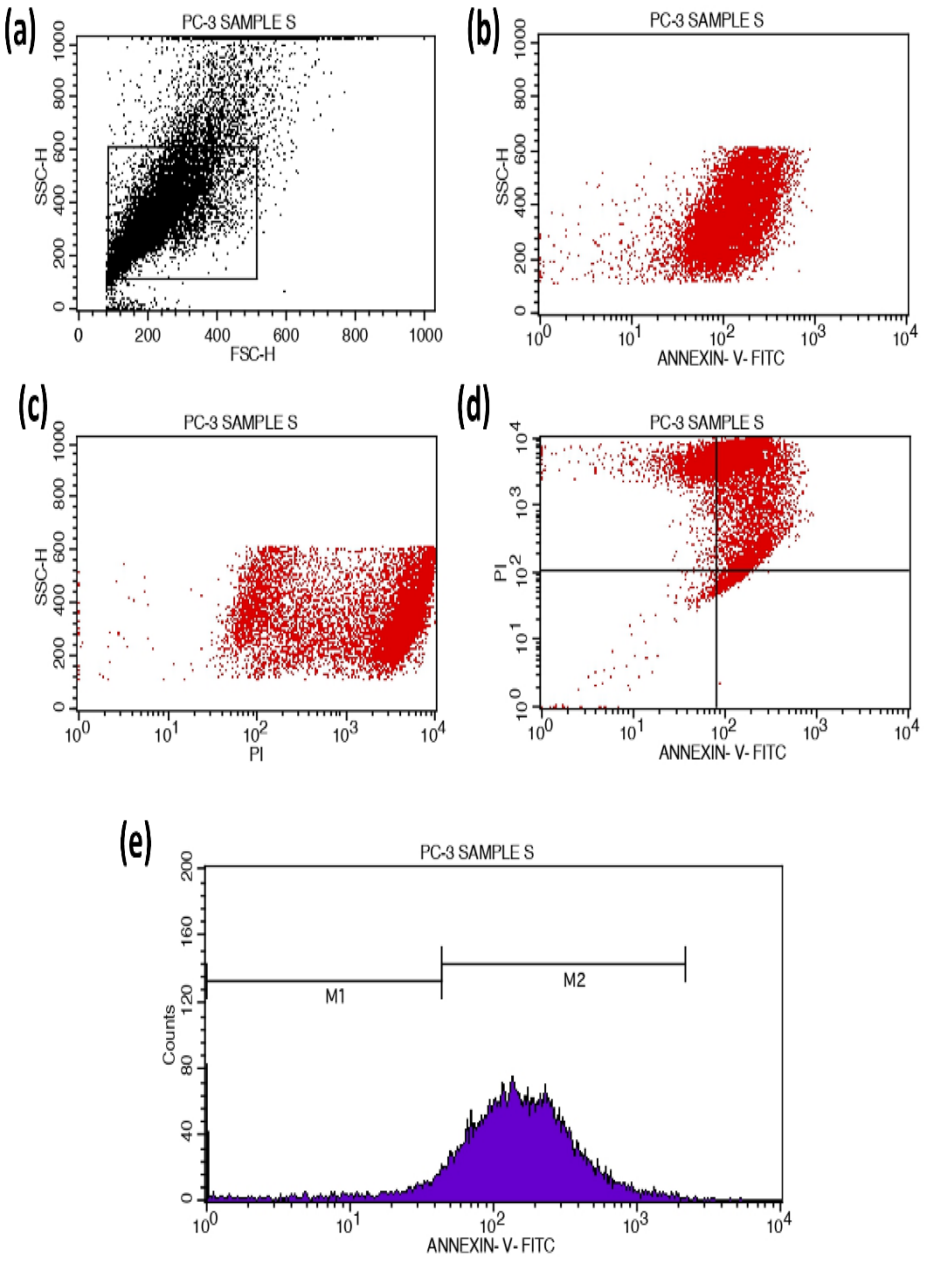

Figure 6.9: Scatter plot exhibiting cytotoxicity studies of tailored silica-coated Ag nanoparticles stimulated apoptosis on PC-3 Cell monolayer by cell cycle investigation. Graphs showing percentages of (a) live cells (b) in early apoptosis, (c) cells in late apoptosis, and (d) cells in necrosis were (e) acquired through the autogating operation of flowcyto-software.

All-inclusive results indicate the emergence of the tremendous potential of silver nanoparticles and silica-coated silver yolk-shell nanoparticles, having exceptionally worthy in the biomedical field.

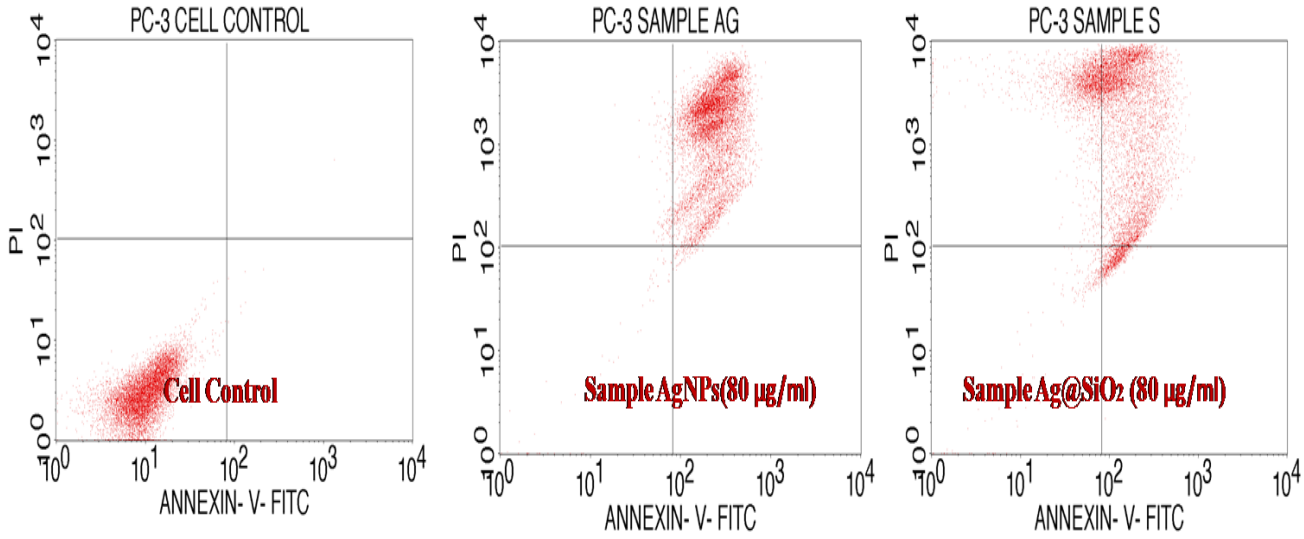

Figure 6.10: Annexin V - PI expression study of the test compounds, Ag nanoparticles, and silica-coated Ag nanoparticles against PC-3 cell line by employing BD FACS Calibur, Cell Quest™ Pro Software (Version: 6.0)

Mechanism of action- Ag and core-shell Ag nanoparticles exhibit excellent properties for cancer therapies. The mechanism of action of Ag nanoparticles (as shown in fig.6.11) against cancerous cells is dependent upon the multiplication of ROS (reactive oxygen species), straightly (generating O_2^- via donating electron to molecular oxygen) as well as incidentally impeding with functions and structure of mitochondria, which resulted into O_2^- cascade by the electron transport chain. Reactive oxygen species are derivatives of biological oxygen catabolism and consist of hydroxyl radical, hydrogen peroxide, and superoxide anion.

Under physiological surroundings, such molecules are maintained at minimal levels with the advantage of antioxidant pool of the cell, becoming important in various signaling routes. However, the abundance of ROS is associated with oxidative stress. The augmentation in the ROS extent generated through Ag nanoparticles manifestation prompts cytotoxicity, reduces rate of cell proliferation, induces destruction of macromolecules and organelles, and eventually leads to cell death. It is noteworthy to mention that reactive oxygen species inducers are principally crucial for commanding cancer advancement because tumor cells induce elevated level of ROS in comparison with healthy(normal) cells, shaping them effortlessly liable to oxidative-stress-prompted destruction, as shown in Fig.6.7. Ag nanoparticles can activate ROS production which resulted in cell death, this phenomenon also triggered through disturbing the proficiency of antioxidant molecules in the cells by the Ag nanoparticles.

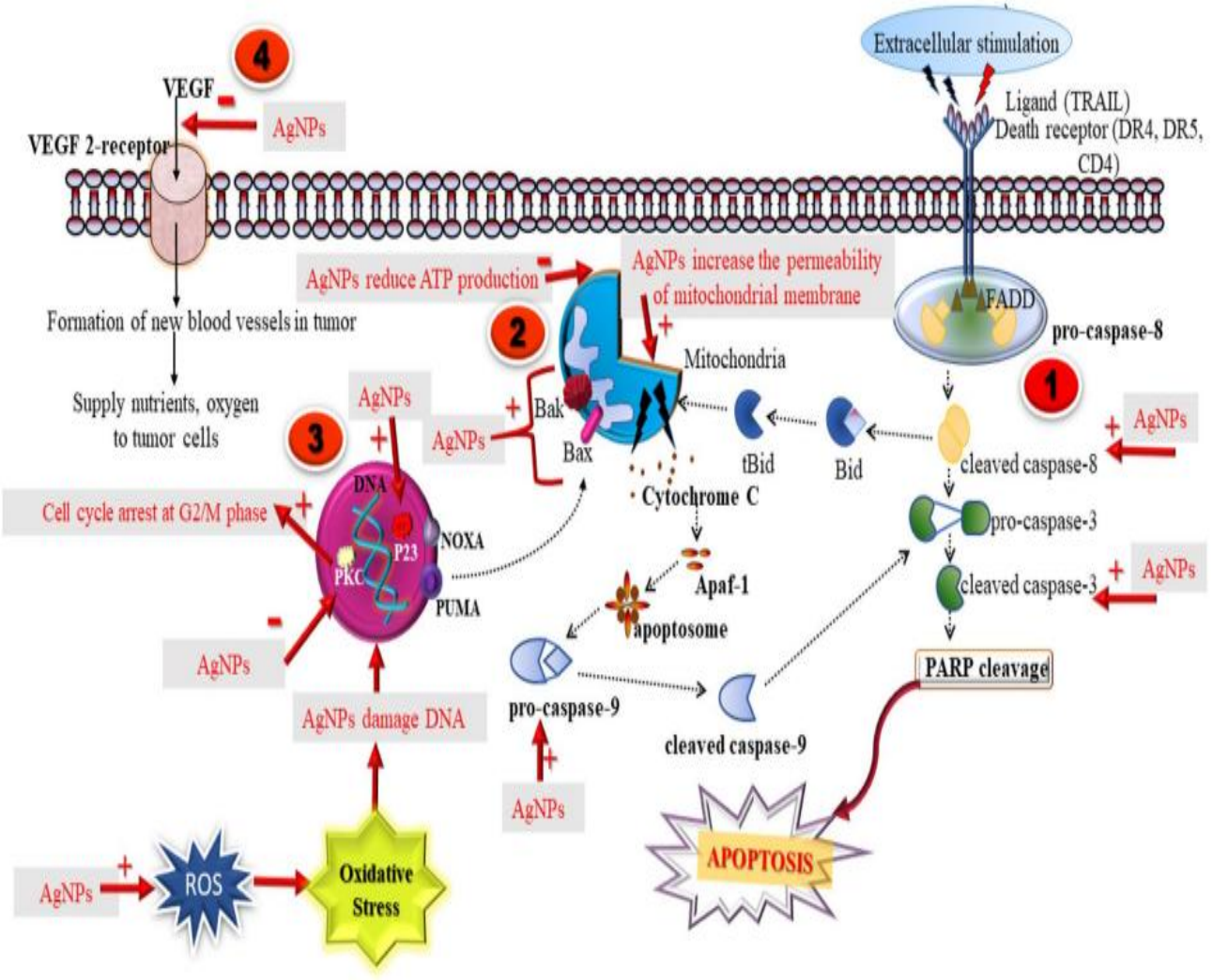

Figure 6.11: Schematic representation of apoptosis induced by Ag nanoparticles[9].

6.5. Conclusions

In the present work, rounded silver nanoparticles, and silica encapsulated silver nanoparticles were decorously modeled, and later on, we mainly emphasized their disease-repelling activities. The finely prepared nanoparticles were appraised for their anticancer activity in this context. We have examined the apoptotic activities of both the synthesized nanoparticles by flowcytometry. Notable strides have been made toward utilising engineered silver and related nanoparticles for prostate in vitro cancer treatment. Visible morphological alteration was seen after treatment with both the nanoparticles on the confluency of PC-3 cell monolayer. Silica-coated silver nanoparticles show little effects compared to the bare silver nanoparticles, attributed to the biocompatible nature of silica. However, it still shows worthwhile anticancerous activity due to the release of silver ions from the porous silica layer and silver ions anchored to the layer of the nanoparticles. These studies will focus on

nanoparticle-cell intercommunication and will also tremendously contribute to the expansion of improvement in the field of nanomedicine. To conclude, we can state that current work combines nanotechnology and cancer biology, resulting in potentially potent anti-cancerous agents for a long-lasting period. It was noteworthy that both nanoparticles have shown effectiveness in anticancerous eccentricities. So, it is proposed that both of the nanoparticles could be used as therapeutic agents for anticancer treatments in the future for the purpose of treatment of prostrate cancer.

References

1. Tan W, Wang K, He X, et al. Bionanotechnology based on silica nanoparticles. *Med Res Rev*. 2004;24(5):621-638. doi:10.1002/med.20003
2. Khorrami S, Zarrabi A, Khaleghi M, Danaei M, Mozafari MR. Selective cytotoxicity of green synthesized silver nanoparticles against the MCF-7 tumor cell line and their enhanced antioxidant and antimicrobial properties. *Int J Nanomedicine*. 2018;13:8013-8024. doi:10.2147/IJN.S189295
3. Dhanalekshmi KI, Meena KS. Comparison of antibacterial activities of Ag@TiO2 and Ag@SiO2 core-shell nanoparticles. *Spectrochim Acta - Part A Mol Biomol Spectrosc*. 2014;128:887-890. doi:10.1016/j.saa.2014.02.063
4. Khan S, Ansari AA, Khan AA, Al-Kattan W, Al-Obeed O, Ahmad R. Design, synthesis and in vitro evaluation of anticancer and antibacterial potential of surface modified Tb(OH)3@SiO2 core-shell nanoparticles. *RSC Adv*. 2016;6(22):18667-18677. doi:10.1039/c5ra17906h
5. Sriraman SK, Aryasomayajula B, Torchilin VP. Barriers to drug delivery in solid tumors. *Tissue Barriers*. 2014;2(3):e29528-1-e29528-10. doi:10.4161/tisb.29528
6. Zhang XF, Liu ZG, Shen W, Gurunathan S. Silver nanoparticles: Synthesis, characterization, properties, applications, and therapeutic approaches. *Int J Mol Sci*. 2016;17(9). doi:10.3390/ijms17091534
7. Gavas S, Quazi S, Karpinski T M. Nanoparticles for cancer therapy: current progress and challenges. *Nanoscale Res Lett*. 2021;16 :173. doi:10.1186/s11671-021-03628-6
8. Buttacavoli M, Albanese NN, Di Cara G. Anticancer activity of biogenerated silver nanoparticles: An integrated proteomic investigation. *Oncotarget*. 2018;9(11):9685-9705. doi:10.18632/oncotarget.23859
9. Jain N, Jain P, Rajput D, Patil UK. Green synthesized plant-based silver nanoparticles: therapeutic prospective for anticancer and antiviral activity. *Micro Nano Syst Lett*. 2021;9(1). doi:10.1186/s40486-021-00131-6

10. Kovács D, Igaz N, Gopisetty MK, Kiricsi M. Cancer Therapy by Silver Nanoparticles: Fiction or Reality? *Int J Mol Sci*. 2022;23(2). doi:10.3390/ijms23020839
11. Gabizon AA, de Rosales RTM, La-Beck NM. Translational considerations in nanomedicine: The oncology perspective. *Adv Drug Deliv Rev*. 2020;158:140-157. doi:10.1016/j.addr.2020.05.012
12. Miranda RR, Sampaio I, Zucolotto V. Exploring silver nanoparticles for cancer therapy and diagnosis. *Colloids Surfaces B Biointerfaces*. 2022;210(November 2021):112254. doi:10.1016/j.colsurfb.2021.112254
13. Bastos V, Ferreira-de-Oliveira JMP, Carrola J, et al. Coating independent cytotoxicity of citrate- and PEG-coated silver nanoparticles on a human hepatoma cell line. *J Environ Sci (China)*. 2017;51:191-201. doi:10.1016/j.jes.2016.05.028
14. Azizi M, Ghourchian H, Yazdian F, Bagherifam S, Bekhradnia S, Nyström B. Anti-cancerous effect of albumin coated silver nanoparticles on MDA-MB 231 human breast cancer cell line. *Sci Rep*. 2017;7(1):1-18. doi:10.1038/s41598-017-05461-3
15. Kokura S, Handa O, Takagi T, Ishikawa T, Naito Y, Yoshikawa T. Silver nanoparticles as a safe preservative for use in cosmetics. *Nanomedicine Nanotechnology, Biol Med*. 2010;6(4):570-574. doi:10.1016/j.nano.2009.12.002
16. Mauricio MD, Guerra-Ojeda S, Marchio P, et al. Nanoparticles in medicine: A focus on vascular oxidative stress. *Oxid Med Cell Longev*. 2018;2018. doi:10.1155/2018/6231482
17. Malekzadeh M, Yeung KL, Halali M, Chang Q. Preparation and antibacterial behaviour of nanostructured Ag@SiO2-penicillin with silver nanoplates. *New J Chem*. 2019;43(42):16612-16620. doi:10.1039/c9nj03727f
18. Dadashpour M, Firouzi-Amandi A, Pourhassan-Moghaddam M, et al. Biomimetic synthesis of silver nanoparticles using Matricaria chamomilla extract and their potential anticancer activity against human lung cancer cells. *Mater Sci Eng C*. 2018;92(June):902-912. doi:10.1016/j.msec.2018.07.053
19. Najahi-Missaoui W, Arnold RD, Cummings BS. Safe nanoparticles: Are we there yet? *Int J Mol Sci*. 2021;22(1):1-22. doi:10.3390/ijms22010385
20. Abdel-Fattah WI, Ali GW. On the anti-cancer activities of silver nanoparticles. *J Appl Biotechnol Bioeng*. 2018;5(1). doi:10.15406/jabb.2018.05.00116
21. Miranda RR, Sampaio I, Zucolotto V. Exploring silver nanoparticles for cancer therapy and diagnosis. *Colloids Surfaces B Biointerfaces*. 2022;210(August 2021). doi:10.1016/j.colsurfb.2021.112254

22. Silvestri B, Armanetti P, Sanità G, et al. Silver-nanoparticles as plasmon-resonant enhancers for eumelanin's photoacoustic signal in a self-structured hybrid nanoprobe. *Mater Sci Eng C*. 2019;102(April):788-797. doi:10.1016/j.msec.2019.04.066
23. Dung TTN, Nam VN, Nhan TT, et al. Silver nanoparticles as potential antiviral agents against African swine fever virus. *Mater Res Express*. 2019;6(12). doi:10.1088/2053-1591/ab6ad8
24. Dawadi S, Katuwal S, Gupta A, et al. Current Research on Silver Nanoparticles: Synthesis, Characterization, and Applications. *J Nanomater*. 2021;2021. doi:10.1155/2021/6687290
25. Venugopal K, Rather HA, Rajagopal K, et al. Synthesis of silver nanoparticles (Ag NPs) for anticancer activities (MCF 7 breast and A549 lung cell lines) of the crude extract of Syzygium aromaticum. *J Photochem Photobiol B Biol*. 2017;167:282-289. doi:10.1016/j.jphotobiol.2016.12.013
26. Venugopal K, Rather HA, Rajagopal K, et al. Synthesis of silver nanoparticles (Ag NPs) for anticancer activities (MCF 7 breast and A549 lung cell lines) of the crude extract of Syzygium aromaticum. *J Photochem Photobiol B Biol*. 2017;167:282-289. doi:10.1016/j.jphotobiol.2016.12.013
27. Lai CS, Chen YC, Wang HF, Ho HC, Ho RM, Tsai DH. Gas-phase self-assembly of uniform silica nanostructures decorated and doped with silver nanoparticles. *Nanotechnology*. 2017;28(3). doi:10.1088/1361-6528/28/3/035602
28. Al-Sadoon MK, Rabah DM, Badr G. Enhanced anticancer efficacy of snake venom combined with silica nanoparticles in a murine model of human multiple myeloma: Molecular targets for cell cycle arrest and apoptosis induction. *Cell Immunol*. 2013;284(1-2):129-138. doi:10.1016/j.cellimm.2013.07.016
29. Barui A, Kotcherlakota R, Patra C. Medicinal applications of metal nanoparticles:*Metal: Synthesis and Applications in Pharmaceutical Sciences*. Metal Nanoparticles; 2018;101-153. doi:10.1002/9783527807093
30. Barnali Ashe. A Detail investigation to observe the effect of zinc oxide and Silver nanoparticles in biological system. *Master Thesis*. 2011;(January):1-228. file:///Users/melinaki/Documents/Papersoldmac/Papers/2011/Melina/Unknown/2011 Melina.pdf%5Cnpapers:/dfa503e6-d258-4223-9ef8-d69bedc66f2d/Paper/p3470
31. Kudelski A, Wojtysiak S. Silica-covered silver and gold nanoresonators for raman analysis of surfaces of various materials. *J Phys Chem C*. 2012;116(30):16167-16174. doi:10.1021/jp304409x

32. Singh P, Katkar PK, Patil UM, Bohara RA. A robust electrochemical immunosensor based on core-shell nanostructured silica-coated silver for cancer (carcinoembryonic-antigen-CEA) diagnosis. *RSC Adv*. 2021;11(17):10130-10143. doi:10.1039/d0ra09015h
33. Arifin E, Lee JK. The distance-dependent fluorescence enhancement phenomena in uniform size Ag@SiO2@SiO2 (dye) nanocomposites. *Bull Korean Chem Soc*. 2013;34(2):539-544. doi:10.5012/bkcs.2013.34.2.539
34. Li C, Mei J, Li S, et al. One-pot synthesis of Ag@SiO2@Ag sandwich nanostructures. *Nanotechnology*. 2010;21(24). doi:10.1088/0957-4484/21/24/245602
35. Pfeffer CM, Singh ATK. Apoptosis: A target for anticancer therapy. *Int J Mol Sci*. 2018;19(2). doi:10.3390/ijms19020448
36. Yakop F, Abd Ghafar SA, Yong YK, et al. Silver nanoparticles Clinacanthus Nutans leaves extract induced apoptosis towards oral squamous cell carcinoma cell lines. *Artif Cells, Nanomedicine Biotechnol*. 2018;46(sup2):131-139. doi:10.1080/21691401.2018.1452750
37. Pistritto G, Trisciuoglio D, Ceci C, Alessia Garufi, D'Orazi G. Apoptosis as anticancer mechanism: Function and dysfunction of its modulators and targeted therapeutic strategies. *Aging (Albany NY)*. 2016;8(4):603-619. doi:10.18632/aging.100934
38. Prasannaraj G, Venkatachalam P. Green engineering of biomolecule-coated metallic silver nanoparticles and their potential cytotoxic activity against cancer cell lines. *Adv Nat Sci Nanosci Nanotechnol*. 2017;8(2). doi:10.1088/2043-6254/aa6d2c

Chapter 7

Comparative Antimicrobial Studies of Ag Nanoparticles and Ag@SiO_2 Core-shell Nanoparticles Against Microbes

7.1. Introduction

In the current era, nanotechnology has gained major attention in medicine because it provides the excellent advantage of working at the molecular level. With the swift development in the nanotechnology arena, the implementation of nanoparticles[1] procured fascination in the biomedical field. The employment of nanotechnology for rapid disease diagnosis, prevention and treatment is designated as nanomedicine. Nanomedicine is a very fast-growing area that can transform healthcare. Among all the nanoparticles, metallic nanoparticles are acquiring attention for their considerable applications in nanomedicine. Notwithstanding, hardly a few nano-based products elevated from metal are presently in use for therapeutic purposes.[2],[3] Betwixt-and-between, the silver nanoparticle is the most promising product because of its excellent antimicrobial properties.[4],[5] Silver was accustomed to conserving water since old and is considered the cradle of anti-disease resources by Hippocrates[6]. There are proof that, to avert the septicemia of the soldier's wound, Egyptians utilized coins made of silver during ancient wars.[7],[8] Silver compounds were also used against wound infections during the First World War.[9] After reaching the nanoscale, particles of silver have a miraculous change in physicochemical properties and turn out to have exceptional biological activities.[10] The uniqueness of silver nanoparticles broaden their pertinency in anti-bacterial, and anti-fungal therapy.[11],[12],[13]

Amid numerous kinds of nanoparticles accessible at the current time, nanoparticles having core-shell architectonic, possess astounding properties, collaborating multiple functionalities into a sole hybrid nanocomposite[14]. Assorted pattern of efforts was given for the study of the anti-cancerous, anti-bacterial, and anti-fungal effectiveness of silver nanoparticles. Still, scant or no attention is given to the comparative study of silver and yolk-shell silver silica nanoparticles. On that account, the present study was focused on learning about the antifungal and antibacterial effects of chemically prepared bare and coated silver nanoparticles and evaluating a comparative analysis of the activity of both nanoparticles. Alteration in silver nanoparticle's functionality with silica gives the nanoparticle idiosyncratic effects, because of the biocompatibility, hydrophilicity, and optical transparency along with thermal and chemical stability of the silica; unexpectedly in aqueous media also[15]. The flexibility of silica in surface moderation as well as in synthesis demeanour, offers an outstanding edge to the employment of this material for therapeutic purposes[16] because, for the applicability in medicine, immunocompatibility is a prerequisite condition that will clinch the non-toxic nature of the material[17],[18].

Antimicrobial chemotherapy[19] demands attention because, lately, resistance to antibiotics by disease-engendering fungus and bacteria has grown at a breathtaking pace and thus become significant trouble. Bacterial and fungal contaminations are a colossal source of disease. To overcome this resistance mechanism of pathogenic microbes[16], consideration has been given to silver nanoparticles

as an encouraging tool since they work miraculously on a span of targets in contrast to antibiotics, which have a particular site of execution[20], a possible mechanism has been shown in Fig.7.1.

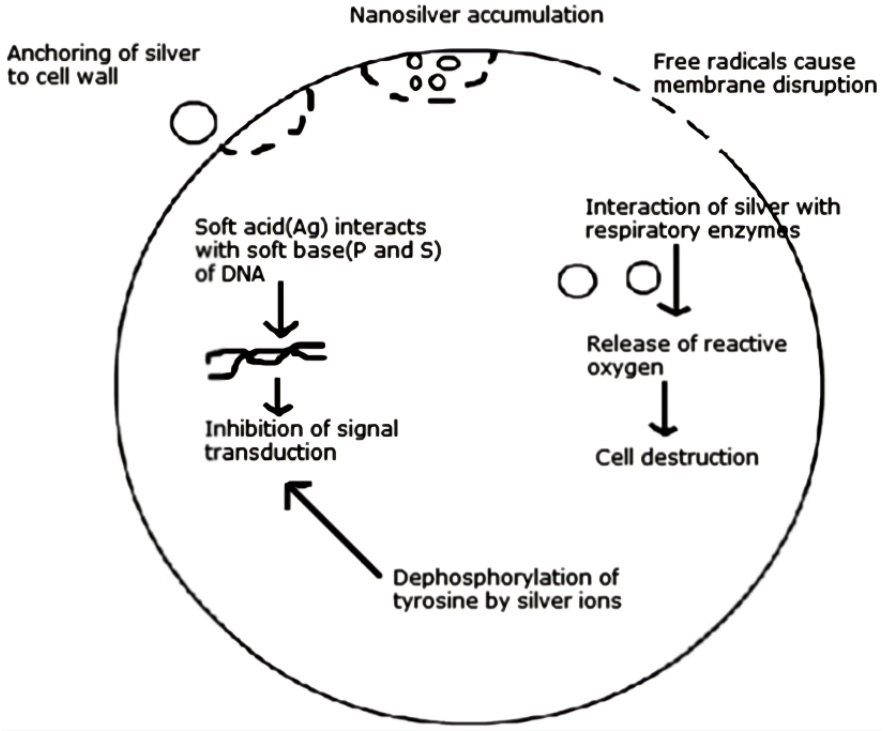

Figure 7.1: Schematic representation of different methodologies of AgNPs action on bacteria.[21]

Silver nanoparticles showcased magnificent outcomes in detecting and remedying microbial infections by enabling the pick out of target pathogens, reactive and combinatorial freightage of antibiotics, successful antibacterial vaccination, and swift detection of pathogens.[22]

The present study pivots on miraculous antimicrobial activities of silver and silica-coated silver nanoparticles at odds with disease-causing bacterial and fungal strains like- Escherichia coli (Gram -ve), Bacillus cereus (Gram +ve), and Candida albicans simultaneously. We selected E.coli because it is associated with food poisoning, the uppermost cause of urinary tract infection (75% to 95%),[23], seizures, bleeding,[24],[25] confusion, neonatal meningitis,[7] and even kidney failure.[20],[26],[27] Bacillus cereus is also associated with gastrointestinal infection[28] whereas Candida albicans infects primarily-immunocompromised patients and causes candidiasis ,named fungal infection. Detailed anti-bacterial and anti-fungal studies of both the tailored nanoparticles were brought off. Furthermore, briefly, their comparative studies were also carried out, pictorial representation is given in Fig.7.2. For anti-bacterial as well as anti-fungal studies; the disc-diffusion method and MIC-Assay were accomplished.

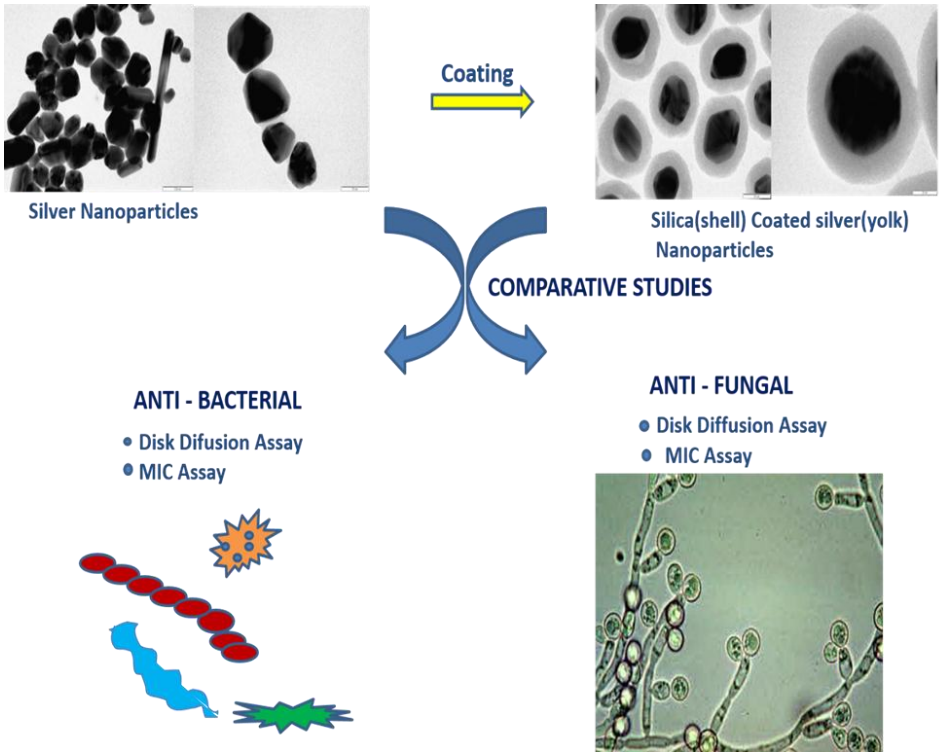

Figure 7.2: Schematic showing present work: Fabrication of silver nanoparticles followed by its coating with silica. Detailed anti-bacterial and anti-fungal studies of both the engineered nanoparticles were brought off, furthermore, briefly, their comparative studies were also carried out. For the observation of anti-bacterial as well as anti-fungal studies; the disc-diffusion method and MIC-Assay were worked.

7.2. Materials and methods

All the reagents required for synthesising and coating silver nanoparticles were procured from Sigma. Materials used for experimentation of antimicrobial activity were bought from HiMedia. Aqueous solutions were processed by using sterilized double-distilled water. The reagents/chemicals employed were of analytical grade, so utilized precisely without additional purification.

7.3. Materials and conditions used for assessment of antibacterial activity of the synthesized nanoparticles

The agar well diffusion technique was utilized to assay the bactericidal and fungicidal action of prepared silver nanoparticles and silica-coated silver nanoparticles[30]. For this purpose, two distinct strains of bacteria were employed: Escherichia coli (Gram-ve) and Bacillus- cereus (Gram+ve). The antimicrobial activity of both nanoparticles was calculated and compared with the control (ciprofloxacin). The microbial culture of bacterial strain was cultivated on nutrient broth and subsequently dabbed on Petri dishes consisting of agar media. Three wells were drilled onto the agar

facet utilizing an autoclaved well-cutter in each Petri plate. Afterwards, suspension of both the nanoparticles (1ml; 0.5mg/ml) in the first plate and (1ml; 1mg/ml) in the second plate were swaged into each of the two wells of the Petri plates, and 40 µl of standard drug ciprofloxacin, were supplemented. All of the plates were then incubated at 37°C straight for 24 hours. Subsequently, the antibacterial activities of both nanoparticles were corroborated by considering the zone of inhibition (in mm) fabricated surrounding the well.

The minimum inhibitory concentration (MIC) assay[31] was also exercised to unearth the antimicrobial efficacy of nanoparticles. For this experiment, five multifarious concentrations of nanoparticles were taken(10µg/ml-50µg/ml).

7.4. Materials and conditions employed for assessment of antifungal activity of the synthesized nanoparticles.

The fungicidal action of both the nanoparticles was decided via employing the Kirby - Bauer agar-well disc diffusion method[21]. Stock fungal strain of Candida albicans was put together and maintained in a media solution. Emended media for Candida albicans (i.e., Dextrose + peptone + $NH_4H_2PO_4$ + KNO_3 + $CaCl_2$ and agar) liquified in double-distilled water. The prepared media was then autoclaved at 15 lbs pressure for 15 minutes at 121°C. The standard drug Itraconazole was used as a control. We employed two different concentrations of both nanoparticles to examine their antifungal activities.

Similarly, like in antibacterial studies, a minimum inhibitory concentration (MIC) assay was used to discover the antifungal effects of nanoparticles. The colloidal nanoparticles were diluted to acquire the finishing concentration extending from 50µg/ml to 10µg/ml and then added to the microtiter plates. Then it was inoculated for a whole 1 day. The fungal growth was reckoned by observing absorption (OD) at 600nm using a microtiter plate.

7.5. Results and discussion

Even though there is an incredible pace of development in the field of nanoscience, relatively very few details are accessible about the upshot of the nanoparticle conjugation process with microbes and their following consequences. Nowadays, various nanoparticles have been utilised as a drug vector, but their synergistic effect inside the human body has not been prophesied completely.

7.5.1. Antibacterial activity

These days, nanoparticles are very favored among researchers as materials that can kill microorganisms[32]. The benefit of wielding nanoparticles is the insufficiency of confrontation of micro-organisms to their functioning system and majestic application chances. Both the synthesized nanoparticles were highly efficacious in two of the above-mentioned conditions. Owing to the same reason, the bactericidal ramifications of both the nanoparticles opposed to multi-drug resistant bacteria,

challenge and attracts researchers to move forward with this work because of lofty surface-area to volume proportion and extraordinary physical and chemical qualities.

The swift reproduction period of bacteria is among the prominent causes of bacterial infections[33]. Nevertheless, the same reason could be an exemplary strategy to obstruct the viable infection because silver and its related nanoparticles are very fruitful in restraining microbes and have lethal effects on bacteria in a dose and time-dependent fashion[34]. Here, an improvised agar-well method was employed in order to appraise the antibacterial action of both nanoparticles, displayed in Fig.7.3. Two distinct bacterial strains were taken for this purpose, i.e. Escherichia coli (Gram -ve) and Bacillus cereus (Gram +ve)[35]. The nanoparticles were allowed to interact with the bacterial strains in a freshly seeded plate containing medium. 25ml sterile nutrient -agar was sowed in each Petri-plate using a glass rod along with day aged culture of gram +ve and gram -ve bacterial strains distinctly.

In each of the Petri plates, three wells were grooved onto the agar facet, by using an autoclaved well-cutter. Subsequently, 40 µl of standard drug ciprofloxacin and suspension of both the nanoparticles (1ml; 0.5mg/ml) in the first plate and (1ml; 1mg/ml) in the second plate protruded into each of the two wells of the Petri-plates were augmented. Afterwards, every plate was inoculated. Eventually, the antibacterial activities of both nanoparticles were validated by calculating the zone of inhibition (in mm) formed around the well, as displayed in table no.7.1 and table no.7.2. It was unearthed from the results, the bacteria that were employed for the experiment died even by using a low concentration of silver along with silica-coated silver nanoparticles and in a shorter time duration.

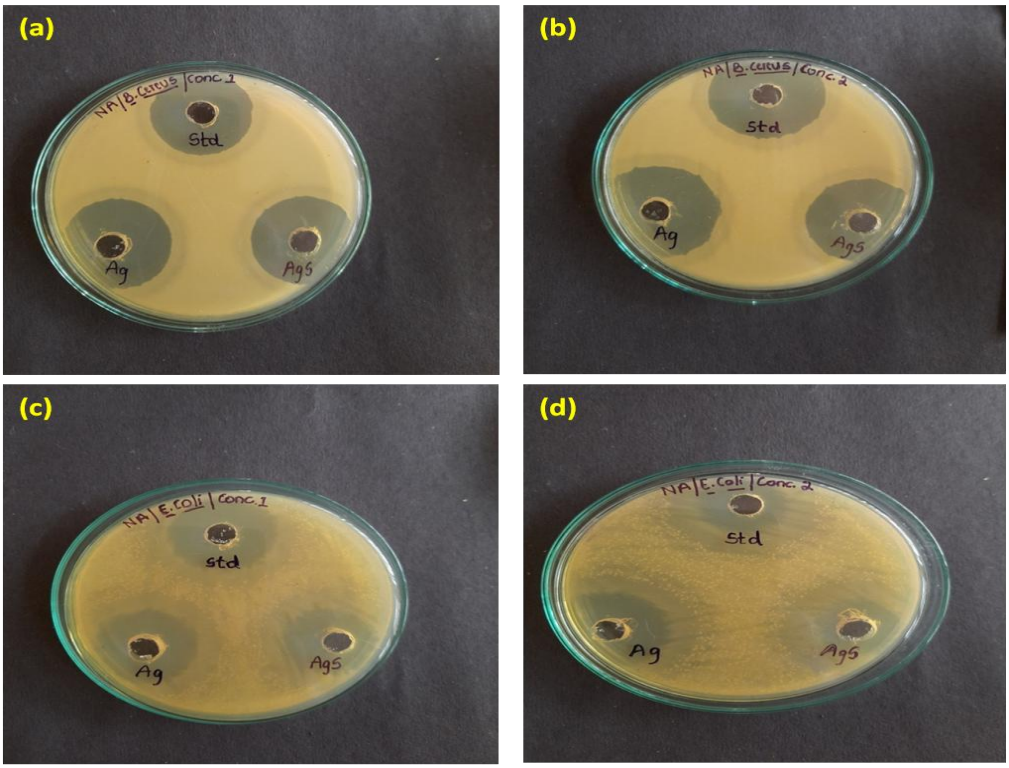

Figure 7.3: Anti-bacterial activity of nanoparticles against (a) Gram-positive bacteria Bacillus cereus by employing concentration 1 and (b)concentration 2. (c) anti-bacterial activities of both the nanoparticles at concentration 1 (0.5mg/ml) against Gram-negative bacteria Escherichia coli; (d) at concentration 2 (1mg/ml).

The minimum inhibitory concentration (MIC) assay was harnessed to discover the minutest concentration of synthesized nanoparticles against bacterial strains, which is exhibited in Fig. 7.4 as well as in table nos.7.1 and 7.2. MIC assay has been carried out by repeating the experiment five times, using different concentrations (10µg/ml- 50µg/ml) of nanoparticles. The lethal effects of both the nanoparticles against bacteria are almost alike or minutely less just in the case of coated nanoparticles. The results obtained from MIC are in virtuous agreement with the disc diffusion results. Results are shown here in the following table-

Table 7.1- Inhibition zone diameter (mm) induced by Ag NPs and Ag@SiO_2NPs by employing two different concentrations against Gram -ve bacteria.

Escherichia coli (Gram -ve)				
Sample Name	**Drug vol.**	**Control (mm±standard deviation)**	**AgNPs (mm±standard deviation)**	**Ag@SiO_2NPs (mm±standard deviation)**
Conc.1(0.5mg/ml)		**19±0.5**	**17±1**	**10±1**
Conc.2(1mg/ml)		**22±1**	**20±1**	**17±1**

Table 7.2- Inhibition zone diameter (mm) induced by Ag NPs and Ag@SiO_2NPs by employing two different concentrations against Gram +ve bacteria.

Bacillus cereus (Gram +ve)				
Sample Name	**Drug vol.**	**Control (mm±standard deviation)**	**AgNPs (mm±standard deviation)**	**Ag@SiO_2NPs (mm±standard deviation)**
Conc.1(0.5mg/ml)		**23±1**	**20±1**	**10±1**
Conc.2(1mg/ml)		**24±1**	**22±2**	**21±1**

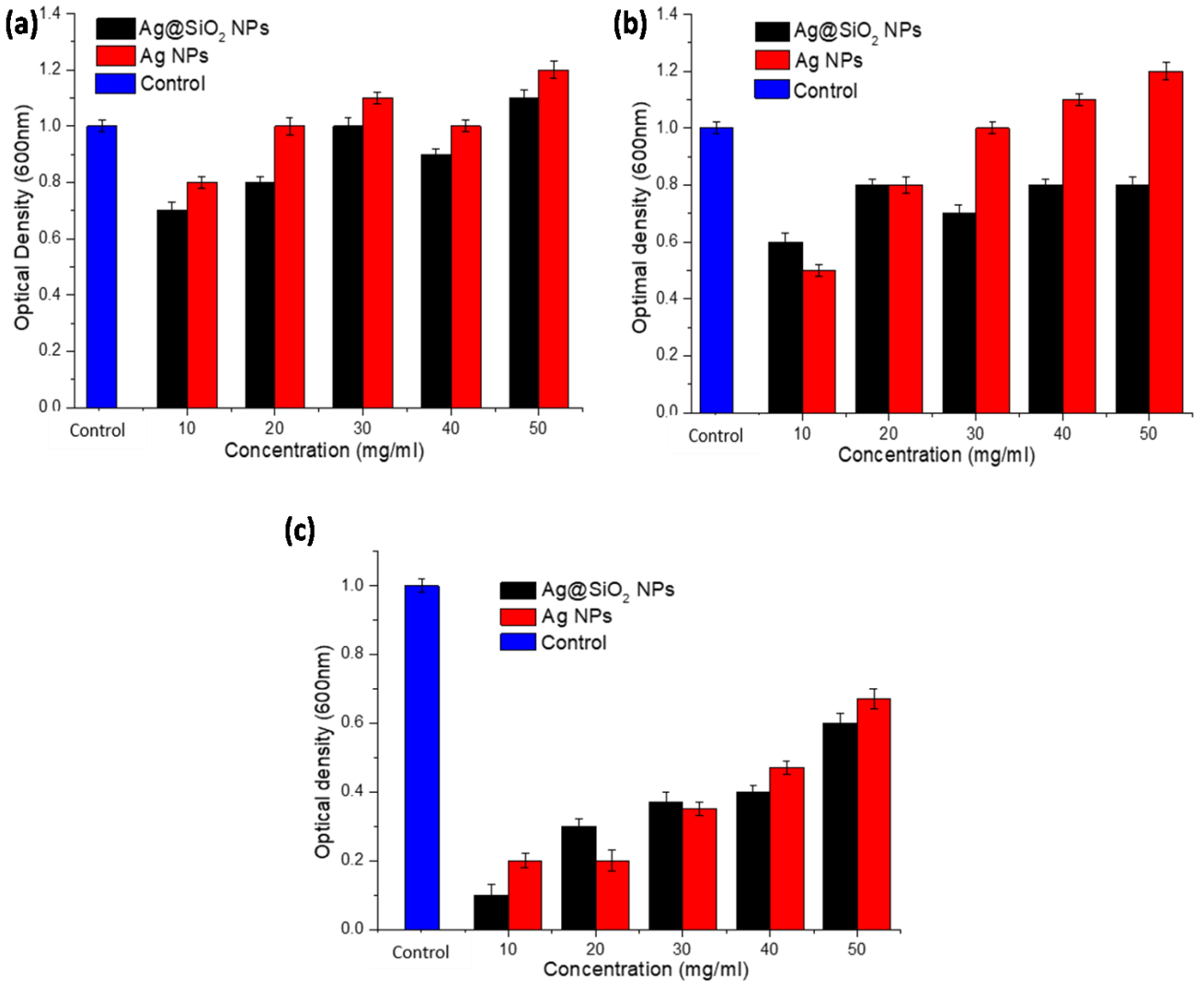

Figure 7.4: Minimum inhibitory concentration (MIC) against Gram-positive bacteria Bacillus cereus; Ag nanoparticles (denoted in red-colored bars) and Silica coated Ag nanoparticles (shown in black-colored bars). (b) - MIC against Gram-negative bacteria- Escherichia coli for measuring the activity of Ag nanoparticles (indicated in the red-colored bar) and Silica coated Ag nanoparticles (displayed in black-colored bars); (c) - Minimum inhibitory concentration (MIC) against Fungus, Candida- albicans; Ag nanoparticles (denoted in red-colored bars) and Silica coated Ag nanoparticles (shown in black colored bars).

Mechanism of action- There is a typical difference between the structure of the cell wall of Gram +ve and Gram -ve bacteria, as displayed in Fig.7.5. Gram -ve bacteria possess a distinguished cytoplasmic membrane, an outermost membrane having a fine peptidoglycan surface as well as an external layer containing lipopolysaccharide conversely Gram +ve bacteria possess broad peptidoglycan covering accompanying teichoic acid[36]. Because of this difference in the cell wall, nanoparticles (silver and silica-coated silver nanoparticles) behave differently on Gram + ve and Gram - ve bacteria[37]. In spite of the fact that the technique by which nano-scaled silver and its associated

nanoparticles work are not completely known, there are few possible common mechanisms on which the toxicity of nanoparticles works[38], as mentioned here-

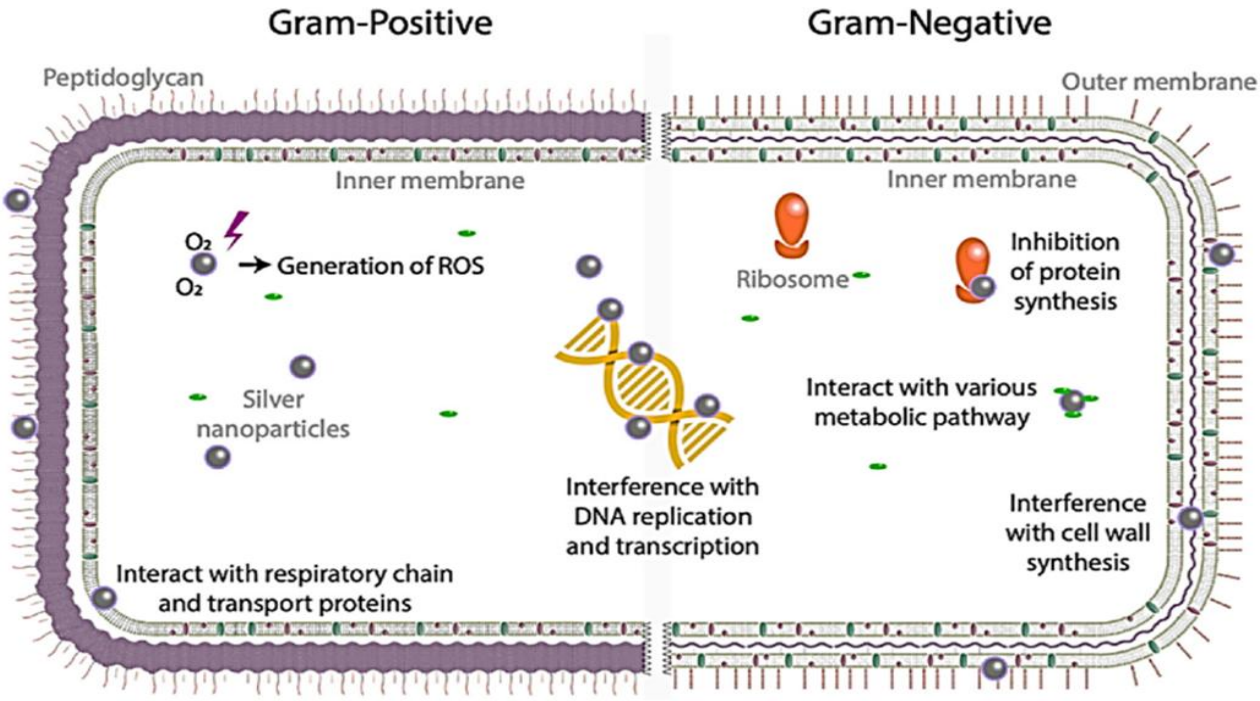

Figure 7.5: Possible bactericidal process of Ag Nps in Gram +ve and Gram –ve bacteria[39].

-Both the nanoparticles interact with bacterial proteins by merging the potent effects of thiol (SH) groups, which induces the appeasement of the proteins, and leads to bacterial inactivation.[40],[31]

-Because of the electrostatic attraction and rapport with sulfur proteins, ions of nanoparticles can cohere with the cell wall as well as with the cytoplasmic - membrane.

-Formation of ROS (reactive oxygen species) through the nanoparticles.[41]

-Disordering of DNA and ATP production due to intake of free silver ions[31]. As we know, silver nanoparticles regularly release silver ions, which was supposed to be the process of killing microorganisms.

7.5.2. Antifungal activity

Fungi cause various frantic diseases and remedy of such infection is very necessary because common drugs (amphotericin B, Nystatin, itraconazole, etc) available on the market used for treatment cause severe aftereffects such as liver and renal dysfunction[39],[42]. Antifungal pursuit of both the nanoparticles was availed by Kirby - Bauer agar- well disc diffusion method[43], as displayed in Fig.7.6. Table no.3 shows that the stock fungal strain of Candida albicans was put together and maintained in a media solution. Emended media for Candida albicans (i.e., Dextrose + peptone + $NH_4H_2PO_4$ + KNO_3 + $CaCl_2$ and agar) liquified in double-distilled water. The well-prepared media was autoclaved at 15

lbs pressure for 15 minutes at 121°C. The standard drug Itraconazole was used as a control. To explore their antifungal activeness, we implemented two varied concentrations of bare Ag nanoparticles and silica-encapsulated Ag nanoparticles. Ag nanoparticles exhibited towering antifungal- action in comparison to Ag@SiO_2 nanoparticles. The control exhibits 14mm and 13mm of inhibition zone by using the first and second concentrations, respectively, as shown in table no.7.3. Ag nanoparticles show an inhibition zone of 13mm when using the first concentration, whereas Ag@SiO_2 nanoparticles show a 12mm zone of inhibition. On the other hand, by using the second concentration, Ag nanoparticles and Ag@SiO_2 nanoparticles show 11mm and 10mm of the zone of inhibition respectively.

The MIC assay of nanoparticles was also evaluated against Candida albicans, shown in Fig.7.5 (c). Colloidal nanoparticles were diluted to attain the final concentration extending from 50µg/ml to 10µg/ml and further prefixed in the microtiter plates. Then it was kept for incubation at 37°C for 24 hours. The growth of the fungus was calculated by observing absorption (OD) at 600nm with the help of a microtiter plate.

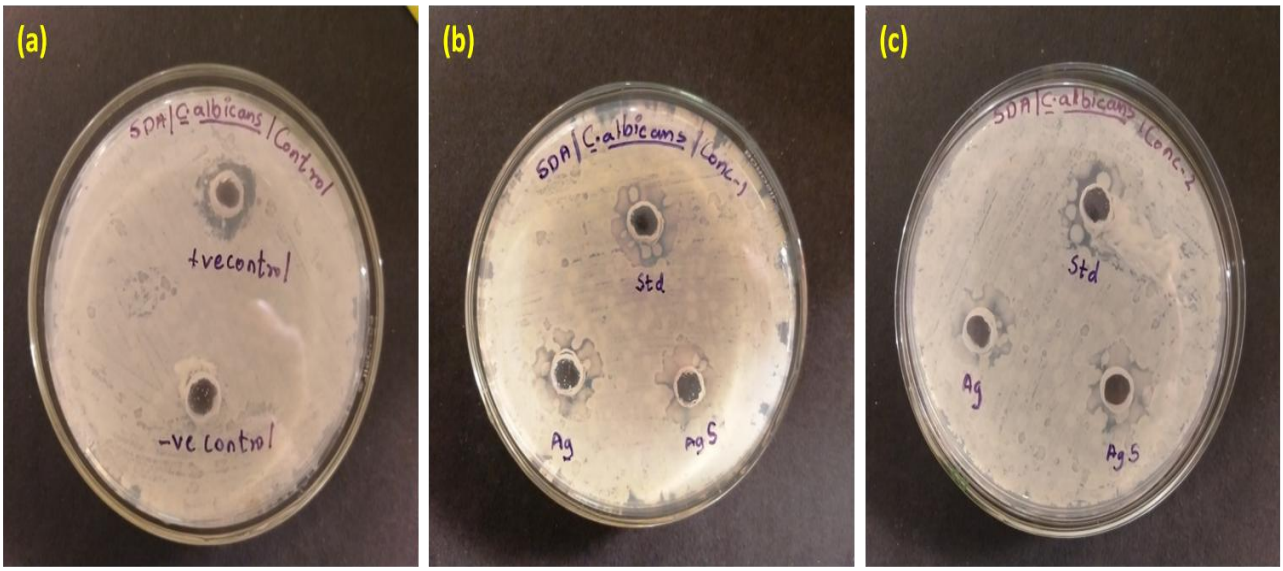

Figure 7.6: Anti-fungal activity of nanoparticles against Candida albicans (a) using positive and negative control. (b) On concentration 1, (c) On concentration 2.

Table 7.3- Inhibition zone diameter (mm) induced by Ag NPs and Ag@SiO_2NPs by employing two different concentrations against Candida albicans.

Candida albicans				
Sample Name	**Drug vol.**	**Control (mm±standard deviation)**	**AgNPs (mm±standard deviation)**	**Ag@SiO_2NPs (mm±standard deviation)**

Conc.1(0.5mg/ml)	**13±1**	**11±1**	**10±1**
Conc.2(1mg/ml)	**13±0.5**	**9±1.1**	**12±0.5**

7.6. Conclusions

The current section emphasizes spherically shaped bare silver nanoparticles and decorously modelled silica-encapsulated silver nanoparticles, further explaining their disease-repelling activities. In this respect, the properly prepared nanoparticles were appraised for their specific antibacterial and antifungal pursuit. Silica-coated silver nanoparticles show diminutive effects as compared to the bare silver nanoparticle, attributed to the biocompatible nature of silica. However, still, shows worthwhile antimicrobial activity because of the delivery of silver ions via the penetrable silica layer as well as the ions of silver inclined onto the nanoparticles. These studies will focus on nanoparticle-microbe interactions and will also tremendously contribute to the expansion of improvement in the field of nanomedicine. In short, the present chapter put together nanotechnology and microbiology contributing to potent anti-bacterial and anti-fungal agents for a long-lasting period. It was interesting to note that both nanoparticles have aced the effectiveness on antimicrobial queernesses.

References

1. Firdhouse MJ, Lalitha P. Biosynthesis of silver nanoparticles using the extract of Alternanthera sessilis-antiproliferative effect against prostate cancer cells. *Cancer Nanotechnol*. 2013;4(6):137-143. doi:10.1007/s12645-013-0045-4
2. Tolaymat TM, El Badawy AM, Genaidy A, Scheckel KG, Luxton TP, Suidan M. An evidence-based environmental perspective of manufactured silver nanoparticle in syntheses and applications: A systematic review and critical appraisal of peer-reviewed scientific papers. *Sci Total Environ*. 2010;408(5):999-1006. doi:10.1016/j.scitotenv.2009.11.003
3. Makvandi P, Wang C yu, Zare EN, Borzacchiello A, Niu L na, Tay FR. Metal-Based Nanomaterials in Biomedical Applications: Antimicrobial Activity and Cytotoxicity Aspects. *Adv Funct Mater*. 2020;30(22). doi:10.1002/adfm.201910021
4. Prasannaraj G, Venkatachalam P. Green engineering of biomolecule-coated metallic silver nanoparticles and their potential cytotoxic activity against cancer cell lines. *Adv Nat Sci Nanosci Nanotechnol*. 2017;8(2). doi:10.1088/2043-6254/aa6d2c
5. Mansour HH, Eid M, El-Arnaouty MB. Effect of silver nanoparticles synthesized by gamma radiation on the cytotoxicity of doxorubicin in human cancer cell lines and experimental animals. *Hum Exp Toxicol*. 2018;37(1):38-50. doi:10.1177/0960327116689717

6. Ahmed S, Mudasir A, Babu L S, Ikram S. A review on plants extract mediated synthesis of silver nanoparticles for antimicrobial applications: A green expertise. *J Adv Res*. 2016;7(1): 17-28. doi:10.1016j.jare.2015.02.007
7. Khatami M, Sharifi I, Nobre MAL, Zafarnia N, Aflatoonian MR. Waste-grass-mediated green synthesis of silver nanoparticles and evaluation of their anticancer, antifungal and antibacterial activity. *Green Chem Lett Rev*. 2018;11(2):125-134. doi:10.1080/17518253.2018.1444797
8. Sun Y A, Chen L T, Hsu S Y, Hu C C, Tsai D H. Silver Nanoparticles-Decorating Manganese Oxide Hybrid Nanostructures for Supercapacitor Applications. *Langmuir*. 2019. 35, 44, 14203-14212. doi:10.1021/acs.langmuir.9b02409
9. Yesilot S, Aydin C. Silver nanoparticles; a new hope in cancer therapy? *East J Med*. 2019;24(1):111-116. doi:10.5505/ejm.2019.66487
10. Zhang Z, Shen W, Xue J, et al. Recent advances in synthetic methods and applications of silver nanostructures. *Nanoscale Res Lett*. 2018;13. doi:10.1186/s11671-018-2450-4
11. Faramarzi MA, Sadighi A. Insights into biogenic and chemical production of inorganic nanomaterials and nanostructures. *Adv Colloid Interface Sci*. 2013;189-190:1-20. doi:10.1016/j.cis.2012.12.001
12. Abd-elnaby HM, Abo-elala GM, Abdel-raouf UM, Hamed MM. Antibacterial and anticancer activity of extracellular synthesized silver nanoparticles from marine Streptomyces rochei MHM13. *Egypt J Aquat Res*. 2016. doi:10.1016/j.ejar.2016.05.004
13. Abdel-Fattah WI, W Ali G. On the anti-cancer activities of silver nanoparticles. *J Appl Biotechnol Bioeng*. 2018;5(1):43-46. doi:10.15406/jabb.2018.05.00116
14. Aslan K, Wu M, Lakowicz JR, Geddes CD. Fluorescent core-shell Ag@SiO2 nanocomposites for metal-enhanced fluorescence and single nanoparticle sensing platforms. *J Am Chem Soc*. 2007;129(6):1524-1525. doi:10.1021/ja0680820
15. Arifin E, Lee JK. The distance-dependent fluorescence enhancement phenomena in uniform size Ag@SiO2@SiO2 (dye) nanocomposites. *Bull Korean Chem Soc*. 2013;34(2):539-544. doi:10.5012/bkcs.2013.34.2.539
16. Guerrero-Martínez A, Pérez-Juste J, Liz-Marzán LM. Recent progress on silica coating of nanoparticles and related nanomaterials. *Adv Mater*. 2010;22(11):1182-1195. doi:10.1002/adma.200901263
17. Li M, Luo Z, Zhao Y. Self-Assembled Hybrid Nanostructures : Versatile Multifunctional Nanoplatforms for Cancer Diagnosis and Therapy. *Chem.Mater:* 2018. 30, 1,25-53. doi:10.1021/acs.chemmater.7b03924
18. Kudelski A, Wojtysiak S. Silica-covered silver and gold nanoresonators for raman analysis of

surfaces of various materials. *J Phys Chem C*. 2012;116(30):16167-16174. doi:10.1021/jp304409x

19. Beyth N, Houri-Haddad Y, Domb A, Khan W, Hazan R. Alternative antimicrobial approach: Nano-antimicrobial materials. *Evidence-based Complement Altern Med*. 2015;2015. doi:10.1155/2015/246012
20. Dey A, Dasgupta A, Kumar V, Tyagi A, Verma AK. Evaluation of the of antibacterial efficacy of polyvinylpyrrolidone (PVP) and tri-sodium citrate (TSC) silver nanoparticles. *Int Nano Lett*. 2015;5(4):223-230. doi:10.1007/s40089-015-0159-2
21. Burdușel AC, Gherasim O, Grumezescu AM, Mogoantă L, Ficai A, Andronescu E. Biomedical Applications of Silver Nanoparticles : An Up-to-Date Overview. *Nanomaterials(Basel)*. 2018:1-24. doi:10.3390/nano8090681
22. Sintubin L, Verstraete W, Boon N. Biologically Produced Nanosilver : Current State and Future Perspectives. *Biotechnology and Bioengineering*. 2012;24570:1-15. doi:10.1002/bit.24570
23. Sunderam V, Thiyagarajan D, Lawrence AV, Mohammed SSS, Selvaraj A. In-vitro antimicrobial and anticancer properties of green synthesized gold nanoparticles using Anacardium occidentale leaves extract. *Saudi J Biol Sci*. 2019;26(3):455-459. doi:10.1016/j.sjbs.2018.12.001
24. Esfanddarani HM, Kajani AA, Bordbar AK. Green synthesis of silver nanoparticles using flower extract of Malva sylvestris and investigation of their antibacterial activity. *IET Nanobiotechnology*. 2018;12(4):412-416. doi:10.1049/iet-nbt.2017.0166
25. Maeda H, Khatami M. Analyses of repeated failures in cancer therapy for solid tumors : poor tumor - selective drug delivery , low therapeutic efficacy and unsustainable costs. *Clin Transl Med*. 2018:1-20. doi:10.1186/s40169-018-0185-6
26. Qais FA, Shafiq A, Khan HM, et al. Antibacterial effect of silver nanoparticles synthesized using Murraya koenigii (L.) against multidrug-resistant pathogens. *Bioinorg Chem Appl*. 2019;2019. doi:10.1155/2019/4649506
27. Tiwari AP, Rohiwal SS. Chapter 2. Synthesis and Bioconjugation of Hybrid Nanostructures for Biomedical Applications. Micro and Nano Technologies.2019;(January).17-41. doi:10.1016/B978-0-12-813906-6.00002-0
28. Allafchian AR, Banifatemi SS, Jalali SAH. Synthesis and Characterization of Ag/SiO2 Nanoparticles Embedded in TPS and TEOS Sol-gel Matrix with Excellent Antibacterial Activity. *Nanosci &Nanotechnology-Asia*. 2017;8(1):33-40. doi:10.2174/2210681207011704191502 09
29. Singh P, Katkar PK, Walski T, Bohara RA. Three in-one fenestrated approaches of yolk-shell, silver-silica nanoparticles: A comparative study of antibacterial, antifungal and anti-cancerous applications. *Heliyon*. 2023;9(8):e18034. doi:10.1016/j.heliyon.2023.e18034

30. Guzman M, Dille J, Godet S. Synthesis and antibacterial activity of silver nanoparticles against gram-positive and gram-negative bacteria. *Nanomedicine Nanotechnology, Biol Med*. 2012;8(1):37-45. doi:10.1016/j.nano.2011.05.007
31. Marambio-Jones C, Hoek EMV. A review of the antibacterial effects of silver nanomaterials and potential implications for human health and the environment. *J Nanoparticle Res*. 2010;12(5):1531-1551. doi:10.1007/s11051-010-9900-y
32. Singh H, Du J, Yi TH. Kinneretia THG-SQI4 mediated biosynthesis of silver nanoparticles and its antimicrobial efficacy. *Artif Cells, Nanomedicine Biotechnol*. 2017;45(3):602-608. doi:10.3109/21691401.2016.1163718
33. Peng H, Borg RE, Nguyen ABN, Chen IA. Chimeric Phage Nanoparticles for Rapid Characterization of Bacterial Pathogens: Detection in Complex Biological Samples and Determination of Antibiotic Sensitivity. *ACS Sensors*. 2020. doi:10.1021/acssensors.0c00654
34. Zhang XF, Liu ZG, Shen W, Gurunathan S. Silver nanoparticles: Synthesis, characterization, properties, applications, and therapeutic approaches. *Int J Mol Sci*. 2016;17(9). doi:10.3390/ijms17091534
35. Elena S, Gomes D, Esteruelas G, et al. Metal-Based Nanoparticles as Antimicrobial Agents : An Overview. *Nanomaterials(Basel)*.2020:1-39. doi: 10.3390/nano10020292
36. P L. Difference Between Gram Positive and Gram Negative Bacteria Stunning images of cells Discover how scientists use Main Difference – Gram Positive vs Gram Negative Bacteria. *Pediaa*. 2017;(April):13. doi:researchgate.net/publication/315757324
37. Tian Y, Qi J, Zhang W, Cai Q, Jiang X. Facile, one-pot synthesis, and antibacterial activity of mesoporous silica nanoparticles decorated with well-dispersed silver nanoparticles. *ACS Appl Mater Interfaces*. 2014;6(15):12038-12045. doi:10.1021/am5026424
38. Marambio-Jones C, Hoek EM V. A review of the antibacterial effects of silver nanomaterials and potential implications for human health and the environment. *J Nanoparticle Res*. 2010;12(5):1531-1551. doi:10.1007/s11051-010-9900-y
39. Anees Ahmad S, Sachi Das S, Khatoon A, et al. Bactericidal activity of silver nanoparticles: A mechanistic review. *Mater Sci Energy Technol*. 2020;3:756-769. doi:10.1016/j.mset.2020.09.002
40. Devi JS, Bhimba BV. Antibacterial and antifungal activity of silver nanoparticles synthesized using Hypnea muciformis. *Biosci Biotechnol Res Asia*. 2014;11(1):235-238. doi:10.13005/bbra/1260
41. Tang X. Potential antibacterial mechanism of silver nanoparticles and the optimization of orthopedic implants by advanced modification technologies. *Int J Nanomediciene.*2018:3311-3327. doi: 10.2147/IJN.S165125

42. Hoehamer CF, Cummings ED, Hilliard GM, Rogers PD. Changes in the proteome of Candida albicans in response to azole, polyene, and echinocandin antifungal agents. *Antimicrob Agents Chemother*. 2010;54(5):1655-1664. doi:10.1128/AAC.00756-09
43. Loo YY, Rukayadi Y, Nor-Khaizura MAR, et al. In Vitro antimicrobial activity of green synthesized silver nanoparticles against selected Gram-negative foodborne pathogens. *Front Microbiol*. 2018;9(JUL):1-7. doi:10.3389/fmicb.2018.01555

Chapter 8

RECOMMENDATIONS

8.1. Recommendations

Detection of CEA levels in adults is crucial for early diagnosis of cancer. Immobilization of immunoreagent onto the surface of the electrode is the fundamental aspect of the fabrication of an efficient electrochemical immunosensor. Recently, indium-tin-oxide (ITO or InSnOx) coated glass substrate is a miniaturized lab-on-a-chip related concept that is an n-type highly degenerated and wide energy gap semi-conductor, which is sturdy and metamorphic. The application of ITO electrodes is acceptable based on their user-friendly characteristics: their unique optical transparency, wide electrochemical working window, high electrical conductivity, excellent substrate adhesion, stable electrochemical and physical properties, conveniently etched, patterned, micro arrayed, and low cost. The use of ITO for sensing applications can be prominently enhanced by introducing nanoparticles on its surface. Metal nanoparticles provide a biocompatible microenvironment for biomolecules and significantly increase the surface-to-volume ratio of an immobilized biomolecule on the electrode surface, ultimately influencing electrical signal enhancement. Analysts in nano biosensors are always enthusiastic about finding new materials with suitable properties to enhance the behaviour of biosensors. Composite nanoparticles are suited to form a continuous electric field and increase the transferred ratio of electrons compared to single nanoparticles. So, they can effectively fasten the regeneration process of sensors.

Nanocomposite materials display unique qualities: optical, catalytical, quantum size effect, electrochemical properties, etc. The employment of such hybrid nanomaterials administers the mixture of extraordinary anti-microbial, anti-cancerous, and physicochemical qualities of compounds, resulting in better signals while detecting antigens. Yolk-shell-based silica-coated silver nanoparticles are prominently used in the biomedical field along with bare silver nanoparticles for various biological applications. The antibacterial and anticancerous effectiveness of AgNPs is enhanced based on their wide-reaching whole surface area per unit volume.

Detailed anti-cancerous, anti-bacterial and antifungal studies of both the engineered nanoparticles were brought off. Furthermore, briefly, their comparative studies were also carried out. In general, Ag NPs release their ions under specific physiological conditions. Such ions assemble on the functional (phosphoryl-, sulfhydryl-) enzymatic groups and proteins, which are prominent for the intrinsic metabolism of bacterial cells. As a result, vital enzymes become inactivated and deoxyribonucleic acid drops its ability to replication, and changes in the cell membrane structure take place. Therefore, bacteria and fungi were inactivated also. For anti-bacterial as well as antifungal studies; the disc-diffusion method and MIC-Assay were worked. For the observation of anti-cancerous activities, an MTT assay has been executed. Additionally, the determination of apoptotic cells was

found by flow cytometry. The grounds of the present study are to combine the advantages of metal nanoparticles, i.e., silver, with silicon dioxide (SiO_2) on an ITO flat substrate to design a novel electrochemical immunosensor for sensitive and selective detection of CEA. Along with this, the current study also highlights the antibacterial, antifungal, anti-cancerous properties of silver and silica-coated silver nanoparticles in a comparative way.

8.2. Competent component of the thesis

The prepared silver nanoparticles were obtained through an improvised chemical reduction method by employing trisodium citrate dehydrate ($Na_3C_6H_5O_7.2H_2O$) as a capping and reducing factor. The layering of silica on the outer surface of silver was implemented by a modified "Stober"(sol-gel) procedure. Silica provides a biocompatible environment. UV-Vis-spectrum, FTIR, XRD, SEM, EDX, TEM, RAMAN, DLS-histogram, Zeta potential, AFM distinguished the structure & properties of Ag nanoparticles and silica-coated Ag nanoparticles, as it is displayed in the Fig 8.1.

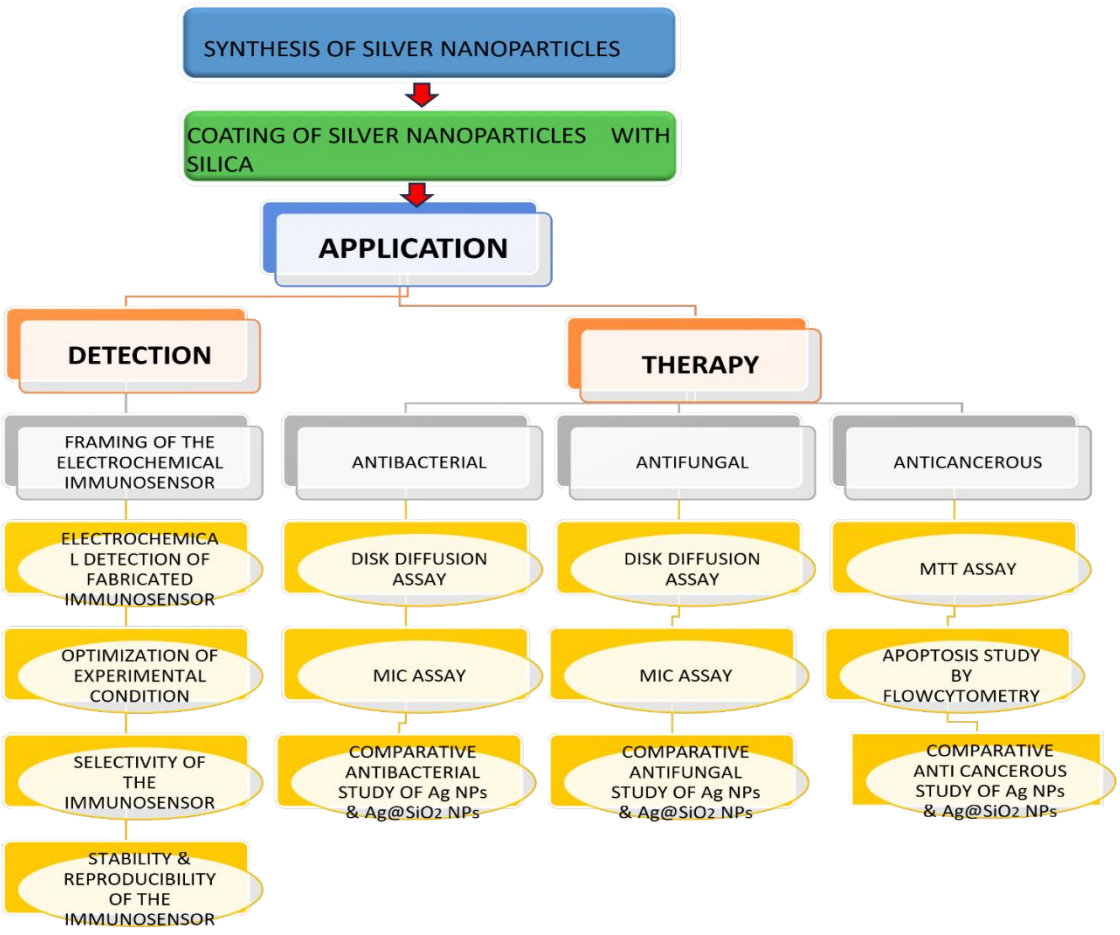

Figure 8.1: Schematics of the present work.

The UV-visible spectroscopy exhibited that the Ag nanoparticles showed a sharp characteristic peak at 420 nm in UV-visible absorption spectra. After the deposition of the silica layer on Ag nanoparticles, the peak shifted to a longer wavelength. The shell thickness after coating with silica in

terms of SPR (surface plasmon resonance) signal was attributed to the growing local refractive index of the nanoparticles. Due to this, red shifting of the peaks took place. XRD diffraction was used to determine the difference in the crystal structure between the two nanoparticles. XRD formats of both nanoparticles were documented in the range of 10° to 80°. There are three characteristic diffraction peaks at 38.2°, 44.03°, and 64.2°, which are analogous to the (111), (200), and (220) Bragg reflections of face-centered-cubic (fcc) crystal shape of silver nanoparticles were visible. The peaks at (200), and (220) planes were slighter intense whereas, the peak located at (111) planes was more intense. The frail and extensive peak at 2θ values of around 22° can be designated to a definite layer of silica.

Measurement of functional groups were carried out by FTIR analysis in the colloidal solution. The sole purpose of FTIR was to study the formation of silica layer on the Ag nanoparticles. When we observe the FTIR of Ag nanoparticles, there are visible pics on 1637.73 cm^{-1}, 2119.06 cm^{-1} and at 3331.39 cm^{-1}. And in the FTIR of $Ag@SiO_2$ nanoparticles, the data revealed that the peaks attributed to 1638.48 cm^{-1} and 2123.94 cm^{-1} may be ascribed to the presence of silica on the surface of particles (Si-O-Si and Si-O). In addition, the band at 3340.79 cm^{-1} were ascribed to C-N stretching which represents the aliphatic amine. RAMAN-spectroscopic assessment was implemented to learn the nanoparticles' vibrational characteristics. It was found that the synthesized particles exhibited good stability. Ag nanoparticles exhibited two significant peaks at approximately 1569 $cm^{-1}$and 1396 cm^{-1}, whereas $Ag@SiO_2$ nanoparticles show much smaller scattering at 1630 cm^{-1} and 1328 cm^{-1}.

The TEM interpretation was executed to examine the configuration and volume of the Ag nanoparticles and $Ag@SiO_2$ nanoparticles. The operating voltage was between 20 to 200 kV with resolution 2.4 A°. There was extensive size distribution of the silver nanoparticles, started from 30 to 100 nm with mean size of 50 nm and the average size of $Ag@SiO_2$ nanoparticles was 80 nm.

Topological studies of both the nanoparticles were observed by AFM on glass-slides. AFM micrographs illustrate the matching height description of the prepared silver and $Ag@SiO_2$ nanoparticles. The maximal number of Ag nanoparticles are detected in the size span of 30 to 80nm. There are several larger particles are also present according to the study of AFM data, but as followed by histogram scanning their number is bounded. As suggested by line analysis, the height profile of the nanoparticles is in the same span, as confirmed by TEM analysis. The AFM images show that once coated with silica, the size of the nanoparticles extended, i.e. approx—80 nm.

The stability of both nanoparticles was measured in terms of zeta potential using a zeta sizer. The prepared colloidal nanoparticles are maintained by a net negative charge on their facet and stay in solution caused by joint electrostatic-repulsive force. It is understood that because the adherent citrate ions Ag nanoparticles have a negative charge, simultaneously due to this, a repulsive potential drives

the particles to prevent aggregation. Hence, there is no need for any additional stabilizing agent, and particles in the suspension remain steady. It was found that incorporating even a tiny quantity of silica promptly reduces the zeta potential. The colloidal stability of the Ag nanoparticles is -27.7mV and Ag@SiO_2 nanoparticles are -21.7mV.

The hydrodynamic diameter of Ag nanoparticles was determined using a dynamic-light-scattering (DLS) experiment. DLS of Ag nanoparticles colloidal solution commences from 10 to 200 nm, besides a mean volume of 50nm. While, the DLS of the Ag@ SiO_2 nanoparticles colloidal solution were in the range of 50 to 200nm, besides a mean diameter of 80nm. The DLS results are almost similar to the TEM results.

The electrochemical experiments related to the fabrication of immunosensors were carried out by cyclic voltammetry (CV) studies. Electrochemical–impedance spectroscopy (EIS) was also part of the study and has been implied to observe the electron transfer resistance. It is a label-free technique to determine antigen-antibody interactions on the electrode surfaces by measuring their capacitance and interfacial charge transfer resistance. As soon as a target protein binds to the pre-functionalized probe surface, the electrode–solution interface impedance changes, and these changes are detected electrically over a range of measurement frequencies.

There are several experimental specifications which needed to be optimized in order to manufacture an immunosensor. The antigen concentration (CEA) was optimized first to enrich the sensitivity. It was unveiled that even with such low concentrations of CEA, well defined voltammetry peaks can be found. Furthermore, with the rise in the concentration of CEA, the peak-current intensities lengthen. Whereas significant enhancement of the concentration of CEA, leads to a high signal, and it also followed the towering background at a similar time because of the non-specific adsorption process. It was monitored that the current scale versus CEA is straight from the span of 0.5 ng/ml to 10 ng/ml, and it is appropriate for the computable task.

The highest signal-to-noise proportion was conceivably attained with 10 µl of CEA concentration. So, 10 µl of antigen was chosen as the optimized condition. The limit of the detection of this procedure was considered to be 0.01ng/ml. The string of 6 repeated quantifications in addition to CEA-concentrations of 0.5ng/ml to 10ng/ml was taken.

The electrochemical reactions that occur in an immunosensor have greatly influenced the pH of the detection suspension. Protein denaturation can occur if pH is unsuitable. The pH of the solvent buffer was explored thoroughly to obtain an excellent electric-current signal. Maintaining the CEA-concentration persistent (10 µl), the outcome of the pH value of the buffer solution on the intensity of the current was calculated by keeping the span of the pH from 5.0 to 6.0 and after reaching maximum

current at pH 6.0, the intensity of the current reduced correspondingly once the pH-value elevated from 6.0 to 7.5. This suggests that pH 6.0 is more advantageous to the current response of the sensor assembly system. So, pH 6.0 was selected as the most favourable value. By using PBS buffer at pH 6.0, precisely elaborated cyclic voltammogram and satisfactory response to CEA were perceived.

By maintaining the concentration of the CEA-20ng/ml, the impact of time of the incubation was examined in the period of 0-30 min. It was observed that, within the first 17 min., ΔI quickly elevated, and once the incubation time was longer than 17 minutes, it came to a constant value. So, 17min was identified as an excellent condition for incubation. Considering practicability in a genuine way of life, the room temperature was selected to carry on all the experiments.

Agar well diffusion technique was employed to assay the antibacterial and antifungal activity of the prepared silver nanoparticles and silica-coated silver nanoparticles. For this purpose, two distinct bacterial strains were used, i.e. Escherichia coli (Gram -ve) and Bacillus- cereus (Gram +ve). And the antimicrobial activity of both nanoparticles was calculated compared with the control (ciprofloxacin). Two concentrations from the suspension of both nanoparticles were taken for analysis. Subsequently, the antibacterial activities of both nanoparticles were corroborated by considering the zone of inhibition (in mm) fabricated surrounding the well.

The minimum inhibitory concentration (MIC) assay was also exercised to unearth the antimicrobial efficacy of nanoparticles. For this experiment, five multifarious concentrations of nanoparticles were taken (10µg/ml-50µg/ml).

The antifungal maneuvre of Ag nanoparticles and $Ag@SiO_2$ nanoparticles was decided by employing Kirby - Bauer agar-well disc diffusion method. The stock fungal strain of Candida albicans was put together and maintained in a media solution. We employed two different concentrations of both nanoparticles to examine their antifungal activities. Similarly, like in antibacterial studies, a minimum inhibitory concentration (MIC) assay was used to discover the antifungal effects of nanoparticles.

To analyze the cytotoxic activity of colloidal silver and silica-coated silver nanoparticles, MTT (3-(4, 5-dimethyl thiazolyl-2)-2, 5-diphenyltetrazolium bromide)-assay was used by utilizing PC-3 cells. The assay computed the pace by which the cell proliferate and contrastingly metabolic set of events occurs which resulted in necrosis or apoptosis. Five different concentrations (10, 20, 40, 60, 80 µg/ml) of test-sample (nanoparticles) were taken to carry out the analysis. Finally, the absorbance was calculated by utilizing a microtiter plate reader at two different wavelengths i.e., 570nm as well as at 630nm. The growth inhibition percentage was evaluated by analyzing the nanoprarticles' potency to

inhibit the cell growth by 50% (IC50value.). Additionally, apoptotic studies of both the synthesized nanoparticles were carried out by flow cytometric studies.

8.3. Conclusions

1] Silver colloidal solutions were synthesized following the chemical reduction method via the altered version of the already known Turkevich method.

2] Encapsulation of silver nanoparticles with silica was accomplished by improvised Stober method followed by characterization of silver nanoparticles and silica-coated silver hybrid nanoparticles.

● The UV-visible spectroscopy revealed a sharp characteristic peak and after accumulation of the silica layer on Ag nanoparticles, the peak moved towards a longer wavelength.

● The UV-visible spectroscopy revealed a sharp characteristic peak and after accumulation of the silica layer on Ag nanoparticles, the peak moved towards a longer wavelength.

● XRD diffraction was employed to regulate the difference of the crystal structure betwixt the two nanoparticles. It also exhibited the phase purity of both synthesized nanoparticles. The synthesized nanoparticles are crystalline having a spherical structure.

● FTIR, EDX, and RAMAN-spectroscopic evaluation were implemented to learn the functional groups, chemical composition, and vibrational characteristics of the nanoparticles respectively. It was discovered that the prepared nanoparticles displayed good stability.

● EDX confirmed the purity of both the nanoparticles.

● The TEM and SEM interpretations confirmed the spherical size of both the nanoparticles, and it was clearly visible that the silica shell consistently encapsulates silver core particles.

● The dynamic-light-scattering (DLS) assessment are nearly identical to the TEM results.

● Topological characterization (AFM) of both the prepared nanoparticles demonstrates the matching height elucidation, and the height profile of the nanoparticles is in the same range, as confirmed by TEM investigation.

● It is noteworthy to mention that all of the characterization techniques divulged the average size of the Ag nanoparticles and $Ag@SiO_2$ nanoparticles were 50 nm and 80 nm simultaneously.

● The steadiness of both the prepared colloidal nanoparticles were computed in terms of zeta potential. The synthesized nanoparticles sustained a net negative charge on their surface and remained in a solution prompted by joint electrostatic-repulsive force. Both the synthesized nanoparticles manifest good stability and later employed for medical and health care applications due to their exceptional chemical and physical properties.

3] The electrochemical disposal immunosensor was fabricated by immobilizing anti-CEA onto $Ag@SiO_2$ nanoparticles encapsulated ITO solid surface for the specific detection of CEA.

● The presence of silica-coated silver nanoparticles on the flat surface of the electrode, gives an excellent voltammetric advantage, fine stability, and noteworthy biocompatibility towards the detection and additionally gives extensive binding sites for the involved immune reactions.

● A potent interconnection between the response of the stripping current of the altered ITO flat surface and the particular logarithmic rate of the concentration of CEA was established extended from 0.5ng mL^{-1} to 10ng mL^{-1} with the minimum detection limit of 0.01ng/ml.

● This empirical, low-cost, and flexible electrochemical immunosensor allows a more uncomplicated immunoassay for the detection of CEA, which can provide the goal of CEA detection in clinical analysis in the future and such strategy could be utilized to manufacture immunosensors for other aimed targets also.

4] Detailed anti-bacterial and anti-fungal studies of both the engineered nanoparticles were brought off, furthermore, briefly, their comparative studies were also carried out. For the observation of anti-bacterial as well as anti-fungal studies; the disc-diffusion method and MIC-Assay were worked.

5] We have examined the anticancerous activities of both the synthesized nanoparticles by flowcytometry. Visible morphological alteration was seen after treatment with both the nanoparticles on the confluency of PC-3 cell monolayer. Silica-coated silver nanoparticles show little effects compared to the bare silver nanoparticles, attributed to the biocompatible nature of silica. However, it still shows worthwhile anticancerous activity due to the release of silver ions from the porous silica layer and silver ions anchored to the layer of the nanoparticles. These studies will focus on nanoparticle-cell intercommunication and will also tremendously contribute to the expansion of improvement in the field of nanomedicine. So, it is proposed that both of the nanoparticles could be used as therapeutic agents for anticancer treatments in the future for the purpose of treatment of prostrate cancer.

8.4. Summary of thesis

Chapter 1 describes all the necessary information about nanoparticles and brief knowledge of nanotechnology, the history of nanoparticles, classification of nanoparticles based on dimension, origin as well as on morphology, consolidation of nanotechnology and life sciences, the influence of nanotechnology on life sciences, their impact on the diagnostic field, the influence of nanotechnology in the field of drug-delivery, influence in tissue-engineering, synthesis of silver nanoparticles, various chemical synthesis routes of silver nanoparticles and silica-coating method of silver nanoparticles.

Chapter 2 gives detailed information about hybrid nanoparticles and approaches to the synthesis of hybrid nanoparticles, components involved in designing hybrid nanostructures, hybrid silver nanoparticles and nanostructures- nanowires, nanospheres, and nanocubes, various modes of synthesis of hybrid silver nanostructures- etching method, double-reductant method, synthesis of silver core-shell nanoparticles- organic coated hybrid silver nanoparticles, inorganic coated hybrid silver nanoparticles, core-shell nanoparticles with the metal core, bimetal nanoparticles or metal core metal-shell nanoparticles, applications of hybrid silver nanoparticles- antibacterial effectiveness of hybrid silver nanoparticles, anticancerous approaches of hybrid silver nanoparticles, hybrid silver nanoparticles applications in detection.

Chapter 3 describes characterization techniques used to determine the chemical and physical properties of silver nanoparticles and silica-coated silver nanoparticles. This chapter also deals with the techniques involved in the study of antimicrobial and anticancerous activities of silver nanoparticles and silica-coated silver nanoparticles.

Chapter 4 deals with the synthesis methods of silver and silica-coated silver nanoparticles. It also covers the physical and chemical studies of silver and silica-coated silver nanoparticles.

Chapter 5 introduces the design and fabrication of an electrochemical immunosensor based on carcinoembryonic antigen (CEA). Optimization of experimental condition during fabrication of immunosensor. Characterization of immunosensor by cyclic-voltammetry and electrochemical impedance spectroscopy as well as morphological studies by scanning electron microscopy.

Chapter 6 deals with the evaluation of the anti-cancer potential of silver nanoparticles and silica-coated silver nanoparticles. It covers the cytotoxic studies of both the nanoparticles by MTT (3-(4, 5-dimethyl thiazolyl-2)-2, 5-diphenyltetrazolium bromide) colorimetric assay. This chapter also deals with the programmed cell death mechanism induced by silver nanoparticles and silica-coated silver nanoparticles.

Chapter 7 focuses on comparative antibacterial and antifungal studies of silver nanoparticles and silica-coated silver nanoparticles. Both nanoparticles were utilized in different concentrations. Antibacterial activity was performed against Gram –ve bacteria- Escherichia coli and Gram +ve bacteria- Bacillus- cereus. Whereas, antifungal activities were studied against fungal strains of Candida albicans. For the study of antibacterial and antifungal activities-disk diffusion method and minimum inhibitory concentration, methods were employed.

Chapter 8 deals with the summary, conclusion as well as recommendations of the thesis.

8.5. Future scope of the thesis

Silver and silica-coated silver nanoparticles: For therapy (Alternative to commercially available anti-cancerous drugs and drug-resistant microorganisms)

The Synthesized silver and silica-coated silver nanoparticles possess great anticancerous and antimicrobial activity. Furthermore, they are biocompatible. For the treatment of various infections rendered by drug-resistant fungi and bacteria, silver and silica-coated silver nanoparticles can be employed as an effective antimicrobial candidate alternatively than the employment of conventional old antibiotic therapies to cure infections. Apart from this, both synthesized nanoparticles are also effective against cancerous cells and can be utilized as a potential anticancerous agent.

Silver and silica-coated silver nanoparticles: For diagnosis (early detection of life-threatening disease)

The synthesized nanoparticles detected CEA (carcinoembryonic-antigen) by fabricating an immunosensor. The sensor fabrication method by utilizing the prepared nanoparticle is more beneficial than that of another electrode because it is made from a low-cost ITO (Indium tin oxide) flat substrate, and it can be reproduced in batches. This direct, cost-effective, and flexible electrochemical immunosensor makes possible a more economical and straightforward immunoassay for CEA, which can enable the detection of CEA. It can serve the purpose of CEA detection in future clinical diagnosis, and this strategy could also be used to develop immunosensors for other targets.